PROTON MAGNETIC RESONANCE SPECTROSCOPY (^{1}H-MRS) OF INTRACRANIAL LESIONS:

Assessment of differences between tumours and Tumour like lesions & its applicability in brain lesion characterization

Thesis

Submitted to

The Tamil Nadu Dr.M.G.R.Medical University, Chennai
for the award of the Degree of
Doctor of Philosophy

by

Dr.N.CHIDAMBARANATHAN

DEPARTMENT OF NEUROLOGY & NEUROSURGERY,
APOLLO HOSPITALS, 21, GREAMS LANE,
CHENNAI 600006.

January 2011

CERTIFICATE

This is to certify that the thesis entitled "**Proton Magnetic Resonance Spectroscopy (^{1}H-MRS) of Intracranial Lesions: Assessment of differences between Tumours and Tumour like lesions & its applicability in brain lesion characterization**" is an original research work done by me, and it was not used previously either partly or fully for the award of any Degree, Diploma, Associate ship, fellowship or other similar title.

Place: Chennai-6
Date:

Dr N Chidambaranathan,
Consultant Radiologist, Department of Radiology & Imaging Sciences,
Apollo Hospitals, Chenna-600 006

CERTIFICATE

This is to certify that the thesis entitled "**Proton Magnetic Resonance Spectroscopy (^{1}H-MRS) of Intracranial Lesions: Assessment of differences between Tumours and Tumour like lesions & its applicability in brain lesion characterization**" submitted **by Dr.N.CHIDAMBARANATHAN** for the Award of the degree of Doctor of Philosophy in Medicine, is a bonafide record of research done by him during the period of study under our supervision and guidance, and that it has not formed the basis for the award of any Degree, Diploma, Associate ship, Fellowship or other similar title. We also certify that this thesis is his original independent work. We recommend that this thesis should be placed before the examiners for their consideration for the award of the Ph.D Degree.

GUIDE

Prof.PRITHIKA CHARY
MD, DM, Ph D, MNAMS (Neurology)
MCh (Neurosurgery)
Senior Consultant Neurologist and Neurosurgeon,
APOLLO HOSPITALS,
21, Greams Lane,
CHENNAI -600 006.

CO-GUIDE

Prof.K.GANAPATHY
MS[Neuro], FAMS, FICS, FACS, Ph D
Senior Consultant Neurosurgeon,
APOLLO SPECIALITY HOSPITALS
320 Anna Salai Teynampet,
CHENNAI -600 035

Place: Chennai

Date:

This Thesis is dedicated to my Parents
Swaminathan Natesan, Punithavalli Natesan
and all my Teachers especially
LateProf. ARCOT GAJARAJ and Late Dr. IQBAL AHMED

I am indebted to my father for living,
but to my teacher for living well

– Alexander the Great

ACKNOWLEDGEMENTS

This work would not have materialised but for the support and guidance from **Dr PRITHIKA CHARY**, my Guide and Supervisor who has been a constant source of inspiration and endless encouragement. I am greatly indebted to her for making this study possible.

I am extremely grateful to my Co-Guide, **Dr K GANAPATHY** for the unstinted help, guidance and supervising my research work in an untiring manner.

I express my sincere thanks to **Dr V S MALLIKARJUN** and **Dr MITRA GHOSH,** consultant pathologists, for their useful interaction and for providing histo-pathological reports.

I am indebted to my radiology colleagues **Dr V MALATHI** and **Dr S NOOR BASHA** for their professional support and for helping me in every possible way.

I have been most fortunate in securing the guidance and advice of **Mr THENNARASU** of the Department of Bio-Statistics, Sankar Nethralaya, Chennai who was instrumental in carrying out the relevant statistical work.

I owe special thanks and gratitude to **Mr M S MURALI MURUGAVEL**, Assistant Professor, Indian Institute of Technology Madras, for helping me in data analysis.

I thank my colleague **Dr JAYARAJ GOVINDARAJ** for all the help rendered

I thank all the **MRI Technologists** who have put in considerable effort and have cooperated enthusiastically in carrying out this study.

Every one of my colleagues in the Department of **Radiology and Imaging** S**ciences**, Department of **Neurology** and **Neurosurgery** have helped me in his or her own way. I am grateful to each of them for their stimulating questions and keen interest in the subject.

I thank all the staff in the **Medical Record Section,** Apollo Main Hospitals and Apollo Speciality Hospitals, Chennai, for their ever readiness to help me at every stage.

My sincere thanks to **Dr Radha Rajagopalan**, Director of Medical Education and **Dr Sathyabhama**, Director of Medical Services and Members of the Ethical committee for facilitating my progress in carrying out this study.

I express my deep appreciation & heartfelt thanks to Padma Vibushan **Dr Pratap C Reddy**, Chairman, Apollo Hospitals Group and **Mrs Preetha Reddy**, Managing Director for all their constant support and encouragement.

This work would not have been possible without strong support at home from my wife and each member of my family who provided a conducive atmosphere and cheerfully put up with all my procrastinations.

Last but not the least, my deep gratitude goes to each one of the patients and their relatives in the study who unmindful of personal inconvenience allowed me to scan & acquire data several times, thus contributing significantly in my attempt to enrich current scientific knowledge.

Coming together is a beginning,
Keeping together is progress,
Working together is success – *Henry Ford*

N. Chidambaranathan

CONTENTS

LIST OF TABLES

LIST OF ILLUSTRATIONS

LIST OF CHARTS & GRAPHS

ABSTRACT

Characterization of intracranial mass lesions, based on structural Magnetic Resonance Imaging (MRI) alone may be difficult. In such cases Proton Magnetic Resonance Spectroscopy (1H-MRS) along with other non-invasive techniques represents an advance in the specificity of brain lesion diagnosis.

PURPOSE: a) To determine if there are specific MRS findings which could help differentiate between neoplastic and non –neoplastic lesions and also to identify the presence or absence of MRS features which could help differentiate one type of neoplasm from another b)To determine if MRS findings could help grade gliomas pre operatively; c) To determine if MRS findings could help differentiate irradiated residual/ recurrent tumours from radiation necrosis. d) To determine if MRS findings could help differentiate necrotic tumours from infective lesions such as abscesses.

METHODS: In vivo proton MR spectroscopy was performed on 1.5 Tesla MR system using standard imaging head coil. 91 patients with intracranial masses were subjected to single voxel spectroscopy. Of the 91 cases that were studied, 70 were Neoplastic and 21 were Non-neoplastic lesions. 75 patients had a histopathological diagnosis and in16 patients presumptive diagnosis was made based on post treatment clinical response, or by serial imaging studies. 15 healthy volunteers were evaluated as a control group. The metabolic area ratios NAA / Cho; NAA / Cr and Cho / Cr were evaluated.

2D-CSI, multi- voxel study was performed in 15 patients, in whom, lesions were ill-defined or infiltrative on MR imaging sequences. On the basis of spectral and distribution patterns of the pathologic spectra seen at MR spectroscopy, a qualitative analysis was done.

RESULTS: Statistical analysis was made by Univariate analysis ANOVA and independent t-test(two sample t-test or student's t-test) and the Multivariate analysis Binary Logistic regression analysis. the **sensitivity, specificity, Positive predictive value, Negative Predictive value and accuracy** for determining **malignant lesions**

with MRI guided ^{1}H-MRS were **90.9%, 97.9%, 97.6%, 92%, and94.3%** respectively**.**

Cho / Cr area ratio was statistically found to be more significant in differentiating neoplastic from non-neoplastic lesions ;.Mean Cho / Cr area ratio for neoplastic tumours (3.87 ± 2.20) was greater than that of non-neoplastic lesions (1.2 ± 0.66) with a P value of <0.001.

2. **Decrease of NAA / Cho area ratio was statistically more significant in differentiating high grade from low grade gliomas:** The mean NAA / Cho area ratio of high grade gliomas (0.27 ± 0.12, *n* = 25) was lesser than the mean NAA / Cho area ratio of low grade gliomas (0.64 ± 0.17, *n* = 18) with a p value < 0.001.

3. **Cho / Cr area ratio was more statistically significant (**with a P value of <0.001) **in discriminating recurrence of tumour from post radiation necrosis / post operative changes.** The mean Cho / Cr area ratio (4.06 ± 1.18) of recurrent / residual tumors was significantly higher than the Cho / Cr area ratio (0.94 ± 0.49) of post operative gliosis / post radiation necrosis

4. Tuberculous abscess depicted an isolated broad lipid peak at 0.9 ppm; Cho / Cr ratio was more statistically significant (with a p value of <0.001) in differentiating infective lesions from neoplastic lesions.

5. Pyogenic abscesses exhibited amino acid residues (valine, leucine), lactate, alanine and acetate.

6. Among the three metabolite ratios**, none of the ratios are statistically significant in differentiating high grade gliomas from metastases** in SV MRS. MV-MRS technique was useful in assessing response to radiation therapy in peri enhancing areas and in differentiating infiltrative tumour from circumscribed lesion

CONCLUSIONS: In vivo proton MR spectroscopy was useful in a) differentiating neoplasm from non- neoplastic lesions, b) differentiating low grade from high grade neoplasms, c) differentiating recurrence of the tumour from radiation necrosis and d) differentiating cystic tumours from cerebral abscesses.

ABBREVIATIONS

MRI	-	Magnetic Resonance Imaging
MRS	-	Magnetic Resonance Spectroscopy
CE-MRI	-	Contrast Enhanced Magnetic Resonance Imaging
SV MRS	-	Single voxel Magnetic Resonance Spectroscopy
MV MRS	-	Multivoxel Magnetic Resonance Spectroscopy
1H-MRS	-	Proton Magnetic Resonance Spectroscopy
FLAIR	-	Fluid Attenuation Inversion Recovery
DWI	–	Diffusion weighted imaging
Ppm	-	parts per million
NAA	-	N Acetyl Aspartate
\Cho	-	Choline
Cr	-	Creatine
Lac	-	Lactate
Lip	-	Lipid
Glx	-	glutamate
Gly	-	Glycine.
AA	-	Amino acid.
MI	-	Myoinositol.
GBM	-	Glioblastoma Multiforme.
PNET	-	Primitive Neuro ectodermal Tumour
FCD	-	Focal Cortical Dysplasia

TB	-	Tuberculous
TDL	-	Tumefactive demyelinating lesion
HPE	-	Histopathological examination
GA	-	glatiramer
IFN-β	-	Interferon
MS	-	multiple sclerosis
NAWM	-	Normal appearing white matter
Gd	-	Gadolinium
CNS	-	Central Nervous system
CT	-	Computed Tomography
SNR	-	Signal-to-Noise Ratio
SVS	-	Single-Voxel Spectroscopy
CSI	-	Chemical-Shift Imaging
RF	-	Radiofrequency
3D.MRSI	-	Three Dimensional Magnetic Spectroscopic Imaging.
SPECT	-	Single-Photon Emission Computerized Tomography
SRS	-	Stereotactic Radiosurgery
PET	-	Positron Emission Tomography
FDG	-	fluoro-2-deoxy-D-glucose
CNI	-	Cho-NAA index
AVM	–	Arterio Venous Malformations
SE	-	Spin-Echo

TE	-	Time to echo
TR	-	Time of repetition
PRESS	-	Point-Resolved Spectroscopy
CHESS	-	chemical-shift selective saturation
PPV	-	Positive Predictive Value
NPV	-	Negative Predictive Value
ROC	-	Receiver Operating Characteristic
AUC	–	Area Under Curve
TP	-	True Positive
FN	-	False Negative
TN	-	True Negative
FP	-	False Positive
ANOVA	-	analysis of variance
LR	-	logistic regression
CI	–	confidence interval
<	-	less than
➢	-	more than
n	-	number
Gy	-	grey
RT	-	radiotherapy
Post – Op	-	post operative
Fig.	-	Figure
etc	-	etcetera
Viz	-	Namely
et al	–	and others

PROFORMA

Name:	Age:	Sex:
Occupation:	Sl.No:	IP/OP No:
Address:	Ph.No:	Date:
Ref Dr:	Ph.No:	

Clinical complaints:

Headache, seizure, loss of consciousness, altered sensorium

Past History:

H/O Tuberculosis, surgery , any relevant treatment history.

Clinical diagnosis:

Other diagnostic test: CT Brain, chest X-ray

MRI Evaluation:

a) MRI Finding

Nature	Solid / cystic /mixed / hemorrhagic/
Location	
T1WI	
T2WI	
Flair	
DW / ADC	
I.V Contrast	
Size	
Diagnosis	
HPE	

b) MRS finding:

	Width	Area	Height
NAA			
Cr			
Cho			

Ratios:

	Area ratios	Height ratios
NAA / Cr		
NAA / Cho		
Cho / Cr		

2) Presence of other metabolites

Lipid	
Lactate	
Amino acid	
Acetate	
Alanine	
Glutamate	
Glycine	
Succinate	
Scyillo inositol	

MRS Report:

Neoplastic	
Non neoplastic	

MRS Grading of glioma

Low grade	
High grade	

MR with pathological correlation:

CHAPTER 1

INTRODUCTION

Many diseases of the Central Nervous system (CNS) are life threatening, although many of them are potentially treatable conditions. Early diagnosis is necessary for appropriate treatment. In the past few decades, non-invasive modalities such as Computed Tomography (CT) and Magnetic Resonance Imaging (MRI) have established themselves in the diagnosis of various CNS diseases. MRI is superior to CT due to its inherent sensitivity, specificity, better soft tissue contrast and multiplanar capability.

MRI provides significantly more information about intrinsic tissue characterization- a capability, which should be exploited by the neuro-radiologist to determine tumour type. This ability to discriminate differences in tissues by variation in signal intensities parallels findings on gross pathology and applies to several areas pertinent to tumour imaging. Besides having multiplanar capabilities and excellent soft tissue contrast, the different pulse sequences used, help in morphological evaluation of various tumours and their components.

Specific diagnosis of brain tumours can often be achieved with MRI on the basis of several specific intensity patterns, using T1 weighted images (T1WI) and T2 weighted images (T2WI). MRI uniquely depicts intra-tumoural haemorrhage or necrosis. Some components of tumours may have specific and pathognomonic signal intensities. Fat containing neoplasms (eg. teratoma, lipoma, dermoid) are easily identified on MRI since fat is high intensity on T1WI and parallels the intensity of subcutaneous fat. Profound hypervascularity associated with certain tumours like hemangioblastoma is shown on spin-echo images as linear or serpentine regions of

signal void vessels within neoplastic masses. Intratumoral vascularity can be confirmed by using gradient echo imaging or MR Angiography, which demonstrates these vessels as hyper intense structures. Markedly hypercellular neoplasms especially those with minimal cytoplasm are, characteristically, of relative low intensity on T2WI and approximate the intensity of normal gray matter due to lower water content (higher solid component).

MR imaging has made it easier to detect and differentiate intracranial mass lesions. Nevertheless, it is sometimes impossible to base a diagnosis solely on clinical and neuro-radiologic findings. Open biopsy is often required before commencing specific treatment. This happens even in cases where surgery is not the first choice in the final treatment. In this context, additional information provided by other non invasive radiological techniques can be of great value for taking clinical decisions, regarding patient management and hopefully in the future, avoiding invasive surgery.

In addition to conventional MR imaging techniques a variety of advanced techniques have found their place in clinical practice or are the subject of intense research. These advanced techniques offer more than the anatomic information provided by the conventional MR imaging sequences. They generate physiologic data and information on chemical composition. The current advanced techniques include perfusion imaging, diffusion-weighted imaging (including diffusion tensor imaging), Magnetic Resonance spectroscopy, Blood Oxygen Level–Dependent (BOLD) imaging, and the largely experimental molecular imaging. Currently, the first three techniques are more commonly used

Proton Magnetic Resonance Spectroscopy:

In vivo **Proton Magnetic Resonance Spectroscopy** (^{1}H MRS) **is a non-invasive technique and provides metabolic information, complementary to the anatomical changes, found in radiological examinations. This has proved useful, in providing additional information in various brain diseases. MRS is a non-invasive physiological imaging of the organ, that measures relative levels of various tissue metabolites.** Because of differences in the cell type and growth characteristics of tumours, it is likely that tumour types will have unique individual metabolic 'fingerprints'.

The most useful nuclei for human spectroscopy are hydrogen, phosphorus, sodium and to a lesser extent, carbon. Proton (hydrogen) Magnetic Resonance spectroscopy (^{1}HMRS) has a greater signal-to-noise ratio (SNR) and better spatial resolution than phosphorus spectroscopy and is more easily integrated with MRI in a single examination. ^{1}HMRS has the potential to record biochemistry in vivo, which can help in tissue characterization. Magnetic Resonance Spectroscopy (MRS) utilizes the principle that nuclei in different chemical structures have different characteristic resonance patterns, depending on the neighboring chemical structures and the interactions between these various chemical structures. MRS detects the chemical composition of the tissue under study and the associated software displays a waveform with peaks that correspond to the various chemicals detected.

The technique of spectroscopy is widely applied in chemistry for the analysis of compounds in solution, and is a powerful tool for determining the structure of biological macromolecules. Similarly, MR (Magnetic Resonance) spectroscopy can be used to identify important molecules in living tissue. Protons often are used for MR spectroscopy because of their high natural abundance and high nuclear magnetic sensitivity. Despite the huge number of bio molecules in tissue, relatively few are identifiable in vivo because only freely mobile compounds, that are present in substantial concentrations, emit enough signals to be detected. The concentrations of metabolites of interest are in the millimolar range for example water protons are a thousand times as common. For this reason, water resonance has to be suppressed so that the other molecules can be detected. The diagnostically resolvable hydrogen MR spectra may be obtained using clinical instruments (1.5 T or greater) and routinely used surface coils.

A basic step in spectroscopy is localization of the region of interest in all three spatial dimensions, yielding the volume of interest. This can be performed using two methods: single-voxel spectroscopy (SVS) or Multi voxel spectroscopy (MV-MRS), chemical-shift imaging (CSI). In clinical practice, SVS is the easier and faster technique for obtaining metabolic information. The voxel (volume element) being sampled has a minimum size of 1 cm^3, using current equipment. At least 128 signal averages are required to obtain interpretable spectra within a clinically acceptable time period.

A homogeneous magnetic field is an important prerequisite for obtaining resolvable spectra. Shimming the field in the region of interest, to the resonance of water, ensures the homogeneity of the field. Water is the dominant peak in all

hydrogen spectroscopy. When the analogue-to-digital conversion is carried out, the intensity of all metabolites is scaled, relative to that of water. The most common technique used to suppress the water peak is chemical-shift selective suppression. In some instances, it may also be desirable to suppress the signal from lipids because lipid peaks are large and may obscure some metabolites of interest.

Although most modern clinical MR spectroscopy units are capable of echo times as short as 20 milliseconds, adequate MR spectra may be obtained using echo times as long as 136 to 272 milliseconds. Using long echo times, the signal from most metabolites in the brain is lost. Conversely, short echo times allow for identification of many other metabolites.

MRS, therefore, allows visualization of molecular processes as opposed to structural and anatomic imaging of tissues and organs and thereby provides direct biochemical information. Common metabolites studied with MRS include N-acetylaspartate (NAA), Choline (Cho), Creatine (Cr), myo-inositol (mI), Glutamate (Glu)/ Glutamine (Gln), amino acids, lipids, lactate, succinate and so on.

The metabolites thus detected are expressed as ratios such as NAA / Cho; NAA / Cr; Cho / Cr; Cho/ NAA and so forth based on their area and/or height. These ratios are compared to the normal assigned ratios of the control groups or to the normal portion of brain in the same individual as a reference. Unfortunately, there is no tumor-specific metabolite that is detectable with in vivo MR spectroscopy.

Proton MR Spectroscopy gives important information in the differential diagnosis of brain tumours through analysis of metabolites of the normal brain and tumours. MRS is a non-invasive means of evaluating brain tumours, by investigating the spatial distribution of metabolic changes in brain lesions. It is possible to detect specific patterns in the changes of metabolite concentrations compared with those in the normal brain.

Several studies (1,2) have shown that a common feature of many rapidly growing tumours is an increased choline to creatinine ratio, and a decreased *N*-acetylaspartate to creatinine ratio, and an increased lactate level. Decrease in overall level of choline, creatinine, *N*-acetylaspartate and increase in lipid/lactate indicate necrotic processes. These changes in brain metabolite level/patterns have been used to grade the tumours, and to monitor and assess the effects of therapy.

Although it is possible to clearly distinguish glial neoplasms from normal brain tissue by MRS, controversy exists regarding the reliability of MRS in distinguishing different histological grades of astrocytomas and other brain tumours.

Bruhn et al, (3) in a qualitative comparison of in vivo MR spectroscopic findings and histologic data from a variety of brain tumours showed that histologically similar tumours exhibit similar spectra while histologically different tumours exhibit quite different spectral patterns. Indeed, the relative concentration of these metabolites

has been shown to differ depending on whether the tissue is neoplastic or non-neoplastic, rapidly proliferating or slow growing.

Apart from intracranial mass lesions MRS is also widely used in evaluating infarcts, white matter disorders, trauma, metabolic disorders, neuro degenerative disease, epilepsy, encephalopathy, parkinsonism among others. Its applications have also expanded to other regions such as breast and prostate MRS is also an useful tool to monitor therapy and to provide prognostic information in certain conditions (4).

CHAPTER -2

2.1. NEED FOR THIS STUDY

- Some Non-Neoplastic lesions particularly inflammatory lesions, pseudotumour, encephalitis, demyelination may have spectral patterns similar to neoplasm.
- High grade gliomas often have false negative spectroscopy for tumours
- It is often difficult to distinguish cerebral abscess from necrotic primary or metastatic brain tumours. These lesions have different treatment regimens and prognosis.
- Tuberculoma/cerebral abscess / parasitic cysts pose a diagnostic problem particularly in Indian patients.
- In post treatment follow up patients with brain tumour, a clear distinction between tumour recurrence and radiation necrosis can often be challenging.

2.2. HYPOTHESIS:

MRS may be helpful in differentiating neoplasm from non-neoplastic lesions. In MRS the specific relative metabolic peak ratios obtained from different regions of brain tumours could be used to histologically classify astrocytomas

- MRS can provide biochemical information that can narrow the differential diagnosis for cystic masses in general and may permit differentiation of brain abscess from cystic or necrotic tumour.

2.3. OBJECTIVES

- To determine if there are specific MRS findings which could help differentiate between neoplastic and non –neoplastic lesions and also to identify the presence or absence of MRS features which could help differentiate one type of neoplasm from another.

- To determine if MRS findings could help grade gliomas pre operatively.

- To determine if MRS findings could help differentiate irradiated residual/ recurrent tumours from radiation necrosis.

- To determine if MRS findings could help differentiate necrotic tumours from infective lesions such as abscesses.

CHAPTER 3

REVIEW OF LITERATURE

"Reading makes a full man, meditation a profound man, discourse a clear man."

Benjamin Franklin

3.1. History

The world of nuclear spins is a true paradise for theoretical and experimental physicists. It supplies simple test systems for demonstrating the basic concepts of quantum mechanics and quantum statistics (4). Nuclear spin systems possess unique properties that pre-destinate the physicists for testing novel experimental concepts in molecular studies.

All science is interdisciplinary – from magnetic moments to molecules to men- as quoted by **Paul C. Lauterbur**(5). Nuclear magnetic resonance began within physics, at a confluence among particle physics, condensed matter physics, spectroscopy, and electromagnetics (4).

Key experiments of magnetic resonance started with the famous molecular beam experiments by **Isidor I. Rabi** (6-7) acknowledged in 1944, followed by the classical NMR experiments by Edward M. Purcell (8) and Felix Bloch (9).

The first successful nuclear magnetic resonance (NMR) experiment was carried out in 1946 independently by two scientists in the United States.

Felix Bloch, working at Stanford University, and **Edward Purcell,** from Harvard University, found that when certain nuclei were placed in a magnetic field, they absorbed energy in the radiofrequency range of the electromagnetic spectrum, and re-emitted this energy when the nuclei were transferred to their original state (8-9). The strength of the magnetic field and the radiofrequency matched each other as had been demonstrated earlier by Sir Joseph Larmor (Irish physicist 1857-1942). This is known as the Larmor relationship (i.e., the angular frequency of precession of the nuclear spins being proportional to the strength of the magnetic field). This phenomenon was termed NMR and later was referred as Magnetic Resonance Imaging (MRI)

This discovery heralded the birth of NMR spectroscopy. This soon became an important analytical method in the study of the composition of chemical compounds. For this discovery Bloch and Purcell were awarded the Nobel Prize for Physics in 1952.

Purcell et al (8) and **Bloch et al** (9) elucidated the principles of nuclear magnetic resonance in 1946. Five years later, **Proctor and Yu** (10) proposed that the resonance frequency of a nucleus depends on its chemical environment, which produces a small, but perceptible, change in the Larmor resonance frequency of that nucleus. This nuclear behaviour is termed "chemical shift," and is caused by the magnetic fields generated by circulating electrons surrounding the nuclei interacting with the main magnetic field.

Later the optical detection schemes by Alfred Kastler (11), leading to a prize in 1966. Other physics Nobel laureates have been associated in various ways with magnetic resonance: John H. Van Vleck developed the theory of dia- and paramagnetism and introduced the moment method into NMR, Studies of Nicolaas Bloembergen had a major impact on early relaxation theory and measurements; Karl Alex Müller contributed significantly to electron paramagnetic resonance; Norman F. Ramsey was responsible for the basic theory of chemical shifts and J couplings; and Hans G. Dehmelt has developed pure nuclear quadruple resonance theory(4).

A major improvement in the signal-to-noise ratio of NMR was achieved in 1964 by the enunciation of the Fourier transform spectroscopy principle. The basic principle, parallel data acquisition, leading to the multiplex advantage, was applied already by Michelson in 1891 for optical spectroscopy (12) and explicitly formulated by Fellgett in 1951 (13). The application of radio frequency (RF) pulse excitation was suggested by Weston A. Anderson to Richard r. Ernst for a detailed experimental study in 1964 (14-16). It was known for a long time that the frequency response function (spectrum) of a linear system is the Fourier transform of the impulse response (free induction decay). This was already implicitly evident in the work of Jean Baptiste Joseph Fourier who investigated as early as 1822 heat conduction in solid bodies (17). In 1957, Lowe and Norberg proved that this relation was also valid for spin systems, despite their strongly nonlinear response characteristics (18). The first applications of random noise excitation in NMR were proposed independently by Russel H.Varian (19) and by Hans Primas

(20), for broadband testing and for broadband decoupling, respectively. The first successful experiments using random noise irradiation led to heteronuclear “noise decoupling” (21), a method that proved to be essential for the practical success of carbon-l 3 resonance in chemical applications.

In 1971, **Reinhold Raiser** (22) and **Richard r. Ernst** (23) independently demonstrated stochastic resonance as a means to improve the signal-to-noise ratio of NMR by broadband irradiation. A third approach, rapid scan spectroscopy, initially proposed by Dadok and Sprecher (24), achieved a virtually simultaneous excitation of all spins by a rapid frequency sweep through the spectrum (25, 26). Finally, by computer synthesis, it was possible to compute an excitation function with a virtually arbitrary excitation profile. This was originally utilized for decoupling purposes by Tomlinson and Hill (27). Among the broadband excitation techniques, pulse excitation is the only one that allows for a rigorous analytical treatment, irrespective of the complexity of the spin system. Pulsed NMR experiments were suggested already by Felix Bloch in his famous 1946 paper (9), and the first time-domain magnetic resonance experiments were performed in 1949 by H.C. Torrey (28) and, in particular, by **Erwin L. Hahn** (29) **who may be regarded as the true father of pulse spectroscopy**. He invented the spin echo experiment and devised extremely important and conceptually beautiful solid state experiments (30, 31). Pulse Fourier transform spectroscopy not only revolutionized high resolution liquid state NMR spectroscopy, but also unified NMR methodology across all fields. It provided also the basis for the development of multidimensional NMR spectroscopy.

A new approach to measure two-dimensional (2D) spectra was proposed by Jean Jeener at an Ampere Summer School in Basko Polje, Yugoslavia, 1971 (32). This two-pulse experiment by Jean Jeener is the forerunner of a whole class of 2D experiments (33) that can also be expanded to multidimensional spectroscopy. The credit for development of the basic procedure for recording a 2D or 3D NMR image of an object goes to Paul Lauterbur (34).

In 1971, **Raymond Damadian** observed that some malignant tissue, obtained from implanted tumors removed from rats, had longer NMR relaxation times than many normal tissues (5).

Commencing from 1972, Sir Peter Mansfield worked on Multi-pulse line narrowing experiments (35) and Image formation in NMR, by a selective irradiation process (36). One of the major practical difficulties encountered with MRI, at that time was the time taken to acquire the data. The breakthrough came in 1977 with the introduction of echo-planar imaging (EPI) (37). This snap-shot technique meant that in principle, complete two-dimensional images could be obtained in extremely short times. However, to reach these acquisition times, yet another step was necessary. This was the introduction of active magnetic screening (38, 39). An important area of application of EPI has been foetal imaging during the third trimester. This lead to multiple uses of EPI namely Whole Body Echo-Planar MR Imaging, Ultra-fast magnetic resonance scanning of the liver with echo-planar imaging, Transectional echo planar imaging of the heart in cyanotic congenital heart disease and Echo-Volumar Imaging(40-43).

Nuclear magnetic resonance (NMR) spectroscopy is unique among the methods available for three-dimensional structure determination of proteins and nucleic acids at atomic resolution, as the NMR data can be recorded in vivo. Before 1967, important qualitative NMR features of amino acids and proteins had already been noted and tentatively rationalized (44-48). It had been well documented, that the spectrum of a globular protein is more complex than the sum of the NMR lines, from the constituent amino acid residues in the polypeptide chain. From 1970 onwards Kurt Wüthrich had worked on NMR spectroscopy to determine protein and nucleic acid structure and its use in structural biology and biological research (49-51).

Magnetic resonance spectroscopy of intact biological tissues was first reported by Moon and Richards(52) using P-31 MRS to examine intact red blood cells in 1973, and Hoult et al. (53) using P-31 MRS to examine excised leg muscle from the rat in 1974. Since then MRS has been applied to almost every organ of the body including brain, heart, liver, kidney, prostate, and extremities.

Protons (1H) have traditionally been used for MR spectroscopy because of their high natural abundance in organic structures and high nuclear magnetic sensitivity compared with any other magnetic nuclei (54).Moreover, diagnostically resolvable hydrogen MR spectra may be obtained with clinical instruments (1.5 T or greater) and routine surface coils. Phosphorus 31 MR spectroscopy has also been used clinically to study changes in high energy metabolism in a number of pathologic processes (2).

3.2. Basic physics of MRI and MRS.

Before going into the physics and fundamentals of MRS a quick look into the basic MR physics and sequences is essential. MRI is a complex and most preferred modality for the definitive evaluation and follow-up of most brain tumours. The technical aspects of MRI are beyond the scope of this review. Very briefly, the patient is placed in a strong magnetic field which causes the protons in the water molecules of the body to align parallel or antiparallel with the field. Then a radiofrequency (RF) pulse is introduced which excites these spinning protons and causes them to move out of alignment with the magnetic field. When the RF excitation stops, the protons return to their resting state within the main magnetic field, giving off the RF energy acquired during the application of RF pulse. This released RF energy signal is spatially localized by the rapid turning on and off of spatially varying magnetic field gradients. This RF signal is detected by radio antennae (coils) within the scanner and used to generate the image. Each proton's behaviour reflects the chemical microenvironment of that proton. The differences in the behaviour of the protons result in differences in the MR appearances of each tissue (55, 56). The amount of signal, a tissue produces, is dependent on the number of mobile hydrogen protons, the speed with which the tissue is moving, the tissue's T1 relaxation time (the time needed for the protons within the tissue to return to their original state of magnetization) and the tissue's T2 relaxation time (the time required for the protons perturbed into coherent oscillation by the radiofrequency pulse to lose this coherence) (54, 56).

The standard MRI pulse sequence for eliciting anatomic and pathologic detail is a spin echo sequence. T1-weighted images (short TR; short TE) provide better anatomic detail, while T2 weighted images (long TR; long TE), which are more sensitive to water content, are more sensitive to pathology. The intermediate or proton density images (long TR; short TE) provide improved contrast between lesions and cerebrospinal fluid. Fluid-attenuated inversion recovery (FLAIR) is another pulse sequence that is useful in detecting low contrast lesions. With FLAIR (long T1, long TR, and variable TE), the CSF signal is nulled, enabling pathology adjacent to the CSF to be seen more clearly. There is also less gray to white matter contrast, providing a bland background against which lesions are readily seen (57). The administration of contrast agents during T1- weighted MR scans, greatly increases the sensitivity to differentiate abnormal from adjacent normal signals. (57).

MRI is evolving rapidly. Echo planar MRI, Diffusion-weighted MR imaging, perfusion-weighted MR imaging and MRS are applications which could sometimes obviate the necessity for an invasive diagnostic procedures. These MRI techniques could also serve to guide stereotactic brain biopsies to the most representative areas, with potentially the highest grade of tumour and also to suggest the best sampling area to differentiate recurrent tumour from radiation necrosis .

3.2.1. Magnetic resonance spectroscopy (MRS)

Magnetic Resonance Spectroscopy (MRS) is a non-invasive method of analyzing tissue metabolism in vivo and provides information on the

composition and spatial distribution of cellular metabolites (58, 59). Most MRS studies are done with proton (1-H) or phosphorus-31. The tissue's chemical environment determines the frequency of a metabolite peak in an MRS spectrum.

Protons that can be used for MRS include: ^{1}H, ^{31}P, ^{13}C, ^{23}Na, ^{7}Li, ^{19}F, ^{14}N, ^{15}N, ^{17}O, ^{39}K The most commonly studied nuclei are ^{1}H and ^{31}P. This study uses Proton (^{1}H).

Because we divide the signal from each voxel into a smaller number of components (chemically distinct species) the SNR of spectra is lower than that of MR images: to obtain an acceptable level of SNR in reasonable imaging times, much larger voxels are required for MRS than MRI—typically MRS uses voxel sizes of 1 to 8 cm^3, whereas voxels for imaging are 1 to 5 mm^3.

The Larmor equation describes the resonant precession frequency of a nuclear magnetic moment in an applied static magnetic field.

$$\mathbf{w} = \mathbf{g} B_o$$

w = precessional frequency

g = gyromagnetic ratio (MHz/Tesla)

[42.58 MHz/Tesla for hydrogen nuclei]

B_o = magnetic field (Tesla)

If all the proton nuclei in a mixture of molecules had the same Larmor frequency, the MR spectra would be limited to a single peak. However, the

magnetic B_0 field "seen" by a nucleus is shielded by the covalent electron structure surrounding the nucleus. Electrons are negatively charged and have spin properties. Thus, when placed in an externally applied magnetic field, electrons will precess and induce a small magnetic field around the nuclei.

These local magnetic fields generated by the surrounding electrons can add or subtract from the applied magnetic field B_0. Consequently, the nuclei experience slightly different magnetic fields based on chemical structures. Due to this small change in the local magnetic field, nuclei will resonate at slightly shifted Larmor frequencies.

Nuclei with different chemical neighbours will have slightly different resonance frequencies given by J coupling, also known as scalar coupling or spin-spin splitting. This refers to the interaction of two nuclear spins on the same molecule by means of distortions in their electron clouds. J coupling interactions are responsible for the **Chemical shifts** in **ppm** and are **independent** of the strength of the applied field B_0 and therefore, the instrument frequency **Chemical shifts** are measured in **Hz** are field and frequency **dependent.**

In the frequency domain, the area under a specific peak is proportional to the number of protons precessing at that frequency. A parts per million (ppm) scale is used. Water is scanned at the center frequency, that position is then assigned 4.7 ppm.

Local magnetic field inhomogeneities widen and distort the spectral lines. Improved magnetic field homogeneity increases SNR and narrows

peak widths-thus improving both sensitivity and spectral resolution. Maximum homogeneity is accomplished by adjusting DC currents in the gradient coils and room temperature shim coils—a process known as **shimming**. The importance of suppressing the water signal lies in the fact that the metabolites of interest have a signal one hundred times smaller than that of the water peak, and without water suppression they would be poorly resolved.

3.2.2. Proton Spectroscopy – Technical considerations

Single -voxel (SV MRS) versus Multi-voxel MRS (MV-MRS) techniques (58)

Single Voxel Proton MRS : At present two Single Voxel proton localization techniques are employed in clinical MRS Studies (59).

STEAM – **St**imulated **E**cho **A**cquisition **m**ode

PRESS – **P**oint **R**esolved **S**pectro**S**copy

3.2.2.1a. SV MRS with PRESS

Water-suppression

The 90° pulse excites a slice. The first 180° pulse refocuses the transverse magnetization in a row of tissue within the slice. The second 180° pulse refocuses the magnetization within a column of the row, leaving a single voxel. Then, the signal represents a combination of spins in that voxel precessing at slightly different frequencies (function of time). Fourier

transform of signal represents number of spins at a given frequency in a voxel (function of frequency) (60).

The effect of echo time in SE single voxel spectroscopy (SVS).

Left: TE=30ms; Right: TE=144 ms. TE controls the T_2 "contrast" of the spectral peaks in the same way tissue T_2 contrast is controlled in MR imaging. As shown, Glx (glutamine) and myo-inositol (mI) have short T_2 values and are not visible on long TE spectra.

3.2.2.1b. SV-MRS with STEAM (60)

Water-suppression: The 90° pulse excites a slice. A second 90° pulse refocuses the transverse magnetization in a row of tissue within the slice. A third 90° pulse refocuses the magnetization within a column of the row, leaving a single voxel.

Negative to STEAM: rephasing only about 50% of the original generated transverse magnetization (low SNR).

Advantages of STEAM (60)

STEAMS enables observation of proton metabolites that have short T2 relaxation process, such as Myo-inositol (mI), glutamate(Glu), Glutamine (Gln) , because echo times(TEs) less than 20 millisecond can be used ; with PRESS these proton metabolites cannot be observed. STEAM also affords more effective suppression of water resonance signals because water suppression chemical shift- selective (CHESS) pulse applied. This can be

placed not only at the preparation phase of the volume localization pulse sequence but also within the localization sequence (at the TM phase of the STEAM sequence) without penalty to the TE being used. This is a major advantage, especially when short TEs (<20msec) are used. At short TEs, the signal intensity of the water resonance can be several folds greater than at higher TEs. Thus higher or more water suppression pulses must be used to attenuate the water signal.

In PRESS, the water suppression CHESS pulses can be placed only at the beginning of the localization pulse sequence.

Disadvantage of STEAM (60)

There are two major disadvantage of STEAM

a) There is a theoretical factor of 2 losses in signal intensity.

b) STEAM is much more susceptible to motion, multiple quantum effects (i.e. homonuclear coupling) and diffusion processes, which in lead to difficulties in phasing and baseline correction in the spectrum.

The twofold signal loss in signal intensity in the STEAM sequence is due to the imperfect refocusing of the spin magnetization when the second 90 degree pulse is applied, which rotates only half the spin of interest into the longitudinal axis; this part of magnetization eventually generates the stimulated echo. The other half of the spin magnetization that remains in the transverse axis is dephased by the TM spoiling gradient and does not lead to any rephased magnetization, at the time of acquisition.

Advantage of PRESS

The major advantage of the PRESS sequence is the theoretical twofold gain in signal intensity compared to the STEAM sequence. PRESS is also much less sensitive to patient motion, homonuclear coupling effects, and eddy current effects (60).

3.2.2.2.Multivoxel MRS (MV-MRS) (58)

MV-MRS is normally called either Chemical Shift Imaging (CSI) or spectroscopy Imaging ((SI) because the signal intensity peak resonance areas, or ratios of peak areas or signal intensities of the metabolites can be converted to an image format and overlaid onto anatomic MR Images, thus showing a qualitative or quantitative distribution of metabolites within the brain area examined . Utilizing the CSI or SI multi-voxel technique, one can obtain spectroscopic information from multiple adjacent volumes over a large region of interest in a single measurement. Volume elements as small as 1 mL can be examined at a reasonable acquisition times, namely 6 to 12 minutes.

Phase encoding gradients can be utilized, as in imaging, in order to encode spatial information. Selective 90° RF pulse and slice-select gradient generates a transverse magnetization within the slice. Orthogonal magnetic field gradients of short duration serve to phase encode the data in 2D. Data are sampled at multiple times. 3D Fourier inverse transformation gives frequency information over the 2D slice. Spectra will then be generated for all voxels within the box.

Either PRESS or STEAM pulse sequence is used for volume selective pulse sequence for CSI/SI Multivoxel technique, which defines a large slice. Spatial localization is achieved by phase encoding in one dimension (1D CSI/SI,) two dimensions (2D CSI/SI), or three dimensions (3D CSI/SI).

The 1D CSI/SI generates a column of n volume elements within the defined slice (n= number of phase-encoding steps in a defined phase encoding direction).

The 2D CSI/SI generates $n_1 \times n_2$ adjacent volume elements within a defined slice plane.

The 3D CSI/SI generates multiple defined adjacent slice planes with $n_1 \times n_2 \times n_3$ spectroscopy volume elements or voxels.

3.3. What is the difference between MRS and MRI?

MRI and MRS are basically not different; both techniques are governed by same the physical principle of Magnetism. They differ only in the manner in which the data are processed and presented (58).

In MRI the data is collected and analyzed in time domain signal, to obtain information about the nuclear relaxation time (T1 and T2) and this is processed to generate an anatomic image. In MRS, the time domain information is converted to a frequency domain via Fourier transformation of the FID time domain signal (58).

Differences between MRI and MRS

Table No: 3-1

	MRI	MRS
Molecule	Water	Biochemicals
Nucleus	^{1}H	^{1}H, ^{31}P, ^{13}C
Chemical shift	Unavoidable nuisance	Exploits CS (PPM)
Voxel dimension	1mm x 1mm x 1mm	10mm x 10mm x 10mm
Scan time	< 1 sec. to a few minutes	5 to 15 minutes
Spatial coverage	volume	Single voxel or a slice
Field homogeneity	A few PPM	< 1 PPM
Information	Mostly qualitative	Mostly quantitative

3.3.1. SELECTION OF TE:

The change in echo time (TE) influences the information obtained and the appearance of the spectra (61). The choice of TE is decided depending upon the lesion. The various TE used are TE-35, 135 and 270. The presence of lactate in TE-35 is confirmed by inverted doublet at TE-144.

Carles Majos et al (62) attempted to classify brain tumours by studying the influence of TE in 151 cases by comparing the spectra obtained at two different TE (30ms and 136ms).They reported that tumour classification was slightly better with short TE(81%) than at long TE (78%). Meningioma was the only group in which long TE enabled better classification.

3.4. IMPORTANT BRAIN METABOLITES (63):

NAA (N-acetylaspartate)

The presence of NAA is attributable to its *N*-acetyl methyl group, which resonates at 2.0 ppm .This peak also contains contributions from the less-important *N*-acetyl groups. NAAis accepted as a neuronal marker, and as such, its concentration will decrease with any insults to the brain (64). The exact role of NAA in the brain is not known. Glutamate and *N*-acetylaspartyl-glutamate are colocalized with NAA in neurons. Breakdown of *N*-acetyl-aspartyl-glutamate releases both NAA and glutamate, and subsequent breakdown of NAA leads to aspartate. These compounds are excitatory amino acids and are increased following ischemic events. It is possible that, in the near future, concentrations of *N*-acetyl-aspartyl-glutamate and glutamate may serve to monitor treatments designed to protect brain tissues by blocking excitatory amino acids. NAA is not present in tumours outside the central nervous system. Canavan disease is the only disease in which NAA is increased. In normal spectra, NAA is the largest peak.

Cho (choline/phosphocholine/glycerophosphorylcholine)

The peak for Cho occurs at 3.2 ppm . It contains contributions from glycerophosphocholine, phosphocholine, and phosphatidylcholine and therefore reflects total brain choline stores. Cho is a constituent of the phospholipid metabolism of cell membranes and reflects membrane turnover, and it is a precursor for acetylcholine and phosphatidylcholine (64*).*The latter

compound is used to build cell membranes, whereas the former is a critical neurotransmitter involved in memory, cognition, and mood. Therefore, increased Cho probably reflects increased membrane synthesis and/or an increased number of cells.

Cr (creatine/phosphocreatine)

The peak for Cr is seen at 3.03 ppm and contains contributions from Cr, Cr phosphate, and to a lesser degree, g-aminobutyric acid, lysine, and glutathione. An additional peak for Cr may be visible at 3.94 ppm. Therefore, the Cr peak is sometimes referred to as "total Cr." Cr probably plays a role in maintaining energy-dependent systems in brain cells by serving as a reserve for high energy phosphates and as a buffer in adenosine triphosphate and adenosine diphosphate reservoirs (65). Cr is increased in hypometabolic states and decreased in hypermetabolic states. In normal spectra, Cr is located to the immediate right of Cho and is the third-highest peak. Because this peak remains fairly stable even in face of disease, it may be used as a control value.

Lac (Lactate)

The lactate peak has a particular configuration. It consists of two distinct, resonant peaks called a "doublet" and is caused by the magnetic field interactions between adjacent protons (J coupling). This lactate doublet occurs at 1.32 ppm. A second peak for lactate occurs at 4.1 ppm. Because this latter peak is very close to the water, it is generally suppressed.

NeuroRx. 2005 April; 2(2): 197–214

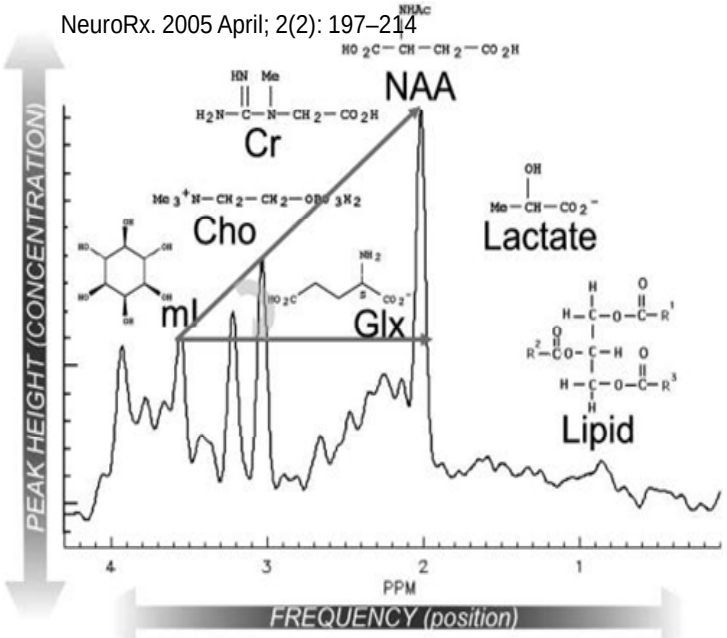

A. Fig. 1a: Magnetic Resonance Spectroscopy (MRS): single voxel proton MRS using point resolved spectroscopy for water and lipid suppression (TE:144)
The "X" axis represents frequency position of the proton containing metabolites displayed as peaks related to chemical shift from zero point displayed in units of parts per million
"Y" axis peak height representing metabolites concentration
Normal spectral pattern : ml , Cho, Cr, Glx, NAA and lip from right to left

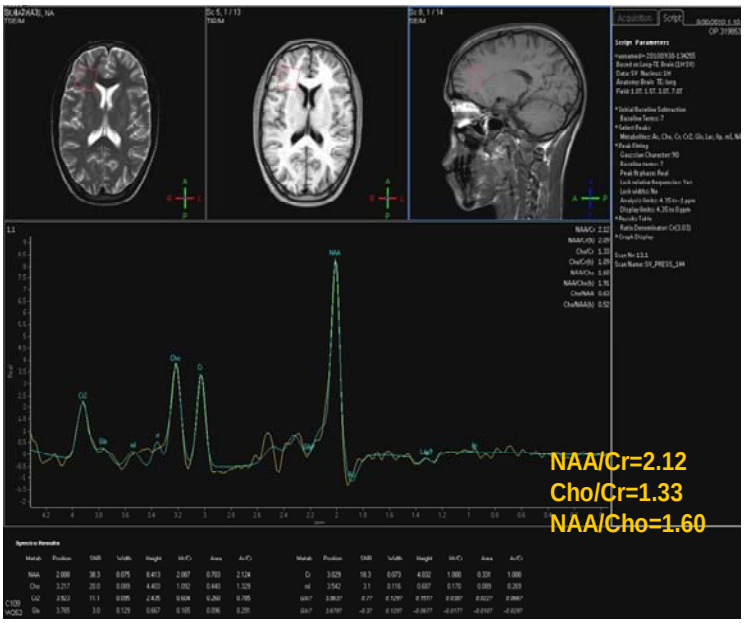

Fig. 1. B. Control MRS: single voxel MRS in frontal lobe showing normal spectral pattern with metabolites ratios

:

Normally, lactate levels in the brain are low. The presence of lactate generally indicates that the normal cellular oxidative respiration mechanism is no longer in effect, and that carbohydrate catabolism is taking place (66). Lactate can play a role as a neuromodulator by altering the excitability of local neurons . Confirmation that a peak at 1.32 ppm corresponds to lactate may be done by altering the TE. At a TE of 272 milliseconds, lactate projects above the baseline, whereas at a TE of 136 milliseconds,the lactate doublet is inverted below the baseline.

mI (Myoinositol)

Myoinositol is a metabolite involved in hormone-sensitive neuroreception and is a possible precursor of glucuronic acid, which detoxifies xenobiotics by conjugation (67). The myoinositol peak occurs at 3.56 ppm. Decreased myoinositol content in the brain has been associated with the protective action of lithium in mania and the development of diabetic neuropathy (68). In addition, a triphosphorylated derivative of myoinositol, myoinositol- 1,4,5-triphosphate, is believed to act as a second messenger of intracellular calcium-mobilizing hormones (68). The combination of elevated myoinositol and decreased NAA may be seen in patients with Alzheimer disease (69). The myoinositol peak is significant in tissues outside the central nervous system, for example, in head and neck carcinomas.

Glutamate and Glutamine

Glutamate is an excitatory neurotransmitter,which plays a role in mitochondrial metabolism

(67).Gamma-amino butyric acid is an important product of glutamate. Glutamine plays a role in detoxification and regulation of neurotransmitter activities (70).These two metabolites resonate closely together and they are commonly represented by their sum as peaks located between 2.1 and 2.5 ppm.

Alanine

Alanine is a nonessential amino acid whose function is uncertain. Its peak occurs between 1.3 and 1.4 ppm and therefore may be overshadowed by the presence of lactate. Alanine, like lactate, inverts when the TE is changed from 136 to 272 milliseconds.

Lipids

Membrane lipids in the brain have very short relaxation times and are normally not observed unless very short TEs are used. The protons of lipids produce peaks at 0.8, 1.2,1.5, and 6.0 ppm. These peaks comprise methyl, methylene, allelic, and the vinyl protons of unsaturated fatty acids (71). These metabolites may be increased in high-grade astrocytomas and meningiomas and may reflect necrotic processes (70). However, it is also important to remember that normal lipid resonances arising from fat may be the result of voxel contamination by fat located in the subcutaneous scalp; they are normally much less intense or absent at a TE of 272 milliseconds because of their short relaxation times.

3.5. Diagnostic Performance: MR Imaging & 1H-MR Spectroscopy versus MR Imaging Alone

Moller-Hartmann et al (72) reported on 176 consecutive patients. The final diagnosis in most patients was established by histology within 10 days of single-voxel 1H-MR spectroscopy. One pair of radiologists interpreted only the MR images; a second pair examined the MR imaging and MR spectra based on a qualitative interpretation of the metabolite peaks. All radiologists were unaware of the final diagnosis. The type and grade of lesion were correctly identified in 97 of 176 (55%) cases based on MR imaging alone. The remaining diagnoses were incorrect (15%) or indeterminate (30%). The addition of 1H-MR spectroscopy information statistically significantly increased the proportion of correctly diagnosed cases to 71% (124/176) ($P <$ .01). There were no cases where a correct diagnosis on MR imaging was mistakenly discarded due to the 1H-MR spectroscopy findings.

A second, smaller, study by **Ando et al** (73) compared contrastenhanced MR imaging (CE-MR imaging) to CE-MR imaging and 1H-MR spectroscopy in 20 patients with suspected residual or recurrent tumour after therapy. The method of final diagnosis was inconsistent between patients, relying on either pathologic or clinical findings. Fourteen patients had a final diagnosis of residual or recurrent tumour, and 6 had treatment-related changes. The authors retrospectively selected a Cho/Cr ratio of greater than 1.5 to be indicative of tumour. Based on this threshold, the addition of 1H-MR spectroscopy information to CE-MR imaging findings marginally increased sensitivity from 12 of 14 (86%) to 14 of 14 (100%) (P=0.79) without altering specificity (4 of 6; 67%).

3.6. NEOPLASTIC VERSUS NON-NEOPLASTIC LESIONS.

Nail Bulakbasi, et al (74) evaluated forty-nine patients with histologically proved brain tumours to assess the diagnostic effectiveness of MR spectroscopy and apparent diffusion coefficient (ADC). MR spectroscopy could differentiate benign from malignant tumors but was not useful in grading malignant tumors. The most significant parameter used to differentiate benign tumors from the control group was the alanine /Cr ratio (P <.001), and it mainly distinguished the meningiomas from other tumours. NAA/Cho and NAA/Cho + Cr ratios were also useful to differentiate the benign tumors from the control group (P < .05). The NAA/Cho, NAA/Cr, NAA/Cho + Cr, lactate/Cr, and lactate/lipid ratios (P< .001) were significantly effective in the differentiation of malignant tumours from the control group, followed by Cho/Cr and lipid/Cr ratios (P < .05). In the differentiation of malignant tumours from benign ones, the NAA/Cho, NAA/Cho +Cr, lactate/Cr, and alanine/Cr ratios (P < .001) were statistically more significant than the NAA/Cr and lactate/lipid ratios (P < .05). No significant difference was noted between the Cho/Cr and lipid/Cr ratios in the differentiation of benign versus malignant tumours. Except for the lipid/Cr ratio (P < .05), none of the spectroscopic parameters were useful in grading the malignant tumours.

In the differentiation of malignant from benign tumours, NAA / (Cho), NAA/Cho + (Cr), lactate/Cr, and Alanine/Cr ratios (P < .001) were statistically more significant than NAA/Cr and lactate/lipid ratios (P < .05).

Increase in lipid/Cr and alanine/Cr ratios could distinguish metastasis and meningiomas from other tumours, respectively ($P < .001$).

S. D. Rand, R. Prost et al (75) evaluated the accuracy of single-voxel, image-guided proton MR spectroscopy in distinguishing normal from abnormal brain tissue and neoplastic from nonneoplastic brain disease in fifty-five lesions in 53 patients. Spectra were interpreted qualitatively by visual inspection by nonblinded readers (prospectively) with the benefit of prior clinical data and imaging studies, and by blinded readers (retrospectively). The nonblinded readers interpreted the spectra as diagnostic or not, and, if diagnostic, as neoplastic or nonneoplastic. The blinded readers classified the spectra as diagnostic or not, and, if diagnostic, as normal or abnormal and as neoplastic or nonneoplastic (when abnormal). The diagnostic accuracy averaged across four blinded readers in differentiating patients from control subjects was0.96, while the area under the aggregate (pooled interpretations) ROC curve approached unity. Accuracy in the nonblinded and blinded discrimination of neoplastic from nonneoplastic disease was 0.96 and 0.83, respectively. The area under the aggregate ROC curve in the blinded discrimination of neoplasm from nonneoplasm was 0.89.

Carles Majo´s, Margarida Julia`-Sape et al (62) classified the brain Tumor by Proton MR Spectroscopy based on comparison of diagnostic accuracy using short and long TE techniques . One hundred fifty-one studies of patients with brain tumors (37 meningiomas, 12 low grade astrocytomas, 16 anaplastic astrocytomas, 54 glioblastomas, and 32 metastases) were retrospectively selected from a series of 378 consecutive examinations of

brain masses. Single voxel proton MR spectroscopy at TE 30 ms and 136 ms was performed with point-resolved spectroscopy in all cases. Tumor classification was slightly better at short TE (123 [81%] of 151 cases correctly classified) than at long TE (118 [78%] of 151 cases correctly classified). Meningioma was the only group that showed higher sensitivity and specificity at long TE. Improved results were obtained when both TE were considered simultaneously: the suggested diagnosis was correct in 105 (94%) of 112 cases when both TE agreed, whereas the correct diagnosis was suggested by at least one TE in 136 (90%) of 151 cases. The author found that short TE provided slightly better tumour classification, and results improved when both TE are considered simultaneously. Meningioma was the only tumour group in which long TE performed better than short TE.

Carles Majo´s, MD, Juli Alons et al (76) evaluated the utility of ^{1}HMRS in the clinical categorization of primitive neuroectodermal tumors (PNETs) in adults. In vivo proton MR spectroscopy was performed with an echo time of 136 msec in nine adults with PNET, and findings were retrospectively compared with spectroscopic findings of 22 meningiomas, 12 low-grade astrocytomas, eight anaplastic astrocytomas, 23 glioblastomas, and 21 metastases. Nine resonances were semiquantitatively evaluated. The resonances of choice for identifying PNET were alanine ($P < .001$) and glutamate and glutamine ($P = .004$), both decreased with respect to meningioma; choline increased with respect to low-grade ($P < .001$) and anaplastic astrocytoma ($P = .055$); and lipids at 1.30 ppm decreased and choline and other trimethyl-amine-containing compounds increased with

respect to glioblastoma ($P < .001$ and $P = .004$, respectively) and metastasis ($P < .001$ and $P = .021$, respectively). Further,they developed an algorithm for bilateral differential diagnosis between PNET and other tumor types. The leave-one-out method was used to test the five possible differential situations in the retrospective data set, with the following results: PNET versus meningioma, 31/23/5/3 (number of total/correct/unclassifiable/incorrect procedures); PNET versus low-grade astrocytoma, 21/19/2/0; PNET versus anaplastic astrocytoma, 17/6/9/2; PNET versus glioblastoma, 32/28/2/2; and PNET versus metastasis, 30/27/1/2. In total, 131 consecutive procedures produced 103 (79%) correct classifications and nine (7%) misclassifications. Twenty-five (78%) of 32 possible procedures in the prospective independent test set produced correct classifications and four (13%) produced incorrect classifications.

Witold Gajewicz et al (77) evaluated the use of ^{1}HMRS in the differential diagnosis of neoplastic brain tumors and tumor-like processes. 29 patients with ambiguous CT images of brain mass lesions were examined by MRI. 1H MRS was applied in this group as the primary option to improve differential diagnosis. In all tumors, the analyzed ratios NAA/Cr, Cho/Cr and Cho/NAA proved to be significantly different from the control group, in both parietal white matter and occipital grey matter, and at both of the echo times used ($p < 0.05$). Additionally, there was a weakly significant difference in the mI/Cre ratio between the group of glioblastomas and the controls ($p=0.05$). NAA/Cr, Cho/Cr and Cho/NAA – proved to be significantly different from the control group, in both parietal white matter and occipital grey matter and

at both of the echo times used ($p < 0.05$). In the tumour-like lesions , the NAA/Cr ratios appeared not to differ significantly from the occipital grey matter controls at both TEs, but there was a statistically significant difference in this ratio from the parietal white matter controls at both TEs.

W. Hollingworth et al (78) conducted "A Systematic Literature Review of Magnetic Resonance Spectroscopy for the Characterization of Brain Tumors". Of the 22 studies that measured diagnostic performance, the largest head-to-head comparison of MR imaging alone versus MR imaging and 1H-MR spectroscopy provided encouraging findings that 1H-MR spectroscopy can make a significant contribution to diagnosis for patients with indeterminate brain lesions. A number of large diagnostic performance studies have demonstrated that 1H-MR spectroscopy can accurately distinguish between high-and low-grade astrocytomas. They presented guidelines to help focus future research in this area.

Isabella Maria Burtscher et al (79) studied 26 patients with intracranial tumours. MR spectroscopic findings were evaluated for the distribution pattern of pathologic spectra (NAA/Cho ratio <1) across the lesion and neighboring tissue, for signal ratios in different tumour types, and for their potential to improve preoperative diagnostic accuracy. Gliomas and lymphomas showed pathologic spectra outside the area of contrast enhancement while four nonastrocytic circumscribed tumours (meningioma, pineocytoma, metastasis, and germinoma) showed no pathologic spectra outside the region of enhancement. No significant correlation was found between different tumour types and signal ratios. They demonstrated that

distribution patterns of pathologic spectra NAA/Cho ratio across the lesion and neighbouring tissue could help in differentiating well circumscribed lesions from infiltrating lesions. However, diagnostic accuracy was not improved in terms of differentiating the types of infiltrative or circumscribed lesions.

The diagnostic value of MRS was evaluated by **Wilken, et al.,** (80) for differentiating focal brain lesions of unknown etiology in 17 pediatric patients from 1-14 years of age. MRS correctly identified 14 out of 17 abnormalities. Overall, the sensitivity and specificity of MRS for detection of neoplasm were 92% and 80%, respectively.

Fayed N et al (81) studied 35 consecutive patients with single brain tumors to determine whether histological grade of tumors may be predicted by means of conventional gadolinium-enhanced MRI and proton magnetic resonance spectroscopy. They found that gadolinium-enhancement measured with the CNR (CNR > 35.86) predicted malignancy at 82.6% sensitivity and 91.7% specificity (area under the curve, 0.88; 95% confidence interval [CI], 0.73-0.97). With regard to MRS a choline/creatine ratio higher than 1.56 predicted malignancy at 88.9% sensitivity and 91.7% specificity (area under the curve, 0.94; 95% CI, 0.78-0.99). When we combined the CNR value, the choline/creatine ratio, and the presence of lactates in a model of discriminant analysis the predictive power improved significantly with an area under the curve of 0.99% (95% CI, 0.87-1). However, the used techniques were unable to distinguish metastases from high-grade gliomas accurately.

Kostas N.Fountas et al (82) in their study "In-vivo Proton MR spectroscopy of Brain tumours" had stated that the NAA / Cr and Cho /Cr ratio help specify the presence or absence of neoplasm. They studied 71 patients with the radiographic diagnosis of astrocytoma to assess non-invasive histologic grading of solid astrocytomas using proton magnetic resonance spectroscopy. An increased concentration of Cho and decreased concentrations of Pcr-Cr and NAA were detected. The concentrations of Lac, Lip and MI varied inconsistently, even among tumors of the same histologic grade. The Cho/Pcr-Cr ratio was calculated. This ratio was found to be 2.15 +/- 0.26 in 27 patients with astrocytomas grade I and II, 2.78 +/- 0.09 in 18 patients with grade III, and 5.40 +/- 0.16 in 26 patients with grade IV. They concluded that, Cho/Pcr-Cr was a very important and statistically significant marker ($p = 0.043$) determining the degree of intracranial astrocytoma malignancy

Magalhaes A, Godfrey W et al (83) in their study, "Proton magnetic resonance spectroscopy of brain tumors correlated with pathology" had concluded that the mean Cho/Cr was 3.35 for nine patients with Grade 4 astrocytomas; 1.62 for three patients with Grade 3 astrocytoma; 1.50 for three patients with Grade 2 astrocytoma; and 1.49 for one patient with Grade 1 Astrocytoma. They concluded that MRS ratios can be used to differentiate malignant and non-malignant lesions from normal brain tissue and that high-grade astrocytomas have higher Cho/Cr ratios compared with low-grade astrocytomas.

Jennifer Butzen et al (84) evaluated a logistic regression (LR) pattern recognition model for the discrimination of neoplastic from nonneoplastic brain lesions with MR imaging–guided single-voxel proton MRS data**.** (86 neoplasms and 13 nonneoplastic lesions) The Logistic regression model output was the probability of tumor, for which a cutoff value was chosen to obtain comparable sensitivity and specificity. The LR sensitivity and specificity were compared with those of qualitative blinded interpretations from two readers (designated A and B), qualitative unblinded interpretations (in aggregate) from a group of five staff neuroradiologists and a spectroscopist, and a quantitative Cho/NAA amplitude ratio > 1 threshold for tumor. An LR cutoff probability for tumor of 0.8 yielded a specificity of 87%, a comparable sensitivity of 85%, and an area under the ROC curve of 0.96. Sensitivities, specificities, and ROC areas (where available) for the other methods were, on average, 82%, 74%, and 0.82, respectively, for readers A and B, 89% (sensitivity) and 92% (specificity) for the group of unblinded readers, and 79% (sensitivity), 77% (specificity), and 0.84 (Az) for the Cho/NAA . >1 criterion. McNemar's analysis yielded significant differences in sensitivity (n;86 neoplasms) between the LR and reader A, and between the LR and the Cho/NAA > 1 criterion. The differences in specificity between the LR and all other methods were not significant (n;13 nonneoplasms). Metz's analysis revealed a significant difference in Az between the LR and the Cho/NAA ratio criterion.

Veena Arpit Nagar et al (85) evaluated 20 patients with intracranial tumours and 15 patients with non neoplastic lesions. Spectra were analysed for peak heights of Cho), Cr, NAA, Lac and Lip. Normalised Cho (nCho) ratios, computed by dividing maximum Cho in the lesion by the normal-appearing brain, were compared between intracranial tumours and non-neoplastic disease. Meningiomas displayed homogeneously elevated Cho. Malignant tumours, especially large glioblastoma multiforme, displayed inhomogeneity of metabolites within the tumour. All tumours had elevation of nCho >1 (mean 1.91 +/- 0.65), and non-neoplastic diseases had tumour nCho <1 (mean 0.91 +/- 0.46), which was significantly lower (P <0.05). Two patients with non-neoplastic lesions, one with subacute cerebral infarction and the other with cryptococcoma, had elevated Cho compared to normal tissue (false positive rate 13%). It was concluded that using semi-automated MRSI method, a simplified normalized Cho algorithm provides a method to distinguish intracranial tumours from non-neoplastic disease.

Kumar.A. et al (86) Evaluated 60 patients and 25 healthy volunteers by 1H-MRS to evaluate the utility of 1H-MRS in adult brain tumours and their differentiation from similar-appearing space-occupying lesions. The Cho/Cr ratio was significantly raised in low and high-grade glioma and meningioma patients (1.85 +/- 0.36, 3.50 +/- 1.00 and 6.65 +/- 2.83 respectively), as compared with the control group (1.16 +/- 0.18); and NAA/Cr and NAA/Cho ratios were found to be lower than normal values in their study (P<0.01). However, in the non-neoplastic lesions, the Cho/Cr

ratios were not statistically significant. The tubercular lesions revealed an average Cho/Cr ratio of 1.24 +/- 0.18, while it was 1.14 +/- 0.07 for infarcts

Kimura et al. (87) evaluated the proton MR spectra obtained from the lesions in 45 patients, to differentiate ring-like enhanced lesions on Gd-enhanced MR brain images. The rate of misdiagnosis was found to be lowest at the threshold level of 2.48 for the Cho/Cr obtained from the whole lesions, which included the enhanced rim and the non-enhanced inner region. That is, the positively predictive values of a Cho/Cr greater than 2.48 for diagnosing metastasis or glioblastoma was 88.9 and 60.0%, respectively, and the positively predictive value of a Cho/Cr less than 2.48 for diagnosing radiation necrosis or cerebral infarction was 71.4 and 100%, respectively. For further differentiating between metastasis and glioblastoma, information about the presence and absence of an NAA peak and lipid- or lactate-dominant peak was found to be useful. In 73.7% of metastasis cases a lipid-dominant peak was observed in the whole lesion without an NAA peak in the inner region, whereas the same pattern was observed in only 10% of the glioblastoma cases. They found that the point of maximum discrimination between brain tumors and non-neoplastic lesions was a Choline/Creatine ratio of 2.48.

Lin et al. (88) evaluated 15 patients with MRS. MRS was useful to aid in differentiating between tumour and other pathologies, including infarction and demyelinating plaque (n=6), radiation necrosis (n=5), and edema (n=5). Subsequent clinical management was based on MRS interpretation, and patients were then followed to determine if MRS interpretation correlated with clinical outcome or surgical findings. Mean follow-up was 12.5 months.

MRS accurately predicted the pathological nature and clinical outcome of lesion in 15 out of 16 (96%) situations. They found that MRS was 88% sensitive and 100% specific for detecting neoplasm.

Carles Majo's et al, (89) retrospectively evaluated 84 solid brain lesions (68 glial tumors and 16 pseudotumoral lesions) using Single-voxel spectra at TE 30 ms (short TE) and 136 ms (long TE) to assess the potential usefulness and the added value of single-voxel proton MR spectroscopy in Differentiating between tumors and pseudotumoral lesions. Differences between tumors and pseudotumors were found in myo-inositol ; $P < .01$) at short TE, and (NAA; $P < .001$), glutamine (Glx; $P < .01$), and choline (CHO; $P < .05$) at long TE. Classifiers suggested tumor when mIns/NAA ratio was more than 0.9 at short TE and also when CHO/NAA ratio was more than 1.9 at long TE. Classifier accuracy was tested in the test-set with the following results: short TE, 82% (23/28); long TE, 79% (22/28).

Chris Dowling et al (90) conducted a study on 29 patients with intracranial lesions prior to surgery and correlated the MRS findings with histopathological diagnosis. It was observed that when there was an increase in Choline and decrease in NAA resonances, histologic findings was positive for tumor. When Choline and NAA resonances were below the normal range, histologic findings were variable, ranging from radiation necrosis, astrogliosis, to mixed tissues that contained some low-, intermediate-, and high-grade tumor.

Adamson, et al. (91), conducted a study to determine the influence of MRS findings on the treatment of 78 patients suspected of having brain tumours. MRS had a potential positive influence on treatment in eight (16%) patients with positive findings and in 15 (52%) patients with negative findings, in two (3%) patients, MRS had a potential negative influence. The authors concluded that MRS may play a beneficial role in managing suspected brain tumours.

Mishra AM, Gupta RK et al, (92) and **Gajewicz et al, (**77) in their studies measured the use of 1H-MR spectroscopy for distinguishing tumour from non-neoplastic lesions. Gajewicz et al included only 2 non-neoplastic lesions and was of limited value. *Mishra, et al* (92) differentiated 52 histopathologically proved tumour cysts, abscesses, or benign cysts by using single voxel 1H-MR spectroscopy and diffusion-weighted MR imaging. The authors reported the sensitivity and specificity of 1H-MR spectroscopy to be 96% (95% CI, 83%–99%) and 100% (95% CI, 86%– 100%) respectively. This compares favorably with diffusionweighted imaging where specificity remained high (100%), but sensitivity was diminished (72%).

3.7. High- versus Low-Grade Astrocytoma

The MR-spectroscopy characteristics of astrocytoma include a significant reduction in NAA, a moderate reduction in Creatine, and an elevation of Choline. MR spectroscopy may allow characterization of metabolic changes associated with tumor growth, degree of malignancy, grading of tumors, response to treatment, and the sequelae of treatment.

(83,90,93). NAA levels are low in all astrocytomas but are lowest in grade-IV tumours. (94, 83) Conversely, Choline is always elevated in solid astrocytomas, but is more so in those of higher grades. The presence of lactate generally reflects necrosis and, therefore, a higher degree of malignancy.

Herminghaus, et al., (94) performed $^{(1)}$ H MRS in 101 patients, with neuroepithelial brain tumors prior to surgery and in 19 healthy volunteers, to measure the total Cho-concentrations (tCho). Histological diagnoses were confirmed postsurgically according to the WHO classification. Measured tCho-compound signal intensities were corrected for coil loading, numbers of acquisitions and voxel size, and tCho concentrations calculated as institutional arbitrary units. They were matched with the mean immunohistochemical marker of cell proliferation, the Ki-67 (MIB.1) labeling index. Compared with low-grade tumors (i.e. WHO grade I/II) and normal white brain matter, high-grade tumors (i.e. WHO grade III/IV) revealed significantly ($p < 0.05$) elevated labeling indices paralleled by increasingly elevated tCho-concentrations. In contrast tCho-concentrations in low-grade tumor did not differ significantly from physiological values. A highly significant positive correlation ($p < 0.0001$, $r(2) = 0.81$) was found between the tCho-concentration and the labeling index. It was concluded that the determination of tCho-concentrations using in vivo (1)H MRS could provide a novel and noninvasive assessment of the proliferative activity of neuroepithelial brain tumors, pointing at (1)H MRS as a useful method for differentiating proliferating from non-proliferating tissues. Hence, potential indications for the clinical application of (1)H MRS are grading tumors presurgically, early

detection of anaplastic transformation, and monitoring treatment. MRS yielded an overall grading success rate of 86%, while 1-H MRS produced a 95% success rate in differentiating low-grade from high-grade tumours.

M.Elizabeth Meyerand, et al (95) conducted a study on "Classification of Biopsy-Confirmed Brain Tumors Using Single-Voxel MR Spectroscopy". 27 patients with biopsy-confirmed brain tumours (13 with glioblastoma multiforme, six with anaplastic astrocytoma, and eight with low-grade astrocytoma) were evaluated with single-voxel spectra. The patients were divided into groups based on the histologic subtype of their tumour for different treatment protocols. Metabolic peak areas were normalized for each metabolite (choline, creatine, N-acetylaspartate, lactate) to the area of the unsuppressed water peak and to the area of the creatine peak. Kruskal-Wallis nonparametric analysis of variance (ANOVA) tests showed statistically significant differences among the tumour groups for all the area ratios. The lactate/water ratio could be used to distinguished all three tumour groups, whereas the Choline/water ratio distinguished low-grade astrocytomas from the two high-grade groups. Both the Choline and lactate ratios could be used to separate the high-grade from the low-grade tumours. They had concluded that Specific metabolic peak area ratios acquired from regions of contrast-enhancing brain tumor can be used to classify astrocytomas according to their histopathologic grade.

Andreas Stadlbauer, et al (96) in their study, "Preoperative Grading of Gliomas by Using Metabolite Quantification with Proton MR

Spectroscopic Imaging" had reported that imaging with high spatial resolution Proton MR spectroscopic allows preoperative grading of gliomas.

Meng Law, et al (97) in their study "High-Grade Gliomas and Solitary Metastases: Differentiation by Using Perfusion and Proton Spectroscopic MR Imaging" had concluded that perfusion weighted and spectroscopic MR imaging enable distinction between solitary metastases and primary high-grade gliomas .Their study population was fifty-one patients with a solitary brain tumour (33 gliomas, 18 metastases). Of the 18 patients with metastases, 12 underwent perfusion-weighted MR imaging and six underwent spectroscopic MR imaging. Of the 33 patients with gliomas, 22 underwent perfusion-weighted MR imaging. The peritumoral region was defined as the area in the white matter immediately adjacent to the enhancing (hyperintense on T2-weighted images, but not enhancing on postcontrast T1-weighted images) portion of the tumor. Spectra from the enhancing tumor, the peritumoral region, and normal brain were obtained from the two-dimensional spectroscopic MR acquisition. Spectroscopic imaging demonstrated elevated choline levels (choline-to-creatine ratio was 2.28 +/- 1.24) in the peritumoral region of gliomas but not in metastases (choline-to-creatine ratio was 0.76 +/- 0.23). The difference was statistically significant (P =.001).

Tien, et al. (98), conducted MRS imaging on 10 normal adults and 46 patients with primary brain tumours; 29 Glioblastoma Multiformes (GBMs), five anaplastic astrocytomas, and 12 low-grade astrocytomas. The spectra of patients with low-grade gliomas (grades 1 and 2) exhibited decreased N-acetylaspartate (12 of 12) and slightly increased Choline (11 of 12) compared

with the spectra of normal brains. In patients with GBMs this comparison yielded markedly decreased N-acetylaspartate (29 of 29) and prominently increased Choline (27 of 29). Lipid signal was seen in high-grade tumours, especially in GBMs (12 of 20). Lactate peaks occurred in high-grade tumours (anaplastic astrocytomas and GBMs, 29 of 34), as well as in low-grade tumours (four of 12). The Creatine signal was slightly lower in all gliomas than is seen in healthy brain tissue. The lowest N-acetylaspartate, Choline and creatinine levels, in conjunction with the highest lactate levels, were usually found in necrotic portions of high-grade tumours. Results show that gliomas tend to demonstrate decreased N-acetylaspartate, increased Choline and decreased Creatine, with a lactate peak common in higher-grade tumours. Ultimately, diagnosis is made histologically after surgical biopsy or resection.

Harish Poptani, Rakesh K. Gupta et al (99) assessed the use of in vivo proton MR spectroscopy for characterization of intracranial mass lesions and to ascertain its reliability in grading of gliomas in 120 patients. All high-grade gliomas (n = 37) showed high choline and low or absent *N*-acetyl-L-aspartate and creatine along with lipid and/or lactate, whereas low-grade gliomas (n = 23) were characterized by low *N*-acetyl-aspartate and creatine and high choline and presence of only lactate. *N*-acetylaspartate/ choline ratio was significantly lower and choline/creatine ratio was significantly higher in high-grade gliomas than in low-grade gliomas. Presence of lipids suggested a higher grade of malignancy. All metastases (n = 7) showed lipid and lactate, whereas choline was visible in only four cases. Epidermoids showed resonances from lactate and an unassigned resonance at 1.8 ppm.

Meningiomas could be differentiated from schwannomas by the presence of alanine in the former. Among the infective masses, pyogenic abscesses (n = 6) showed resonances only from cytosolic amino acids, lactate, alanine, and acetate; and tuberculomas (n = 11) showed only lipid resonances

Meng Law, Stanley Yang et al (93) evaluated the sensitivity, specificity, PPV, and NPV of perfusion MR imaging and MR spectroscopy compared with conventional MR imaging in grading primary gliomas. One hundred sixty patients with a primary cerebral glioma underwent conventional MR imaging, dynamic contrast-enhanced T2*-weighted perfusion MR imaging, and proton MR spectroscopy. Gliomas were graded as low or high based on conventional MR imaging findings. The rCBV measurements were obtained from regions of maximum perfusion. Cho/ cr , Cho/NAA and NAA/cr Metabolite were measured at a TE of 144 ms. Tumor grade determined with the three methods was then compared with that from histopathologic grading. Threshold values of 1.08 and 1.56 for Cho/Cr and 0.75 and 1.60 for Cho/NAA provided the minimum C2 and C1 errors, respectively,for determining a high-grade glioma. The combination of rCBV, Cho/Cr, and Cho/NAA resulted in sensitivity, specificity, PPV, and NPV of 93.3%, 60.0%, 87.5%, and 75.0%, respectively. Significant differences were noted in the rCBV and Cho/Cr, Cho/NAA, and NAA/Cr ratios between low- and high-grade gliomas ($P < .0001$, .0121, .001, and .0038, respectively .They concluded that, the rCBV measurements had the most superior diagnostic performance (either with or without metabolite ratios) in predicting glioma grade. Threshold values can be used in a clinical setting to evaluate tumours

preoperatively for histologic grade and provide a means for guiding treatment and predicting postoperative patient outcome.

Negendank et al (4) studied 86 cases of glial tumours and showed each type and grade of tumour was metabolically heterogeneous with significant overlap in spectral Cho/Cr and NAA/Cr ratio in low and high grade. All tumours demonstrate increased Cho/Cr and decreased NAA/Cr. Lactate occurred infrequently and in all grades. Mobile lipids, on the other hand, occurred in 41% of high-grade tumours with higher mean amounts found in glioblastomas. This result, coupled with the recent demonstration that intratumoral mobile lipids correlate with microscopic tumour cell necrosis, led to the hypothesis that mobile lipids observed in vivo in 1H-MR spectroscopy may correlate independently with individual prognosis.

A comparative study was conducted of 28 healthy volunteers and 18 patients with gliomas, all patients undergoing in vivo proton MRS (100). MRS analysis was able to distinguish the normal brain from gliomas, and low-grade from high-grade astrocytomas.

Alvaro Magalhaes et al (83) studied 27 patients who had suspicious brain tumours with MR spectroscopy. They correlated that Cho/NAA and Cho/Cr are higher for high grade glioma and the values are 6.53 and 3.35 for Grade IV, 1.85 and 1.62 Grade III, 2.21 and 1.50 Grade II and 1.45 and 1.49 for Grade I.

Carles Majos et al (76) studied the utility of proton magnetic resonance (MR) spectroscopy in the clinical categorization of primitive neuro-ectodermal tumors (PNETs) in adults. According to them the resonances of choice for identifying PNET were alanine ($P < .001$) and glutamate and glutamine ($P = .004$), both decreased with respect to meningioma; Choline increased with respect to low-grade ($P < .001$) and anaplastic astrocytoma ($P = .055$); and lipids at 1.30 ppm decreased and choline increased with respect to glioblastoma ($P < .001$ and $P = .004$, respectively) and metastasis ($P < .001$ and $P = .021$)**.**

W.Hollingworth, L.S. Medina et al (78) reviewed various studies and reported, that five studies examined the sensitivity and specificity of 1H-MR spectroscopy for differentiating high- from low-grade tumours. Among those, two studies described (101,102) provided information on tumour grading. In both studies, 1H-MR spectroscopy was very accurate in differentiating high- and low-grade tumours, achieving an AUC (Area under the Curve) of 94% (0.05 SE) and 96% (0.03 SE) in the studies that used long and short echo times, respectively.

Herminghaus et al (94) also used automated spectral analysis derived from a 126 patients. This algorithm was validated in an independent cohort of 90 patients with histopathologically graded tumours (30 grade I/II, 29 grade III, 31 grade IV). The sensitivity and specificity of 1H-MR spectroscopy for differentiating high- and low-grade tumours in this independent cohort was 95% (86%–98%; 95% confidence interval [95% CI]) and 93% (95% CI, 79%–98%) respectively. This diagnostic accuracy diminished in the

differentiation of grade III and grade IV tumours, with 6 of 31 grade IV tumours mistakenly assigned to grade III status.

Astrakas et al (103) prospectively recruited 66 patients with histologically confirmed brain tumours (grade I, 13; grade II, 30; grade III, 7; grade IV, 16). Multivoxel 1H-MR spectroscopy analysis focused on the voxel with the highest Cho. The best diagnostic accuracy was achieved by an amalgam of Cho, Cr, and lipids and/or lactate (L) (Cho/Cr + 0.49 L/Cr). This linear combination resulted in an AUC of 96% (0.02 SE). At a threshold value of 1.8, the sensitivity and specificity of 1H-MR spectroscopy for diagnosing high-grade tumours were 96% (95% CI, 78%–100%) and 88% (95% CI, 75%–96%), respectively.

In contrast to the preceding work, Law et al (93) observed much lower diagnostic accuracy in a retrospective cohort of 160 patients with histopathologically confirmed lesions (120 grade III/IV, 40 low-grade) evaluated with multi-voxel 1H-MR spectroscopy, CE and perfusion MR imaging. A blinded interpretation of the Cho/NAA ratio had a sensitivity of 73% (95% CI, 64%–80%) and specificity of 63% (95% CI, 47%–76%) at a threshold value of 1.66; this was less accurate than MR perfusion and no better than CE-MR imaging.

Huang Y, Lisboa PJ et al 2003, Majos C, Alonso J, Aguilera C, et al.2003,2004, & Mishra AM, Gupta RK, 2004, indicated that ^{1}H-MR spectroscopy resulted in accurate diagnoses in 78% to 96% of cases, though these accuracy figures will be dependent upon case mix.

3.8. Metastases versus High grade Gliomas:

Meng Law et al, (97) in their study "High-Grade Gliomas and Solitary Metastases: Differentiation by Using Perfusion and Proton Spectroscopic MR Imaging" have concluded that perfusion weighted and spectroscopic MR imaging enable distinction between solitary metastases and primary high-grade gliomas .Their study population was fifty-one patients with a solitary brain tumor (33 gliomas, 18 metastases). Conventional, contrast enhanced perfusion-weighted, and proton spectroscopic MR imaging before surgical nine, spectroscopic MR imaging were done; and two underwent both. Of the 18 patients with metastases, 12 underwent perfusion-weighted MR imaging and six underwent spectroscopic MR imaging. Of the 33 patients with gliomas, 22 underwent perfusion-weighted MR imaging. The peritumoral region was defined as the area in the white matter immediately adjacent to the enhancing (hyperintense on T2-weighted images, but not enhancing on postcontrast T1-weighted images) portion of the tumor. Spectra from the enhancing tumor, the peritumoral region, and normal brain were obtained from the two-dimensional spectroscopic MR acquisition. Spectroscopic imaging demonstrated elevated choline levels (choline-to-creatine ratio was 2.28 +/- 1.24) in the peritumoral region of gliomas but not in metastases (choline-to-creatine ratio was 0.76 +/- 0.23). The difference was statistically significant (P =.001).

J.K.Smith et al (104) have concluded that metastases show moderate to marked reduction in NAA, low Cr and high Cho. These features are similar to astrocytomas and they are differentiated from it by the sharp margin of

metastatic lesions. In a study of 18 patients with brain metastases, all but two of the lesions exhibited decreased N-acetylaspartate, as well as a peak corresponding to lactate or lipid (57). Of the lesions that were followed after treatment, all those showing decreases in the volume of the enhancing lesion also showed reductions in lactate, lipid and Choline peaks. Lesions that showed increased enhancement on long-term follow-up also had a corresponding increase in Choline and lactate or lipid peaks. From this study, it appears that adding MRS to a conventional MRI examination enables more reliable identification of active tumours, and also the ability to determine if lesions are responding to therapy. In some cases, adding MRS to MRI may yield additional information.

Lukas L, Devos A, Suykens JA, et al.,(101,102) evaluated the differentiation of metastases from high-grade astrocytoma by using long and short echo time 1H-MR spectroscopy. This study retrospectively assembled a cohort of patients from multiple hospitals. The MR hardware varied between hospitals, but spectroscopy was performed using standardized protocols. Both studies used automated spectral analysis for diagnostic classification. At long and short echo times, the area under the ROC curve (AUC) for differentiating glioblastomas from metastases was relatively poor (AUC = 64% [0.10 SE] and 59% [0.10 SE], respectively). This is statistically significantly better than chance alone; however, it is not high enough to suggest that 1H-MR spectroscopy can be relied upon to differentiate metastases from glioblastomas.

Opstad et al, (105) reviewed 47 patients with pathologically proven glioblastomas and metastases; 7 patients were later excluded due to poor quality spectra. The authors focused on the lipid peak-area ratio derived from short echo time, single-voxel 1H-MR spectroscopy. They defined this as the ratio of L1 (the combined alanine, lactate, δ 1.4 macromolecule, and δ 1.3 lipid peak) to L2 (the combined δ 0.9 lipid and δ 0.87 macromolecule peaks). Using this ratio, they reported an AUC of 84% with both sensitivity and specificity equal to 80% at a threshold value of 2.9. The authors speculated that the difference in lipid profiles may be related to differences of membrane structure of infiltrative versus migratory tumour cells or to lipid metabolism.

3.9. Recurrent/Residual Tumour versus Treatment-Related Change

MRS was able not only to facilitate diagnosis and accurate classification of de novo brain tumours but also to allow differentiation of recurrent tumour and tumour progression from radiation necrosis, post-treatment effects, or edema (106-109). **Castillo M et al** (107) stated that, MRS was useful in evaluating the response to therapy in patients with brain tumours. Radiation necrosis occurs from approximately 6 to 24 months after completion of therapy, was seen more commonly with high grade astrocytomas, and was indistinguishable from recurrent tumour by conventional gadolinium–enhanced MRI. Elevated Lac level were seen in Proton MR spectra of patients who have received 40 Gy or more of radiation to the brain, even when the conventional MRI study does not demonstrate any structural abnormality within the resection bed.

Castillo M et al (107) studied 25 patients with cerebral astrocytoma who received a combination of radiation and chemotherapy and demonstrated increased Cho/NAA and Cho/Cr ratio as well as the presence of Lac, in case of recurrent tumour, compared to markedly decreased level of NAA, Cho, and Cr and the presence of a broad intense peak between 0 and 2.0ppm in case of radiation necrosis. This peak between 0 and 2.0ppm, consists of free fatty acid, Lac and amino acids. However, because most therapy-induced tissue damage occurs in combination with areas of viable tumour, single-voxel techniques were not optimal for evaluation of these patients; 3D MR spectroscopic imaging is preferable for distinguishing among areas of residual or recurrent tumour, radiation necrosis and viable normal brain tissue. Sensitivity and specificity of ^{1}HMRS for the detection of residual/recurrent tumour in radiated patients in their series were 71% and 100%, respectively and serial MRS in the same series allowed differentiation of necrosis and tumour progression; progressive decreases in Cho levels and mild increase in NAA levels correlated well with therapy success (107).

Chan Y l (108), **Jaysundar Rama,** (109) reported contradictory results; the reasons for differences in results may include the fact that Cho levels may be elevated in early radiation induced lesions because of demyelination and reactive astrocytosis.

Conventional MR and MR spectroscopic imaging was conducted on 31 children with neuroglial brain tumours by **Tziak, et al.,** (106). MR spectroscopic imaging improved the assessment of paediatric brain tumours by adding biochemical information regarding tumour involvement and by

depicting residual or recurrent tumour outside the Gd-DTPA enhanced tumour bed. The authors recommend the use of MR spectroscopic imaging in addition to conventional MR imaging in assessing paediatric brain tumours.

Castillo M et al (107), **Chan Y l** (108), **Jaysundar Rama,** (109), stated that 3D.MRSI is preferable for distinguishing areas of residual or recurrent tumour, radiation necrosis and viable normal tissue. Elevated Lac level were seen in Proton MR Spectra of patients who have received 40 Gy or more of radiation to the brain, even when the conventional MRI study does not demonstrate any structural abnormality within the resection bed.

Kimura, et al, (110), compared the usefulness of MRS to that of contrast-enhanced MRI and of single-photon emission computerized tomography (SPECT) in evaluating the response of metastatic brain tumours to Stereotactic Radio-surgery (SRS). The study evaluated 40 patients, with a total of 47 metastatic brain tumours. The primary lesion was identified in all cases. SRS was effective in 37 lesions. The effectiveness of SRS was observable by MRI from 1-3 months or longer after SRS. With SPECT, a decrease in the ratio of lesion to normal brain was observable at between two weeks and two months after surgery. With MRS, results were observable between one week and one month after SRS. The authors concluded that MRS may be a more sensitive tool in evaluating the response to SRS than SPECT or MRI and that it can be used earlier for this purpose.

An MRI and a positron emission tomography with [2-18F] fluoro-2-deoxy-D-glucose (FDG-PET) were performed seven months after

radiotherapy on a patient treated by stereotactic radiotherapy for recurrence of an initially resected low-grade astrocytoma as described by **Schlemmer, et al.,** (111). MRI follow-up examination showed a mass lesion indicative of high-grade tumour progression. In contrast, proton MR spectroscopy (1-H MRS) indicated radiation necrosis, which was confirmed histopathologically in surgical specimens. Subsequent follow-up examinations up to 19 months after surgery showed no evidence of tumour recurrence.

Traber et al (112) presented data on 43 patients, with high-grade astrocytomas sequentially tracked with multiple-voxel 1H-MR spectroscopy until completion of radiation therapy. An increased Cho peak (50% higher than contra lateral tissue) was 72% (95% CI, 53%–86%) sensitive and 82% (95% CI, 48%–98%) specific in distinguishing tumor from radiation-induced necrosis. **Ando et al**, (113) in a study described in more detail previously, examined 20 patients with CE-MR imaging and 1H-MR spectroscopy. Based on a Choline-to-Creatine ratio diagnostic threshold of 1.5, 1H-MR spectroscopy had a sensitivity of 64% (95% CI, 35%–87%) and a specificity of 83% (95% CI, 36%–100%) in distinguishing tumor from radiation-induced necrosis.

Lichy et al (114) used multi-voxel spectroscopy in 24 patients with irradiated gliomas. The final diagnosis was determined by clinical and imaging follow-up. Using the Cho/Cr ratio with a diagnostic threshold of 2, the authors identified 13 of 15 (87% [95% CI, 60%–98%] sensitivity) recurrent or residual tumours and 8 of 9 (89% [95% CI, 52%–100%] specificity) radiation-related changes.

Plotkin et al (115) investigated the value of single-voxel 1H-MR spectroscopy at 3T in a prospective study of 25 patients with suspected recurrent glioma based on MR imaging after treatment with surgery, interstitial radiation therapy, external radiation therapy, or chemotherapy. The final diagnoses were based on a minimum of 6 months' clinical follow-up and repeat MR imaging examinations. A combined diagnostic threshold of Cho/ NAA (>1.17) and Cho/Cr (>1.11), resulted in 89% sensitivity and 83% specificity for identifying tumour. However, the authors also observed that sensitivity (95%) and specificity (100%) were higher still with single-photon emission CT.

Tumour Extent before Treatment

McKnight et al (116) prospectively recruited 44 patients with suspected glioma before image-guided resection or stereotactic biopsy of the tumour. Data from the preoperative multi-voxel ^{1}H-MR spectroscopy study was used to select 4 potential targets for biopsy in each patient. In practice, the authors were unable to obtain biopsy samples at each target, and their analysis was based on 100 samples, of which only 7 were classified as non-

tumour. The authors based diagnosis on the Cho-NAA index (CNI), where CNI is the number of standard deviations between the Cho to NAA ratio within a given voxel and that of the control voxels. At a threshold CNI of greater than 2.5, the authors reported 90% (95% CI, 84%–96%) sensitivity and 86% (95% CI, 56%–100%) specificity for predicting the presence of tumour in the biopsy sample. The overall AUC for CNI was 94% (95% CI, 87%–99%). Up to half of the T2-hyperintense lesion outside of the gadolinium-enhanced lesion contained CNI greater than 2.5. This suggests that 1H-MR spectroscopy might have a considerable therapeutic impact on surgical and radiation target volumes.

3.10. Non neoplastic lesions:

Gupta RK et al (117,118) found that tubercular lesions exhibited strong lipid resonance, ascribed to mobile lipids within the caseous material which are minimally visible on MR imaging. Their main observation was absence of Choline and NAA or reduced Cho/Cr ratio in tubercular lesions. **Poptani,H, Rakesh, K. Gupta** et al (99,119) reported that among the infective masses, six pyogenic abscesses showed resonances only from cytosolic amino acids, lactate, alanine, and acetate; and eleven tuberculomas showed only lipid resonances.

3.10.1.Infections (abscesses) and cystic tumours:

Rakesh Gupta et al (120,121) evaluated twenty-seven patients with a total of 33 pyogenic brain abscesses and three patients with a total of 12 tuberculous abscesses with in vivo MR spectroscopy and MT MR imaging.

All 27 patients with pyogenic brain abscesses had lipid and lactate levels of 1.3 ppm and amino acid levels of 0.9 ppm with or without the presence of succinate, acetate, alanine, and glycine, while the three patients with tuberculous abscesses showed only such lipid and lactate levels. The MT ratio from the wall of the pyogenic abscesses was significantly higher ($P < .001$) than that from the tuberculous abscess wall.

The mean MT ratio from the wall of the pyogenic brain abscesses measured 25.56 ± 1.61 (n = 33). The mean MT ratio from the wall of the tuberculous abscesses measured 19.89 ± 1.55 and was found to be significantly lower ($P < .001$) than the wall of the pyogenic brain abscess, normal cortical and deep gray matter, and white matter. They concluded that it might be possible to differentiate tuberculous abscesses from pyogenic abscesses by using MT MR imaging and in vivo MR spectroscopy.

Chang KH et al, (122) evaluated 40 proton MR spectra obtained from cystic contents of various intracranial cystic masses in 39 patients, In most gliomas and metastases, only a lactate resonance was observed. There was a trend toward a higher lactate peak in high-grade gliomas. A few tumors, including malignant gliomas and metastases, showed lipid signal combined with lactate signal. In abscesses, there were various combinations of lactate, acetate, succinate, amino acids (including valine, alanine, and/or leucine), and/or unassigned resonances.

Grand S, et al, (123) Cytosolic amino acids are found only inside the pyogenic abscesses cavity and are not demonstrated in proton MRS of intracranial tumours with cystic or necrotic degeneration in vivo; therefore,

they considered specific markers for abscesses. They studied, 34 patients with cystic intra-cerebral masses (28 tumours and six abscess) in in-vivo ^{1}HMRS to differentiate necrotic tumour from brain abscess. Amino acid concentrations were determined in vitro in 13 purulent samples from brain and non brain tissues and in nine aseptic fluids from the necrotic brain tumours at 2D MRS and liquid Chromatography. Amino acids were identified in vitro in both purulent and aseptic samples. Amino acid concentration measured in the aseptic fluids at both liquid chromatography and 2D MRS were far below the detection thresh hold of in vivo ^{1}HMRS. Quantitative results obtained at 2D MRS showed no overlap in the ranges of amino acid concentrations in purulent and aseptic samples. In vivo the proton spectra obtained with a 136msec TE revealed amino acids (inverted peak at 0.9ppm) in only the pyogenic abscesses. They concluded that detection of amino acid resonance at 0.9ppm in MRS was a promising tool in distinguishing bacterial abscess from cystic brain tumours.

Shukla-Dave, et al., (124) evaluated 51 patients with intracranial cystic lesions (21 abscesses, 20 gliomas, three Hydatid cysts, three arachnoid cysts, one glio-ependymal cyst, one xanthogranuloma, one infarction and one acoustic neuroma) using conventional MRI and in vivo MRS. MRS accurately predicted the pathology in 92% of the cases, leading the authors to conclude that MRS complements and enhances MRI in characterizing cystic intracranial mass lesions.

3.10.2.DEMYELINATION:

MR images with contrast revealed enhancement in active multiple sclerosis lesions. It has been shown by **Arnold DL, Matthews PM** (125,126) that NAA is decreased in patients with chronic multiple sclerosis in whom axonal loss has occurred. Conversely, in acute plaques, NAA may be normal, indicating that the axons have not yet disappeared or have been permanently damaged. In addition, resonances corresponding to free lipids (0.9 to 1.6ppm) have been observed in chronic multiple sclerosis plaques and may reflect disintegration of myelin (124).

Bitsch A, Bruhn H, Vougioukas V, et al. (127) described that, the elevated Cho resonance peaks are compatible with the proliferation of the cellular elements of the immune system and astroglia. Reactive astrogliosis is conspicuous in demyelinating disease.

Moreover, Choline-containing compounds and myo-inositol (mI) were both found to be elevated within Multiple Sclerosis plaques, suggesting enhanced membrane turnover (124,127).

A multi-center study was conducted on patients with primary progressive multiple sclerosis (PPMS) **Narayana, et al.,** (128). The average NAA/Cr ratio in patients with PPMS was significantly lower than that in normal controls, and no significant differences were observed in this ratio between lesion-containing regions and normal-appearing tissues.

3.11. Summary of review of literature:

A Technology Assessment conducted by Tufts-New England Evidence-based Practice Center for the Agency for Healthcare Research and Quality (AHRQ) evaluated the use of MRS in brain tumours (2003)(129). The conclusion stated that "human studies conducted on the use of MRS for brain tumours demonstrate that this non-invasive method is technically feasible and suggest potential benefits for some of the proposed indications. However, there is a paucity of high quality direct evidence demonstrating the impact on diagnostic thinking and therapeutic decision making. In addition, the techniques of acquiring the MRS spectra and interpreting the results are not well standardized. In summary, (129) while there are a large number of studies that confirm MRS' technical feasibility in the diagnosis of brain tumours, there are very few published studies to evaluate its diagnostic accuracy and whether it can positively affect diagnostic thinking and therapeutic choice. Those studies that do address these areas often have significant design flaws including inadequate sample size, retrospective design and other limitations that could bias the results." (129).

W. Hollingworth et al, (78) performed an updated systematic review of 26 studies (published during 2002-2004) evaluating diagnostic performance, diagnostic impact, therapeutic impact, or health impact of 1H-MR spectroscopy. They observed that no articles evaluated patient health or cost-effectiveness. Methodologic quality was mixed; most used histopathology as the reference standard but did not specify blinded interpretation of histopathology. Several studies have found that 1H-MR

spectroscopy is highly accurate for distinguishing high- and low-grade gliomas, though the incremental benefit of 1H-MR spectroscopy in this setting is less clear. Interpretation for the other clinical subgroups is limited by the small number of studies. They concluded that the current evidence on the accuracy of 1H-MR spectroscopy in the characterization of brain tumours is promising. However, additional high-quality studies are needed to convince policy makers. They presented guidelines to help focus future research in this area. The conduct of additional, well-designed, prospective studies aiming to replicate this head-to-head comparison will provide the more definitive evidence that policy makers seek before making coverage decisions.

Sufficient evidence exists in several published, peer reviewed scientific studies which establishes the value of MRS in distinguishing high and low grade gliomas, in defining recurrent tumour from radiation induced necrosis and in paediatric treatment planning.

Pioneering investigation of MR spectroscopy in infective lesions of the brain particularly in tuberculous versus pyogenic abscesses has been done by Gupta RK et al (117,118) in North India. However, in this part of South India, the role of 1H-MR spectroscopy in the assessment of all intracranial lesions and particularly to differentiate neoplastic from non-neoplastic lesions has not been clearly determined.

With wider availability of good MRI scanners and the desire to pursue high quality diagnostic imaging, it is a challenge to overcome this current deficiency and this study would serve as a catalyst in bringing about a change in the practice of modern MR Imaging technique.

CHAPTER 4

MATERIALS AND METHODS

4.1 Study design, setting and population

The study was done in the Department of Radiology and Imaging sciences Apollo Hospitals, a multi disciplinary tertiary care private Hospital in Chennai, India. . The study group comprised predominantly patients belonging to the middle and higher socio-economic status. The study population was the referral patients with clinical / diagnostic evidence of an intracranial space occupying lesion based on CT/MR Imaging investigations. Most of the patients were referred by the departments of neurology, neurosurgery or internal medicine. A few patients were also referred from the department of paediatrics, infectious disease and endocrinology.

The cases included in this study were acquired between the period April 2005 and December 2009.

4.1.1Sampling Technique

The technique proposed for selecting this sample is PURPOSIVE SAMPLING. The investigator selects the patients who are judged to be typical of the population to be studied.

A. Inclusion criteria

Referred patients to the MRI department who were shown to have an intracranial space occupying lesion on MR Imaging were included in this study.

B. Exclusion Criteria

- Lesions close to the skull base and close to the calvarium where it was not technically feasible to acquire Magnetic Resonance Spectroscopy (MRS) data.
- Lesions less than 2x2x2 cm in size as reduced voxel size might not display a good spectral pattern.
- Vascular lesions eg, aneurysms, A- V malformations, infarctions, primary haemorrhage or lesions with haemorrhage.
- Diffuse neuro-degenerative and metabolic disorders.

C. Sample size

350 patients with intracranial space occupying lesions evaluated by conventional MR imaging underwent proton MR spectroscopy.

182 patients who satisfied the above criteria were initially taken up for the study. However, sixty four cases had to be excluded from the study for the following reasons :

a) Non-availability of histo-pathological verification in 22 patients, due to unwillingness for surgery.

b) Non-availability of follow up of 42 cases (those left the hospital due to various reasons)

Of the remaining one hundred and eighteen patients, 27 patients had to be excluded from the final statistical analysis for the following reasons:

a) 17 patients: MRS spectra did not have one or two of NAA/Cr, Cho/Cr, and NAA/Cho due to technical issues including artefacts, noise due to structures like bone or CSF adjacent to the lesion.

b) 10 patients: Classified as a miscellaneous neoplastic or non – neoplastic group. The number of cases in a particular subgroup were only two or three, no useful statistically valid results could be obtained by analysing these sub groups. (*eg, three cases of Lymphoma , two cases of central neurocytoma, one PNET, one case of choroid plexus papilloma and one epidermoid. In the non neoplastic group, there were two patients with focal cortical dysplasia).*

Thus the number of cases subjected to statistical evaluation was restricted to ninety one (n=91).

D. Control group:

Fifteen healthy volunteers were evaluated as a control group that comprised eight males and seven females ranging from 7 to 68 years of age (mean age, 40.3 years). (Table No: 4.1)

Informed consent was obtained from all the subjects / parents / guardians before the study.

4.1.2. MR Imaging and MR Spectroscopy measurements and evaluation

All patients were examined using a 1.5-T superconducting MR imager Philips INTRA, (with software RELEASE 11.1.4.3CE0344) Netherland) with a standard circularly polarized *SENSE* head coil.

Computer and software equipment:

Image analysis was performed in the advanced workstation with the view-forum *5.IVILI2006 CE0344* **Philips Medical systems, Netherland B.V** Veenpluis 4-6, 5684 PC BEST. Netherland software package supplied by the manufacturer.

In each patient, axial T1-weighted TSE (650/14 ms [TR/TE]) spin-echo (SE), T2-weighted (2000/80 ms) turbo SE, and fast fluid-attenuated inversion recovery (FLAIR) (9000/ 2500/110 ms [TR/TE/TI]) images were obtained by using 5-mm section thickness, 210-mm field of view (FOV), and 160 × 256 matrix size. After intravenous administration of gadodiamide 0.1 mml/kg (Omniscan; Amersham Health, Carrington Hill, Ireland), contrast-enhanced T1-weighted SE sequences were obtained in axial, coronal, and sagittal planes in all patients.

Image analysis:

Morphological appearance of the lesion/ lesions i.e, site, size, shape, extent, signal intensity, pattern of enhancement, degree of peri- lesional oedema, presence or absence of haemorrhage, necrosis/ cystic components and presence or absence of mass effect on adjacent structures and midline

shift was evaluated on conventional MR imaging. In all cases normal areas, lesion, cystic/necrotic and peri tumoral regions were defined on the basis of following the imaging features:

Normal tissue, an area having no enhancement and normal signal intensity on T2 –WI, FLAIR (Fluid attenuated Inversion recovery) and DW Images;

L**esion**, a region containing a well defined solid portion ,contrast enhancement and abnormal signal intensity on T2 WI,FLAIR and DW Images ;

Cystic components were differentiated as both areas of hyperintensity on T2 WI and areas of hypointensity on FLAIR images. Necrotic components were differentiated on contrast –enhancement T1 WI as the interior of enhanced lesions;

Peri-tumoral area, a region containing no enhancement and signal intensity on T2 WI, FLAIR and DW Images;

Hemorrhagic lesions, area hyperintensity on unenhanced T1 WI and dark on gradient echo MR Images.

Proton MR Spectroscopy

MR spectra were acquired on a clinical 1.5-T system with a prototype quadrature receive/transmit head coil The point-resolved spectroscopy (PRESS) pulse sequence was used with chemical-shift selective saturation

(CHESS) water suppression, with imaging parameters of 2000/144 ms(TR/TE) and conventional post processing techniques. Additional spectra with a TE of 31ms were obtained in some cases in which mobile lipid resonances obscured metabolites in the range of 0.5 to 1.5 ppm. Cubic or nearly cubic MR spectroscopic single voxels were centered over solid portions of the lesions to avoid necrotic debris with metabolically inactive tissue or edema. A compromise between partial volume effects with large voxels and poor signal-to-noise ratio with small voxels determined a typical voxel size of 2x2x2 cm3 **(MR spectroscopy was not performed for lesions less than approximately 2 cm3 in size).** Regions that showed enhancement on previous studies with IV gadolinium complexes were sampled whenever possible. Localizer images and spectra were typically acquired within 45 minutes.

The single-volume spectroscopy (SVS) technique can be considered a limitation, as multi voxel techniques can provide smaller volume of interest and a better evaluation of tumour heterogeneity, avoiding sampling error (89).

Hence, in addition to the SVS technique, two-dimensional chemical shift imaging (2D-CSI), multi- voxel study was performed in 15 patients, in whom; lesions are ill-defined or infiltrative on MR imaging sequences. For the 2D-CSI technique, a data set was obtained from a selected volume of 18 to 135 cm3 (minimum, 3 x 4 x 1.5 cm; maximum, 10 x 9 x 1.5 cm) by using an SE sequence with phase-encoding gradients in two directions, automatic shimming, and gaussian water suppression. Measurement parameters used in 2D-CSI were 1500/270 (135 in two cases)/ 2(1 in six cases)

(TR/TE/excitations); 16 x 16 phase-encoding steps; 160 x 160-mm field of view; 15-mm section thickness; and 1024 data points. Data sets of 1.5 cm3 resolution were acquired within 12 minutes (6 minutes in the six measurements with one excitation).

a) **Spectral pattern:** Nine major metabolite resonances in single- voxel MR spectra were obtained from lesions. Assignment of the resonance of interest, included N-acetyl-aspartate(NAA) at 2.02ppm, Creatine (Cr) at 3.03ppm, Choline (Cho) at 3.20ppm,Lipid (Lip0.9) at 0.09ppm and (Lip 1.3) at 1.30ppm glutamate & glutamine (Glx) at 2.35ppm and glycine and /or myo-inositol(Gly/Mi) at 3.55ppm. Two doublets inverted owing to phase modulation duo to J coupling are defined, corresponding to lactate (Lac) at 1.35ppm & to Alanine (Ala) at 1.47ppm. Cr(3.03ppm) is chosen as reference resonance for correction of possible shifting in the frequency domain.

Peak location, Amplitude, & Areas under the peak of Cho, Cr, NAA, are analyzed**.**

b) **Metabolite ratios:** Metabolite values were calculated automatically from the area under each metabolite peak by using the standard commercial software program provided by the manufacturer. Peak integral values were normalized to the internal Cr peak. Metabolite area and amplitude ratios of NAA/Cr, Cho/Cr and NAA/Cho were calculated by the inbuilt software in analysis package.

In addition to the above ratios, the peaks of Gly,Mi, Glx, lactate, lipids alanine and aminoacid were difficult to approximate credibly by manual means, and were thus evaluated only qualitatively “Four Point scale method’ as very high (+++), high (++), present (+) & absent (–)

MRS was then interpreted by two unblinded radiologists (same radiologists with three years experience in MRI) with clinical and MR Imaging findings. The Spectra were interpreted by visual inspection, analogous to the qualitative interpretation of graphical data and the ratios so obtained were interpreted to characterize and grade lesions based on studies conducted by Nail Bulakbasi et al (74); Meng law et al, 2003(93).

The conventional MR images and MRS were graded for each tumour according to the two-tier imaging grading system (130,131): low- versus high-grade gliomas. Gliomas of different histologic types were graded I to IV, according to the degree of malignancy. Grade I and II gliomas were taken together as **low-grade** and grade III and IV were considered **high-grade** gliomas.

A consensus was reached on the conventional grading of each lesion based on eight criteria: contrast material enhancement, border definition, mass effect, signal intensity heterogeneity, hemorrhage, necrosis, degree of edema, and /or crossing the midline (130,131).

Evaluation of Multivoxel MR Spectroscopy

Measurements performed with multivoxel spectroscopy were excluded from the statistical analysis, based on the hypothesis that different tumour types show varying distribution patterns of pathologic spectra. On the basis of spectral and distribution patterns of the pathologic spectra seen at MR spectroscopy, a qualitative analysis was done.

MR spectroscopic results were evaluated for the distribution of normal or pathologic spectra across the lesion and neighbouring radiologically normal-appearing tissue.

Spectra were defined as **pathologic spectra** when the ratio of *N*-acetylaspartate/choline-containing compounds (NAA/Cho) was less than 1. Distribution patterns of pathologic spectra were classified in two groups: those limited to the region corresponding to the contrast enhancement, (intra-tumoral) and those outside the region corresponding to the contrast enhancement (peri-tumoral /perienhancing area) based on the study conducted by Isabella Maria Burtscher, et al 2000(79).(Table No: 4-4)

4.2. Reference standard

In the neoplastic lesions and other surgically resected or stereotactically biopsied neoplastic- like lesions, the appearance of metabolites and metabolite ratios of the intracranial lesions was determined preoperatively and the tumor types were histopathologically classified according to WHO criteria (130,131,132) low-grade astrocytomas

(astrocytoma grade II), high-grade astrocytomas (anaplastic astrocytoma grade III, and glioblastoma multiforme grade IV); Grade I and II gliomas were taken together as low-grade, and grade III and IV were high-grade gliomas.(Table No:4-3)

Of the 91 cases that were studied 70 were Neoplastic and 21 were Non-neoplastic lesions. Of 70 case of the neoplastic group, histo-pathological diagnosis of 68 cases was established by stereotactic biopsy or open biopsy and open biopsy in all neoplastic lesions except for two patients were a presumptive diagnosis of metastasis was made based on clinical grounds and circumstantial supporting evidence. (One patient was with biopsy proven carcinoma breast and another patient with bronchogenic carcinoma with multiple intracranial lesions.)

Of the 21 non-neoplastic lesions, histopathological diagnosis was obtained in 7 cases (by stereotactic biopsy in 4 cases and by aspiration of pus material in 3 cases of cerebral abscesses). Remaining 14 cases were managed medically. The presumptive diagnosis in these cases was based on post treatment clinical response, or by serial imaging studies or laboratory tests.

Data obtained was compared between tumour types in order to assess which findings are characteristic of each type and the utility of each metabolite resonance signal in classifying the different tumours and inflammatory lesions. Significance of difference between various groups for each metabolite was assessed.

Table No: 4.2 Types of Lesions studied (n=91)

Neoplastic group	**n=70**
HIGH GRADE gliomas	n=25
LOW GRADE GLIOMAS	n=18
MENINGIOMA	n=7
POST OP RECURRENCE	(n=6)
METASTASIS	(n=14)
Non – neoplastic group	**n=21**
INFECTIONS	n=13
DEMYELINATION	n=4
Post operative gliosis /post RT Changes	n=4

4.3. Statistical Analysis - Method

Sensitivity, specificity, Positive Predictive Value (PPV), and Negative Predictive Value (NPV) were calculated for the possible correct identification of malignant lesion as per analysis done by Meng law et al (93). According to Meng Law et al (93), Sensitivity, specificity, PPV, and NPV were calculated for correct identification of high-grade gliomas. Tumors classified as high grade and found at histologic examination to be high grade were considered true-positive findings; low-grade gliomas that were histologically confirmed as low grade were considered true-negative findings.

In this study, Sensitivity, specificity, PPV, and NPV were calculated for correct identification of malignant lesion. Hence, lesions classified as **malignant group** *(high grade gliomas, recurrent gliomas and metastasis*) and found at histologic examination to be high grade gliomas or metastases were considered true-positive findings; **benign lesions group** (*Low grade gliomas, Meningioma and non-neoplastic lesions*) that clinically improved after specific treatment or were histologically confirmed as benign lesions were considered true-negative findings.

SENSITIVITY & SPECIFICITY

Sensitivity and specificity are statistical measures of the performance (133) of a binary classification test. **Sensitivity** (also called **recall rate** in some fields) measures the proportion of actual positives which are correctly identified as such (e.g. the percentage of sick people who are correctly identified as having the condition). **Specificity** measures the proportion of negatives which are correctly identified (e.g. the percentage of healthy people who are correctly identified as not having the condition). These two measures are closely related to the concepts of type I and type II errors. A theoretical, optimal prediction can achieve 100% sensitivity (i.e. predict all people from the sick group as sick) and 100% specificity (i.e. not predict anyone from the healthy group as sick).

POSTIVE PREDICT VALUE & NEGATIVE PREDICT VALUE

The **positive predictive value**, or **precision rate**, or **post-test probability of disease**, is the proportion of patients with positive test results who are correctly diagnosed. It is the most important measure of a diagnostic

method as it reflects the probability that a positive test reflects the underlying condition being tested for. Its value does however depend on the prevalence of the disease, which may vary. In essence, the PPV is a special application of Bayes' theorem(133).

Receiver Operating Characteristic (ROC)

The diagnostic performance of a test or the accuracy of a test to discriminate diseased cases from normal cases is evaluated using Receiver Operating Characteristic (ROC) curve analysis (134). ROC curves can also be used to compare the diagnostic performance of two or more laboratory or diagnostic tests .

The ROC curve (134)

In a Receiver Operating Characteristic curve (ROC) the true positive rate (Sensitivity) is plotted in function of the false positive rate (100-Specificity) for different cut-off points. Each point on the ROC plot represents a sensitivity/specificity pair corresponding to a particular decision threshold. A test with perfect discrimination (no overlap in the two distributions) has a ROC plot that passes through the upper left corner (100% sensitivity, 100% specificity). Therefore the closer the ROC plot is to the upper left corner, the higher the overall accuracy of the test (Zweig & Campbell, 1993).

AREA UNDER CURVE

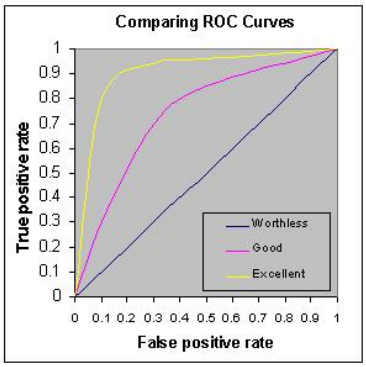

Fig.4.1

The graph at right shows three ROC curves representing excellent, good, and worthless tests plotted on the same graph. The accuracy of the test depends on how well the test separates the group being tested into those with and without the disease in question. Accuracy is measured by the area under the ROC curve. An area of 1 represents a perfect test; an area of 0.5 represents a worthless test. A rough guide for classifying the accuracy of a diagnostic test is the traditional academic point system:

- 0.90-1 = excellent (A)
- 0.80-0.90 = good (B)
- 0.70-0.80 = fair (C)
- 0.60-0.70 = poor (D)
- 0.50-0.60 = fail (F)

In this study, NAA/CR, CHO/CR and NAA/CHO Vs Control ratios were compared using ANOVA test, because these ratios followed the normal distribution when test of normality was applied. Student's t-test was used for the comparison between a) Neoplastic and Non neoplastic lesions, b) Low- and High-grade gliomas, c) High grade gliomas and Metastases and d) Post radiotherapy changes and Residual / Recurrent tumours**.**

All the analysis were done by using SPSS-**S**tatistical **P**ackage for the **S**ocial **S**ciences for Windows.14.1 version, probability value **p** value less than 0.05 was considered as statistically significant difference.

Univariate analysis (135)

Univariate analysis is the simplest form of quantitative (statistical) analysis (135). The analysis is carried out with the description of a single variable and its attributes of the applicable unit of analysis. For example, if the variable age was the subject of the analysis, the researcher would look at how many subjects fall into a given age attribute category.

ANOVA

In statistics, **analysis of variance (ANOVA) (135)** is a collection of statistical models, and their associated procedures, in which the observed variance in a particular variable is partitioned into components due to different sources of variation. In its simplest form ANOVA provides a statistical test of whether or not the means of several groups are all equal, and therefore generalizes *t*-test to more than two groups. ANOVAs are helpful because they possess an advantage over a two-sample t-test. Doing multiple two-sample t-tests would result in an increased chance of committing a type I error. For this reason, ANOVAs are useful in comparing three or more means.

INDEPENDENT T-TEST

Introduction

The independent t-test (135), also called the two sample t-test or student's t-test is an inferential statistical test that determines whether there is

a statistically significant difference between the means in two unrelated groups.

Multivariate analysis (136 & 137)

Statistical procedure for analysis of data involving more than one type of measurement or observation. It may also mean solving problems where more than one dependent variable is analyzed simultaneously with other variables.

Binary Logistic regression analysis

In statistics, **logistic regression** (sometimes called the **logistic model** or **logit model**) is used for prediction of the probability of occurrence of an event by fitting data to a logit function logistic curve. It is a generalized linear model used for binomial regression. Like many forms of regression analysis, it makes use of several predictor variables that may be either numerical or categorical

In this study, data were analyzed with multivariate repeated-measures analysis (*Binary Logistic regression analysis)* of variance among the groups to compare neoplastic versus non-neoplastic , low grade versus high grade, and high grade versus metastasis

All the analysis were done by using SPSS. **S**tatistical **P**ackage for the **S**ocial **S**ciences for Windows.14.1 version, probability value (*p)* less than 0.05 was considered as statistically significant difference.

Table No: 4-1

Metabolites Area ratio and Amplitude ratio in Healthy individuals - Control (n=15)

S. No.	Sex	Age	NAA/ Cr	NAA /Cr (Ht)	CHO /Cr	CHO / Cr (Ht)	NAA/ CHO	NAA/CHO (Ht)	CHO/ NAA	CHO/NAA (Ht)
1	**M**	**28**	2.57	2.43	1.57	1.36	1.64	1.79	0.61	0.56
2	**M**	**47**	2.29	2.02	1.51	1.17	1.52	1.74	0.66	0.58
3	**M**	**45/**	2.2	2.24	1.37	1.07	1.61	2.09	0.62	0.48
4	**F**	**30/**	2.5	2.38	1.29	1.05	1.94	2.27	0.51	0.44
5	**F**	**13**	2.45	2.26	2.12	1.41	1.16	1.6	0.86	0.63
6	**M**	**68**	2.25	2.06	1.94	1.21	1.61	1.6	0.75	0.59
7	**M**	**23**	2.12	2.09	1.33	1.09	1.6	1.91	0.63	0.52
8	**M**	**65**	2.19	1.97	1.33	1.16	1.64	1.7	0.61	0.59
9	**M**	**36**	2.52	2.28	1.43	1.17	1.76	1.95	0.57	0.51
10	**F**	**34**	1.88	2.13	1.02	1.07	1.84	1.99	0.54	0.5
11	**F**	**7**	2.74	2.52	1.27	1.06	2.16	2.38	0.46	0.42
12	**F**	**27**	2.35	2.25	1.37	1.04	1.71	2.16	0.58	0.46
13	**F**	**29**	2.25	2.18	1.21	0.98	1.86	2.22	0.54	0.45
14	**F**	**38**	2.73	2.31	1.59	1.25	1.72	1.85	0.58	0.54
15	**M**	**35**	2.48	2.38	1.55	1.31	1.59	1.75	0.62	0.57
Mean			2.37	2.23	1.46	1.16	1.69	1.93	0.61	0.52
Standard deviation			0.23	0.16	0.28	0.13	0.22	0.25	0.10	0.06

DISTRIBUTION PATTERN OF PATHOLOGIC SPECTRA IN MV MRS

Spectra were defined as pathologic when NAA/Cho was less than 1/1.

TABLE No: 4-3

S.NO	PATIENT DEATAIL	H.P.E DIAGNOSIS	NO OF LESIONS	NUMBER OF CASES WITH PATHOLOGIC SPECTRUM	
				Limited to contrast Enhancing Area (Intra-Tumoral)	Outside contrast Enhancing Area (Peri-Tumoral)
1	M 47	Fibrillary Astrocytoma – grade 2	1	1	NIL
2	F 63	MENINGIOMA	1	1	NIL
3	M 32	DNET	1	1	NIL
4	F 48	Oligodentroglioma Grade 2	1	1	NIL
5	M 68	Anaplastic astrocytoma Gr 3	1	1	1
6	M 48	GBM – grade 4	1	1	1
7	M 28	GBM Grade 4	1	1	1
8	M 58	Metastases	2	1	NIL
9	M 65	Metastasis	1	1	NIL
10	F 68	LYMPHOMA	1	1	1
11	M 65	Post radio-therapy case of grade 3 astrocytoma(recurrence)	1	1	1
12	F 55	Post operative & post Radiotherapy case of Grade 3(radiation change with recurrence)	1	NIL	1
13	M 63	Post Radiotherapy case of grade 2 Astrocytoma Recur.	1	1	NIL
14	33 F	Post RT case of grade 2 astrocytoma No residual / recurrence	1	NIL	NIL
15	41 F	POST RADIOTHERAPY F/U case of GRADE 3 ASTROCYTOMA	1	1	NIL

CHAPTER- 5

ANALYSIS AND RESULTS

5.1. Age Distribution of patients in this study.

Table No: 5-1

Descriptive Statistics

	N	Minimum	Maximum	Mean ±S.D
Age	91	5	84	42.69±17.162
Valid N	91			

Fig No: 5-1

Age

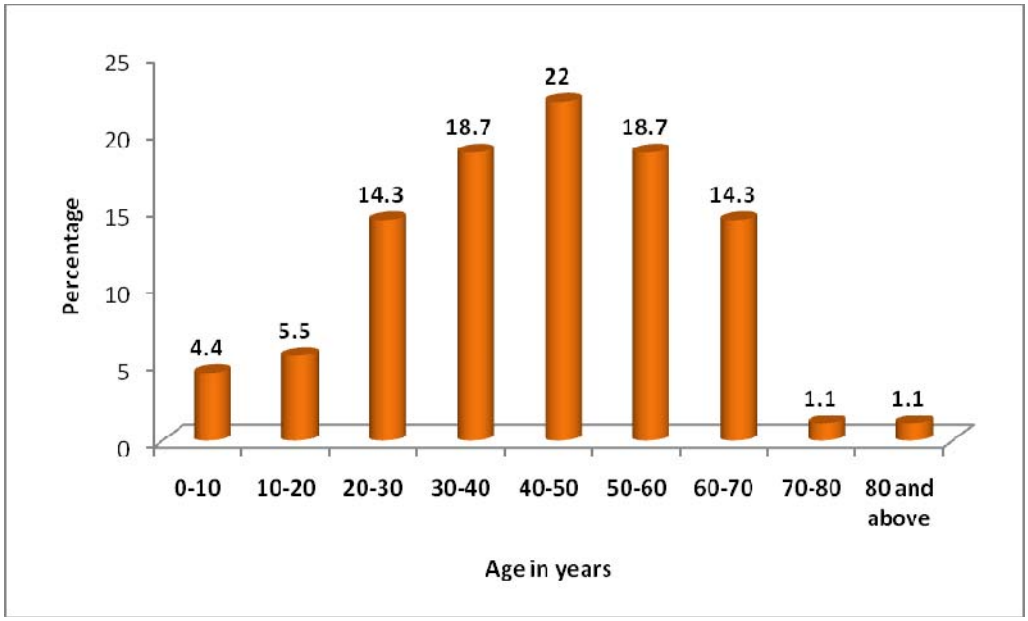

5.2. Sex Distribution of patients in this study.

Table. No: 5-2

Sex	No. of patients	Percentage
Female	36	39.6
Male	55	60.4
Total	91	100.0

Fig No: 5-2

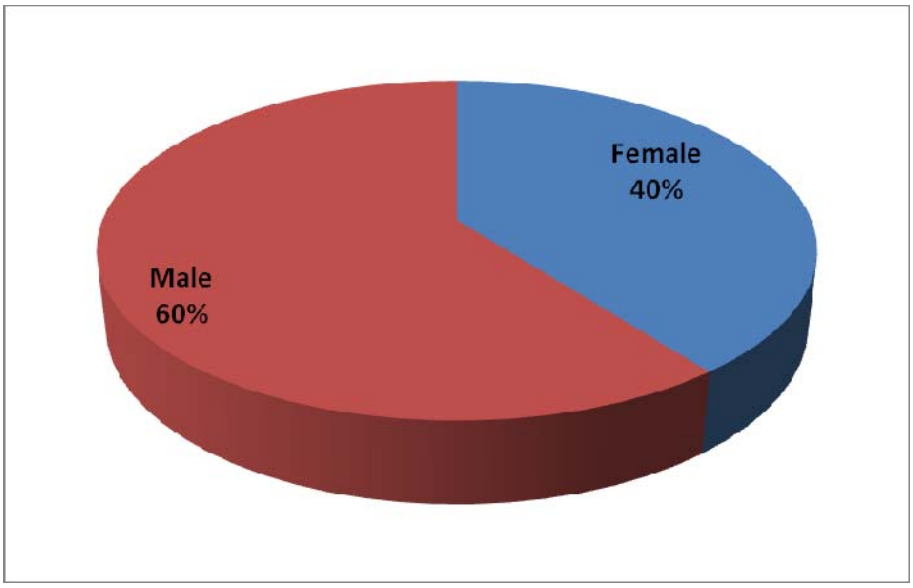

The objective of the study was:

a) to ascertain if MRS could assist in distinguishing neoplastic from non-neoplastic lesions and the lesion was neoplastic, whether it was high or low grade, and thereafter if high grade whether the lesion was a primary malignant lesion or a metastasis.

b) In postoperative or post radiation patients with recurrent symptoms or a lesion, whether the changes seen on imaging were due to surgery or radiation or due to recurrence of the tumour.

5.3. Malignant lesion versus benign lesion

Sensitivity, specificity, Positive Predictive Value (PPV), and Negative Predictive Value (NPV) were calculated for correct identification of malignant lesion as per analysis done by Meng law et al (93). Hence, lesions classified as malignant lesions group (*high grade gliomas, recurrent gliomas and metastasis*) and found at histopathologic examination (HPE) to be high grade gliomas or metastases were considered true-positive findings; benign lesions group(*low grade gliomas, Meningioma and non-neoplastic lesions*) that were histologically confirmed or showed clinical improvement after specific treatment as benign lesions were considered true-negative findings. Based on MRI & MRS findings, those lesions classified as malignant one

which turned out to be benign on HPE were considered as false positive and the those lesions classified as benign that were found to be malignant lesions on HPE were considered as false negative The **sensitivity, specificity, positive and negative predictive values** for determining a malignant lesion was calculated. Receiver operating characteristic (ROC) curve analysis was used to evaluate the accuracy for detection of malignant lesion

Table. No: 5-3 Results of sensitivity and specificity

Estimate	No.
TRUE POSITIVE	40
TRUE NEGATIVE	46
FALSE POSITIVE-	1
FALSE NEGATIVE-	4
TOTAL	91

Table. No: 5-4 Estimation of sensitivity, specificity, positive and negative predictive values

	Estimate	95% CI
Sensitivity	0.909	[0.788 to 0.964]
Specificity	0.979	[0.889 to 0.996]
PPV	0.976	[0.874 to 0.996]
NPV	0.92	[0.812 to 0.968]
LR+	42.727	[6.132 to 297.701]
LR-	0.093	[0.036 to 0.237]

Inference: In this study, the sensitivity, specificity, PPV, and NPV for determining malignant lesions and non malignant lesions with MRI aided MRS were 90.9%, 97.9%, 97.6%, and 92%, respectively.

Figure No: 5-3

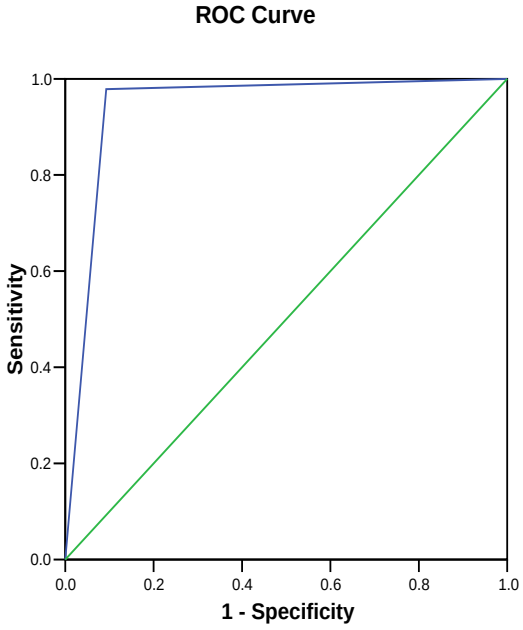

Diagonal segments are produced by ties.

Table No: 5-5

Area Under the Curve (AUC):

Test Result Variable(s): FINAL MRI & MRS DIAGNOSIS

Area	Std. Error (a)	Asymptotic Sig. (b)	Asymptotic 95% Confidence Interval	
			Lower Bound	Upper Bound
0.943	0.029	0.000	0.886	0.999

Receiver Operating Characteristic (ROC) curves: ROC plot represents a sensitivity/specificity pair corresponding to 0.9-1 representing grade "excellent" ; the Area Under the Curve is 0 .943. Therefore, ROC curve analysis (Fig: 5-2) shows the 94.3% accuracy for determination of malignant lesions.

5.4. Neoplastic lesions versus non neoplastic lesions:

Of the 91 cases that were studied 70 were Neoplastic and 21 were Non-neoplastic lesions. Of 70 cases in the neoplastic group, histo-pathological diagnosis of 68 cases was established by stereotactic biopsy or craniotomy and open biopsy. In two patients a presumptive diagnosis of metastasis was made based on clinical grounds. Of the 21 non-neoplastic lesions, definitive diagnosis was obtained by either stereotactic biopsy or by aspiration of pus material in 7 cases. In 14 cases non neoplastic lesions managed medically, a presumptive diagnosis was made based on post treatment clinical response, or by serial imaging studies or laboratory tests.

High grade tumours, low grade tumours, meningiomas, post operative recurrence of tumours and metastases were grouped under neoplastic lesions (n=70). Infective lesions, demyelination and post operative gliosis /and post radiotherapy changes were grouped under non neoplastic lesions (n=21).

The spectra from the healthy volunteers revealed a consistent pattern of the major peaks of NAA, Cr, Cho. No lactate or lipid resonances were visible in any of the healthy subjects studied. The mean NAA/Cr, Cho/Cr, and NAA/Cho ratios from the 15 volunteers (Table No: 4-1) were 2.37 ±0.23 1.46 ±0.28 and, 1.69 ± 0.22 respectively.

The area ratios of NAA / Cr, Cho / Cr and NAA / Cho in these neoplastic and non neoplastic lesions were utilized for statistical evaluation by ANOVA method and compared to the mean area ratio values of control population.(n=15).

In this study, mean NAA/CR, CHO/CR , NAA/CHO area ratio and Control ratios were compared **using ANOVA test.** Student's t-test was used for the comparison between a).neoplastic and non neoplastic lesions, b) low- and high-grade gliomas, c) High grade gliomas and Metastases, d) post radiotherapy changes and residual / recurrent tumours**.**

Multivariate analysis - Binary Logistic regression analysis was used for prediction of the probability of metabolite ratio and their ratio variations from the normal control ratios to distinguish a non neoplastic from neoplastic lesion, low grade versus high grade gliomas, and high grade gliomas versus metastasis.

Analysis was done by using SPSS. **(S**tatistical **P**ackage for the **S**ocial **S**ciences) 14.1 version, A probability value *p* less than 0.05 was considered as a statistically significant difference.

5.4.1 A. Univariate analysis - Neoplastic versus Non-neoplastic lesions

5.4.1. A. a. a) NAA/CR ratio

Table No: 5-6

	N	Mean±S.D	P value
Neoplastic	70	1.21±0.763	
Non-neoplastic	21	1.17±0.665	
Control	15	2.37±0.234	<0.001
Total	106	1.36±0.801	

Fig No: 5-4

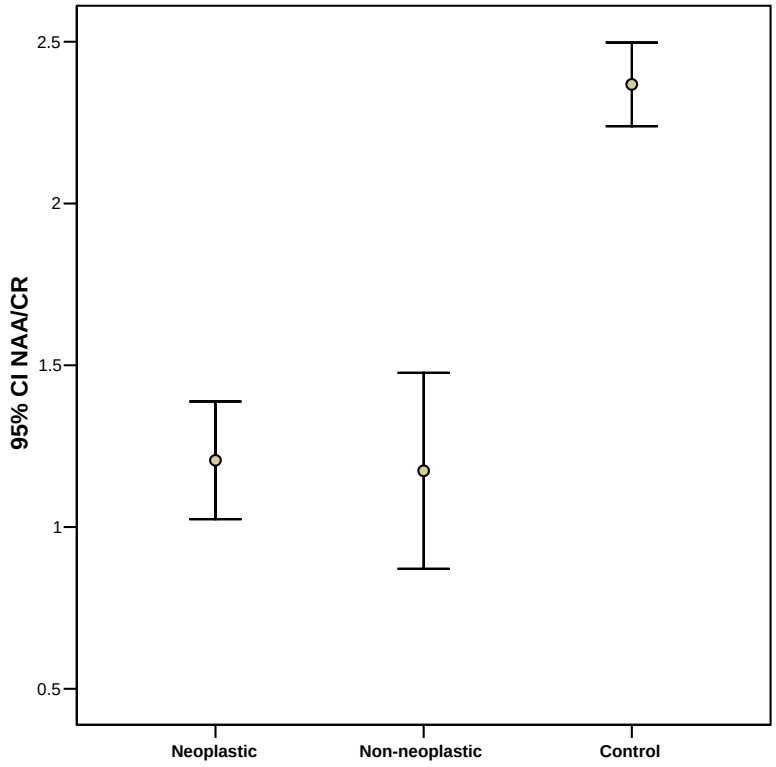

It was observed that the NAA / Cr ratio for neoplastic (1.21 ± 0.76; n=70) and non neoplastic lesions (1.17 ± 0.66; n=21) showed no gross difference (p=0.861), yet the control group ratio (2.37 ± 0.23; n=15) was significantly different from the lesions with a P value of <0.001 which is statistically significant at 1% level.(Table No:5-6)

Hence, NAA/Cr area ratio did not provide any significant difference in neoplastic and non neoplastic lesion but it differentiates them from control group. Area NAA/Cr ratio was useful to exclude whether abnormality was present or not. This is due to the fact that any pathology, whether it is neoplastic / non- neoplastic, causes an alteration in the NAA content owing to neuronal loss or modification and a significant change from the normal mean (2.37 ± 0.23) value. The Cr content is quite stable with only mild reduction due to altered metabolism and hence used as a reference or control.

5.4.1. A.b Neoplastic vs Non-neoplastic lesions : b) CHO / CR ratio

Table No: 5-7

	N	Mean ± S.D	P value
Neoplastic	70	3.87±2.206	<0.001
Non-neoplastic	21	1.20±0.662	
Control	15	1.46±0.277	
Total	106	3.00±2.187	

Fig No: 5-5

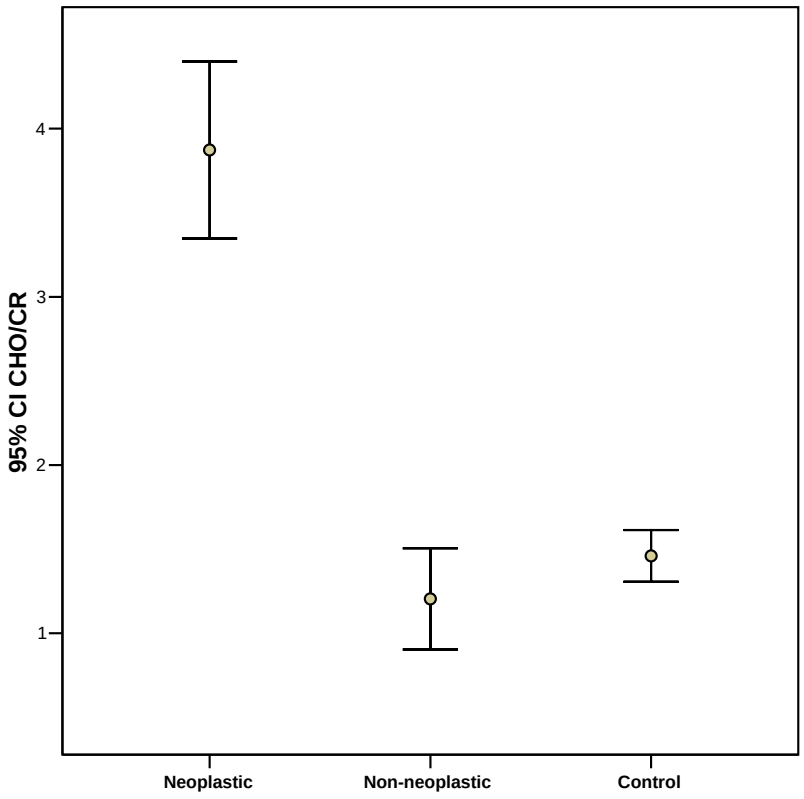

It was observed that the Mean Cho / Cr ratio for Neoplastic tumors was 3.87± 2.20 (n=70) and that for Nonneoplastic lesions was 1.2 ±0.66 (n=21). It showed a statistically significant difference ($p<0.001$).The Mean Cho / Cr of control was 1.46 ± 0.28 (n=15). There was a statistically significant variation in the Cho / Cr ratios between the neoplastic, non neoplastic lesions and control with a P value of <0.001 which is statistically significant at 1% level. (Table No: 5-7)

Hence, neoplastic lesions are clearly differentiated from non-neoplastic and normal control population when the Cho/Cr ratio is studied. Choline being associated with cell membrane turnover was noted to be high in lesions with rapid cellular turnover such as in malignancies. This is the reason for the discernibly high ratio in neoplastic lesions as compared to the other two entities.

5.4.1. A.c Neoplastic vs. Non-neoplastic lesions: c) NAA/CHO

Table No: 5-8

	N	Mean±	P value
Neoplastic	70	0.45±0.286	<0.001
Non-neoplastic	21	0.98±0.724	
Control	15	1.69±0.221	
Total	106	0.73±0.597	

Fig No: 5-6

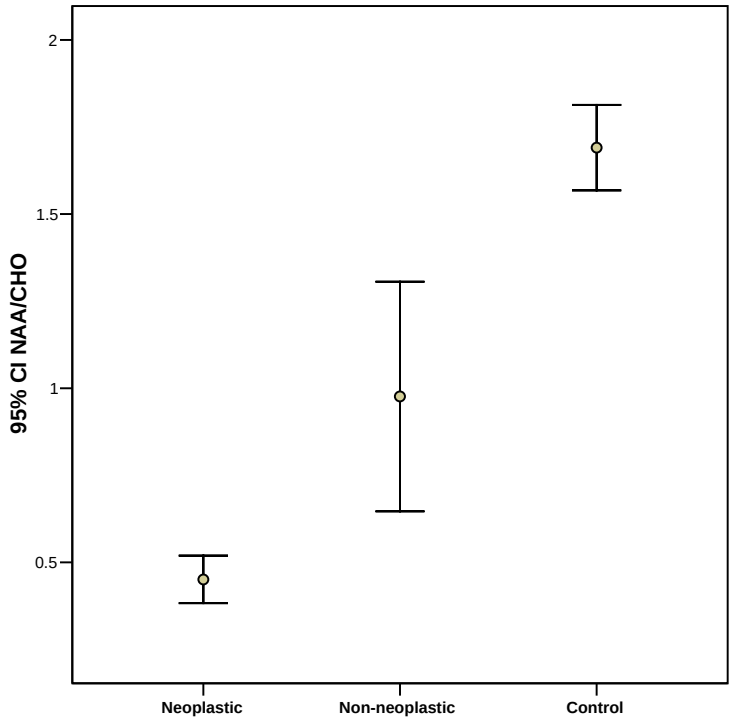

It was observed that the Mean NAA / Cho ratio for Neoplastic tumors was 0.45 ± 0.29 (n=70) and that for Non-neoplastic lesions was 0.98 ± 0.72 (n=21). The Mean NAA/Cho of control was 1.69 ±0.22 (n=15). There was a statistically significant difference in the NAA / Cho ratio of the control group as compared to the Neoplastic / non neoplastic lesions with a P value of <0.001 which is statistically significant at 1% level. (Table No: 5-8) It was also observed that the ratio range of the neoplastic lesions was narrow making their probability more specific as compared to the wide range of non neoplastic lesions.(graph fig: 5-6)

Decrease in NAA/Cho ratios was also significant MR spectroscopic parameters in the differentiation of neoplastic lesion from non neoplastic lesions.

This suggests that a larger neuron functionality loss and larger membrane turnover differentiate neoplastic lesions from an inflammatory process.

5.4.1 B) Binary Logistic regression analysis - Neoplastic vs Non-neoplastic lesions

Table No: 5-9

Variables in the Equation

		B	S.E.	Wald	df	Sig.	Exp(B)
Step 1(a)	NAACR	1.624	.977	2.763	1	.096	5.072
	CHOCR	-2.264	.718	9.951	1	.002	.104
	NAACHO	.774	1.313	.348	1	.555	2.169
	Constant	1.029	1.067	.929	1	.335	2.798

a Variable(s) entered on step 1: NAACR, CHOCR, NAACHO.

From the above table No: 5-9, it is observed that only one p value i.e, Cho/Cr is less than 0.05; therefore, among three metabolites ratio, only Cho/Cr area ratio is more statistically significant (p=0.002) in differentiating neoplastic from non-neoplastic lesions.

5.5. High grade gliomas versus low grade gliomas:

5.5.1 **High grade gliomas**

Of the 25 cases of high grade gliomas in this study (7 were grade III astrocytomas and 18 were Glioblastoma multiforme), 16 were predominantly solid and infiltrative lesion and 9 had cystic / necrotic areas within the solid lesion.

Moderate to gross edema and mass effect was present in 24. Foci of hemorrhagic areas were noted in 10.

Lesions in 16 patients showed restriction on diffusion, 8 lesions showed focal areas of restriction and 4 lesions showed T2 shine through effect. All the lesions were heterogeneously hypointense on T1WI and heterogeneously hyperintense on T2WI and FLAIR Sequences. Almost all the lesions showed moderate to significant heterogeneous enhancement with IV contrast. Three infiltrative lesions could not be measured and the rest ranged from 3cm to 8cm.

The mean NAA / Cr; Cho / Cr and the NAA / Cho ratios of high grade gliomas were 1.01 ± 0.62; 4.09 ± 1.51 and 0.27±0.121 respectively. The significant elevation in the choline levels is due to the large scale cellular turnover and membrane synthesis. Lactate was present in 5 cases and lipids were present in 20 cases.

5.5.2. Low grade gliomas:

Of the 18 low grade gliomas in this study group (13 were Grade 2 astrocytomas, 3 were pilocytic astrocytomas, 1 was a sub-ependymoma , and 1 was a DNET), 11 cases appeared solid and compact with fairly well circumscribed margins and 7 were heterogeneous and mixed with cystic / necrotic areas. All the lesions were hypo intense on T1 and heterogeneously hyper intense on T2W images & FLAIR Sequences.

Two cases showed T2 shine through effect on DW imaging and 6 cases showed mild restriction with low ADC values. 10 cases showed no restriction or T2 shine through. With IV contrast administration 2 cases showed no enhancement, 8 cases showed mild homogeneous enhancement, 2 cases

showed marginal rim enhancement, 2 cases showed moderate enhancement and 2 cases showed significant enhancement. 2 cases showed patchy enhancement.

The lesion was located in the brain stem in 5 cases, in the cerebellum in one , in the frontal lobe in 3 , in the temporal lobe in 3 , in the temporo-parietal lobe in 5 and in the Foramen of Monro in one case . Mild edema was present in 8 cases and hemorrhagic foci in one case. Mild to moderate mass effect was seen in 10 cases. The lesions varied in size from 2 cm to 6 cm.

The mean NAA / Cr; Cho / Cr and the NAA / Cho area ratios of low grade gliomas were 1.06 ± 0.52; 2.12 ± 0.99 and 0.64 ±0.17 respectively. Lactate was present in 8 cases and lipids were present in 6 cases reflecting increased anaerobic metabolism and cellular necrosis. Additionally, high resonance of myoinositol was observed in five cases of low grade astrocytoma

The area ratios NAA / Cho, Cho / Cr and NAA / Cr of the high and low grade gliomas and the mean ratio values of 15 controls were utilized for statistical evaluation and compared.

5.5.3.A Univariate analysis High Grade gliomas VS low grade gliomas

5.5.3.A a) NAA/CR Ratio

Table No: 5-10

	N	Mean±S.D	P value
High grade gliomas	25	1.01±0.619	<0.001
Low grade glioma	18	1.06±0.522	
Control	15	2.37±0.234	
Total	58	1.38±0.779	

Fig No: 5-7

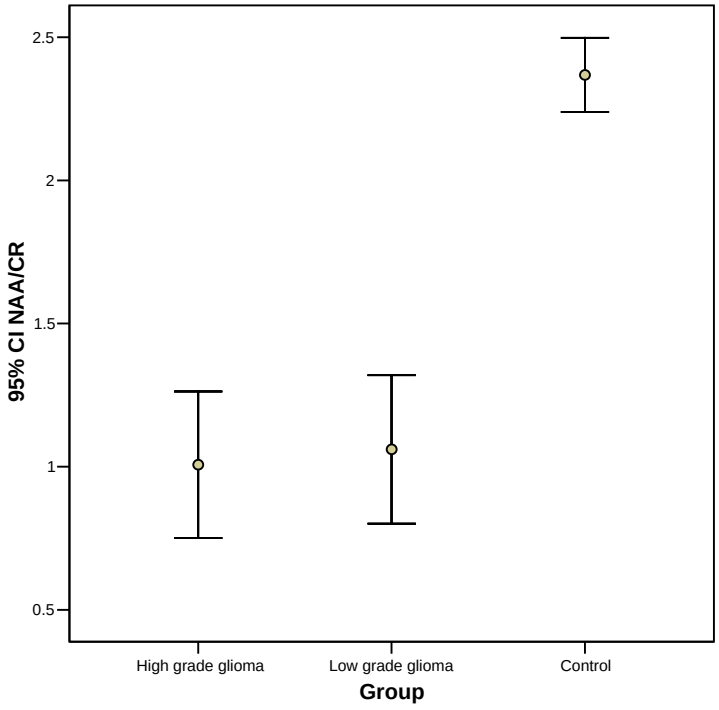

It was observed that the NAA / Cr ratio for high grade gliomas (1.01 ± 0.62; n=25) and low grade gliomas (1.06 ± 0.52; n=18) showed no great difference, (p= 0.766) but the control group ratio (2.37 ± 0.23; n=15) was significantly different from the high and low grade ratios with a P value of <0.001 at 1% level of significance. (Table No: 5-10)

NAA/Cr ratio did not provide any significant difference between high grade and low grade gliomas but it differentiates them from control group. Neuronal loss being a part of the process in both conditions there is no demonstrable change in the NAA / Cr ratios between these two groups.

5.5.3. A.b. High grade vs low grade gliomas: CHO/CR Ratio-

Table No: 5-11

	N	Mean± S.D	P value
High grade glioma	25	4.09±1.512	<0.001
Low grade glioma	18	2.12±0.988	
Control	15	1.46±0.277	
Total	58	2.80±1.618	

Fig No: 5-8

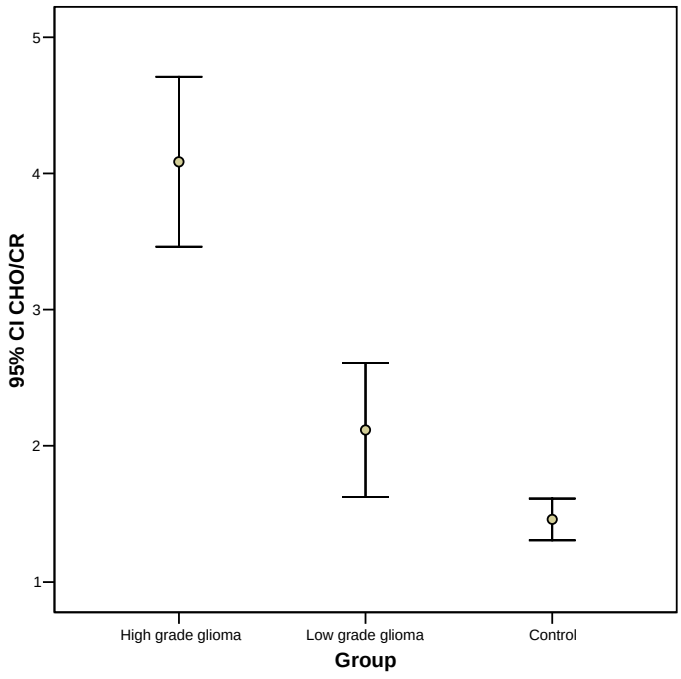

It was observed that the Mean Cho / Cr area ratio for high grade gliomas was 4.09 +/- 1.51 (*n*=25) and that for low grade gliomas was 2.12 ± 0.99 (n=18). The Mean Cho / Cr of control was 1.46 ±0.28 (*n*=15). There is a statistically significant variation in the Cho / Cr ratios between the high grade, low grade gliomas and the control population ratios with a P value of <0.001 which is statistically at 1% level of significance.(Table No:5-11)

It was also noted that the range of the ratios of the glioma group was wide denoting wide range of variations among the same tumor group.

The mean CHO/CR area ratio (2.12 ± 0.99, *n* = 18) in low grade tumours was lesser than the mean high grade tumour CHO/CR area ratio (4.09 ± 1.51, *n* = 25) with p value < 0.001 which is statistically at 1% level of significance.

This increase in Cho/Cr ratio was mainly due to increase in Cho levels because of increased membrane turnover and liberation of unbound Cho-containing compounds caused by the destruction of neurons during the malignant process, rather than a decrease in Cr levels, which was quite constant in various metabolic conditions

Hence, the Cho/Cr ratio was a good MR spectroscopic parameter to demonstrate the grade of malignancy.

5.5.3A.c. High grade vs low grade gliomas: NAA/CHO

Table: no: 5-12

	N	Mean ±S.D	P value
High grade glioma	25	0.27±0.121	<0.001
Low grade glioma	18	0.64±0.169	
Control	15	1.69±0.221	
Total	58	0.75±0.604	

Fig No: 5-9

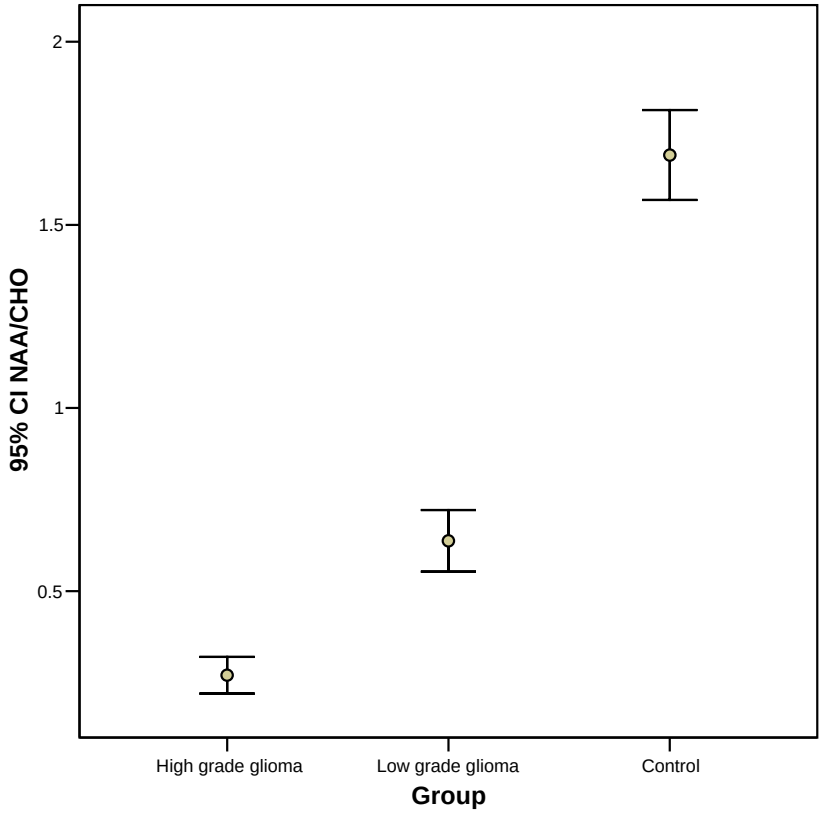

It was observed that the Mean NAA / Cho ratio for high grade gliomas was 0.27 ± 0.12 (n=25) and that for low grade gliomas was 0.64 ± 0.17 (n=18). The Mean NAA/Cho of control was 1.69 ± 0.22 (n=15). There was a statistically significant difference in the NAA / Cho ratio of the control group, the high grade gliomas and the low grade gliomas with a P value of <0.001 which is statistically at 1% level of significance.(Table No:5-12) It was also observed that these ratio ranges are narrow making their probability more specific.

Mean NAA/CHO area ratio of low grade gliomas (0.64 ± 0.17, n = 18) was greater than the mean NAA/CHO area ratio (0.27 ± 0.12, n = 25) of high grade gliomas with a p value < 0.001 in this analysis. A decrease in the NAA/Cho ratio is mainly due to both an increase in Cho levels and a decrease in NAA levels. The NAA / Cho ratio undoubtedly distinguished high or low grade gliomas from the control group thereby helping in confirming an abnormality.

Decrease in NAA/Cho ratios was also significant MR spectroscopic parameters in the differentiation of low grade from malignant high grade tumours.

5.5.3. B)Binary Logistic regression analysis- High grade versus low grade gliomas

Table No: 5-13

Variables in the Equation

		B	S.E.	Wald	df	Sig.	Exp(B)
Step 1(a)	NAA/CR	.960	2.021	.226	1	.635	2.611
	CHO/CR	-1.699	1.256	1.831	1	.176	.183
	NAA/CHO	16.625	7.926	4.400	1	.036	16604073.063
	Constant	-2.703	3.740	.522	1	.470	.067

a Variable(s) entered on step 1: NAA/CR, CHO/CR, NAA/CHO.

The above analysis (Table No: 5-13)shows that only one p value i.e., NAA/Cho is less than 0.05; therefore, among three metabolites ratio, only NAA/Cho area ratio is more statistically significant in differentiating High grade from low grade gliomas .

Eventually, between the high grade and low grade tumours, statistical analysis showed that only the **increase in Cho / Cr ratio and decrease in NAA / Cho area ratios were statistically significant (p=0.036) in distinguishing between the tumour grades.** The NAA / Cho ratio undoubtedly distinguished high or low grade gliomas from the control group thereby helping in confirming an abnormality.

This result concludes that it is possible to discriminate high and low grade tumours on the basis of the area ratios of NAA / Cho and to certain extent from Cho/Cr ratio.

5. 6. High grade Gliomas versus Metastases:

The NAA/CR, CHO/Cr and NAA/CHO area ratio of 25 cases of high grade gliomas, 14 cases of metastases and the 15 control cases were compared and analyzed by using ANOVA method.

5.6.1. Metastases

Of the 14 cases of intracerebral metastases, 6 cases had a known primary; 2 from renal cell carcinoma, 1 from carcinoma of cervix and 3 from the lung. Out of the 14 cases, HPE diagnosis of 10 cases was established by stereotactic biopsy or craniotomy and open biopsy except for two patients where presumptive diagnosis of metastasis was made based on clinical grounds. (one patient with biopsy proven carcinoma breast and another patient with bronchogenic carcinoma with multiple intracranial lesions). In two metastatic adenocarcinomas, MRS suggested as high grade glioma in one case and intraventricular central neurocytoma in another.

All the cases were solid lesions, appearing hypo intense on T1WI and hyper intense on T2WI & FLAIR sequences, except one that presented as a thick walled cystic lesion. 10 of the cases showed a predominantly peripheral intense rim enhancement. Two cases had necrotic areas within. Extensive edema was a common feature in all. 8 cases had multiple lesions. All had elevated lipid. The Cho / Cr peaks were very high as compared to the high grade gliomas.

The cases of metastasis showed mean area ratios as follows: Cho/Cr ratio was 4.88 ± 2.42, NAA/Cr ratio was 1.93 ± 1.0 and NAA/Cho ratio was 0.47±0.247. The height ratios were NAA/Cr = 1.71 ± 1.03 and Cho/Cr = 2.97 ± 1.16. Lipids were consistently observed in all metastatic lesions.

5.6.1A Univariate analysis. High grade gliomas Vs. Metastases:

5.6.1Aa. NAA/CR ratio

Table No: 5-14

	N	Mean ± S.D	P value
High grade glioma	25	1.01±0.619	<0.001
Metastasis	14	1.93±1.003	
Control	15	2.37±0.234	
Total	54	1.63±0.892	

Fig No: 5-10

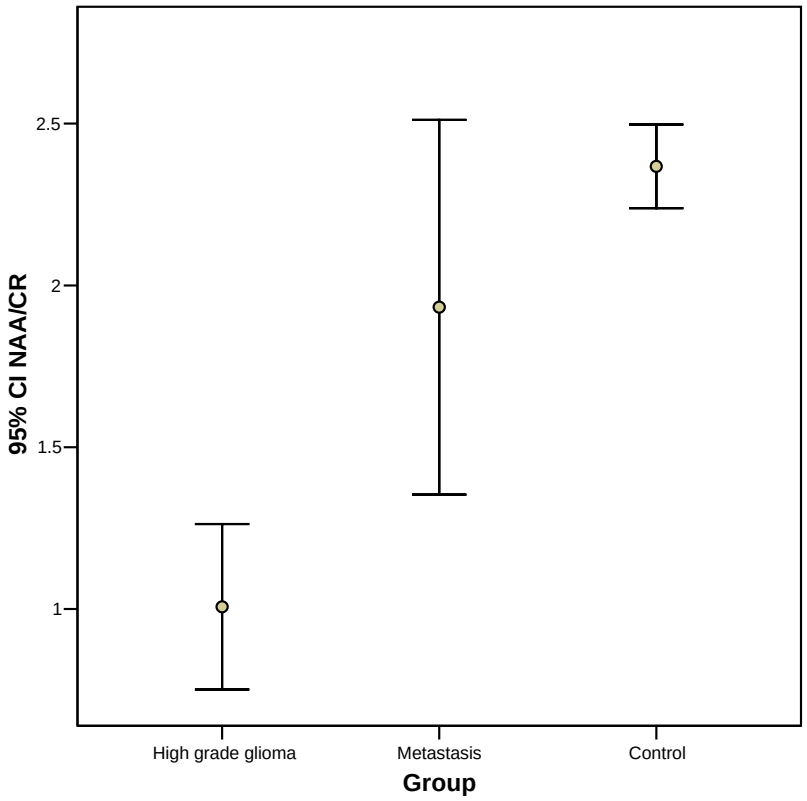

The mean NAA / Cr ratios of the 25 cases of high grade gliomas was 1.01±0.62 and in the 14 cases of metastases was 1.93 ± 1.00.It showed statistical difference (p=0.001). The mean area ratio NAA / Cr in the control group (n=15) was 2.37 ± 0.23 with P value of <0.001 which is statistically significant at 1% level.(Table 5-14)

Hence MRS findings in high grade gliomas differ from metastases group and control group.

5.6.1.A.b High grade gliomas vs. Metastases: b) CHO/CR ratio

Table No: 5-15

	N	Mean±S.D	P value
High grade glioma	25	4.09±1.512	<0.001
Metastasis	14	4.88±2.415	
Control	15	1.46±0.277	
Total	54	3.56±2.080	

Fig No: 5-11

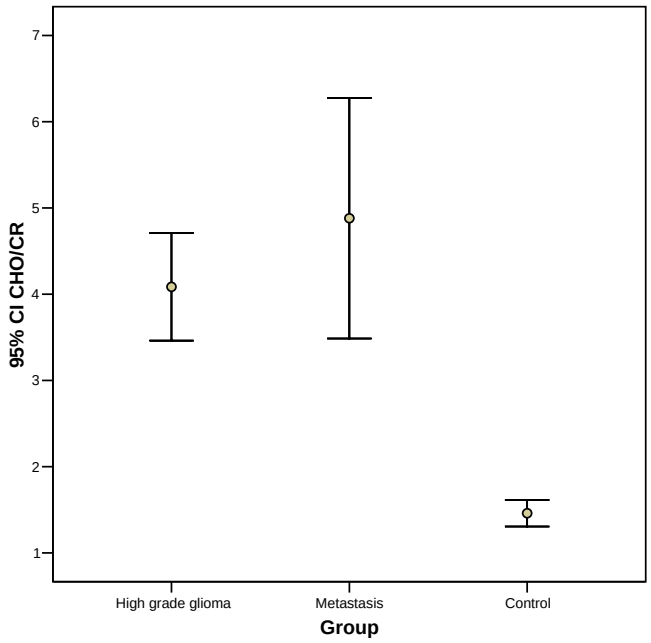

It was observed that the Mean Cho / Cr ratio for the 25 high grade tumours was 4.09±1.51 and 14 metastatic lesions was 4.88 ± 2.41. **There was no significant statistical difference between high grade tumors and metastasis.** The Mean Cho / Cr of control was 1.46 ±0.28 (n=15). There was a statistically significant variation between the Cho / Cr ratios of the tumours (both high grade / metastasis) and the control with a P value of <0.001 which is statistically at 1% level of significance. (Table No: 5-15)

It is also noted that the range of ratios for metastases was wide denoting a significant variation within the group.

5.6.1. A c. High grade gliomas vs. Metastases: c) NAA/CHO ratio

Table No: 5-16

	N	Mean±S.D	P value
High grade glioma	25	0.27±0.121	<0.001
Metastasis	14	0.47±0.247	
Control	15	1.69±0.221	
Total	54	0.72±0.642	

Fig No: 5-12

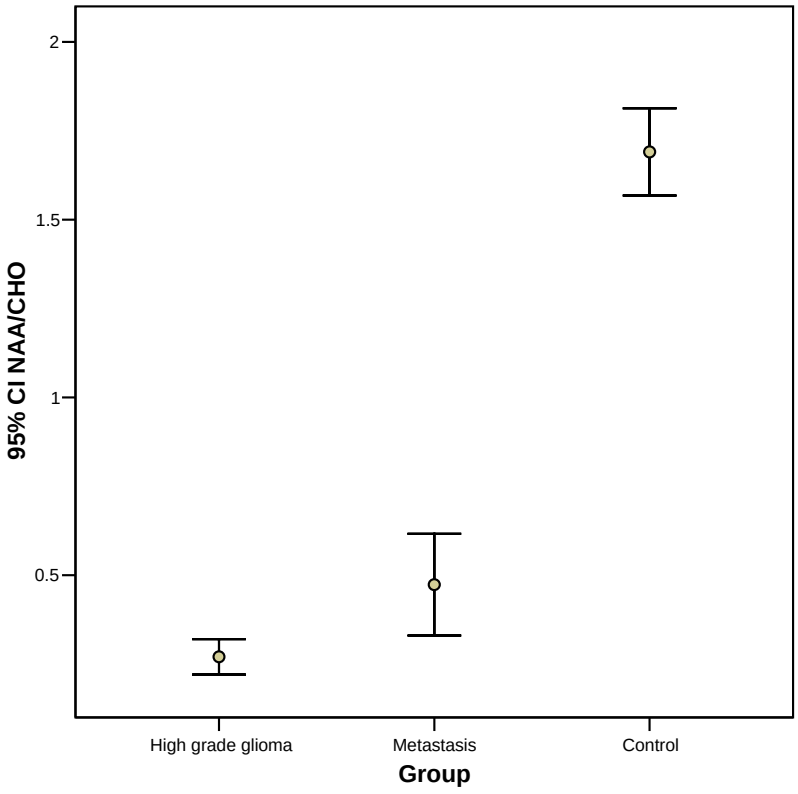

It was observed that the Mean NAA / Cho ratio for the 25 high grade gliomas was 0.27 ± 0.12 and for the 14 cases of metastases was 0.47 ± 0.25. Hence there was a statistical difference between high grade glioma & metastasis with p value ($p<0.001$). The Mean NAA/ Cho of control was 1.69

±- 0.22 (n=15). There was a statistically significant difference in the NAA / Cho ratio of the control group and metastases / high grade gliomas ($p<0.001$) at 1% level of significance. (Table No: 5-16)

There is a statistical difference between the NAA/Cho ratio of high grade gliomas and metastasis with a P value of 0.001 at 1% level of significance**.**

Figure 5-11 shows that these ratio ranges are narrow increasing the probability for distinguishing high grade tumors, metastases and the normal population.

Lipids were found in both conditions and absent in the normal control population.

Eventually it is noted that of the three ratios studied, only the **NAA / Cho ratio shows an appreciable difference between the high grade gliomas & metastases.**

The Cho / Cr shows an overlap between the two with their means almost equal (4.09 ± 1.51 and 4.88 ± 2.41 respectively) with the maximum value and the range being more for the metastases. Hence **Cho / Cr ratio is not ideal to differentiate these two conditions**. This was the reason why in this study we had one false positive and 3 false negative in diagnosing metastases and high-grade gliomas.

5.6.1.B Binary Logistic regression analysis- High grade gliomas vs Metastases

Table No: 5-17

Variables in the Equation

		B	S.E.	Wald	df	Sig.	Exp(B)
Step 1(a)	NAACR	1.098	.766	2.057	1	.152	2.999
	CHOCR	-.101	.253	.161	1	.688	.904
	NAACHO	4.440	3.354	1.752	1	.186	84.795
	Constant	-3.168	1.265	6.276	1	.012	.042

a Variable(s) entered on step 1: NAACR, CHOCR, NAACHO.

In this analysis, (Table No: 5-17) None of the above ratios show p value less than 0.05; therefore, among three metabolites ratio, No one ratio is statistically significant to differentiate high grade gliomas from metastases.

5.7. Post operative / Post radiotherapy changes versus residual / recurrent tumours:

In the post treatment (post surgical / radiotherapy) group (n=10,) the six cases histopathologically proved were five residual/ recurrent tumors and one radiation necrosis.

The diagnosis of post operative changes and /radiotherapy changes was established by clinical response and resolution of lesion on follow up MRI imaging for three cases.

On CEMRI both the recurrent / residual lesion and the post radiotherapy changes showed enhancement and resulting in difficulties in diagnosis.

In this study, one could discriminate between recurrence of tumors and radiation necrosis based both on MRI findings and MRS findings. Six cases were interpreted as recurrence based on the MRI findings (edema, mass effect, enhancement pattern of the lesions) and marked elevation of CHO/ Cr ratio and reduction in the NAA/ CHO ratio, Stereotactic biopsy confirmed this. Lipid and Lactate were present in both conditions. The NAA was reduced in both cases as there is neuronal loss in both. In two out of six cases, both residual lesions and post radiation changes were recognized.

The mean NAA / Cr, Cho / Cr and NAA/Cho area ratios of the 6 cases of recurrent / residual lesions was 0.99 ± 0.24, 4.06 ± 1.18 and 0.81 ± 0.54 respectively ; The mean NAA / Cr, Cho/Cr and NAA/Cho area ratios of 4 cases of post operative / Radiotherapy changes was 1.00 ± 0.42., 0.94 ± 0.49 and 1.02 ± 0.24 respectively.

5.7.1. A Univariate analysis –Post operative / Post Radiotherapy changes VS Residual / Recurrent Tumours :

5.7.1. A.a : NAA/CR Ratio

Table No: 5-18

	N	Mean ±S.D	P value
Post OP/RT changes	4	1.00±0.422	
Recurrence	6	0.99±0.238	<0.001
Control	15	2.37±0.234	
Total	25	1.82±0.732	

Fig No: 5-13

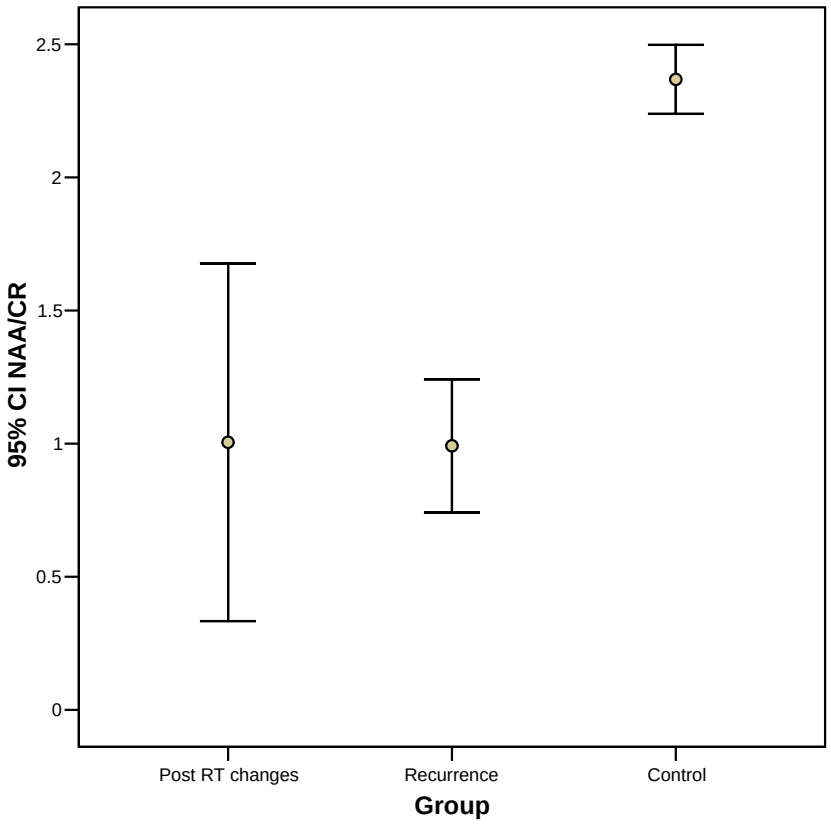

Of the total 10 post operative/radiotherapy cases, 6 were diagnosed to have residual / recurrent changes and 4 were found to have post operative gliosis /post radio radiotherapy changes.

The mean NAA / Cr ratio of the 6 cases of recurrent / residual lesions was 0.99 ± 0.24 and in the 4 cases of post operative / RT changes was 1.00 ± 0.42. The mean area ratio NAA / Cr in the control group (n=15) was 2.37 ± 0.23.(Table No:5-18) There is a significant overlap in the two ratios in recurrence and post Op changes and hence not of significance .The control group however shows a notable difference among the group. **This is due to neuronal loss in both groups**

Post operative / Post Radiotherapy changes VS Residual / Recurrent Tumours:

5.7.1 A. b) CHO/CR ratio

Table No: 5-19

	N	Mean± S.D	P value
Post OP changes	4	0.94±0.487	<0.001
Recurrence	6	4.06±1.181	
Control	15	1.46±0.277	
Total	25	2.00±1.340	

Fig No: 5-14

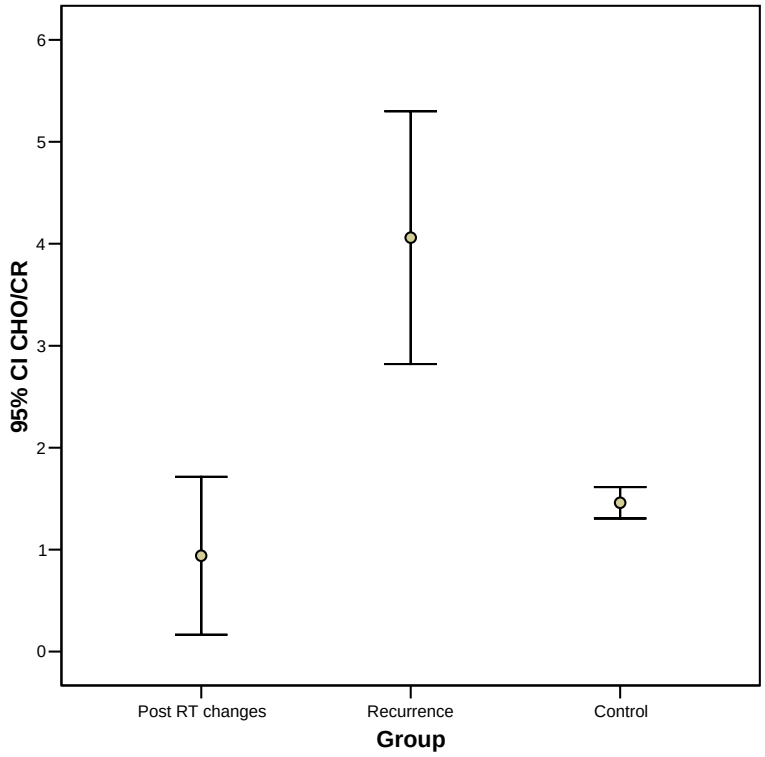

The Mean Cho / Cr ratio of 6 cases of recurrent / residual lesions was 4.06±1.18 and for the 4 cases of post operative gliosis / RT necrosis was 0.94 ± 0.49. The Mean Cho / Cr of controls being 1.46 ±0.28 (n=15). There is a statistically significant variation between the Cho / Cr ratios of the recurrent / residual lesions and the post op / RT changes with a P value of <0.001 which is statistically significant at 1% level of significance.(TableNo:5-19). The control group ratios are similar to post op gliosis / RT changes as there is no tumour in both conditions to increase the choline values.

It is also noted that the range of ratios for recurrence is wide and denotes a significant variation within the group.

The Mean Cho/Cr area ratio (4.06±1.18) of recurrent / residual tumours was significantly higher than the Cho/ Cr area ratio (0.94 ± 0.49) of post operative gliosis/ post radiation.

Hence the metabolic ratio Cho/ Cr is a good marker to discriminate between recurrences from post op / RT changes in this study.

Post operative / Post Radiotherapy changes VS Residual / Recurrent Tumours:

5.7.1.A.c NAA/CHO ratio

Table No: 5-20

	N	Mean ±S.D	P value
Post OP/ RT changes	4	1.02±0.241	<0.001
Recurrence	6	0.81±0.544	
Control	15	1.69±0.221	
Total	25	1.37±0.512	

Fig No: 5-15

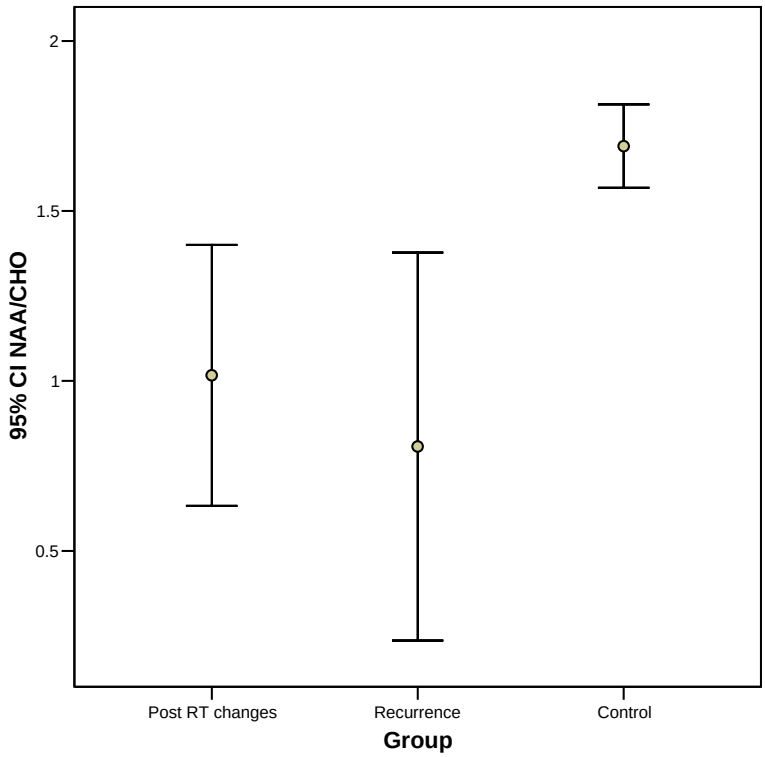

The Mean NAA / Cho ratio for the 6 cases of recurrent / residual lesions was 0.81 ± 0.54 and for the 4 cases of post operative / RT changes was 1.02 ± 0.24. The Mean Cho / Cr of control was 1.69 ±0.22 (n=15). There was a statistically significant difference in the NAA / Cho ratio of the control group as compared to those of the recurrence and post operative / RT changes with a P value of <0.001 at 1% level of significance.(Table No:5-20)

The above analysis shows that, of the three ratios, **the Cho / Cr ratio is the one that is statistically significant in differentiating between recurrence and post OP / RT changes with a P value of <0.001 at 1% level of significance.**

5.8. Distribution of specific metabolites in various intracranial lesions:

The presence of certain metabolites viz., Lipids, Lactate, Glutamine, Alanine, Amino acids, Myoinositol and Glycine were assigned a grade of 1+ to 4+ based on the level of their presence.

In this study, it was found that Lipid at 0.9 -1.4 ppm was grossly elevated in high grade tumours that aided in differentiating them from low grade tumours in which Lipids if present were in small amounts only. The fact that high grade tumours mostly have necrotic portions within, explains the presence of Lipids more consistently in these tumours rather than the low grade counterparts where necrotic areas are rare.

Of the seven cases of Meningioma, six showed the presence of Alanine at 1.48 ppm.

Among the brain abscesses, the tuberculous abscesses showed a grossly elevated Lipid component, whereas, the pyogenic abscesses showed the presence of Amino acids in their spectrum. Amino acids were also noted in the toxoplasmosis.

Among the four cases of demyelination three of them were noted to have Myo-inositol (at 3.5 ppm) in the spectrum.

Lactate was present in the Neoplastic as well as Non-neoplastic lesions with no preponderance in any of the sub group studied. Lactate was noted in five out of twenty five cases in high grade gliomas, eight out of eighteen cases in low grade gliomas, two out of thirteen cases in infective lesions and two out four cases in demyelinating disease.

Glutamate was observed in pyogenic abscess, hydatid cyst, meningiomas, epidermoid, high and few low grade tumours.

5.8. 1 Distribution of LIPID in various intracranial lesions

The distribution of lipids and lactates in various sub groups in the Neoplastic and Non neoplastic lesions the following charts were tabulated.

Table No: 5-21 Distribution of lipid in various intracranial lesions

Groups	Nil	Mild	Moderate	Severe
High grade gliomas (n=25)	4	10	6	5
Low grade gliomas(n=18)	12	3	3	-
Meningiomas (n=7)	5	-	2	-
Post RT changes(n=4)	1	1	2	-
Recurrence(n=6)	2	2	2	-
Metastasis(n=14)	1	2	6	5
Infective Lesions(n=13)	1	2	4	6
Demyelination(n=4)	4	-	-	-

Fig No: 5-16 Distribution of LIPID in various intracranial lesions

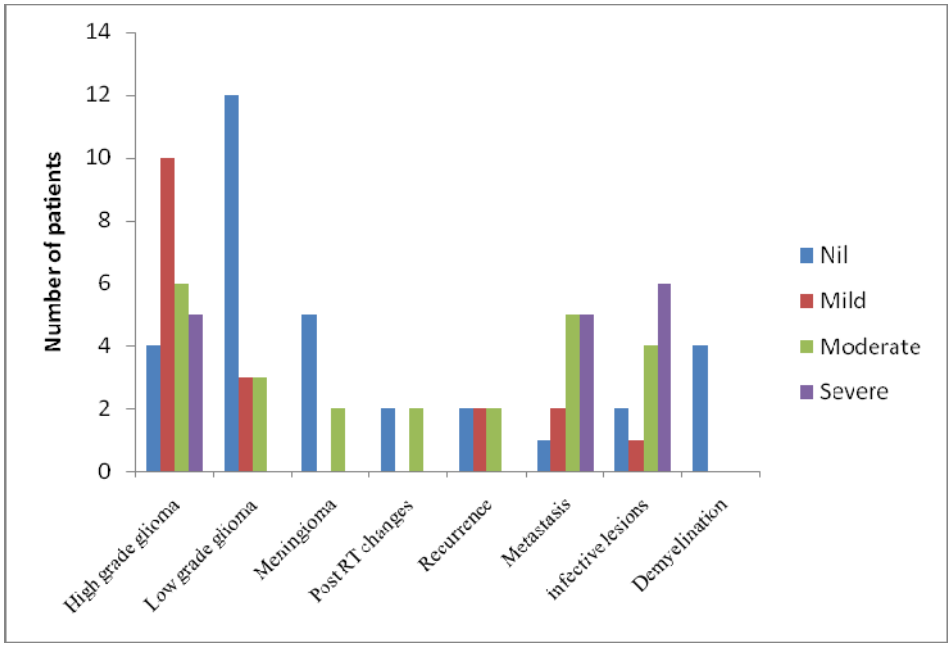

Nil (-);Mild(+); Moderate(++);Severe (+++);

From the above table, it is inferred that, out of the 25 cases of high grade gliomas 21 had a lipid peak with degrees as noted above. On the contrary the low grade gliomas did not have a consistent lipid peak with it being present in 6 cases and absent in 12 cases. Lipids were consistently present in the high grade tumors with a larger peak than in the low grade tumors.

The other neoplastic lesion in the group that had similar lipid peaks was metastasis with lipid being absent only in 1 of 14 cases.

Presence of lipid is a well known association in infective cases, namely the tuberculous lesions due to presence of lipids in the Tubercle bacilli cell wall.

5.8.2 Distribution of Lactate in various intracranial lesions

Table No: 5-22

Groups	Nil	Mild	Moderate	Severe
High grade glioma(n=25)	20	3	-	2
Low grade glioma(n=18)	10	2	4	2
Meningioma(n=7)	7	-	-	-
Post RT changes(n=4)	4	-	-	-
Recurrence(n=6)	5	-	1	-
Metastasis(n=14)	12	-	2	-
infected cyst(n=13)	11	-	1	1
Demyelination(n=4)	2	-	2	-

Fig No: 5-17 Distribution of Lactate in various intracranial lesions

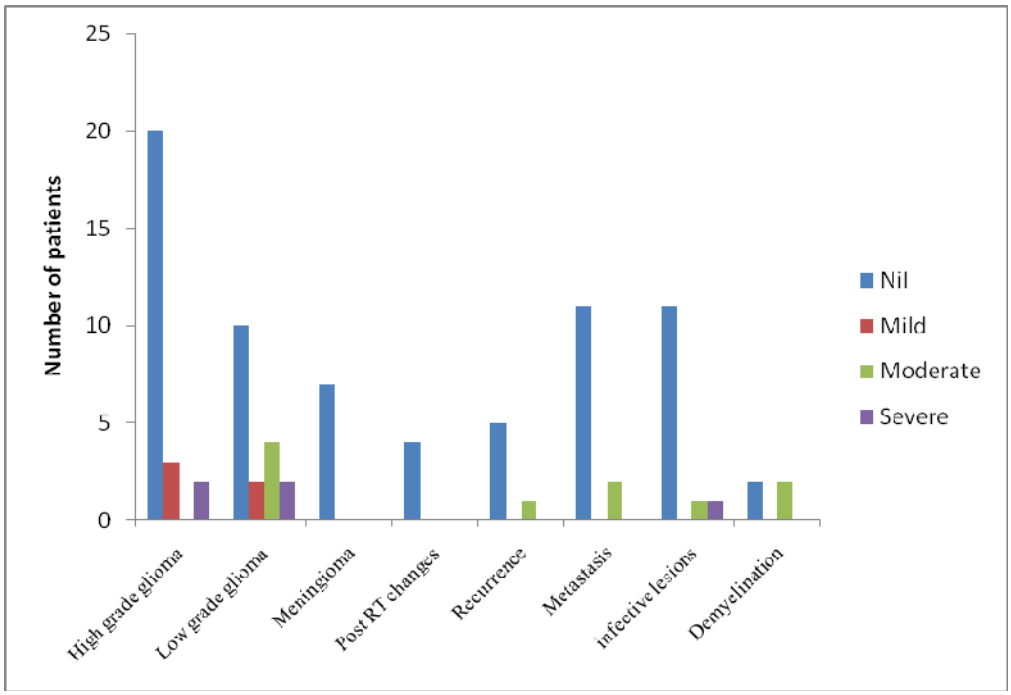

Nil (-);Mild(+); Moderate(++);Severe (+++);

5.9. Non- Neoplastic lesions:

Of the 21 non-neoplastic lesions, histopathological diagnosis was obtained by either stereotactic biopsy in 4 cases or by aspiration of pus material in 3 cases. In the remaining 14 cases of non- neoplastic lesions, a presumptive diagnosis was made either by post treatment clinical response, or by serial imaging CT/ MRI studies or laboratory tests. Among the non neoplastic group, infective lesions (granulomas) were 13, demyelinating diseases were 4 and post op/post radiation changes were 4 .

5.9.1 Infective lesions:

Among the thirteen cases of infective lesions, there were eight granulomatous (tuberculomas), (biopsy proven in two cases and post treatment clinical response in six cases), three histologically proven cases of cerebral abscesses, one case of toxoplasmosis in a patients with immuno-compromised status (HIV positive individual) and one case of intracerebral infected cyst in a patient with hydatid cyst in the liver.

In this study of 13 cases of infective lesions, there was absence of the metabolites NAA, CHO and Cr in two patients. Others showed presence of NAA, CHO and Cr. **All the granulomatous lesions (Tuberculomas) shows moderate to marked elevation of lipid levels (3+or 4+) due to the presence of presence of lipid rich cell wall in the caseous material.**

Table No: 5-23 Analysis of neoplastic Vs infective lesions

	group	N	Mean±S.D	P value
NAA/CR	Neoplastic	70	1.21±0.763	0.762
	Infective	13	1.28±0.808	
CHO/CR	Neoplastic	70	3.87±2.206	<0.001**
	Infective	13	1.04±0.587	
NAA/CHO	Neoplastic	70	0.45±0.286	0.011*
	Infective	13	1.15±0.838	

The Cho/Cr ratio were mildly raised in 8 cases and not raised in 3. These are differentiated from neoplastic lesions by presence of lipid with only mild increase in Choline or no increase in Choline compared to a marked increase in tumors.

It is observed that the Mean Cho / Cr ratio (1.04 ± 0.58) of infective lesions was lesser than the Mean Cho / Cr ratio (3.87± 2.20) of Neoplastic lesions in this study.

The above analysis shows that, of the three ratios, **the Cho / Cr ratio is the one that is statistically significant in differentiating between neoplastic lesions and infective lesions with p value of <0.001 at 1% level of significance. The NAA/Cho ratio is also significant metabolite ratio in differentiating infective lesions from neoplastic lesions with a p value of <0.011.**

The mean NAA / Cr, Cho / Cr and the NAA / Cho area ratios of neoplastic group (*n*=70) were 1.21. ± 0.76, **3.87±2.20** and 0.45 ± 0.29 respectively, the mean NAA / Cr; Cho / Cr and the NAA / Cho area ratios of these infective lesions (*n*=13) were 1.28 ± 0.80; **1.04 ± 0.58** and 1.15 ± 0.83 and metabolic ratio of control group (*n*=15) were 2.37 ±0.23, **1.46 ±0.28** and, 1.69 ± 0.22 respectively.(Table No:5-23)

In this study, three cases were diagnosed as cerebral abscesses. Acetate and amino acid were elevated in two case and lip, lac, glx were elevated in the other case. One case of toxoplasmosis showed normal NAA / Cr ratio with raised Cho / Cr ratio and presence of lipids and amino acids. The amino acids detected at 0.9ppm are the products of proteolysis caused by enzymes released from neutrophil cells. Because these metabolites have never been detected in neoplasms, their detection is strongly indicative of a cerebral abscess .The broad resonance seen at 0.9 ppm in the in vivo spectrum was assigned to cytosolic amino acid residues i.e. valine, leucine.

One known case of hydatid disease of the liver presented with an ~ 4cm cystic lesion with multiple septation and adjacent few daughter cysts with rim enhancement in the right frontal region and MRS showed Lip+++,Lac++ at 1.3ppm, Succinate at 2.4ppm and alanine at 1.4ppm.

In this study**, tuberculomas had moderate to marked elevation of lipid levels (3+or 4+) due to the presence of presence of lipid rich cell wall in the caseous material. The cerebral abscesses displayed Acetate and amino acid at 0.9ppm.**

5.9.2 DEMYELINATION:

The diagnosis of demyelinating diseases was established in one out of four cases as astrocytic gliosis on HPE. In the other three cases, a presumptive diagnosis was made on clinical grounds and or by post treatment clinical response, or by serial imaging CT/ MRI studies. Clinically these patients presented with either symptoms of tingling sensations of the limbs, dysphagia or diplopia.

One of the presumed cases of demyelination was ill-defined, appearing hypo intense on T1 WI and hyper intense on T2 WI and FLAIR sequences. In two other cases, the lesions were multiple, focal, nodular lesions in the white matter with their long axis oriented perpendicular to the ventricles. Lesions were seen involving the brain stem, the thalamus & corpus callosum. One case was unusual simulating a neoplasm with mass effect. All the four patients had solid lesions, two of showing mild enhancement, one showing intense enhancement and one showing no enhancement.

Table No: 5-24 Analysis of Neoplastic Vs Demyelinating lesions

	Group	N	Mean±S.D	P value
NAA/CR	Neoplastic	70	1.21±0.763	0.917
	demyelination	4	1.01±0.202	
CHO/CR	Neoplastic	70	3.87±2.206	0.028*
	Demyelination	4	2.00±0.518	
NAA/CHO	Neoplastic	70	0.45±0.286	0.881
	Demyelination	4	0.37±0.102	

The mean NAA / Cr; Cho / Cr and the NAA / Cho area ratios were 1.01 ± 0.02; 2.00 ± 0.51 and 0.37 ±0.10(*n*=4) respectively, as compared to a metabolic ratio of 2.37 ±0.23, 1.46 ±0.28 and, 1.69 ± 0.22 respectively in the of control group (*n*=15). Compared to the control group, a decrease in NAA/CR and NAA/Cho ratios was a significant MR spectroscopic parameters associated with demyelinating disease**. Cho/Cr is a significant metabolic ratio in differentiating demyelinating lesion from neoplastic lesions (p value of <0.028).(Table No:5-24)**

Of the 4 cases of demyelination, the metabolic ratio analysis was not significantly different from that in low grade gliomas and the other non neoplastic lesions. However, distribution of lesions, location, enhancement pattern on CEMRI and diffusion weighted imaging features have characteristic appearances and MRS is useful in differentiating demyelination from a neoplastic lesion.

5.10. Analysis and Observations on Multi-voxel spectroscopy study:

MR spectroscopic results were evaluated for the distribution of pathologic spectra across the lesion and neighbouring radiologically normal-appearing tissue.

Spectra were defined as **pathologic spectra** when the ratio of *N*-acetylaspartate/choline-containing compounds (NAA/Cho) was less than 1. Distribution patterns of pathologic spectra were classified in two groups: those limited to the region corresponding to the contrast enhancement, (intra-tumoral) and those outside the region corresponding to the contrast enhancement(peri-tumoral /perilesional area) based on an earlier study conducted by Isabella Maria Burtscher, et al 2000.

The Multi- voxel MR spectroscopic distribution patterns of pathologic spectra were correlated with histopathologic findings in 15 patients. They included High grade gliomas, grade III (one), &grade IV astrocytomas(two) and lymphoma (one) . All showed pathologic spectra in both intra-tumoral and peri-tumoralregions. Three low grade gliomas, one Meningioma and two metastases (of adenocarcinoma) showed no pathologic spectra in the peritumoral region.

Five patients with gliomas (post operative and post radiotherapy) were followed up. Of, two cases (grade III anaplastic astrocytomas) showed pathologic spectra in the peritumoral region and intra tumoral region denoting recurrence. The spectra taken, away from the tumour, showed broad based peak between 0.5 and 2 ppm representing lipid and lactate with depressed

Cho and NAA metabolites representing radiation necrosis. In two patients with grade II astrocytomas, the lesion showed pathologic spectra in intratumoral regions representing residual / recurrence of the lesion and no pathologic spectra in the peritumoral region. Another case showed no pathologic spectra both in the intratumoral and peritumoral regions indicating no residual or recurrence of the tumour.

In this Multi voxel MRS study of 15 cases, all high grade gliomas and lymphoma (6 out of 15), showed pathologic spectra (**with NAA/Cho ratios of less than 1)** in both intra-tumoral and peri-tumoral regions. All the low grade gliomas, metastases, and Meningiomas studied with MV MRS (9 out of 15), showed no pathologic spectra in the peritumoral region

The multi-voxel spectroscopy(MV- MRS) results revealed that tumor infiltration beyond the area of contrast enhancement (i.e. beyond the margins of radiologically obvious tumour) in patients with high-grade gliomas disclosed on MR spectroscopy as pathologic spectra with NAA/Cho ratios of less than 1, whereas, relatively discrete or non infiltrativet umours like metastasis did not show this pathological spectra outside the lesion.

5.11 . Summary of Analysis & Results in this study.

1. **Neoplastic vs Non-neoplastic lesions :** Neoplastic lesions were clearly differentiated from non-neoplastic and normal control population when the Cho/Cr ratio is studied. Both Univariate and Multivariate analysis revealed that **among three metabolites ratio, only Cho/Cr area ratio is more statistically significant in differentiating neoplastic from non-neoplastic lesions.** The Mean Cho / Cr area ratio (3.87± 2.20 (n=70)) for Neoplastic tumors was greater than that for Nonneoplastic lesions (1.2 ±.66 (n=21). Decrease in NAA/Cho ratio was also a significant MR spectroscopic parameter in the differentiation of neoplastic lesion from non neoplastic lesions. NAA/Cr area ratio did not provide any significant difference between neoplastic and non neoplastic lesions but it differentiated them from normal brain.

2. **High Grade Gliomas VS Low Grade Gliomas:** Univarient analysis showed that only increase in Cho / Cr ratio and decrease in NAA/Cho area ratios was statistically significant in distinguishing between tumor grades in high grade and low grade tumors. Binary Logistic regression analysis revealed **among three metabolites ratios, only NAA/Cho area ratio was statistically significant in differentiating High grade from low grade gliomas.** Decrease in NAA/Cho area ratios was a significant MR spectroscopic parameters in the differentiation of low grade from malignant high grade tumors. The mean NAA/CHO area ratio (0.27 ± 0.12, n = 25) of high grade gliomas was lesser than mean NAA/CHO area ratio of low grade gliomas (0.64 ± 0.17, n = 18) with a p value < 0.001.

3. **<u>High grade gliomas vs Metastases</u> :** Anova univariate statistical analysis revealed that **there was a statistical** difference between NAA/Cho ratio in high grade gliomas and metastasis (P value of 0.001 at 1% level of significance) whereas, Binary Logistic regression analysis revealed that **among three metabolites ratios, none of the ratios was statistically significant in differentiating high grade gliomas from metastases.**

4. **<u>Post operative / Post radiotherapy changes vs residual / recurrent tumours</u> :**

   The Mean Cho / Cr ratio of recurrent / residual lesions was 4.06 ±1.18, (*n*=6) and for post operative / RT changes were 0.94 ± 0.49,(*n*=4),with a P value of <0.001 which is statistically significant at 1% level .**The Mean Cho/Cr area ratio (4.06±1.18) of recurrent / residual tumors was significantly higher than the Cho/ Cr area ratio (0.94 ± 0.49) of post operative gliosis/ post radiation necrosis .**

   Hence this metabolic ratio, Cho/ Cr is good marker to discriminate between recurrence from post operative / RT changes.

5. **<u>Tuberculosis vs pyogenic lesions</u>:** Tuberculomas revealed that moderate to marked elevation of lipid levels (3+or 4+) due to the presence of presence of lipid rich cell wall in the caseous material .

In tuberculomas (n= 13), Cho/Cr ratio were mildly raised in 8 cases and not raised in 3. However, tuberculomas differentiated from neoplastic lesions by presence of lipid with only mild increase in Choline or no increase

in Choline compared to a marked increase in tumors. In this analysis, Cho / Cr ratio was the one that is statistically significant in differentiating between neoplastic lesions and infective lesions with a p value of <0.001 at 1% level. The NAA/Cho ratio is also significant metabolite ratio in differentiating infective lesions from neoplastic lesions with a p value of <0.011.

Pyogenic abscesses displayed elevation of resonance signal for amino acid (at 0.9 ppm), alanine (at 1.47 ppm), acetate (at 1.92 ppm), pyruvate (at 2.37 ppm), and succinate (at 2.40 ppm), and absent Cho and NAA . Tuberculous abscess showed high lipid and lactate peaks and absent amino acids (leucine, isoleucine, and valine) and succinate peak.

6. Presence of Alanine at 1.48 ppm in Meningioma in six out of seven cases, elevation of Myoinositol (at 3.5 ppm) in demyelination in three out four cases were observed. **Cho/Cr is a significant metabolic ratio in differentiating demyelinating lesions from neoplastic lesions (p value of <0.028).** Compared to the control group, a decrease in NAA/CR and NAA/Cho ratios was a significant MR spectroscopic parameters associated with demyelinating disease**.**

7. In this study, the **sensitivity, specificity, Positive predictive value and Negative Predictive Value** for determining **malignant lesions** and non malignant lesions with MRI guided ^{1}H-MRS were **90.9%, 97.9%, 97.6%, and 92%,** respectively**.** ROC curve analysis showed **94.3% accuracy** for determination of malignant lesion.

CHAPTER 6

DISCUSSION

"An idea that is developed and put into action is more important than an idea that exists only as an idea"

The purpose of this study is to find out if it is possible to improve the preoperative diagnostic efficacy of MR Imaging in characterizing different intracranial lesions by using in addition in- vivo Proton MR Spectroscopy (^{1}H MRS). ^{1}H MRS is a noninvasive technique which provides metabolic information complementary to the anatomical changes found in routine MR Imaging. This has proved useful in providing additional information to differentiate various intracranial diseases. The presence of certain metabolites and their ratio variations from the normal assigned ratios in control populations is said to provide additional useful information which could be of help to (a) Distinguish a non neoplastic from a neoplastic lesion (b) Differentiate high grade from low grade tumours (c) Differentiate Radiation necrosis from Tumour Recurrence (d) Distinguish Metastases from High grade tumors. This information is very important for treatment decisions, planning surgical resection, biopsies, and radiation therapy.

6.1. MRS: Technical considerations

All MR spectroscopic examinations in this study were based on the single-voxel (SVS) technique. This technique can be considered a limitation, as Multi-voxel MR Spectroscopy (MV- MRS) techniques provide smaller volumes of interest and a better evaluation of tumour heterogeneity thereby

avoiding sampling errors (89). Sampling errors in MR spectroscopy may be minimized with the use of two-dimensional chemical-shift imaging, (MV-MRS) in which a grid of voxels is placed over a lesion and a spectrum is generated from each element in the grid, at the cost of increasing the examination time. Hence, in addition to the SVS technique, MV- MRS was performed in 15 patients, in whom, lesions were ill-defined or infiltrative on routine MR imaging sequences, to assess the metabolic nature & the distribution of these metabolites across the lesion and in the neighboring radiologically normal-appearing tissue.

However, single-voxel techniques may have some relevant advantages compared with multivoxel techniques(89). Single-voxel 1H-MR spectroscopy is quicker and easier to evaluate in a standard clinical setting, providing the opportunity to obtain more than one spectrum (ie, spectra at two different TEs) in a reasonable amount of time. In pursuit of this advantage the investigator found that evaluating spectra at both short and long TE improves the level of accuracy. Also, in a recent study, Hourani et al (138) had reported that technical reasons precluded acquisition of multi-voxel data at short TE in their study. This would influence evaluation of some resonances relevant for tumour classification, such as Myo-inositol, GLx and amino acids etc which is under-evaluated at long TE spectroscopy methods.

Rand SD, Prost R, Haughton V, et al.(75) estimated that the diagnostic accuracy of MR spectroscopy in differentiating patients from control subjects was 0.96, and in nonblinded and blinded discrimination of neoplastic from non-neoplastic disease it was 0.96 and 0.83, respectively. However the use of

MR spectroscopy in the differential diagnosis of different tumour types was limited. **Moller-Hartmann et al (72) evaluated that the additional information of MR spectroscopy led to a 15.4% higher number of correct diagnoses and to 6.2% fewer incorrect and 16% fewer equivocal diagnoses than with MR imaging data alone**. Moreover, the additional information did not lead to incorrect diagnoses when compared with structural MRI alone. **Therefore, it is concluded that the biochemical information given by ^{1}H-MRS is a useful additional diagnostic modality for preoperative grading of human gliomas, differentiating contrast-enhancing neoplastic and non-neoplastic lesions such as cerebral metastases, high-grade gliomas and abscesses, and allowing differentiation of non-contrast enhancing lesions such as low-grade gliomas from acute and sub acute infarction.**

In this study, the efficacy of MRS in combination with routine MR imaging to characterize intracranial mass lesions yielded promising results in differentiating malignant (high grade neoplastic lesions) from benign (low grade neoplasms and non - neoplastic lesions) with a sensitivity of 90.9%, specificity of 97.9%, positive predictive value of 97.6%, negative predictive value of 92% and accuracy 94.3%.

6.2. Neoplastic vs. Non neoplastic lesions:

Conventional MR imaging provides important information regarding contrast material enhancement, peri-enhancement edema, distant tumor foci, hemorrhage, necrosis, mass effect, and so on, which are all helpful to

characterize tumor aggressiveness and to assess tumor grade. Dean et al (130) determined that mass effect and necrosis were the two most important predictors of tumor grade. However, often a high-grade glioma may be mistaken for a low-grade glioma when it demonstrates minimal edema, no contrast enhancement, no necrosis, and no mass effect. Similarly in this study, a case of solitary metastasis was incorrectly classified as low grade glioma based on conventional imaging due to lack of edema and significant enhancement.

Conversely, low-grade gliomas can sometimes demonstrate peritumoral edema, contrast enhancement, central necrosis, and mass effect and can be mistaken for a high-grade glioma. Conventional MR imaging readily provides evidence of contrast enhancement, signifying blood-brain barrier breakdown, which is often associated with higher tumor grade. However, contrast material enhancement alone is not always accurate in predicting tumor grade. Ginsberg et al (139) demonstrated that lack of enhancement of supratentorial gliomas does not equate with low-grade gliomas. All low-grade tumors showed contrast enhancement, but almost one-fifth of Glioblastoma multiforme tumors did not. The peritumoral hyperintensity on conventional T2-weighted MR images is nonspecific, representing tumor infiltration, vasogenic edema, or both. Moreover, conventional MR imaging does not provide reliable information on tumor physiology such as microvascularity, angiogenesis, metabolism, micronecrosis, or cellularity, all of which are also important in determining tumor grade. These shortcomings are now partly overcome by the use of MR Spectroscopy.

6.2.1 MRS in Astrocytomas

NAA is a neuronal marker and decreases in all tumors because of the invasiveness of tumour cells within the normal tissue. Proton MR spectroscopy visible Cho-containing compounds include acetyl choline, glycerophosphocholine, and phosphocholine(140). Cho is increased in all tumors because of increased cell membrane turnover (synthesis and/or degradation) and myelin turnover; Cr/phosphocreatine, an indicator of energy metabolism, shows a variable signal intensity in proton MR spectroscopy of intracranial tumours and osmotic balance(118). Presence of the lactate and lipid peaks were usually consistent with aggressive tumours, reflecting increased anaerobic metabolism and cellular necrosis, respectively (118).

Proton MR spectroscopy readily distinguishes normal brain tissues from astrocytomas (3, 5, 74). However, proton MR spectroscopy may not be able to distinguish between different histologic grades of malignancy in astrocytomas (141). Some investigators have proposed that the presence of lactate correlates with a higher degree of malignancy and that it is commonly observed in glioblastoma multiforme (142,143).

The typical proton MR spectroscopic characteristics of astrocytomas include a significant reduction in NAA, a moderate reduction in Cr, and an elevation of Choline (3). Reduction of NAA probably indicates a loss of normal neuronal elements as they are destroyed and/or substituted by malignant cells. In astrocytomas, the NAA is reduced to 40% to 70% of that in normal brain (64). Reduction of Cr is probably related to an altered

metabolism, and elevation of Cho may reflect increased membrane synthesis and cellularity (both of which are present in tumors) (142). Elevation of lactate may reflect tumor hypoxia. The Cho peak also, is increased in the more-malignant astrocytomas (64). Proton MR spectroscopy may be used to distinguish infection from a tumor, due to the fact that the former has extremely low concentrations of Cho (64).

The Cho / Cr ratios (both area and amplitude ratios) were found to be very useful in distinguishing a neoplastic from non neoplastic process, wherein this ratio was grossly elevated in almost all the neoplastic lesions as compared to the non-neoplastic lesions. The mean Cho / Cr area ratio 3.87 ± 2.20 (n=70) in neoplastic tumours was greater than the mean non-neoplastic Cho / Cr area ratio 1.2 ± 0.66 (n=21) with p value <0.001.

It is to be noted that the mean NAA / Cho area ratio 0.45 ±0.29 (n=70) in neoplastic tumours was *lesser than* the mean NAA / Cho area ratio for non-neoplastic lesion 0.98 ± 0.72 (n=21) with a P value of <0.001.

It was observed that the NAA / Cr ratio for neoplastic (1.21 +/- 0.76; n=70) and non neoplastic lesions (1.17 +/- 0.66; n=21) show no gross difference (p=0.861). However, the control group's NAA / Cr ratio (2.37 +/- 0.23; n=15) was significantly different from that of the lesions with a P value of <0.001 which is statistically significant with CI of 95%.

Case No. 1 : Seventeen year old female presented with seizure disorder

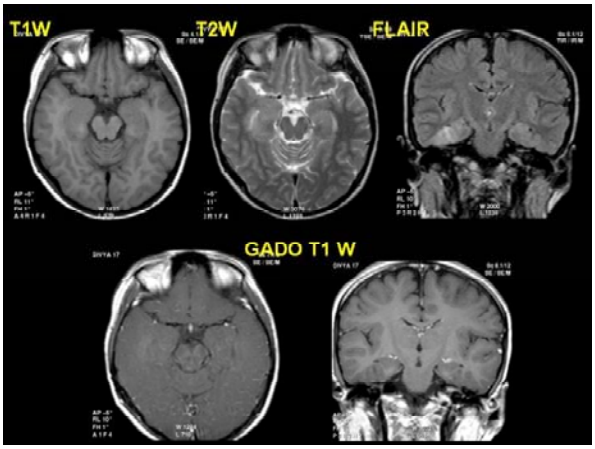

Fig. 2a: MRI shows faint, subtle, signal alteration on T2 WI in the right medial temporal cortex and non-enhancing on Post gadolinium contrast study – A nonspecific finding

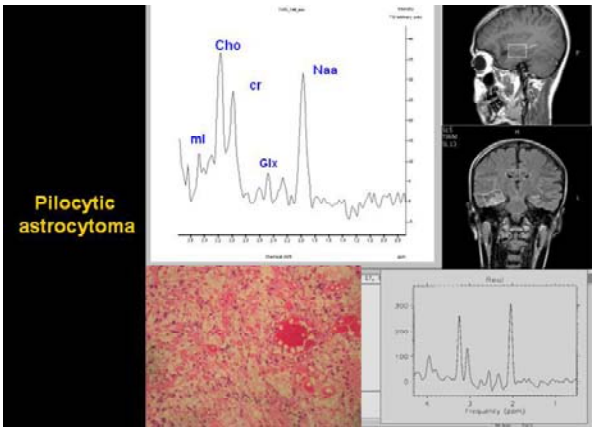

Fig. 2b: MRS reveals increased Cho/Cr ratio with small myoinositol peak at 3.5ppm representing low grade neoplasm

Case No. 2 : Twenty years old male presented with seizure

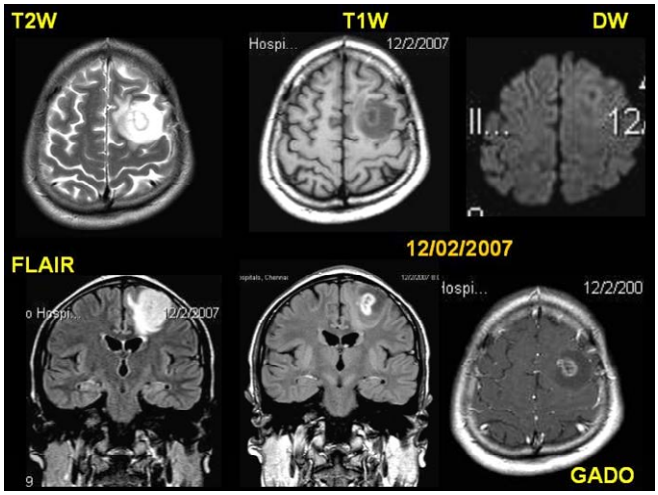

Fig. 3a: MRI shows, a small, nodular, peripheral enhancing lesion in the left frontal cortex mimicking a granuloma

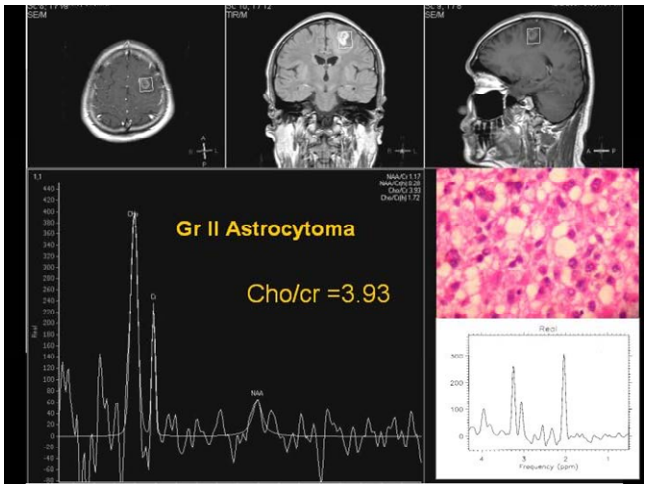

Fig. 3b: MRS reveals increased Cho/Cr ratio (3.93)with marked reduction of NAA peak suggesting a neoplasm ; Stereotactic biopsy : Grade II Astrocytoma

MRS changed the MRI diagnosis

Case No. 2 (contd.) : Post radiation follow up

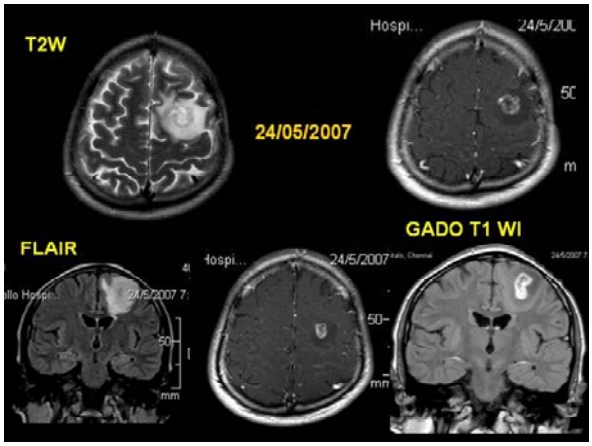

Fig. 3c: MRI after 3 months shows, a small, nodular, peripheral enhancing lesion with perilesional edema in the left frontal cortex as seen in pre-operative study- Recurrence

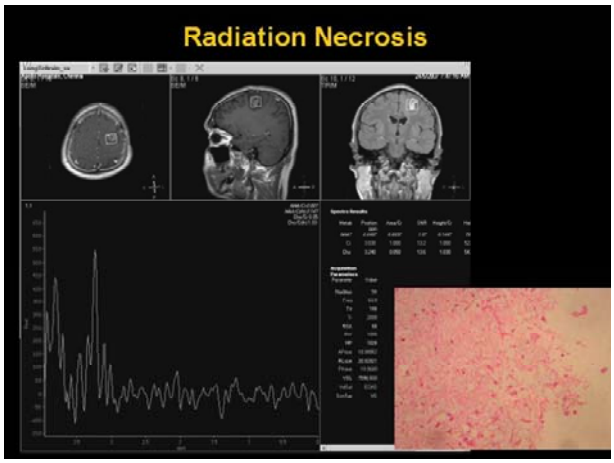

Fig. 3d: MRS reveals mild elevation of Cho peak with non-visualized NAA peak representing reactive changes
Stereotactic biopsy : Radiation changes

Case No. 3 : Twenty seven year old male presented with left side weakness for one week

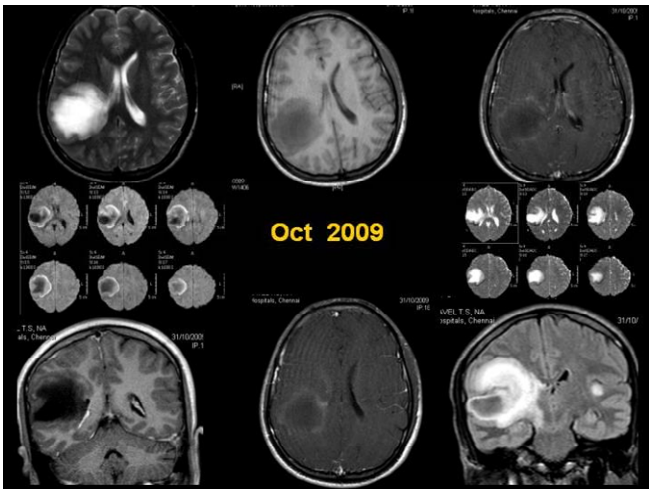

Fig. 4a: MRI shows a large, peripherally faint,indistinct enhancing lesion with perilesional edema and mass effect in the right temporal lobe; lesion reveals a peripheral rim of restricted diffusion on DW images suggesting a neoplasm

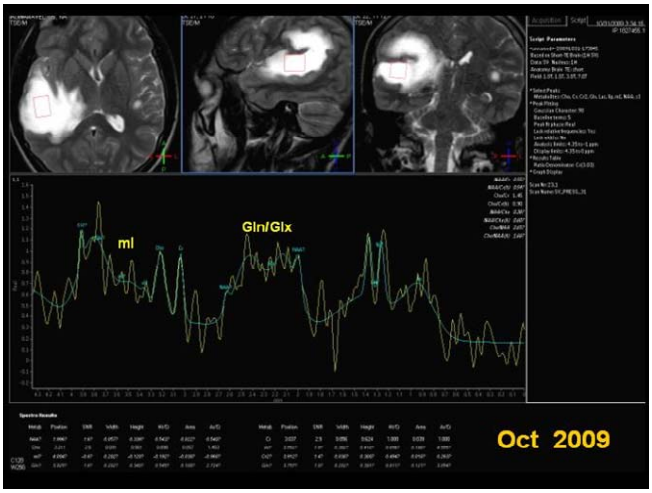

Fig. 4b: MRS reveals a broad peak between 2.1 and 2.5 ppm representing Gly/Gln and a myo-inositol peak; marked reduction in Cho and NAA suggesting non-neoplastic lesion; possibility of demyelinating disease is considered

Case No. 3 (contd.): Post medical treatment Follow up

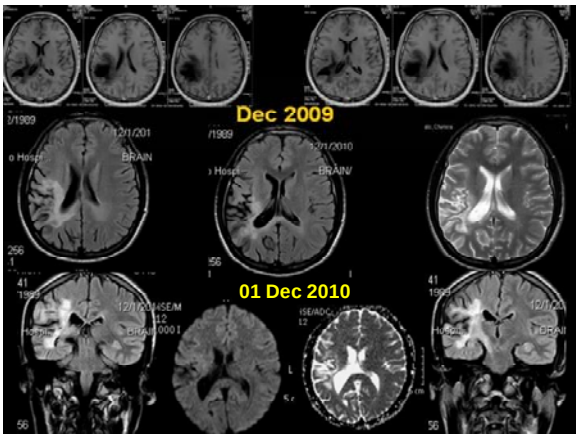

Fig. 4c: MRIs (after 2 months and 14 months)show significant reduction in the size of the lesion on Dec 2009; gliosis in subcortical and deep white matter with wallerian degeneration along the tract on Dec 2010 studies

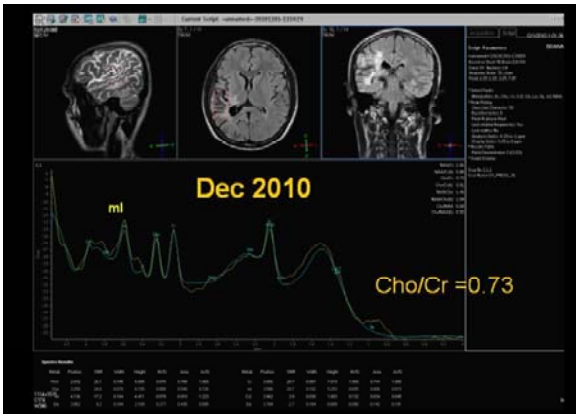

Fig. 4d: MRS reveals a myo-inositol peak; marked reduction in Cho and NAA and broad lipid peak representing chronic demyelinating disease

MRI aided MRS obviated need for biopsy or surgery in this patient

Case No. 4 : Twenty one year old male presented with seizure disorder

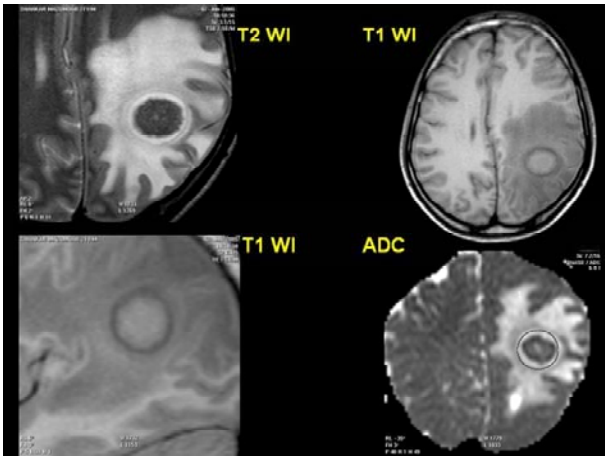

Fig. 5a: MRI shows, a circumscribed nodular, peripheral enhancing lesion with central hypointense area and hyperintense rim on T2 WI in the left parietal lobe ; ? Granuloma. ? Neoplasm

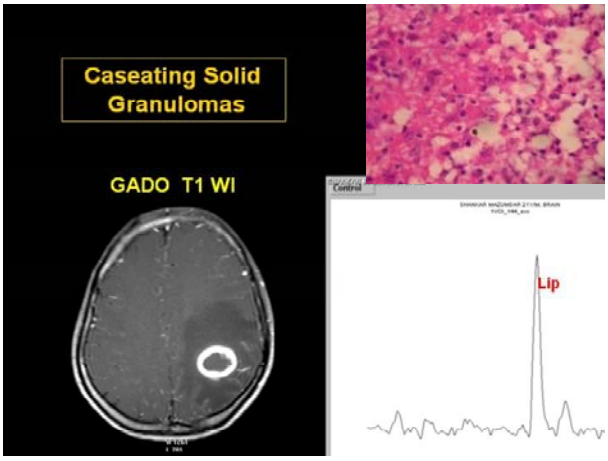

Fig. 5b: MRS reveals a sharp lipid peak at 1.3ppm and absence of Cho, NAA and other metabolites representing Tuberculoma

In this study, the neoplastic lesions can be clearly differentiated from the non-neoplastic and normal control population when the Cho / Cr ratio is studied. Both Univariate and Multivariate analysis reveal that among the three metabolites ratios, only Cho / Cr area ratio is more statistically significant in differentiating neoplastic from non-neoplastic lesions. The mean Cho / Cr area ratio (3.87± 2.20 (n=70)) for neoplastic tumors is greater than that of non-neoplastic lesions (1.2 ±.66 (n=21)). Decrease in NAA / Cho ratio is also a significant MR spectroscopic parameter in the differentiation of neoplastic from non neoplastic lesions. However the NAA / Cr area ratio is not significantly different between neoplastic and non neoplastic groups, but it differentiates them from the control group.

Fayed N, et al (81) in their study has concluded that Cho / Cr ratio higher than 1.56 predicted malignancy at 88.9% sensitivity and 91.7% specificity which also correlates with this study.

Witold Gajewicz et al (77) study on 29 patients have concluded that 1H MRS proved to be a useful tool in establishing tumor type and differentiating between neoplastic and large inflammatory tumor-like lesions, which is consistent with this study. However, their study included only 2 non-neoplastic lesions and was of limited value.

Jennifer Butzen et al (84) have conducted a study on 99 patients and concluded that Cho / NAA amplitude ratio of >1 was the threshold for tumour detection. Though this study had analyzed NAA / Cho area ratio, there was an inverse correlation that majority of the neoplastic cases (except one case of

metastases) had the ratio <0.9. Likewise the NAA / Cho ratio for non neoplastic cases were >0.9 except in 4 cases of infective etiology and 1 case of post-op gliosis. This reduction of NAA / Cho ratio in infective lesion is related to necrosis in chronic abscess or gliosis. However all the cases of demyelination had <0.9 as reduction of NAA and mild elevation of Choline an observation consistent with feature of chronic demyelinating disease. It has been shown that NAA is decreased in patients with chronic multiple sclerosis in whom axonal loss has occurred (**125**).

Mishra et al (92) differentiated 52 histo-pathologically proved tumor cysts, abscesses, or benign cysts by using single voxel 1H-MR spectroscopy and diffusion-weighted MR imaging. The authors reported the sensitivity and specificity of 1H-MR spectroscopy to be 96% (95% CI, 83%–99%) and 100% (95% CI, 86%– 100%) respectively.

In this study, the diagnostic threshold level of Cho / Cr ratio between the neoplastic and non neoplastic lesions was 2.0 with the neoplastic lesions being more than 2 and non-neoplastic lesions being less than that. Similarly the NAA / Cho ratio diagnostic threshold level was 0.9 with neoplastic lesions being less than that and non neoplastic lesions being more. However, this threshold value of NAA / Cho ratio (< 0.9) could also occur in chronic non- neoplastic lesion such as chronic demyelination / chronic cerebral abscess.

Lactate was present in 16 cases of neoplastic lesions and 4 of non neoplastic lesions in this study**,** more commonly in low grade glioma **(**8 out of

18 cases). The elevation of lactate levels is due to anaerobic glycolysis and hypoxia (4). Even though lactate is more likely to be found in high-grade lesions, large studies have shown that lactate cannot be used as a reliable predictor of either malignancy or poor prognosis (4, 96) as was the observation in this study.

Lipid peaks were present in 45 (of 70) patients with neoplastic lesions and 13 (of 21) patients with non neoplastic lesions. Among the neoplasms lipid peaks were high (3 or 4-severe) in high grade tumours, metastasis, lymphomas and PNET. The occurrence of lipids in tumors is indicative of a malignant lesion (4, 144).

Of 25 cases of high grade gliomas, lipids were present in 21 and lactate in 5 cases. In 18 cases of low-grade gliomas Lactate was noted in 8 cases and lipid in 6.

Lipids were present in both neoplastic and non-neoplastic lesions, but the presence of lipid with marked elevation of Cho / Cr ratio with reduction of NAA / Cho was used in differentiating neoplastic from non neoplastic lesions and these findings were in accordance with the study by Bulakbasi et al (74).

Among the non-neoplastic lesions lipids were characteristically seen as a large peak in tuberculomas, abscesses and were found absent in all 4 cases of demyelination.

6.3. Grading of Astrocytomas: High grade versus Low grade gliomas

Preoperative grading of astrocytomas is necessary, because it helps in better treatment planning and management (99).

The decrease in NAA in gliomas and astrocytomas may indicate a decrease or displacement of neurons by the tumor. This study revealed that the NAA signal to be decreased in all astrocytomas, with the higher grade tumours having the lowest levels of NAA. Higher grade astrocytomas tend to have heterogeneous tissue components. It would therefore be reasonable not to find any significant NAA in necrotic regions of malignant gliomas (98).

In this study, the NAA / Cho area ratio was found to be more in the low grade tumors than in the high grade tumors. .

6.3.1 Role of NAA / Cho ratio:

It was observed that the Mean NAA / Cho ratio for high grade astrocytomas was 0.27±0.12 (n=25) and that for low grade gliomas was 0.64 ± 0.17 (n=18) with the NAA / Cho of controls being 1.69 ±0.22 (n=15). There is a statistically significant difference in the NAA/ Cho ratio of the control group (1.69 ± 0.22), the high grade gliomas and the low grade astrocytomas with a P value of <0.001. It was also observed that these ratio ranges in this study were narrow making their probability more specific.

The NAA / Cho ratio undoubtedly distinguished high or low grade gliomas from the control group thereby helping in confirming an abnormality.

In this study, among three metabolites ratio (NAA/Cr, Cho/Cr, & NAA/Cho), only NAA/Cho area ratio is more statistically significant in differentiating High grade from Low grade gliomas (p=0.036).

A decrease in the NAA/Cho ratio is mainly due to both an increase in Cho levels and a decrease in NAA levels.

GBMs have lower NAA content compared to lower grade gliomas, probably because of fewer viable neurons and more tissue necrosis within the tumors. Andreas Stadlbauer et al (145) in their study, observed significantly lower Cho levels and higher NAA levels in grade II tumors (n = 9) compared with grade III tumors (n = 17). The average Cho/tNAA ratio over the voxels in the tumor center showed a distinct difference ($P < .001$) between grade II and III gliomas at a threshold of 0.8 (with ratios <0.8 for grade III). Though in this study NAA/CHO ratio was used rather than the Cho /NAA ratio, it also concurs with the same observation. This study found a very low NAA level due to neuronal damage and very high Choline in GBMs and only a slight reduction of the NAA level in low-grade astrocytomas.

In one case presumptive diagnosis was made as low grade Astrocytoma based on MRI aided MRS findings, and it turned out to be a high grade GR-3 Astrocytoma on HPE. This was probably due to the deceptively well circumscribed margin with mild enhancement and lack of hemorrhage and significant edema. The Cho / Cr area ratio was 2.56 which was in a median position close to the threshold value between the two and was not contributing to the diagnosis. However the NAA / Cho ratio was 0.21

favouring high grade but the misleading morphological pattern was taken onto consideration leading to a false negative diagnosis.

6.3. 2 Role of Cho/Cr ratio:

In all 25 histopathologically proven high grade tumours, the spectral pattern was characterized by dominant high resonance of lactate and lipids and extremely low NAA peak which produced a decrease in the NAA / Cr ratios and an increase in the Cho / Cr ratios (mean 4.09 +/- 1.51). This enabled the correct diagnosis of the tumor type.

The spectra in 18 low grade astrocytomas presented low NAA resonance, higher Choline / Cr ratios (mean 2.12+/-0.99), and lowered NAA / Cr ratios. The resonances of lactate and lipids were also noted in this group, but not as pronounced as in the Glioblastoma group.

There is a statistically significant variation in the Cho / Cr ratios between the high grade, low grade astrocytomas and the control population ratios with a P value of <0.001.

Case No. 5 : Forty six year old male presented with seizure disorder

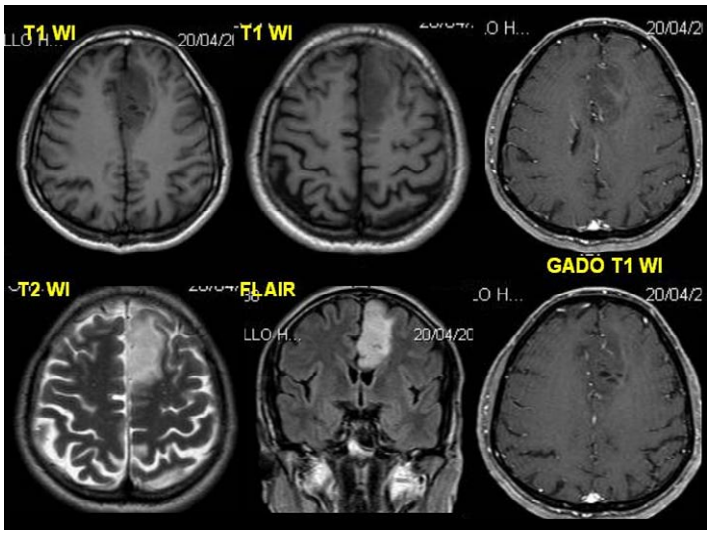

Fig. 6a: MRI shows, signal alteration on T2 WI in the left medial frontal cortex and non-enhancing on Post gadolinium contrast study – A nonspecific finding in the left frontal cortex – Focal cerebritis or neoplasm

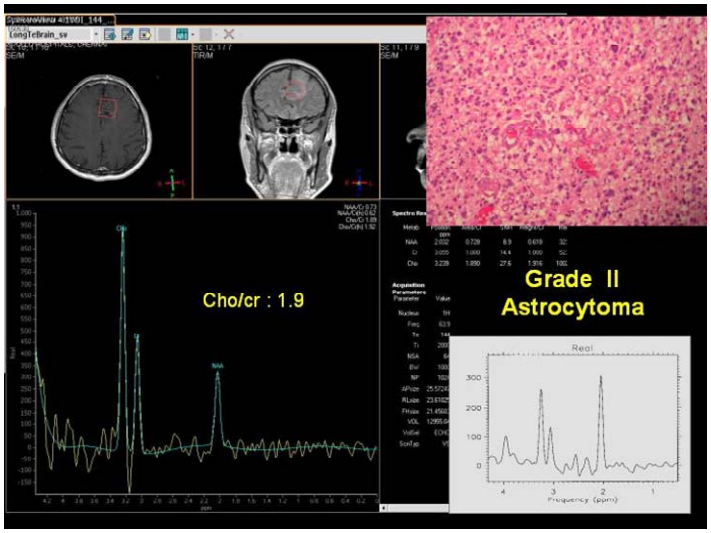

Fig. 6b: MRS reveals increased Cho/Cr ratio (1.9)with mild reduction of NAA peak suggesting a neoplasm ;
Stereotactic biopsy : Grade II Astrocytoma

Case No. 6 : Fifty seven year old male presented headache and seizure -3 months

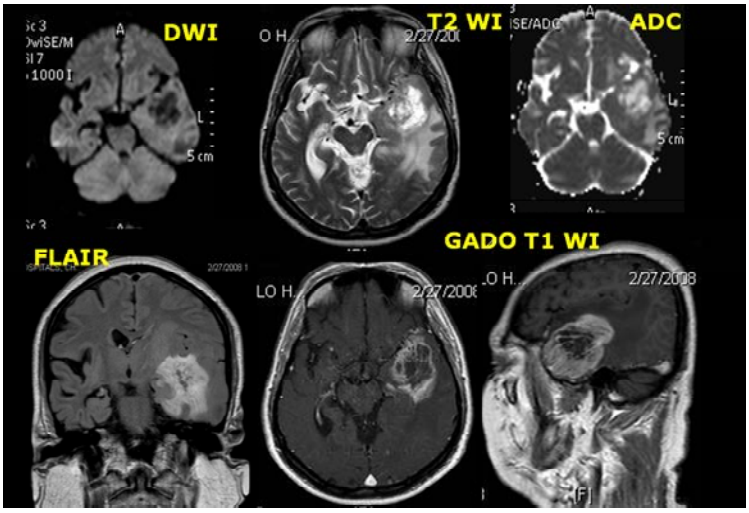

Fig No: 7 A. MRI shows, a large, thick nodular, peripheral enhancing necrotic lesion with edema and mass effect in the left temporal lobe representing high grade neoplasm

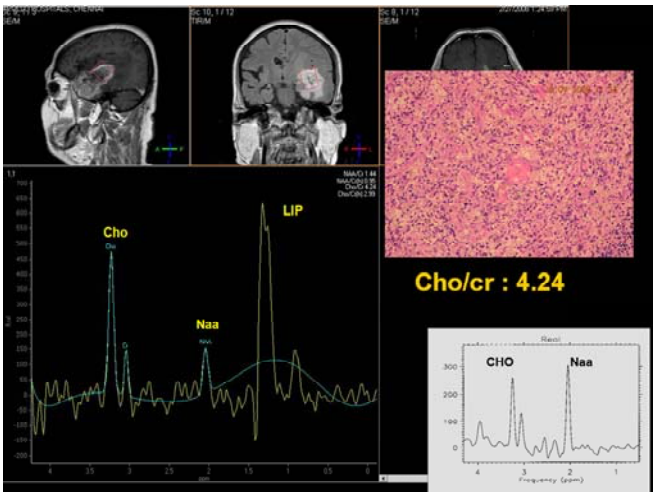

Fig No: 7 B. MRS reveals increased Cho/Cr ratio (4.24)with marked reduction of NAA peak and sharp increased in height of lipid peak - a high grade neoplasm

Biopsy : GBM

Case No. 7 : Twenty six year old male presented with headache and vomiting

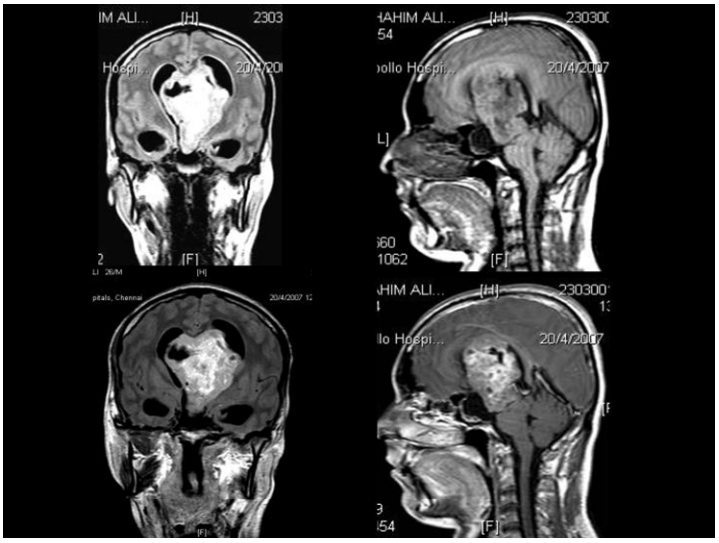

Fig. 8a: MRI shows, a large, midline, solid with cystic areas, intensely enhancing septal mass causing obstructive hydrocephalus-high grade neoplasm

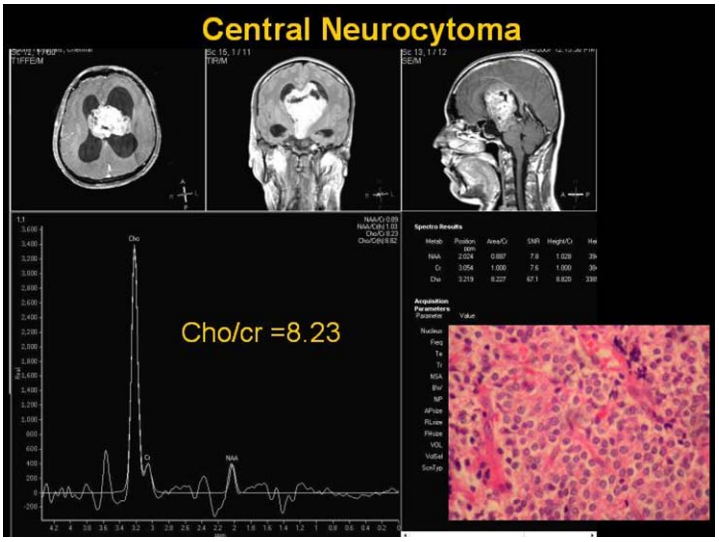

Fig. 8b: MRS reveals sharp increased choline height with Cho/Cr ratio (8.24) with marked reduction of NAA peak;
No lipid or lac peak seen. Biopsy : Central neurocytoma

H.Shimizu et al (146) observed that in 25 patients with brain tumours their **mean Cho / Cr area ratio** for grade II tumours was 1.68 ±0.43; for grade III 3.37 ±1.42 and for GBM was 5.52 ±0.12 ; D. Yang, Y. Korogi et al (147) found that the Means of maximum Cho/Cr and minimum NAA/Cr ratios were 4.73 ± 2.22, and 0.40 ± 0.06, respectively, in the high-grade gliomas and 1.84 ± 1.20, and 1.65 ± 1.61, respectively, in the low-grade gliomas; Kostas N. Fountas et al, (82) found that the Cho/ Cr ratio is a very important malignancy marker for histologic tumor grading of astrocytomas. The greater this ratio, the higher the grade of the astrocytomas. In grade I & II the cho / Cr ratio was 2.15 ± 0.26; 2.78 ± 0.09 in grade III tumours and 5.4 ± 0.16 in grade IV tumours. These results are in concordance with the findings of this study.

Kumar.A et al (86) have observed in 60 patients with intracranial lesions that the Cho/Cr ratio was significantly elevated in low grade, high grade and meningioma patients measuring about 1.85±0.36, 3.5±1.00 and 6.65±2.83 respectively as compared with the control group of 1.16± 0.18. The NAA/ Cho and NAA /Cr ratios were reduced and the above findings were highly significant statistically with confidence level of more than 99% ($p<0.01$). H. Poptani, R.K.Gupta et al (99) have observed that the mean NAA/Cho; Cho / Cr and NAA / Cr ratio in low-grade gliomas were 0.39 ± 0.12; 2.06 ±0.75 and 0.76 ± 0.29 respectively and in high grade gliomas was 0.19 ± 0.08; 2.9 ± 1.1 and 0.42 ± 0.24 respectively. These findings are in concordance with the present study. Similar to this study, the NAA/Cr ratio

did not provide any significant correlation with the degree of malignancy in their studies.

Vuori et al (148) found changes in Cho and Cr levels helpful for differentiation between grade II astrocytomas (four patients) and grade II oligodendrogliomas or oligoastrocytomas (six patients). Grade II astrocytomas showed a modest increase in Cho (69%) and decrease in Cr (-27%), whereas grade II oligodendrogliomas and oligoastrocytomas had a pronounced Cho increase (149%) and Cr increase (58%) compared with age- and sex-matched control subjects. These differences were without overlap between the subgroups, but Vuori et al were not able to define threshold values for differentiation

In this study, summarizing differentiation between the high grade and low grade tumors, univariate analysis shows that only the increase in Cho / Cr ratio and decrease in NAA/Cho area ratios are statistically significant in distinguishing between the tumor grades. Binary Logistic regression analysis reveals among three metabolites ratio, only NAA/Cho area ratio is more statistically significant in differentiating High grade from low grade astrocytomas. Decrease in NAA/Cho area ratios is a significant MR spectroscopic parameter in the differentiation of low grade from malignant high grade tumours. The mean NAA/CHO area ratio (0.27 ± 0.12, $n = 25$) of high grade astrocytomas is lesser than mean NAA/CHO area ratio of low grade gliomas (0.64 ± 0.17, $n = 18$) with a p value < 0.001.

The Cho/Cr ratio was a good MR spectroscopic parameter to assess the grade of malignancy. This increase in Cho/Cr ratio was mainly due to increase in Cho levels which in turn is because of increased membrane turnover and liberation of unbound Cho-containing compounds caused by the destruction of neurons during the malignant process, rather than a decrease in Cr levels, which was quite constant in various metabolic conditions.

Eventually, between the high grade and low grade tumors, statistical analysis shows that the increase in Cho / Cr ratio and decrease in NAA / Cho area ratios were statistically significant in distinguishing between the tumor grades.

Thus, based on this study a diagnostic threshold level of Cho/Cr ratio between the high grade and low grade tumors is 2.5 with the high grade tumors having a higher ratio and low grade tumours having a lower ratio. Similarly the diagnostic threshold level of NAA/Cho ratio is 0.5 with high grade tumors being less and low grade tumors being more.

6.3.3 Role of NAA/Cr ratio:

NAA/Cr ratio did not provide any significant difference between high grade and low grade gliomas but it differentiates them from control group. Neuronal loss being a part of the process in both conditions there is no demonstrable change in the NAA / Cr ratios between these two groups. A decreased NAA/Creatine ratio is consistent with the replacement of healthy neurons by neoplastic cells (149).

6.3.4. Distribution of Lipid & lactate in Low and high grade gliomas.

Lipids were consistently present in high grade tumors and with a larger peak than in the low grade tumors. Of the 25 cases of high grade astrocytomas Lipids were present in 21 cases and lactate was observed in 5 cases. Of the 18 cases of low-grade astrocytomas, Lactate was noted in 8 cases and lipid in 6 cases. R.D.Tien et al (98) has made a similar observation stating that lipids are frequently seen in almost all high grade tumours and that lactate is present in both high and low grade tumours. However the presence of lactate in low grade tumours in this study did not correlate with the observations of Mark.C.Preul et al (150) who have noted that Lactate is more likely to be present in malignant tumors than in low-grade astrocytomas. However, the presence of Lipids in high grade cases is seen to correlate with their observation that it occurs in tumors of higher histo-pathological grade. Lipids correlate with the amount of cellular necrosis which is more in high grade neoplasms.

H. Poptani, R.K.Gupta et al, (99) observed in their study, that most of the high grade gliomas showed the presence of lipids and lactate (n = 25), with lactate in 10 and only lipids in two cases. They have concluded that high grade gliomas can be differentiated from low-grade gliomas on the basis of NAA/Cho and Cho/Cr ratios, along with the presence of lipids or lactate and lipids.

Meng Law et al, (93) compared conventional MRI with perfusion MR and Proton MR spectroscopy in grading glioma and demonstrated that rCBV

measurements and metabolite ratios (Cho/Cr, Cho/NAA, and NAA/Cr) both individually and in combination can increase the sensitivity and PPV when compared with conventional MR imaging alone in determining glioma grade.

Multi-voxel spectroscopy(MV- MRS) revealed that tumor infiltration beyond the area of contrast enhancement (i.e. beyond the margins of radiologically obvious tumour) in all patients (6 out of 6 cases) with high-grade gliomas, is disclosed on MR spectroscopy as pathologic spectra with NAA/Cho ratios of less than 1, whereas, in relatively discrete or non-infiltrative tumours like low grade gliomas (all the 5 out of 5 cases) this pathological spectra outside the lesion were not seen. A similar widespread infiltrative pattern is often seen histo-pathologically in cases of high-grade gliomas (151,152).

6.4. Metastases versus High grade Gliomas.

In adults with multiple brain lesions the primary differential diagnosis is that of metastases. In the presence of a single lesion, differentiating between primary neoplasm and solitary metastasis is often challenging. Unfortunately, Proton MR spectroscopic findings are also nonspecific in this situation (140, 141). Metastases commonly show moderate to marked reduction of NAA, a decreased Cr signal, and elevated Cho. Obviously, these features are identical to those present in astrocytomas (see above). Some metastases (particularly those from breast carcinomas) may also contain lipids (153). Lipid resonance may also be present in high-grade astrocytomas and is caused by the presence of necrosis. Metastases to the brain pose challenging

demands to the spectroscopist, because their small size may require small voxels and a larger number of signal averages. If analyzed with larger voxels, which may include normal surrounding tissues, partial volume artifacts may influence the MR spectra resulting in suboptimal may results.

In this study, metastatic lesions(n=14) showed mean NAA/Cr ratio of 1.93±1.0, mean Cho/Cr ratio of 4.88±2.42, and NAA/Cho ratio of 0.47±0.247.Lipids were consistently observed in metastatic lesions; whereas high grade gliomas(n=25) showed mean NAA / Cr ratios of 1.01±0.62, , Mean Cho / Cr ratio of 4.09±1.51, and Mean NAA / Cho ratio of 0.27 ± 0.12

Eventually it is noted that, of the three ratios(NAA/Cr, Cho/Cr and NAA/Cho), studied only the NAA / Cho ratio shows an appreciable difference between the high grade gliomas and metastases in the Anova univariate analysis with a P value of 0.001 at 1% level of significance. The Cho / Cr shows an overlap between the two with their means almost equal (4.09 ± 1.51 and 4.88 ± 2.41 respectively) with the maximum value and the range being more for the metastases. Hence Cho / Cr ratio is not good at differentiating these two conditions. This was the reason for getting one false positive and three false negatives in diagnosing metastases and high grade gliomas. However, Binary Logistic regression analysis reveals that none of the three metabolite ratios is statistically significant in differentiating high grade gliomas from metastases.

There were three false negatives in this group, where the investigator had interpreted based on MRI aided MRS as a central neurocytoma, low

grade glioma and meningioma. On HPE all turned out to be metastases with no known primary. The diagnosis of central neurocytoma was made owing to the classical location in the foramen of Monroe extending into the left lateral ventricle. The Cho / Cr ratio in this case was however 2.9 as opposed to the mean ratio of metastases in the range of 4.88. The other false negative case diagnosed as low grade glioma, had a well circumscribed 7x 5 x 7 cm lesion in the right fronto temporal region with mild marginal enhancement and with no evidence of edema. The morphology corresponded with a low grade glioma. The 2.26 Cho /Cr ratio and absence of lipid corroborated with the MRI diagnosis. The third false negative case was interpreted as meningioma based on its extra-axial location and a moderately elevated Cho / Cr ratio of 7.22.

Erroneous diagnosis of metastasis: A 66 year old female had an intensely enhancing 2.6 x 2.3 cm lesion in the left posterior parietal region with extensive edema. This was presumed to be a metastasis owing to the disproportionate edema. It turned out to be a grade III Astrocytoma (false positive).

Fayed n et al (81) have observed that a Cho/Cr ratio higher than 1.56 predicted malignancy at 88.9% sensitivity and 91.7% specificity (area under the curve, 0.94; 95% CI, 0.78-0.99) and the presence of lactates improved the diagnostic accuracy of malignancy significantly with an area under the curve of 0.99% (95% CI, 0.87-1). However, the techniques were unable to distinguish metastases from high-grade gliomas accurately. This finding agrees with the findings in the present study.

As in this study, no statistical differences were found between Glioblastoma and metastases in any of the resonances evaluated by Carles majos (89).

Ott.D et al (140) and H.Poptani (99) observed that the spectral pattern in metastases was similar to that in high-grade gliomas and lymphomas as was observed in the present study.

Opstad KS et al (105) in their study of differentiation of metastases from high-grade gliomas, the authors focused on the lipid peak-area ratio derived from short echo time. They defined lipid peak-area as the ratio of L1 (*total peak area at combined Alanine, lactate, δ 1.4 macromolecule and δ1.3lipid peak*) to L2 (*the combined δ 0.9 lipid and δ0.87 macromolecule peak*). Using this ratio, they reported an AUC of 84% with both sensitivity and specificity equal to 80% at a threshold value of 2.9. The authors speculated that the difference in lipid profiles may be related to differences of membrane structure in infiltrative versus migratory tumor cells or to lipid metabolism.

The lipid peak was observed in both high grade gliomas(21out of 25 cases) and metastasis (12 out of 13 cases) in this study.

Nail Bulakbasi et al (74) have also observed that MRS was not very effective in distinguishing tumor types that were in the same grade, such as high-grade astrocytoma versus metastasis as there was no significant difference noted in NAA/Cho, NAA/Cr, NAA/Cr + Cho, Cho/Cr, lactate/Cr, and lactate/lipid ratios among the different histologic subtypes. The lipid/Cr ratio was significantly effective in distinguishing metastases from high and low-grade astrocytomas.

Case No. 8 : 64Yrs male Presented with late onset seizure

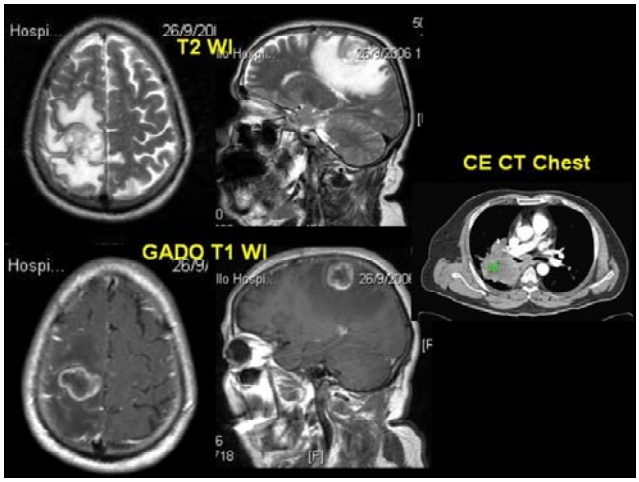

Fig. 9a: MRI shows a thick walled peripheral enhancing nodular lesion with area of necrosis and marked peri-enhancing edema in the right parietal lobe; CT chest reveals central bronchogenic carcinoma

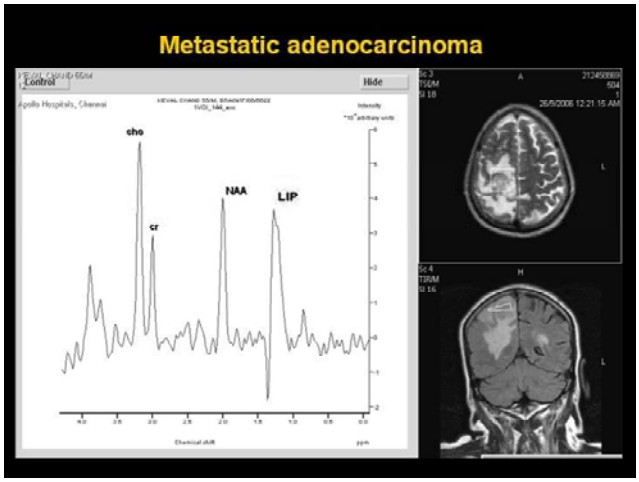

Fig. 9b: MRS reveals increased Cho/Cr ratio (3.1)with mild reduction of NAA peak and lipid elevation suggesting a necrotic neoplasm. Stereotactic biopsy : metastatic adenocarcinoma

Case No. 9 : Thirty one year old male presented with headache and seizure

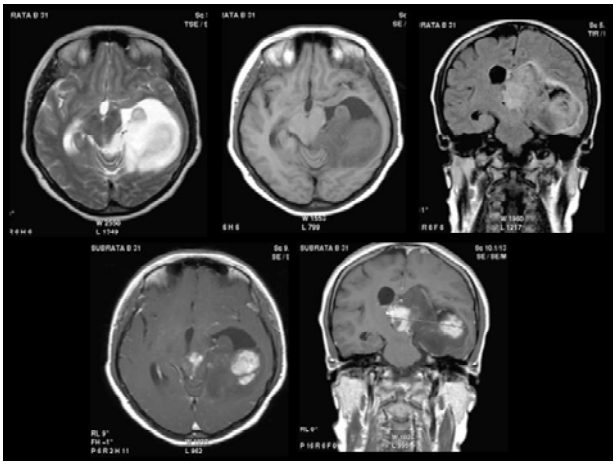

Fig. 10a: MRI shows large bulky, enhancing intra-ventricular mass in left temporal horn infiltrating into temporal lobe suggesting high grade neoplasm

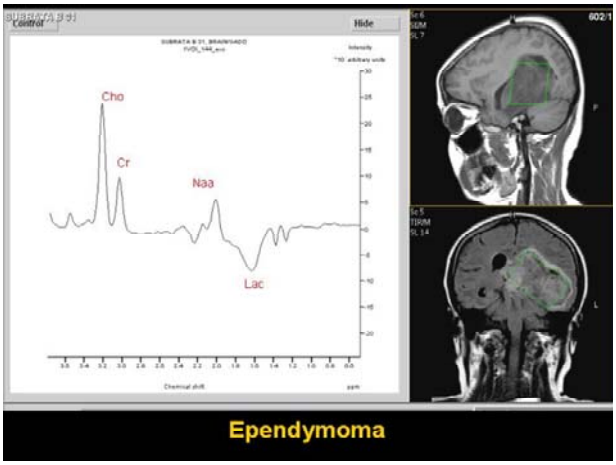

Fig. 10b: MRS reveals increased Cho/Cr ratio with gross reduction of NAA peak and inversion of lactate peak (TE of 144) indicating high grade neoplasm. Biopsy : Ependymoma

Sijens PE, Knopp MV, et al (154) had concluded that brain metastases can be categorized into stages based on the presence of certain metabolites for e.g. as early stage (Cho), intermediate stage (lipid, higher Cho) and late stage metastases (Lact, lower Cho).

In this MV MRS study, all (6 out of 15), high grade glioma and lymphoma showed pathologic spectra (with NAA/Cho ratios of less than 1) in both intra-tumoral and peri-tumoral region. Whereas all (9 out of 15), the low grade gliomas, metastases, and meningioma studied with MV MRS showed no pathologic spectra in the peri-tumoral region.

Meng Law et al (93) using perfusion and MRS to differentiate high-grade gliomas from metastases have observed that the Cho /Cr ratio was elevated (2.28 ±1.24) in the peritumoral regions in gliomas but not in metastases. Elevated Cho levels were observed in the peritumoral region of high grade gliomas but not in metastases by Law M, Cha S, et al(97). These important findings agreed with previous studies (Burtscher et al (79).

Burtscher et al (79) reported that tumour infiltration beyond the area of contrast enhancement or beyond the margins of neuro-radiologically obvious tumour in patients with high-grade gliomas is disclosed on MR spectroscopy as pathologic spectra with NAA/Cho ratios of less than 1. A comparable widespread infiltrative pattern is often seen histopathologically in cases of high-grade gliomas. Circumscribed lesions such as meningiomas, metastases, or abscesses only rarely show histopathologic infiltration of neighbouring

tissue, to show abnormal spectra with NAA/Cho ratios of less than 1 outside the lesion.

As this study of MV MRS had smaller subgroups of two cases of metastases and five cases of high grade gliomas, interpretation of their significance was questionable, with larger numbers are required to be proved further.

6.4.1 Meningiomas:

Meningiomas mostly pose no problem in diagnosis due to their extra axial location, characteristic morphological and enhancement pattern on MR. However, large tumors with extensive edema and mass effect on the brain parenchyma may sometimes pose a problem in interpretation on routine MR Sequences in which case MRS is useful.

The signal of Cho is, however, markedly increased (up 300 times normal) particularly in recurrent meningiomas (141). Lactate and alanine may also be elevated in some meningiomas (3). There is no clear explanation for the increase in alanine in meningiomas. The above proton MR spectroscopic features are seen in typical meningiomas (fibrous type). Atypical and malignant meningiomas, or those that invade the brain, may show resonances in the location of NAA, and differentiating them from astrocytomas may prove difficult.

In this study, of the 7 cases of histopathologically confirmed meningiomas, one was calcified meningioma.

High Choline resonance dominated the spectra, whereas NAA and Creatine were extremely low; these changes produced an increase of the Cho/Cr and decrease in NAA / Cho ratios. The meningiomas showed mean area ratios as follow: Cho/Cr ratio of 5.46±3.93, NAA/Cr ratio of 1.11±0.82 and a NAA/Cho ratio of 0.25±0.14. The mean height ratios were NAA/Cr of 0.39±0.85 and Cho/Cr of 4.55±2.1.

Alanine peaks were present in six out of seven cases. The presence of Alanine peaks at 1.5 ppm was also observed by H.Poptani et al (99) in 12 of the 13 cases of meningioma. The presence of Alanine is considered specific for meningiomas. However, Kugel (141) has found Alanine in only 5 of 8 cases and Ott.D et al (140) has shown its presence in only 4 of 11 cases. Shino et al. (155) reported the presence of the Alanine peak in only 12 of 30 meningiomas they examined.

Case No. 10 : Seven year old child presented with cerebellar ataxia

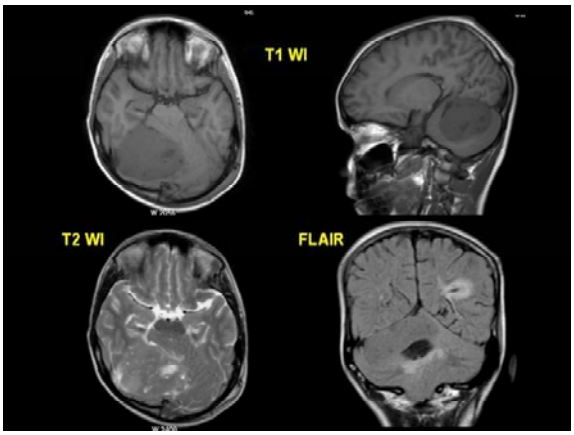

Fig. 11a: MRI shows a large, well-defined extra-axial neoplasm arising from the tentorium on right side causing mass effect on the cerebellum with tonsillar herniation -meningioma

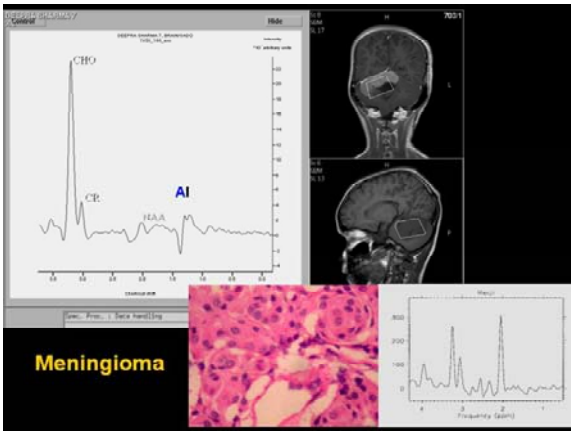

Fig. 11b: MRS(TE144) reveals sharp increased Choline height with Cho/Cr ratio (6.2)with marked reduction of NAA peak;
A small inverted peak at 1.4ppm representing alanine.
Biopsy : Meningioma

Nail Bulakbasi et al (74) have also observed that the alanine/Cr ratio was useful in distinguishing meningiomas from other tumor types ($P < .001$).

Rubaek Danielson et al (156) have observed that when the Alanine peak is present it is still helpful in identifying meningioma, and improves the possibility of the correct diagnosis.

Demir. M.K et al (157) have observed a prominent Choline peak in all meningiomas. Alanine (Ala) was observed in 21 of the 23 meningiomas. NAA and Creatine were not observed or were detected in minimal amounts. The mean Cho/Cr value in the four atypical meningiomas was 4.44+/-0.30 and in the 12 typical meningiomas was 3.39+/-0.52.

Lipid was present in two cases. Lactate was not present in any of the cases, one had Myo-inositol and one had glycine.

6.4.2. LYMPHOMAS:

Four cases of lymphoma were evaluated. It was observed that the metabolite ratios obtained were comparable to those in high grade gliomas. However, the presumptive diagnosis was made based on their characteristic appearances on MRI as a highly cellular enhancing tumor predominantly located in the ependymal surface.

The lymphomas showed mean area ratios as follow: Cho/Cr ratio of 3.89±2.45, mean NAA/Cr ratio of 2.07±1.28 and a NAA/Cho ratio of 0.54±0.21. The height ratios were NAA/Cr of 1.29±0.51 and Cho/Cr of

3.24±1.8. The mean value for this group was between that observed in high grade and low grade tumors in the present cases.

Chang et al (159) have reported that spectroscopic analysis of lymphomas in patients with AIDS demonstrated markedly increased concentrations of Choline, and mild to moderate elevated concentrations of lactate and lipids.

Sharad maheshwari, et al (158) had noted that the spectroscopic findings in lymphoma were similar to that in primary high-grade astrocytoma and metastases. MR spectroscopy showed a marked elevation of Choline and lipids and a significant reduction in Creatine and NAA as seen in other high grade neoplasms. Multi-voxel spectroscopy in a lymphoma showed pathologic spectra with NAA/Cho ratios of less than 1, in both intra-tumoral and peritumoral areas, representing tumor infiltration beyond the area of contrast enhancement (i.e. beyond the margins of radiologically obvious tumour).

6.4.3. Primitive Neuro- Ectodermal Tumour (PNET):

Two cases of PNET were studied and diagnosis arrived at based on their location MR Imaging findings and contrast enhancement pattern . This was confirmed by histopathology. They showed mean area ratios as follow: Cho/Cr ratio of 4.74±3.15, mean NAA/Cr ratio of 1.2±0.1 and a NAA/Cho ratio of 0.69. The mean height ratios were NAA/Cr = 0.39±0.1 and Cho/Cr = 2.84±1.3. Marked increase in Choline and increased Cho/Cr ratio of

lymphoma (n=4) 4.74 ± 3.15 was observed in the PNET tumours as compared to the Cho/Cr ratio of high grade gliomas 4.09± 1.51.

6.5. Tumour Recurrence versus Post operative / Post Radiotherapy changes:

It is often difficult to differentiate recurrent glioma from the effects of post-operative radiotherapy changes by means of conventional diagnostic imaging. Contrast-enhancing lesions detected on routine follow-up MRI, at the site of a previously identified and treated intracranial neoplasm present a significant diagnostic dilemma (160) whether they that have been subjected to radiation, and or surgical resection. Radiation necrosis may be indistinguishable from residual and recurrent tumors by computed tomography, single-photon emission computed tomography, and even Positron Emission Tomographic (PET) imaging (161).

MRI cannot reliably discriminate tumor recurrence or progression from the inflammatory or necrotic changes resulting from radiation, although the latter can be associated with more specific patterns of enhancement, such as "soap bubble" or "Swiss cheese" enhancement. Among the noninvasive methods that are available for diagnosing intracranial tumors, which include SPECT, PET, and diffusion- and perfusion-weighted MRI, it is mainly proton MR spectroscopy that has been used in attempts to differentiate tumor from radiation necrosis.

Mauricio Castillo et al (63) described that histologically, radiation injury is characterized by damage to the vascular endothelium that may result

in ischemia and necrosis. Proton MR spectroscopy shows elevation of lactate in patients who have received 40 Gy or more to the brain (161). This abnormality is appreciable even when the MR imaging studies are normal. Therefore, proton MR spectroscopy may be a promising tool for the detection of radiation injury, before it becomes evident through MR imaging.

MRS is capable of distinguishing between residual or recurrent tumors and pure radiation necrosis as shown by previous studies Herholz, et al. (162), Zeng, et al.(163), Weybright, et al (164), Palumbo, et al.(165), Lin, et al.(166,167). Zeng, et al. (163) showed Cho/NAA and Cho/Cr ratios were significantly higher in recurrent tumor than in regions of radiation injury ($p < 0.01$).

In this study, of the 13 patients referred for follow up after surgical treatment with Radiotherapy (RT) and (with or without chemotherapy), four cases a presumptive diagnosis of post RT changes was made, based on MRI aided MRS . This obviated the necessity of a biopsy. These four cases of post Operative / RT changes, one had HPE diagnosis of radiation necrosis and 3 were followed up and there was no interval change, justifying the diagnosis. Of the 6 cases interpreted as recurrence based on MRI and MRS, all 6 underwent stereotactic biopsy which confirmed recurrence of the tumours.

Analysis of NAA / Cho, Cho/ Cr and NAA / Cr ratios revealed that the Cho / Cr ratio was statistically significant in identifying recurrence with a P value of <0.001 with CI of 95%.

The mean Cho / Cr ratio of the 6 cases of recurrent / residual lesions was 4.06 ± 1.18 and for the 4 cases of post operative / RT changes was 0.94 ± 0.49. that of controls being 1.46 ±0.28 (n=15). There was a statistically significant variation between the Cho / Cr ratios of the recurrent / residual lesions and the post operative / RT changes with a P value of <0.001 which is statistically significant with CI of 95%. The control group ratios are similar to that seen in post op gliosis / RT changes as there is no tumour in both conditions to increase the Choline values. It was observed that the NAA / Cr and NAA / Cho ratios were not statistically significant to distinguish between these two groups, as neuronal loss occurs in both recurrence of tumours and in radiation induced necrotic lesions.

Case No. 11 : Fifty seven year old male, a treated case of carcinoma Nasopharynx with RT, presented with headache for 3 months

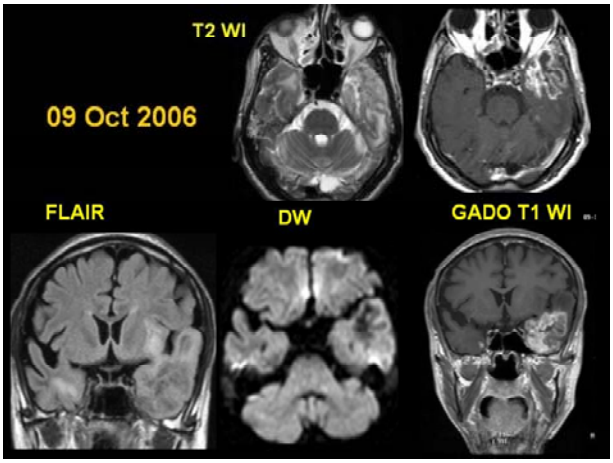

Fig. 12a: MRI shows large, lobulated, thick walled, peripheral enhancing lesion without significant mass effect in the left temporal lobe; another small lesion in the right lobe simulating metastases in view of clinical history.

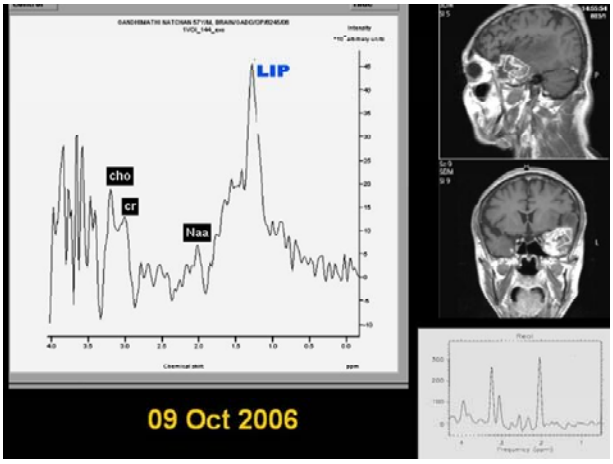

Fig. 12b: MRS reveals a broad based lipid peak between 0.6 and 1.9ppm ; marked reduction in Cho and NAA representing radiation necrosis

Case No. 11 : Follow up

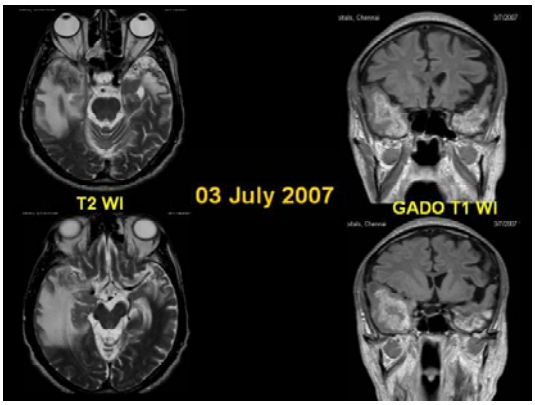

Fig. 12c: MRI after 9 months shows resolution of lesion in the left temporal lobe; lesion in the right temporal lobe appears more pronounced ; distribution of lesions consistent with radiation field

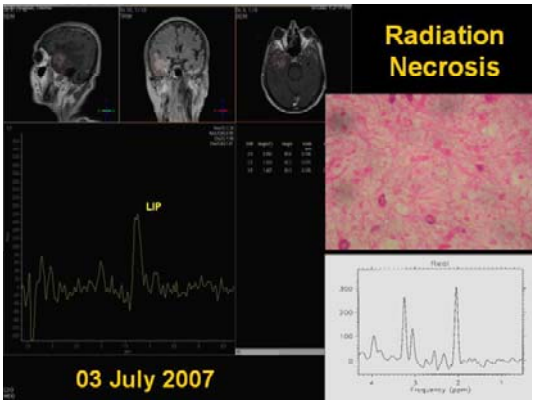

Fig. 12d: MRS reveals a sharp lipid peak at 1.3ppm; marked reduction in Cho and NAA representing radiation necrosis
Stereotactic biopsy of right temporal lesion: Radiation necrosis

Mark.C Preul et al (150) have observed that increasing levels of Cho was noted in tumors interpreted to be progressing and areas believed to be radiation necrosis showed decrease in Choline. Choline signal was low in the areas of radiation changes; while it was high in areas where recurrence predominated. They have concluded that the differentiation between relatively dense areas of tumor recurrence and radiation change may be achieved using H1MRSI.

Zeng, et al. (163) in their study in 2007 observed that Cho/NAA and Cho/Cr ratios were significantly higher in recurrent tumor than in regions of radiation injury ($p < 0.01$).

Rock JP et al (168), Weybright, et al (164) concluded that NAA/ Cr ratio greater than 1.56, NAA/Cho ratio greater than 1.32 that a tissue biopsy will be pure necrosis versus mixed tumor and necrosis. The respective ratios in post RT necrotic lesions, in this study were 1.00 ± 0.42 and 1.02 ± 0.24 and were nearly the same. The minimal difference in the ratios could possibly be due to the small number of four cases (out of 10 cases) of post op / RT changes as opposed to 8 (out of 21) cases in their study.

Patrick Weybright et al (164) performed MRS in 29 patients who had a new contrast-enhancing lesion in the vicinity of a previously diagnosed and treated brain neoplasm. Clinical and imaging follow-up, and histopathology in 16 patients, were used as indicators to establish the identity of the lesion. It was observed that the mean Cho/Cr ratios were 2.52 for tumor, 1.57 for radiation injury, and 1.14 for normal-appearing white matter. When values

greater than 1.8 for Cho/Cr was considered as evidence of tumor, 27 of 28 patients could be correctly classified. They concluded that Cho/Cr and Cho/NAA ratios may be the best numeric discriminators. In the present study the Mean Cho / Cr ratio of 6 cases of recurrent / residual lesions was 4.06 ±1.18 and in 4 cases of post operative / RT changes it was 0.94 +/- 0.49. These findings correlated well with the observations of Patrick Weybright et al (164).

Ando et al, (113) examined 20 patients with CE-MR imaging and ^{1}H-MR spectroscopy. Fourteen patients had a final diagnosis of residual or recurrent tumor, and 6 had treatment-related changes. The authors retrospectively selected a Cho/Cr ratio of greater than 1.5 to be indicative of tumor. Based on this threshold, the addition of 1H-MR spectroscopy information to CE-MR imaging findings marginally increased sensitivity from 12 of 14 (86%) to 14 of 14(100%) (P=0.79) without altering specificity (4 of 6; 67%).

McKnight et al (116) prospectively recruited 44 patients with suspected glioma before image-guided resection or stereotactic biopsy of the tumor. Data from the preoperative Multivoxel 1H-MR spectroscopy study was used to select 4 potential targets for biopsy in each patient. In practice, the authors were unable to obtain biopsy samples at each target, and their analysis was based on 100 samples, of which only 7 were classified as non tumor. The authors based diagnosis on the Cho-NAA index (CNI), where CNI is the number of standard deviations between the Cho to NAA ratio within a given voxel and that of the control voxels. At a threshold CNI of greater than

2.5, the authors reported 90% (95% CI, 84%–96%) sensitivity and 86% (95% CI, 56%–100%) specificity for predicting the presence of tumour in the biopsy sample. The overall AUC for CNI was 94% (95% CI, 87%–99%). Up to half of the T2-hyperintense lesion outside of the gadolinium-enhanced lesion had CNI greater than 2.5. This suggests that 1H-MR spectroscopy might have a considerable therapeutic impact on surgical and radiation target volumes.

Lichy et al (114) used multi-voxel spectroscopy in 24 patients with irradiated gliomas and in one patient with a suspicious lesion on gadolinium-enhanced MRI. The diagnosis was determined by clinical and imaging follow-up. Using the Cho/Cr ratio with a diagnostic threshold of 2, the authors identified 13 of 15 (87% [95% CI, 60%–98%] sensitivity) recurrent or residual tumours and 8 of 9 (89% [95% CI, 52%–100%] specificity) radiation-related changes.

Traber et al (112) presented data of 43 patients, with high-grade astrocytomas sequentially tracked with multiple-voxel 1H-MR spectroscopy until completion of radiation therapy. An increased Cho peak (50% higher than contralateral tissue) was 72% (95% CI, 53%–86%) sensitive and 82% (95% CI, 48%–98%) specific in distinguishing tumour from radiation-induced necrosis.

Based on this study, a diagnostic threshold level of Cho/Cr ratio to discriminate between the recurrence of the tumours and post

radiation necrosis/changes is 2 with the recurrence of tumors having more than that and radiation necrotic changes less than that.

6.5.1. Radiation necrosis

Catillo et al (63) performed serial proton MR spectroscopy in 25 patients with brain tumors treated with a combination of radiation and chemotherapy. In nine patients with tumour recurrence, proton MR spectroscopy showed elevated Cho/NAA, Cho/Cr, and the presence of lactate. Eight patients with radiation necrosis showed highly depressed levels of NAA, Cho, and Cr and an intense and broad peak between 0 and 2.0 ppm. This peak is consistent with tissue necrosis. This cellular breakdown peak probably consists of free fatty acids, lactate, and amino acids (169). Elevated lactate, reflecting severe tissue ischemia and/or mitochondrial damage, was also present in these patients.

Similar findings of a broad based peak between 0.5 and 2 ppm representing lipid and lactate with depressed Cho and NAA metabolites indicated radiation necrosis (later confirmed by HPE) and differentiated from recurrent tumour in this study.

6.5.2.Pseudoprogression: Pseudoprogression, a transient increase in the volume of the enhanced area just after chemo-radiotherapy, especially after Temozolomide has been recognized (170,171) and widely accepted to occur in the management of malignant gliomas.

In the present study, a similar phenomenon was observed after radiotherapy and chemo radiotherapy (Temozolomide) during the follow up of a patient with high grade glioma.

A 33 yr male presented with the manifestation of seizure with weakness on left half of body. He had undergone surgery for a neoplasm in right parietal lobe with the histological diagnosis of Neuroblastoma of CNS . The tumor was partially removed and was treated with fractionated RT followed by chemotherapy (Temozolomide). This combination of chemo & radiotherapy resulted in dramatic clinical improvement. However, 6 months after radiotherapy, he developed seizure and MR images (first follow up study) showed marked irregular peripheral enhancement with central patchy non- enhancing area with edema and mass effect simulating a recurrence of the tumour on MRI ; MRS revealed mildly elevated Cho with depressed NAA with a Cho/Cr ratio of 0.11. The lesion was well controlled by steroids, and the enhanced area decreased in size on follow-up MR, after six months. MRS depicted only a broad peak between 0.4 and 1.6 representing lipid and lactate and absence of Cho and NAA representing treatment related changes. These findings are suggestive of appearances seen in pseudoprogression as outlined below.

Case No. 12 : Thirty three years old male diagnosed to have CNS Neuroblastoma

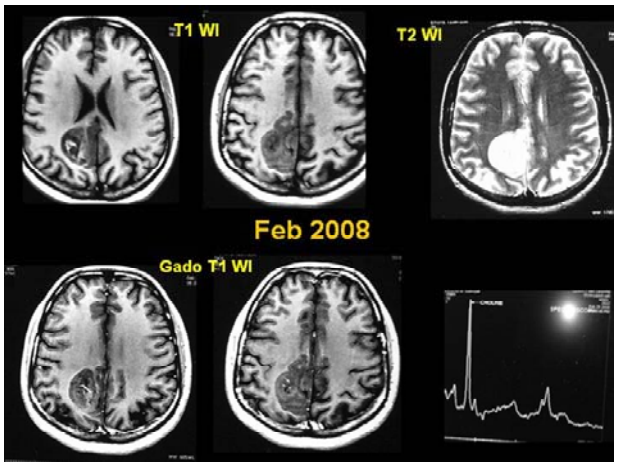

Fig. 13a: Preoperative MRI shows patchy enhancing lesion in right parietal cortex- surgery done ; biopsy :neuroblastoma (grade III)

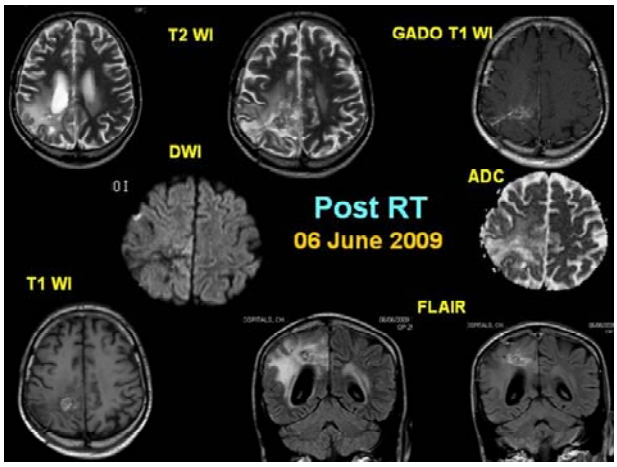

Fig. 13b: Post operative and post radiotherapy follow up of CNS Neuroblastoma- MRI after 15 months shows patchy enhancing areas in the right parietal lobe associated with area of gliosis suggesting doubtful recurrence

Case No. 12 : Post operative & Post RT follow up of CNS Neuroblastoma

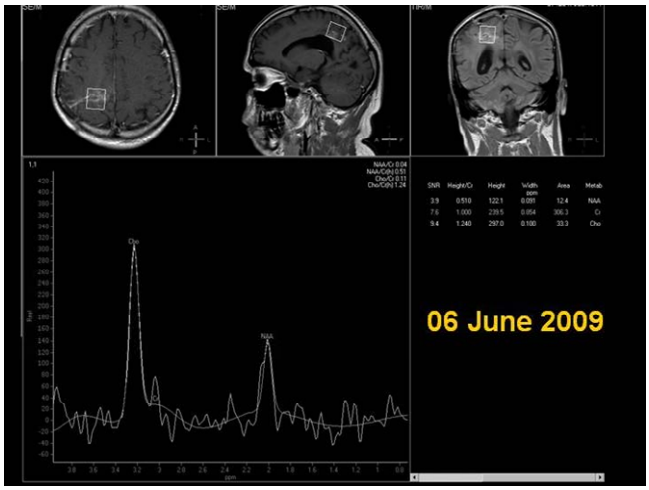

Fig. 13c: MRS reveals marked reduction in NAA and increased Cho/cr ratio suggesting reactive changes ; suggested follow up MRI with MRS

CHAPTER 7

SUMMARY AND RECOMMENDATIONS

"The point of philosophy is to start with something so simple as not to seem worth stating, and to end with something so paradoxical that no one will believe it."

Bertrand Russell

Intracranial lesions are a significant health problem and present several imaging challenges. The role of imaging is no longer limited to merely providing anatomic details of the exact location of the pathology. Advanced Magnetic Resonance Imaging (MRI) techniques allow insight into the chemical makeup of certain compounds within these pathologic lesions.

In vivo Proton MR Spectroscopy (^{1}H MRS), a non-invasive technique which provides metabolic information can complement the anatomical changes found in radiological examinations of various intracranial lesions increasing diagnostic specificity.

The present investigation was carried out a) To determine if there are specific MRS findings which could help differentiate between neoplastic and non –neoplastic lesions and also to identify the presence or absence of MRS features which could help differentiate one neoplasm from another b)to determine if MRS findings could help grade gliomas pre operatively; c) To determine if MRS findings could help differentiate irradiated residual/ recurrent tumours from radiation necrosis. d) To determine if MRS findings could help differentiate necrotic tumours from infective lesions such as abscesses.

TABLE: 7-1

Summary: Distribution of Metabolites & their Ratios in various intracranial lesions

	CHO/CR	NAA/ CHO	LIPID/	Lactate	Specific metabolites
HIGH GRADE GIOMAS(n=25)	4.09±1.512	0.27±0.121	21/25 (84%)	5/25 (20%)	
LOW GRADE GLIOMAS(n=18)	2.12±0.988	0.64±0.169	6/18 (33%)	8/18 (44%)	Myo-inositol - 7/18 (38%)
METASTASES(n=14)	4.88±2.415	0.47±0.247	13/14 (92%)	2/14 (14%)	
MENINGIOMAS(n=7)	5.47±2.45	0.25±0.14	2/7 (28%)	0	Alanine - 6/7 (85%)
TUMOUR RECURRENCES (n=6)	4.06±1.181	0.81±0.544	4/6 (66%)	1/6 (16%)	
POST RADIATION CHANGES (n=4)	0.94±0.487	1.02±0.241	3/4 75%	0	
INFECTIVE LESIONS (n=13)	1.04±0.587	1.15±0.838	12/13 92%	2/13 (15%)	Aminoacid, succinate, in pyogenic abscess
DEMYELINATIONS(n=4)	2.00±0.518	0.37±0.102	0	2/4 (50%)	Myo-inositol in4/4 Glx in 3/4

1. In this study, the **Cho / Cr area ratio was statistically found to be more significant in differentiating neoplastic from non-neoplastic lesions.** Mean Cho / Cr area ratio (3.87 ± 2.20) for neoplastic tumours was greater than that of non-neoplastic lesions (1.2 ± 0.66) with a P value of <0.001 which is statistically at 1% level of significance**.**

2. Decrease in NAA / Cho ratio was also a significant MR spectroscopic parameter in the differentiation of neoplastic lesion from non neoplastic lesions. Mean NAA / Cho area ratio for neoplastic tumours was 0.45 ± 0.29 (n=70) and that for non-neoplastic lesions was 0.98 ± 0.72 (n=21) with a P value of <0.001 which is statistically at 1% level of significance.

Based on these findings in this study, the investigator suggests that two resonance diagnostic threshold ratios could be used to differentiate neoplastic from non-neoplastic lesions:

Cho / Cr area ratio of more than 2 and NAA/Cho area ratio of less than 0.9 may be considered in the diagnoses of a neoplastic lesion. However, it should be remembered that the threshold value of NAA / Cho ratio (< 0.9) might also be obtained in chronic non - neoplastic lesions such as chronic demyelination / chronic abscess etc. in which there is neuronal loss.

2. In this study, the decrease of NAA / Cho area ratio was statistically more significant in differentiating high grade from low grade gliomas. The mean NAA / Cho area ratio (0.27 ± 0.12, *n* = 25) of high grade gliomas was lesser than the mean NAA / Cho area ratio of low grade gliomas (0.64 ± 0.17, *n* = 18) with a p value < 0.001 in this analysis.

Conversely, the mean Cho / Cr area ratio (2.12 ± 0.99, *n* = 18) in low grade tumours was found to be lesser than the mean Cho / Cr area ratio (4.09 ± 1.51, *n* = 25) in high grade tumours with p value < 0.001 which is statistically at 1% level of significance.

The lipid / lactate peak was higher in high-grade malignant tumours than in low-grade tumours.

Based on these findings in this study, the investigator suggests two resonance diagnostic threshold ratios to be used to differentiate high grade gliomas and low grade gliomas amongst the astrocytoma group: **Cho / Cr area ratio of more than 2.5, NAA / Cho area ratio of less than 0.5 and elevated lipid / lactate peak may be considered significant in the diagnosis of high grade gliomas.** However, this threshold value may not be considered for differentiating tumours with the same grade such as high-grade astrocytomas versus metastases or low grade astrocytomas versus non astrocytic gliomas.

3. In this study, **Cho / Cr area ratio was more statistically significant (**with a P value of <0.001) **in discriminating recurrence of tumour from post radiation necrosis / post operative changes.** The mean Cho / Cr area ratio (4.06 ± 1.18) of recurrent / residual tumors was significantly higher than the Cho / Cr area ratio (0.94 ± 0.49) of post operative gliosis / post radiation necrosis.

Based on these findings in this study, the investigator suggests using Cho / Cr diagnostic threshold ratio to differentiate recurrence of the tumour

from post radiation necrosis / changes: **Cho / Cr area ratio of more than 2 may be considered for diagnosis of tumour recurrence.**

4. In this study, among the three metabolites ratios**, none of the ratios are statistically significant in differentiating high grade gliomas from metastases. Hence,** it is suggested by the investigator that 1H-MR spectroscopy cannot be relied upon to differentiate metastases from glioblastomas in SV MRS

5. Tuberculomas showed a mild elevation of Choline and moderate to marked elevation of lipid levels (3+ or 4+) .Tuberculomas were differentiated from neoplastic lesions by presence of lipid with only mild increase in Choline or no increase in Choline compared to a marked increase in tumors. In this study, Cho / Cr ratio was more statistically significant (with a p value of <0.001) in differentiating infective lesions from neoplastic lesions.

Tuberculous abscess depicted an isolated broad lipid peak at 0.9 ppm with absence of other metabolites Cho, NAA and amino acids .

Pyogenic abscesses exhibited broad resonances at 0.9 ppm,(cytosolic amino acid residues (valine, leucine), 1.3 ppm (lactate), 1.5 ppm (alanine), and 1.92 ppm (acetate) with absence of NAA, Cho, and Cr peaks. These metabolites have never been detected in cystic and necrotic brain tumours, and detection of these metabolites- (acetate and succinate) are a specific marker for cerebral abscess.

6. Elevated Choline, markedly reduced NAA and elevated myo-inositol peak were observed in demyelinating disease in this study. **Cho/Cr is a significant metabolic ratio in differentiating demyelinating lesions from neoplastic lesions (p value of <0.028).** Elevation of Myo-inositol peak (at 3.5 ppm) and glutamine peak were consistent findings in demyelination in this study.

7. Presence of Alanine at 1.48 ppm in Meningioma observed in six out of seven cases.

8. Multi-voxel spectroscopy (MV- MRS) results revealed that tumour infiltration beyond the area of contrast enhancement (i.e. beyond the margins of radiologically obvious tumour) in patients with high-grade gliomas disclosed on MR spectroscopy as pathologic spectra with NAA/Cho ratios of less than 1, whereas, relatively discrete or non infiltrative tumours like metastasis did not show this pathological spectra outside the lesion.

Moreover, MV-MRS technique was useful in assessing response to radiation therapy in the peritumoral area. This technique offers more coverage than single voxel technique and provides reliable spectral data to properly identify tumour locations which could be used as accurate target points for stereotactic biopsy.

9. In this study, the **sensitivity, specificity, Positive predictive value, Negative Predictive value and accuracy** for determining **malignant lesions** with MRI guided ^{1}H-MRS were **90.9%, 97.9%, 97.6%, 92%, and94.3%** respectively**.**

The understanding and familiarity of the spectral pattern of the various metabolites and their ratios in various intracranial lesions could be helpful in daily clinical practice to improve diagnostic accuracy to characterise intracranial lesions. In accordance with spectroscopy features and two resonance diagnostic threshold ratios, ^{1}H-MR spectroscopy may play a role in the non invasive assessment of intracranial lesions by suggesting a) a diagnosis of neoplasm or non- neoplastic lesions, b) differentiating low grade from high grade neoplasms c) differentiating recurrence of the tumour from radiation necrosis and d) differentiating cystic tumours from cerebral abscesses.

7.1 CONCLUSION

MR Spectroscopy in addition to appropriate conventional MRI sequences provides useful supplementary information and has a potential to validate treatment strategies. This **c**ould influence decision making with respect to prognosis and therapy in patients with intracranial lesions.

Current Neuro - Imaging techniques enable use of multiple modalities to enhance the accuracy of non-invasive diagnosis. This study emphasizes the utility and validity of a simple add on technique of MRS over MRI to provide additional information in establishing the possible aetiological diagnosis of intracranial lesions.

This study helps radiologists to improve diagnostic accuracy of MRI using the additional modality of MRS. MRS could help in clinical decision making in difficult cases e.g.in distinguishing neoplastic from non-neoplastic lesions.

During the last few years there has been an exponential growth in MRS. The phenomenal advances in neuroimaging of the brain are resulting in a paradigm change in the clinician’s approach to diagnosing and managing intracranial conditions. Advances in the ultra precise delineation of anatomical changes in the brain have resulted in increasing precision in separating normal from abnormal brain tissue. However this has not kept pace with identifying the nature of the abnormal brain tissue. For several decades humankind has preferred non-invasive methods in establishing a definite

pathological diagnosis. This is particularly true for cerebral lesions. This study appears to indicate, that one is now justified, in carrying out larger studies to confirm the present findings that MRS could be a valuable diagnostic tool in identifying certain types of cerebral pathology.

.

7.2 CLINICAL APPLICATIONS & SUGGESTIONS

This study has enabled development of a few guidelines in the use of MR spectroscopy, as an add-on modality, to improve diagnostic accuracy, in certain categories of lesions i.e. neoplasm versus non-neoplasm, high grade tumours versus low grade tumours, high grade tumours versus metastases, recurrent tumours versus radiation necrosis, cystic non-tumoural lesions versus cystic tumours and improved follow up of polyphasic demyelinating conditions i.e. multiple sclerosis

1. It is desirable that all patients with intra cranial space occupying lesions referred for MRI also undergo MRS, to provide additional information which may help differentiate a neoplasm from non-neoplasms. This could avoid surgical treatment in some instances.

2. MRS can be considered as a suitable, complementary modality to be used when a doubt exists in defining whether a tumour is low or high grade.

3. Solitary metastasis always is difficult to diagnose and may be confused with other high grade tumours. While it is challenging to use single voxel MRS technique to distinguish between the two, MV-MRS technique would be more useful to differentiate metastasis from high grade glioma

4. In follow up of treated patients of brain tumour, especially after surgery, radiotherapy and/or chemotherapy, the differentiation

between recurrent tumour and radiation necrosis can be difficult. Making this distinction is critical for treatment and MRS appears to be a useful tool to distinguish between the two.

5. In analyzing the use of MRS in tuberculous and pyogenic abscess, MRS was found to be useful in distinguishing tuberculous from pyogenic abscesses.

6. In polyphasic demyelinating conditions such as Multiple Sclerosis, MRS plays a valuable role not only in initial diagnosis but also in follow up. Degree of neuronal loss, a prognostic factor, can indirectly be titrated through MRS findings on follow up studies.

BIBLIOGRAPHY

1. Bottomley PA, Hart HR, Edelstein WA, et al. **Anatomy and metabolism of normal human brain studied by magnetic resonance at 1.5Tesla.** *Radiology* 1984; 150: 441-446

2. Radda GK, Bore PJ, Rajagoplan B: **Clinical aspect of ^{31}P NMR Spectroscopy.** *Br Medical Bull* 1984; 40:155-159

3. Bruhn H, Frahm J, Gyngell ML, et al. **Noninvasive differentiation of tumors with use of localized H-1 MR spectroscopy in vivo: initial experience in patients with cerebral tumors**. *Radiology* 1989; 172: 541–548

4. Negendank W, Sauter R, Brown T, et al. **Proton magnetic resonance spectroscopy in patients with glial tumors: a multicenter study.** *J Neurosurg* 1996; 84:449-458

5. Castillo M, Kwock L, Mukherji SK. **Clinical applications of proton MR spectroscopy.** *AJNR Am J Neuroradiol* 1996; 17:1–15

4. Richard R. Ernst**. Nuclear Magnetic Resonance Fourier Transform Spectroscopy, Nobel Lecture**, Zurich, Switzerland, December 9, 1992.

5. Paul C. Lauterbur. **All Science is Interdisciplinary – From Magnetic Moments to Molecules to Men, Nobel Lecture**, Biomedical Magnetic Resonance Laboratory, University of Illinois, Urbana, IL 61801, USA, December 8, 2003.

6. I.I. Rabi, J.R. Zacharias, S. Millman, et al. *Phys. Rev*.1938; 53

7. J.M.B.Kellogg, I.I. Rabi, N.F. Ramsey, and J.R. Zacharias. *Phys. Rev.*1939; 55: 318, 1939; 56: 728 & 1940; 57:677

8. E.M. Purcell, H.G. Torrey, R.V. Pound. **Resonance absorption by nuclear magnetic moments in a solid**. *Phys. Rev* 1946; 69: 37-38

9. F. Bloch, W. Hansen, and M.E. Packard, **Nuclear induction.** *Phys. Rev.*1946; 69: 127

10. Protor WG, Yu FC. **The dependence of nuclear magnetic resonance frequency upon chemical shift**. *Physiol Rev* 1950; 70:717

11. J. Brossel and A. Kastler. *Acad. Sci.* 1949; 229: 1213 & A. Kastler, *J.Physique* 1950; 11: 255

12. A.A. Michelson, Phil. Mag. Ser. 5, 1891; 31: 256 & A.A. Michelson, **Light Waves and their Uses,** University of Chicago Press, Chicago, 1902.

13. P. Fellgett, Thesis, Cambridge University, 1951 & P. Fellgett, *J. Phys. Radium,* 1958; 19: 187.

14. R.R. Ernst and W.A. Anderson. *Rev. Sci. Instrum.*1966; 37: 93

15. R.R. Ernst. *Adv. Magn. Reson* 1966; .2: 1

16. W.A. Anderson and R.R. Ernst. US Patent No. 3.475.680 Impulse **resonance spectrometer including a time averaging computer and a Fourier analyzer,** 1969; issued Oct: 28.

17. J.B.J. Fourier. **Theorie analytique de la chaleur , Firmin Didot,** *Pere et fils***,** 1822; Paris.

18. I.J. Lowe and R.E. Norberg . *Phys. Rev*. 1957; 107: 46

19. R.H. Varian, US Patent No. 3.287.629 **Gyromagnetic resonance methods and apparatus,** filed 1956; Aug.:29: issued 1966; Nov: 22

20. N. Wiener, M.I.T. Radiation Lab., Rep.V-16S, 1942; Apr.6, N. Wiener, **Non-Linear Problems in Random Theory,** 1958: Wiley, New York.

21. H. Primas, Helv. *Phys. Acta* 1961; 34: 36

22. R. Kaiser. *J. Magn. Reson*. 1970; 3: 28

23. R.R. Ernst. *J. Magn. Reson*. 1970; 3:10

24. J. Dadok and R.F. Sprecher. *J. Magn. Reson*. 1974; 13: 243

25. R.K. Gupta, J.A. Ferretti, and E.D. Becker. *J. Magn. Reson.* 1974; 13: 275

26. J.A. Ferretti , R.R. Ernst ..*J. Chem. Phys.* 1976; 65: 4283.

27. B.L. Tomlinson and H.D.W. Hill. *J. Chem. Phys*. 1973; 59:1775

28. H.C. Torrey. *Phys. Rev*. 1949; 75: 1326, 1949; 76: 1059

29. E.L. Hahn. *Phys. Rev*. 1949; 76: 145.

30. M. Emshwiller, E.L. Hahn, and D. Kaplan .*Phys. Rev*. 1960; 118: 414.

31. S.R. Hartmann and E.L. Hahn. *Phys. Rev*. 1962; **128**: 2042.

32. J. Jeener .Ampere International Summer School, Basko Polje, Jugoslavia, 1971.

33. R.R. Ernst, G. Bodenhausen, and A. Wokaun. **Principles of NMR in One and Two dimensions**, *Clarendon Press*, Oxford, 1987.

34.P. C.Lauterbur. **Image Formation by Induced Local Interactions: Examples Employing Nuclear Magnetic Resonance.** *Nature 1973*; *242*: 190–191.

35. P Mansfield, P K Grannell, A N Garroway and D C Stalker .**Multi-pulse line narrowing experiments**. *Proc First Specialised Colloque Ampere*, Poland 1973

36. A N Garroway, P K Grannell and P Mansfield. **Image formation in NMR by a selective irradiative process.** *J Phys C* 1974; 7: L457.

37. P Mansfield**. Multi-planar imaging formation using NMR spin echoes**. *J Physics C Solid State Phys* 1977; 10: L55–L58.

38. P Mansfield and B Chapman. **Active magnetic screening of coils for static and time-dependent magnetic field generation in NMR imaging.** *J Phys E:Sci Instrum* 1986;19: 541–546.

39. B Chapman and P Mansfield: **Double active magnetic screening of coils in NMR.** *J Phys D: Appl Phys* 1986; 19: L129–L131

40. M J Stehling, A M Howseman, P Mansfield, B Chapman, et al . **Whole Body Echo-Planar MR Imaging at 0.5 T.** *Radiol 1989*; 170:257–263

41. M K Stehling, R M Charnley, P Mansfieldet al . **Ultra-fast magnetic resonance scanning of the liver with echo-planar imaging.** *Brit J of Radiol* 1990; 63: 430–437

42. A Chrispin, P Small, Mansfield et al .**Transectional echo planar imaging of the heart in cyanotic congenital heart disease.** *Pediatr Radiol* 1986; 16: 293–297

43. P R Harvey and P Mansfield. **Echo-Volumar Imaging (EVI) at 0.5 T: First Whole-Body Volunteer Studies**. *Mag Res Med 1996*; 35: 80–88

44. Saunders, M. and Wishnia, A. **Nuclear magnetic resonance spectra of proteins**. *Ann. N.Y. Acad. Sci.*1958; *70*: 870–874

45. Jardetzky, O. and Jardetzky, C.D. **Proton magnetic resonance spectra of amino acids** *J. Biol. Chem.* 1958; *233*: 383–387

46. Kowalsky, A. **Nuclear magnetic resonance studies of proteins**. *J. Biol. Chem.*1962; **237**: 1807–1819.

47. Mandel, M: **Proton magnetic resonance spectra of some proteins**. *J. Biol. Chem.* 1965; **240**: 1586–1592

48. McDonald, C.C. and Phillips, W.D. **Manifestations of the tertiary structures of proteins in high-frequency nuclear magnetic resonance**. *J. Amer. Chem. Soc.*1967; *89*: 6332–6341

49. Wüthrich, K. **NMR–this other method for protein and nucleic acid structure determination** *Acta Cryst. D* 1995; 51:249–270

50. Wüthrich, K**. NMR in Structural Biology:** A Collection of Papers by Kurt Wüthrich. *World Scientific*, Singapore. 1995

51. Wüthrich, K. **NMR in Biological Research: Peptides and Proteins** .North Holland, Amsterdam 1976

52. Moon RB, Richards JH: **Determination of intracellular Ph by ^{31}P magnetic resonance**. *J Biol Chem* 1973; 248: 7276-7278

53. Hoult DI, Busby SJW, Gadian DG et al. **Observation of tissue metabolites using Phosphorus nuclear magnetic resonance** .*Nature* 1974; 252:285-287.

54. Lenkinski RE, Schnall MD. **MR spectroscopy and the biochemical basis of neurological disease.** In: Atlas SW, ed. *Magnetic Resonance Imaging of the Brain and Spine.* New York: Raven 1991: 1099–1121.

55. Peter Mansfield. **Snap-Shot MRI, Nobel Lecture.** Sir Peter Mansfield Magnetic Resonance Centre, Department of Physics and Astronomy,

University of Nottingham, Nottingham, NG7 2RD, U.K. December 8, 2003

56. Michael L W, Felix W.Wehrli. **Principle of Magnetic Resonance Imaging** .Third edition Vol I: David D Stark & W G Bradley, Mosby 1999

57. Nelson SJ, McKnight TR, Henry RG**. Characterization of untreated gliomas by magnetic resonance spectroscopic imaging.** *Neuroimaging Clin N Am* 2002; 12:599–613

58. Jay J. Pillai, Lester Kwock. **Brain Magnetic Resonance Spectroscopy**. In: John R. Haaga, Charles F. Lanzieri , Robert C.Gilkeson, Eds. *CT and MR Imaging of whole body;* Eds IV St Louis: Mosby, 2003:371-373

59. Bottomly PA. **Spatial localization in NMR spectroscopy in vivo**. *Ann N.Y Acad Sci* 1987; 508:376-385

60. Moonen CTW, Van Zijil PCM, Frank JA at al .**Comparisons of single shot localization method (STEAM and PRESS) for in vivo proton NMR spectroscopy** . *NMR Biomed* 1989; 2:201-208

61. Lin A, Ross BD: **The effect of gadolinium on quantitative short echo time single voxel MRS of treated and untreated brain tumors**. *Proc Intl Soc, Mag Reson Med*, 2000; 9: 270

62. Carles Majós, Margarida et al .**Brain Tumor Classification by Proton MR pectroscopy: Comparison of Diagnostic Accuracy at Short and Long TE;** *AJNR Am. J. Neuroradiology* 2004; 25: 1696 - 1704

63. Mauricio Castillo, Lester Kwock, and Suresh K. Mukherji. **Clinical application of MR spectroscopy.** *AJNR Am J neuroradiology* 1996; 17:1-15.

64. Miller BL. **A review of chemical issues in 1H NMR spectroscopy: N-acetyl-L-aspartate, creatine, and choline.** *NMR Biomed* 1991; 4:47–52.

65. Kreis R, Ernst T, Ross BD. **Development of the human brain: in vivo quantification of metabolite and water content with proton magnetic resonance spectroscopy.** *Magn Reson Med* 1993; 30: 424–437.

66. Sanders JA. **Magnetic resonance spectroscopy.** In: Orrison WW, Lewine JD, Sanders JA, Harthshorne MF, eds. *Functional Brain Imaging.* St Louis: Mosby, 1995:419–467

67. Van der Knaap MS, Ross B, Valk J. **Uses of MR in inborn errors of metabolism**. In: Kucharczyk J, Mosely M, Barkovich AJ, eds. *Magnetic Resonance Neuroimaging. Boca Raton*: CRC Press, 1994:245–318.

68. Ceodan S, Parrilla R, Santoro J, Rico M. **H-1 NMR detection of cerebral/myo-inositol**. *FEBS Lett* 1985; 187:167–172

69. Miller BL, Moats RA, Shonk T, et al. **Alzheimer disease: depiction of increased cerebral myo-inositol with proton MR spectroscopy.** *Radiology* 1993; 187:433–437

70. Michealis T, Merboldt KD, Bruhn H, Dipl Math WH, Frahm J. **Absolute concentrations of metabolites in the adult human brain in vivo: quantification of localized proton MR spectra**. *Radiology* 1993; 187:219–227.

71. Castillo M, Kwock L, Scatliff JH, Gudeman S, Greenwood R**. Proton MR spectroscopic characteristics of a presumed giant subcortical heterotopia.** *AJNR Am J Neuroradiol* 1993; 14:426–429

72. Moller-Hartmann W, Herminghaus S, Krings T, et al**. Clinical application of proton magnetic resonance spectroscopy in the diagnosis of intracranial mass lesions.** *Neuroradiology* 2002; 44:371–81.

73. Ando K, Ishikura R, Nagami Y, et al. **Usefulness of Cho/Cr ratio in proton MR Spectroscopy for differentiating residual/recurrent glioma from non-neoplastic lesions**. *Nippon Igaku Hoshasen Gakkai Zasshi* 2004; 64:121–26.

74. Nail Bulakbasi, Murat Kocaoglu et al .**Combination of Single-Voxel Proton MR Spectroscopy and Apparent Diffusion Coefficient Calculation in the Evaluation of Common Brain Tumors**. *AJNR Am. J. Neuroradiology* 2003; 24: 225 – 233.

75. S. D. Rand, R. Prost, V. Haughton L. Mark et al. **Accuracy of Single-Voxel Proton MR Spectroscopy in Distinguishing neoplastic from Nonneoplastic Brain Lesions** *AJNR Am J Neuroradiology* 1997; *18:1695*–1704.

76. Carles Majós, et al. **Adult Primitive Neuroectodermal Tumor: Proton MR spectroscopic Findings with Possible Application for Differential Diagnosis**. *Radiology* 2002; 225:556-566.

77. Witold Gajewicz et al. **The use of proton MRS in the differential diagnosis of brain tumors and tumor-like processes.** *Med Sci Monit*, 2003; 9(9):MT97-105.

78. W.Hollingworth L, S. Medina et al. **A Systematic Literature Review of Magnetic Resonance Spectroscopy for the Characterization of Brain Tumors**; *AJNR Am J Neuroradiol* Aug 2006.

79. Isabella Maria Burtscher et al. **Proton MR Spectroscopy and preoperative diagnostic accuracy: An evaluation of intracranial mass lesions characterized by stereotactic biopsy findings** .*AJNR Am J Neuroradiology* 2000; 21: 84-93

80. Wilken et al. **Quantitative proton magnetic resonance spectroscopy of focal brain lesions**. *Pediatric Neurology* 2000; 23(1):22-31.

81 Fayed N, Morales H,, Modrego PJ, Pina MA . **Contrast/Noise ratio on conventional MRI and choline/creatine ratio on proton MRI spectroscopy accurately discriminate low-grade from high-grade cerebral gliomas** *Acad Radiol.* 2006 Jun; 13(6):728-37.

82. Kostas N. Fountas Effie Z. Kapsalaki , Stathis et al . **In vivo Proton Magnetic Resonance Spectroscopy of Brain Tumors.** *Stereotactic and Functional Neurosurgery* 2000; 74:83-94.

83. Alvaro Maghales MD, William godfrey et al. **Proton magnetic resonance spectroscopy of brain tumors correlated with pathology** *Acad Radiology* 2005 Jan; 12(1):51-7.

84. Jeniffer Butzen et al. **Discrimination between Neoplastic and Nonneoplastic Brain Lesions by Use of Proton MR Spectroscopy: The Limits of Accuracy with a Logistic Regression Model** .*AJNR Am. J. Neuroradiology* 2000; 21: 1213 – 1219

85. Veena Arpit Nagar, et al. **Multivoxel MR Spectroscopic Imaging – Distinguishing Intracranial Tumours from Non-neoplastic Disease.** *Ann Acad Med Singapore* 2007

86. A.Kumar, S.Kaushik, R.P.Tripathi, P.kaur, et al. **Role of Invivo proton MR Spectroscopy in the evaluation of adult brain lesions. Our preliminary experiences**. *Neurology India* 2003; 51:474-478

87. Kimura T, Sako K, Gotoh T et al**. In vivo single-voxel proton MR spectroscopy in brain lesions with ring-like enhancement.** *NMR Biomed* 2001; 14:339-349.

88. Lin A, et al. **Efficacy of proton magnetic resonance spectroscopy in clinical decision making for patients with suspected malignant brain tumors**. *J Neurooncol* 1999; 45(1):69-81

89. C.Majos, C.Aguilera, J.Alonso, et al. **Proton MR Spectroscopy Improves Discrimination between Tumor and Pseudotumoral Lesion in Solid Brain Masses** *AJNR Am. J. Neuroradiol*. 2009; 30(3): 544 - 551.

90. Chris Dowling et al. **Preoperative Proton MR Spectroscopic Imaging of Brain Tumors: Correlation with Histopathologic Analysis of Resection Specimens** *AJNR Am J Neuroradiology* 2001; 22:604–612.

91. Adamson, et al. **Focal brain lesions: effect of single-voxel proton MR spectroscopic findings on treatment decisions.** *Radiology* 1998; 209, 73-78.

92. Mishra AM, Gupta RK, Jaggi RS, et al**. Role of diffusion-weighted imaging and in vivo proton magnetic resonance spectroscopy in the differential diagnosis of ring-enhancing intracranial cystic mass lesions.** *J Comput Assist Tomogr* 2004; 28:540–47

93. Meng Law, Stanley Yang, Hao Wang et al .**Glioma Grading: Sensitivity, Specificity, and Predictive Values of Perfusion MR Imaging and Proton MR Spectroscopic Imaging Compared with**

Conventional MR Imaging; *AJNR Am J Neuroradiology* 2003; 24:1989–1998

94. Herminghaus et al. **Determination of histopathological tumor grade in neuroepithelial brain tumors by using spectral pattern analysis of in vivo spectroscopic data.** *J Neurosurg* 2003; 98:74–81

95. Elizabeth Meyerand et al**. Classification of Biopsy-Confirmed Brain Tumors Using Single-Voxel MR Spectroscopy.** *AJNR Am J Neuroradiology* 1999; 20:117-123.

96. Andreas Stadlbauer, PhD, Stephan Gruber, PhD et al. **Pre operative Grading of Gliomas by Using Metabolite Quantification with High-Spatial-Resolution Proton MR Spectroscopic Imaging .** *Radiology* 2006; (3):958-69.

97. Meng Law, Cha S, et al. **High-Grade Gliomas and Solitary Metastases: Differentiation by Using Perfusion and Proton Spectroscopic MR Imaging**. *Radiology* 2002; 222:715-721.

98. Tien et al. **Single voxel proton brain spectroscopy exam (PROBE/SV) in patients with primary brain tumors;** *AJR Am J Roentgenology* 1996; 167: 201-209.

99. Poptani H, Rakesh K. Gupta et al .**Characterization of Intracranial Mass Lesions with In Vivo Proton MR Spectroscopy**. *AJNR Am J Neuroradiology* 1995; 16:1593–1603.

100. Tong Z, et al**. In vivo quantification of the metabolites in normal brain and brain tumors by proton MR spectroscopy using water as an internal standard**. *Magn Reson Imaging.* 2004; 22(7):1017-24

101. Devos A, Lukas L, Suykens JA, et al. **Classification of brain tumours using short echo time 1H MR spectra**. *J Magn Reson* 2004; 170:164–75

102. Lukas L, Devos A, Suykens JA, et al. **Brain tumor classification based on long echo proton MRS signals**. *Artif Intell Med* 2004; 31:73–89

103. Astrakas LG, Zurakowski D, Tzika AA, et al. **Noninvasive magnetic resonance spectroscopic imaging biomarkers to predict the clinical grade of paediatric brain tumors**. *Clin Cancer Res* 2004; 10:8220–28

104. .K .Smith et al. **MR spectroscopy of Brain tumors**. *Mag reson clin N Am* 2003; 11:415-429.

105. Opstad KS, Murphy MM, Wilkins PR, et al. **Differentiation of metastases from High-grade gliomas using short echo time 1H spectroscopy**. *J Magn Reson Imaging* 2004; 20:187–92

106. Tzika AA, et al. **Multivoxel proton MR spectroscopy and hemodynamic MR imaging of childhood brain tumors: preliminary observations.** *AJNR, Am J Neuroradiology* 1997; 18:203-18

107. Castillo M, Kwock L. **Proton MR spectroscopic of common brain tumors**. *AJNR Am Neuroimaging Clin North Am 1998;* 8:733-752

108. Chan Y-1, Yeung DKW, Leung S-F, et al. **Proton magnetic resonance spectroscopy of late delayed radiation-induced injury of the brain.** *J Magn Reson Imaging* 1999; 10:130-137

109 Jaysundar Rama, Bakshi A, Singh VP, et al. **Diagnostic potential of proton MRS in differentiating between tumor recurrence and**

radiation necrosis? Paper presented at the *fifth Annual Scientific Meeting of the ISMRM* 1997; Vancouver BC, p 1142

110. Kimura T, Sako K, Tanaka K, et al**. Evaluation of the response of metastatic brain tumors to stereotactic radiosurgery by proton mag-netic resonance spectroscopy,^{201} TlCl single-photon emission com-puterized tomography, and gadolinium-enhanced magnetic reso-nance imaging.** *J Neurosurg* 2004; 100: 835-41.

111. Schlemmer HP, Bachert P, Henze M et al**. Differentiation of radiation necrosis from tumor progression using proton magnetic resonance spectroscopy.** *Neuroradiology* 2002; 44(3):216-22

112. Traber F, Block W, Flacke S, et al. **^{1}H-MR Spectroscopy of brain tumors in the course of radiation therapy: use of fast spectroscopic imaging and single voxel Spectroscopy for diagnosing recurrence**. *Rofo* 2002; 174:33–42

113. Ando K, Ishikura R, Nagami Y, et al. **Usefulness of Cho/Cr ratio in protonMR spectroscopy for differentiating residual/recurrent glioma from non-neoplastic lesions.** *Nippon Igaku Hoshasen Gakkai Zasshi* 2004; 64:121–26

114. Lichy MP, Henze M, Plathow C, et al. **Metabolic imaging to follow stereotactic radiation of gliomas—the role of1HMRspectroscopy in comparison to FDG PET and IMT-SPECT**. *Rofo* 2004; 176:1114–21

115. Plotkin M, Eisenacher J, Bruhn H, et al**. 123I-IMT SPECT and1HMR-spectroscopy at 3.0 T in the differential diagnosis of recurrent or residual gliomas: A comparative study**. *J Neurooncol* 2004; 70:49–58

116. McKnight TR, von dem Bussche MH, Vigneron DB, et al**. Histopathological validation of a three-dimensional magnetic resonance spectroscopy index as a predictor of tumor presence.** *J Neurosurg* 2002; 97:794–802

117. Gupta RK, Pandey R, Khan EM et al. **Intracranial tuberculomas: MRI signal intensity correlation with histopathology and localized proton spectroscopy.** *Magn Res Imaging* 1993;11: 443-449

118. Poptani H, Gupta RK, Jain VK, Roy R, Pandey R**. Cystic intracranial mass lesion: possible role of in vivo MR spectroscopy in its differential diagnosis**. *Magn Reson Imaging* 1995; 13: 1019–1029

119. Dev R, Gupta RK, Poptani H, Roy R, Sharma S, and Husain M. **Role of in vivo proton magnetic resonance spectroscopy in diagnosis and management of brain abscesses**. *Neurosurgery* 1998; 42: 37–43

120. Gupta RK, Kathuria M, Pradhan S. **Magnetization transfer MR imaging in central nervous tuberculosis**. *AJNR Am J Neuroradiol* 1999; 20:867–875

121. Rakesh K. Gupta, Davender K. Vatsal, Nuzat Husain. **Differentiation of Tuberculous from Pyogenic Brain Abscesses with In Vivo Proton MR Spectroscopy and Magnetization Transfer MR Imaging** *AJNR Am J Neuroradiol* 2001;22:1503–1509

122. Chang KH, Song IC, Kim H, et al. **In vivo single voxel proton MR spectroscopy in intracranial cystic masses.** *AJNR Am J Neuroradiol* 1998; 19:401–405

123. Grand S, Passaro G, Ziegler A, et al**. Necrotic tumor versus brain abscess: importance of amino acids detected at 1H MR spectroscopy—Initial results.** *Radiology* 1999; 213:785–793

124. Shukla-Dave A, , et al**. Prospective evaluation of in vivo proton MR spectroscopy in differentiation of similar appearing intracranial cystic lesions.** *Magn Reson Imagin.* 2001; 19(1):103-10.

125. Arnold DL, Matthews PM, Francis G, Antel J. **Proton magnetic resonance spectroscopy of human brain in vivo in the evaluation of multiple sclerosis: assessment of the load of disease.** *Magn Reson Med* 1990; 14:154–159

126. Arnold DL, Matthews PM, Francis GS, O'Connor J, Antel JP. **Proton magnetic resonance spectroscopic imaging for metabolic characterization of demyelinating plaques**. *Ann Neurol* 1992; 31:235–241

127. Bitsch A, Bruhn H, Vougioukas V, et al. **Inflammatory CNS demyelination: histopathologic correlation with in vivo quantitative proton MR spectroscopy.** *AJNR Am J Neuroradiol* 1999; 20:1619–27.

128**.** A Narayana, J. S Wolinsky, S. B Rao, Renjie He, et al.**Trial MRSI** Group **Multicentre proton magnetic resonance spectroscopy imaging of primary progressive multiple sclerosis** . *Multiple Sclerosis*, June 1, 2004; 10(1_suppl): S73 - S78.

129. CareAllies .**Medical Necessity Guidelines Magnetic Resonance Spectroscopy (MRS)** American Medical Association: Chicago, IL. 2007; Number 0244: Page 3

130. Dean BL, Drayer BP, Bird CR, et al. **Gliomas: classification with MR imaging**. *Radiology* 1990; 174:411–415

131. Watanabe M, Tanaka R, Takeda N. **Magnetic resonance imaging and histopathology of cerebral gliomas**. *Neuroradiology* 1992; 34:463–469

132. David N.Louis, Hiroko Ohgaki, Otmar D.Wiestler, B.W.Scheithauer et al. **The 2007 WHO Classification of tumours of the CNS**. *Acta Neuropathologica* 2007; 114(2):97-109

133. CHAP T.LE.Wiley. **Introductory Biostatistics -Interscience.** *A john wiley & sons publication.*2003

134. Box, G. E. P., Hunter, W. G. and Hunter. J. S. **Statistics for Experimenters**. New York: Wiley, 1978.

135 Keppel, G. **Design and Analysis**: *A Researcher's Handbook*. Englewood Cliffs, NJ: Prentice-Hall. 1991.

136 Dillon, W. R. and Goldstein, M. **Multivariate Analysis: Methods and Applications**. New York: Wiley .1984.

137. Agresti, A. **Categorical Data Analysis**. New York: Wiley.1990

138. Hourani R, Brant LJ, Rizk T, et al. **Can proton MR spectroscopic and perfusion imaging differentiate between neoplastic and nonneoplastic brain lesions in adults?** *AJNR Am J Neuroradiol* 2008; 29:366–72

139. Ginsberg LE, Fuller GN, Hashmi M, et al. **The significance of lack of MR contrast enhancement of supratentorial brain tumors in adults: histopathological evaluation of a series.** *Surg Neurol* 1998; 49:436–440

140. Ott D, Hennig J, Ernst T. **Human brain tumors: assessment with in vivo proton MR spectroscopy.** *Radiology* 1993; 186:745–752

141 . Kugel H, Heindel W, Ernestus RI, Bunke J, du Mesnil R, Friedmann G. **Human brain tumors: spectral patterns detected with localized H-1 MR spectroscopy**. *Radiology* 1992; 183:701–709

142. Fulham MJ, Bizzi A, Dietz MJ, et al. **Mapping of brain tumor metabolites with proton MR spectroscopic imaging: clinical relevance** .*Radiology* 1992; 185:675–686

143. Demaerel P, Johannik K, Van Hecke P, et al. **Localized H-1 NMRspectroscopy in fifty cases of newly diagnosed intracranial tumors**. *J Comput Assist Tomogr* 1991; 15:67–76

144. Kuesel AC, Sutherland GR, et al. **^{1}H MRS of high grade astrocytomas: mobile lipid accumulation in necrotic tissue**. *NMR Biomed* 1994; 7:149–155

145. Andreas Stadlbauer, PhD, Stephan Gruber, PhD et al. **Pre operative Grading of Gliomas by Using Metabolite Quantification with High-Spatial-Resolution Proton MR Spectroscopic Imaging**. *Radiology* 2006; 3:958-69

146. Shimizu H, Kumabe T, Tominaga T, et al. **Nonivasive evaluation of malignancy of brain tumors with proton MR spectroscopy**. *AJNR Am J Neuroradiol* 1996; 17:737–747

147. Yang D, Korogi Y, Sugahara T, et al. **Cerebral gliomas: prospective comparison of Multivoxel 2D chemical-shift imaging proton MR spectroscopy, echoplanar perfusion and diffusion- weighted MRI**. *Neuroradiology* 2002; 44:656–666.

148. Vuori K, Kankaanranta L, Hakkinen AM, et al**. Low-grade gliomas and focal cortical developmental malformations: differentiation with proton MR spectroscopy**. *Radiology* 2004; 230: 703–708.

149. Go KG, Kamman RL, Mooyaart EL, et al. **Localized proton spectroscopy and spectroscopic imaging in cerebral gliomas, with comparison to positron emission tomography.** *Neuroradiology*1995; 37:198–206

150. Pruel MC. **Accurate noninvasive diagnosis of human brain tumors by using proton magnetic resonance spectroscopy**. *Nature Med* 1996; 2:323–325

151. Scheithauer BW. **The forms of growth in gliomas and their practical significance**. *Brain* 1940; 63:1–35

152. Burger PC. **Classification, grading and patterns of spread of malignant gliomas.** In: Apuzzo ML, ed. *Neurosurgical Topics: Malignant Cerebral Glioma.* Park Ridge, IL: American Association of Neurological Surgeons; 1990:3–17

153. Sijens PE, van Dijk P, Oudkerk M. **Correlation between Choline level and Gd-DTPA enhancement in patients with brain metastases of mammary carcinomas.** *Magn Reson Med* 1994; 32:549– 555

154. Sijens PE, Knopp MV, Brunetti A et al. **^{1}H MR spectroscopy in patients with metastatic brain tumors: a multicenter study**. Magn Reson Med, 1995; 33: 818-26

155. Shino A, Nakasu S, Matsuda M et al. **Noninvasive evaluation of the malignant potential of intracranial meningiomas performed using proton magnetic resonance spectroscopy**. *J Neurosurg,* 1999; 91: 928-34

156. Rubaek, Danielsen E, Ross B. **Magnetic resonance spectroscopy diagnosis of neurological diseases.** Marcel Dekker, Inc New York, 1999

157. Demir MK, Iplikcioglu AC, Dincer A, Arslan M, Sav A. **Single voxel proton MR spectroscopy findings of typical and atypical intracranial meningiomas**. *Eur J Radiol*. 2006 Oct; 60(1):48-55.

158. Sharad Maheshwari, Suresh Mukherji. **Proton MR Spectroscopy: Clinical Applications** . *Imaging Economics* August , 2002

159. Chang L,Ernst T **. MR spectroscopy and diffusion- weighted MR imaging in focal brain lesions in AIDS**. *Neuroimaging Clin North Am* 1997; 7: 409-426.

160. Ethan A. Smith; Ruth C. Carlos; Larry R. Junck et al. **Developing a Clinical Decision Model: MR Spectroscopy to Differentiate Between Recurrent Tumor and Radiation Change in Patients with New Contrast- Enhancing Lesions** .*AJR* 2009; 192: February

161. Gober JR.. **Noninvasive tissue characterization of brain tumor and radiation therapy using magnetic resonance spectroscopy**. *Neuroimaging Clin North Am* 1993; 3:779–802

162. Herholz K, Coope D, Jackson A. **Metabolic and molecular imaging in neuro-oncology**. *Lancet Neurol.* 2007; (8):711-24

163. Zeng QS, Li CF, Zhang K, Liu H, Kang XS, Zhen JH. **Multivoxel 3D proton MR spectroscopy in the distinction of recurrent glioma from radiation injury**. *J Neurooncol* 2007; 84:63–69.

164. Weybright P, Sundgren PC, Maly P, et al. **Differentiation between brain tumor recurrence and radiation injury using MR spectroscopy.** *AJR* 2005; 185:1471–1476.

165. Tzika AA, Zarifi MK, Goumnerova L, Astrakas LG, Zurakowski D, Young-Poussaint T, et al. **Neuroimaging in pediatric brain tumors: Gd-DTPA-enhanced, hemodynamic, and diffusion MR imaging compared with MR spectroscopic imaging**. *AJNR Am J Neuroradiol.* 2002 Feb; 23(2):322 33.

166. Lin A, Bluml S, Mamelak AN. **Efficacy of proton magnetic resonance spectroscopy in clinical decision making for patients with suspected malignant brain tumors**. *J Neurooncol*. 1999; 45(1):69-81.

167. Lin A, Ross BD, Harris K, Wong W. **Efficacy of proton magnetic resonance spectroscopy in neurological diagnosis and neurotherapeutic decision making.** *NeuroRx*. 2005 Apr; 2(2):197-214.

168. Rock JP, Scarpace L, Hearshen D, et al**. Associations among magnetic resonance spectroscopy, apparent diffusion coefficients, and image-guided histopathology with special attention to radiation necrosis**. *Neurosurgery* 2004; 54(5):1111-7

169. Ende J, Scatliff JH, Powers S, et al**. Spectral proton and P-31 MR Spectroscopy Patterns of Treated Human Brain Tumors**. Presented at the *11th Annual Meeting of the Society of Magnetic Resonance in Medicine*, Berlin, Germany 1992

170. Dieta Brandsma, Lukas Stalpers, Walter Taal, et al. **Clinical features, mechanisms, and management of pseudoprogression in malignant gliomas.** *The Lancet Oncology* 2008; 9, (5): 453 - 461

171. Shin-Ichi Miyatake, Shinji Kawabata, Naosuke Nonoguchi, et al. **Pseudoprogression in boron neutron capture therapy for malignant gliomas and meningiomas.** *Neuro-Oncology* 2009; 11(4):430-436

172. Taal W, Brandsma D, de Bruin HG, et al. **Incidence of early pseudoprogression in a cohort of malignant glioma patients treated with chemo-irradiation with temozolomide**. *Cancer*.2008; 113(2): 405-410

173. Chamberlain MC, Glantz MJ, Chalmers L, Van Horn A, Sloan AE. **Early necrosis following concurrent Temodar and radiotherapy in patients with glioblastoma**. *J Neurooncol* 2007; 82: 81-83

174. Chaskis C, Neyns B, Michotte A, et al. **Pseudoprogression after radiotherapy with concurrent temozolomide for high-grade glioma: clinical observations and working recommendations.** *Surg Neurol.* 2009 Oct; 72(4):423-8.

175. Yamagata NT, Miller BL, McBride D, et al. **In vivo proton spectroscopy of intracranial infections and neoplasms**. *J Neuroimaging* 1994; 4:23–28

176. Kim SH, Chang KH, Song IC, et al**. Brain abscess and brain tumor: discrimination with in vivo H-1 MR spectroscopy**. *Radiology* 1997; 204:239–245

177. Whitener DR. **Tuberculous brain abscess**. *Arch Neurol* 1978; 35: 148–155

178. Jayasundar R, Singh VP, Raghunathan P, Jain K, Banerji AK. **Inflammatory granulomas: evaluation with proton MRS.** *NMR Biomed* 1999; 12:139–144

179. Brenner RE, Munro PMG, Williams SCR, et al. **The proton NMR spectrum in acute EAE: the significance of the change in the Cho:Cr ratio**. *Magn Reson Med* 1993; 29:737–745

180. Hendrikus G. J. Krouwer, Thomas A. Kim, Scott D. Rand**. Single-Voxel Proton MR Spectroscopy of Nonneoplastic Brain Lesions suggestive of a Neoplasm** *AJNR Am J Neuroradiol* 1998; 19:1695–1703

181. Gupta RK, Roy R, Poptani H, et al. **Finger printing of *Mycobacteriumtuberculosis* in intracranial tuberculomas using in vivo, ex vivo and in vitro proton spectroscopy.** *Magn Reson Med* 1996; 36:829–833

182. Gupta RK, Roy R. **MR imaging and spectroscopy of intracranial tuberculomas.** *Curr Sci* 1999; 76:783–788

183. Jinkins JR, Gupta R, Chang KH, et al. **MR imaging of central nervous tuberculosis.** *Radiol Clin North Am* 1995; 33:771–786

184. Mendz GL, McCall MN, Kuchel PW. **Identification of methyl resonances in the ^{1}H NMR spectrum of incubated blood cell lysate.** *J Biol Chem* 1989; 264:2100–2107

185. Chapman M, Murray RO, Stoker DJ. **Tuberculosis of the bones and joints.** *Semin Roentgenol* 1979; 14–282:266

186. Prakash B, Mehta G, Gondal R, Kumar S, Malhotra V. **Tuberculous abscesses of the brain stem.** *Surg Neurol* 1989;32: 445–448

187. Remy C, Grand S, Laı ES, et al. **^{1}H MRS of human brain abscesses in vivo and in vitro.** *Magn Reson Med* 1995; 34:508–514

188. May GL, Sztelma K, Sorrell TC, Mountford CE. **Comparison of human polymorphonuclear leukocytes from peripheral blood and purulent exudates by high resolution 1H MRS.** *Magn Reson Med* 1991; 19:191–198

189. Martı´nez-Pe´rez I, Moreno A, Alonso J, et al**. Diagnosis of brain abscess by magnetic resonance spectroscopy.** *J Neurosurg* 1997; 86:708–713

190. Lai PH, HO JT et al. **Brain abscess and necrotic brain tumor: Discrimination with proton MR spectroscopy and diffusion weighted image**; *AJNR Am J Neuroradiology* 2002; 23; 1369-77

191. Haimes AB, Zimmerman RD, Morgello S, et al. **MR imaging of brain abscess**. *AJNR Am J Neuroradiol* 1989; 10:279–291

192. Bowen BC, Post MJD. **Intracranial infection**. In: Atlas SW, ed. *Magnetic Resonance Imaging of the Brain and Spine.* New York, NY: Raven Press; 1997: 501–538

193. Kohli A, Gupta RK, Poptani H, Roy R**. In vivo proton magnetic resonance spectroscopy in a case of intracranial hydatid cyst**. *Neurology* 1995; 45:562–564

194. Isabella M. Burtscher and Stig Holtas. **In Vivo Proton MR Spectroscopy of Untreated and Treated Brain Abscesses.** *AJNR Am J Neuroradiol* 1999; 20:1049–1053

195. Ernst T, Chang L, Walot I, et al. **Physiologic MRI of a tumefactive multiple sclerosis lesion.** *Neurology* 1998; 51:1486–88 28

196. Narayana PA. **Magnetic resonance spectroscopy in the monitoring of multiple sclerosis.** *J Neuroimaging* 2005; 15:46S–57S25-2

197. Dousset V, Grossman RI, Ramer KN, et al. **Experimental allergic encephalomyelitis and multiple sclerosis lesion characterization with magnetization transfer imaging.** *Radiology* 1992; 182: 483–491

198. Giulian D. **Microglia and neuronal dysfunction.** In: Kettenmann H, Ransom BR, eds. *Neuroglia*. New York: Oxford University Press; 1995:671–684

199. Wekerle H. **Antigen presentation by central nervous system glia.** In: Kettenmann H, Ransom BR, eds. *Neuroglia*. New York: Oxford University Press; 1995:685–699

200. Benveniste E. **Cytokine production.** In: Kettenmann H, Ransom BR, eds. *Neuroglia*. New York: Oxford University Press; 1995:700– 713

201. Roser W, Hagberg G, Mader I, et al. **Proton MRS of gadolinium enhancing MS plaques and metabolic changes in normal-appearing white matter**. *Magn Reson Med* 1995; 33:811–817.

202. Koopmans RA, Li DKB, Zhu G, Allen PS, Penn A, Paty DW**. Magnetic resonance spectroscopy of multiple sclerosis: in-vivo detection of myelin breakdown products**. *Lancet* 1993; 341:631–632

203. B ruhn H, Frahm J, Merboldt KD, et al. **Multiple sclerosis in children: cerebral metabolic alterations monitored by localized proton magnetic resonance spectroscopy in vivo**. *Ann Neurol* 1992; 32:140–150

204. Brand A, Richter-Landsberg C, Leibfritz D. **Multinuclear NMR studies on the energy metabolism of glial and neuronal cells.** *Dev Neurosci*. 1993; 15(35):289–298.

205. Srinivasan R, Sailasuta N, Hurd R, Nelson S, Pelletier D**. Evidence of elevated glutamate in multiple sclerosis using magnetic resonance spectroscopy at 3 T.** ***Brain***. 2005 May; 128(Pt 5):1016–1025

206. Khan OA, Bauserman SC,Rothman MI,et al . **Concurrence of multiple sclerosis and brain tumor: clinical considerations.** *Neurology*. 1997 May 48(5):1330-3

207. Amit M Saindane , Cha S, Law M, et al. **Proton MR spectroscopy of tumefactive demyelinating lesions.** *AJNR Am J Neuroradiol* 2002; 23: 1378–86

208. Matthews PM, De Stefano N, Narayanan S, et al. **Putting magnetic resonance spectroscopy studies in context: axonal damage and disability in multiple sclerosis**. *Semin Neurol.* 1998; 18:327–336

209. Narayanan S, Caramanos Z, Arnold D. **The effect of glatiramer acetate treatment on axonal integrity in multiple sclerosis** *Mult Scler.* 2004; 10 (suppl 2)(S256):Abstract P633

210. Balasrinivasa R. Sajja, Jerry S. Wolinsk and Ponnada A. Narayana, **Proton Magnetic Resonance Spectroscopy in Multiple Sclerosis.** *Neuroimaging Clin N Am*. 2009 Feb; 19(1): 45–58

211. Arnold DL**. Evidence for neuroprotection and remyelination using imaging techniques**. *Neurology*.2007 May 29; 68(22 Suppl 3):S83–90. Discussion S91-86.

212. Khan O, Shen Y, Caon C, et al. **Axonal metabolic recovery and potential neuroprotective effect of glatiramer acetate in relapsing-remitting multiple sclerosis**. *Mult Scler.* 2005 Dec; 11(6):646–651

213. Comi G, Filippi M, Wolinsky JS. **European/Canadian multicenter, double-blind, randomized, placebo-controlled study of the effects of glatiramer acetate on magnetic resonance imaging--measured disease activity and burden in patients with relapsing multiple sclerosis. European/Canadian Glatiramer Acetate Study Group**. *Ann Neurol.* 2001 Mar; 49(3):290–297.

214. Paty DW, Li DK. **Interferon beta-1b is effective in relapsing-remitting multiple sclerosis. II. MRI analysis results of a**

multicenter, randomized, double-blind, placebo-controlled trial. UBC MS/MRI Study Group and the IFNB Multiple Sclerosis Study Group. *Neurology* 1993 Apr; 43(4):662–667.

215. Gruber S, Mlynarik V, Moser E. **High-resolution 3D proton spectroscopic imaging of the human brain at 3 T: SNR issues and application for anatomy-matched voxel sizes**. *Magn Reson Med* 2003; 49:299–306

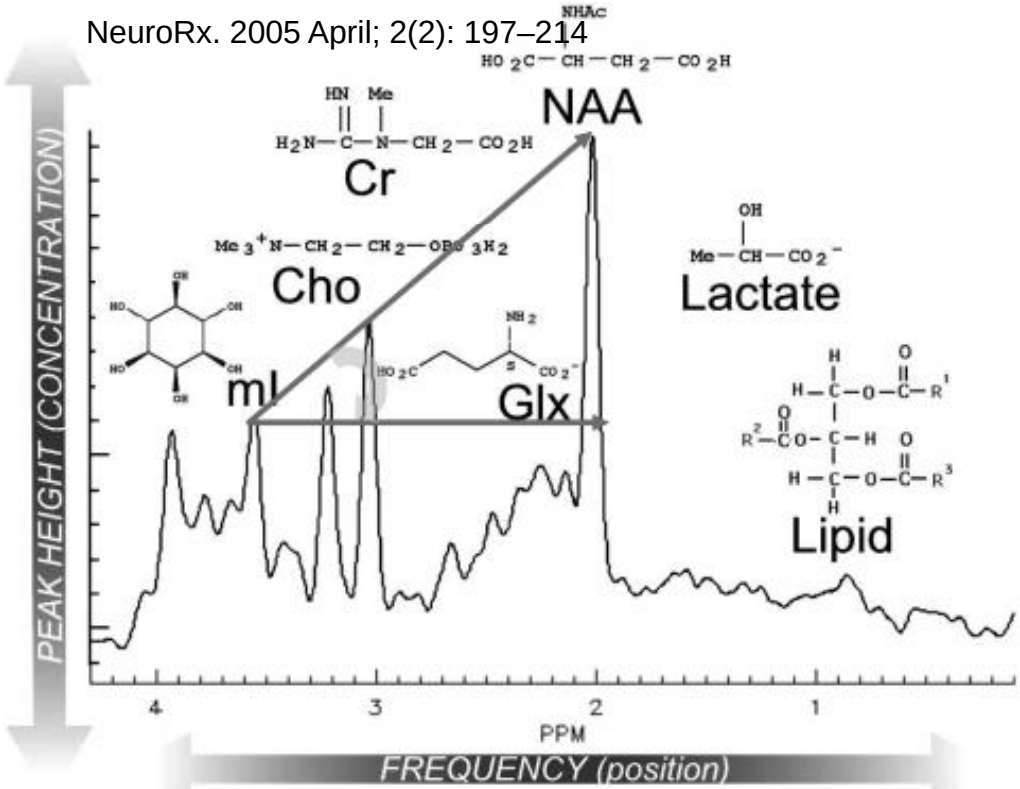

A. **Fig. 1a: Magnetic Resonance Spectroscopy (MRS): single voxel proton MRS using point resolved spectroscopy for water and lipid suppression (TE:144)**
The "X" axis represents frequency position of the proton containing metabolites displayed as peaks related to chemical shift from zero point displayed in units of parts per million
"Y" axis peak height representing metabolites concentration
Normal spectral pattern : mI , Cho, Cr, Glx, NAA and lip from right to left

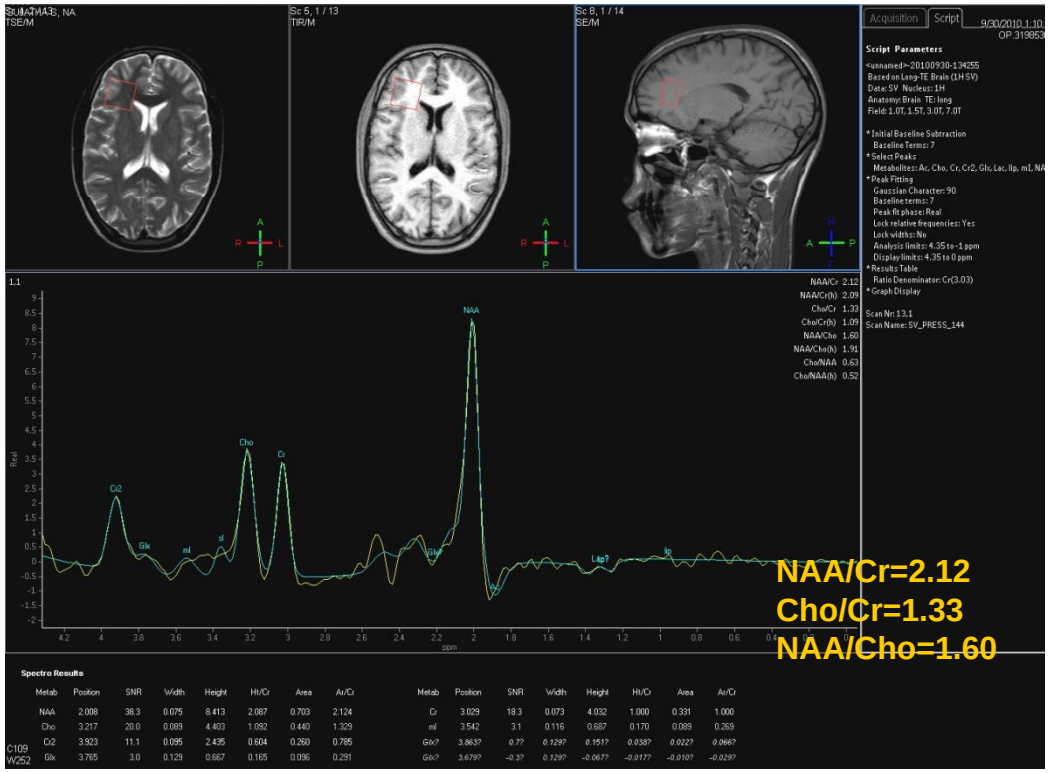

Fig. 1. MRS in (control) Healthy individual : single voxel MRS in frontal lobe showing normal spectral pattern with metabolites ratios

:

Case No. 1 : Seventeen years, female presented with seizure disorder

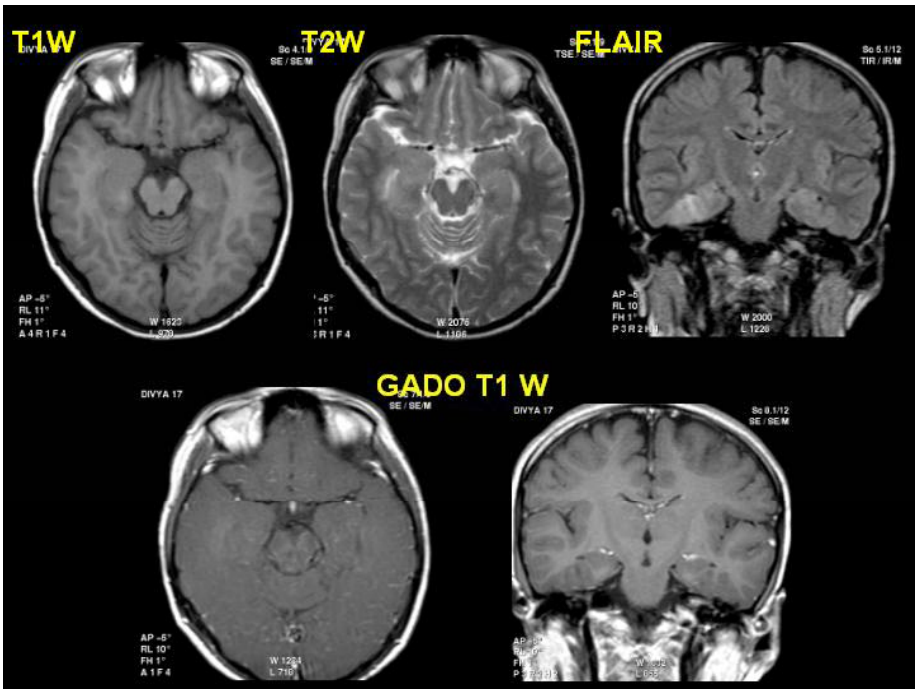

Fig. 2a: MRI shows faint, subtle, signal alteration on T2 WI in the right medial temporal cortex and non-enhancing on Post gadolinium contrast study – A nonspecific finding

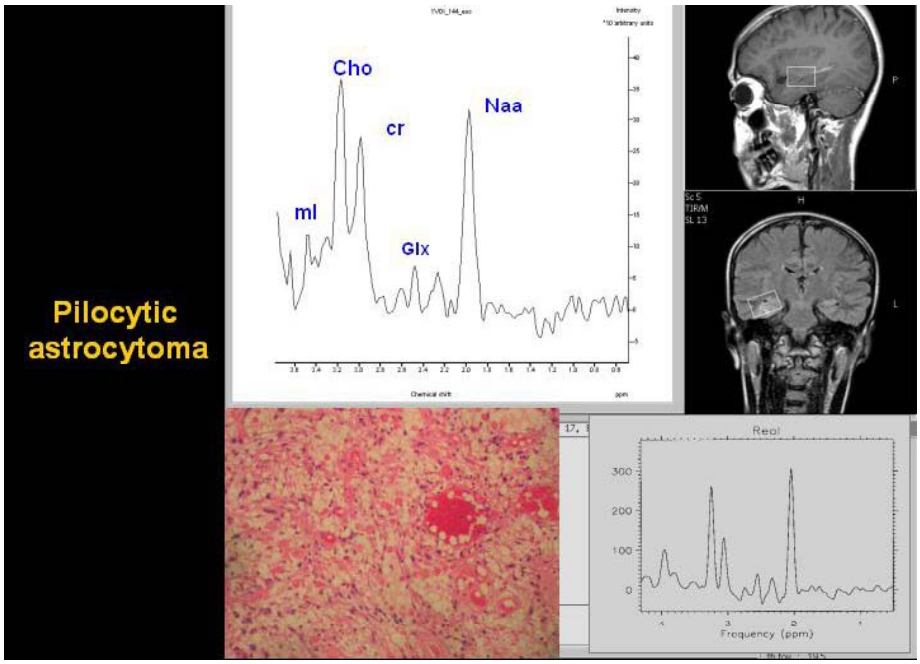

Fig. 2b: MRS reveals increased Cho/Cr ratio with small myoinositol peak at 3.5ppm representing low grade neoplasm

Case No. 2 : Twenty years, Male presented with seizure

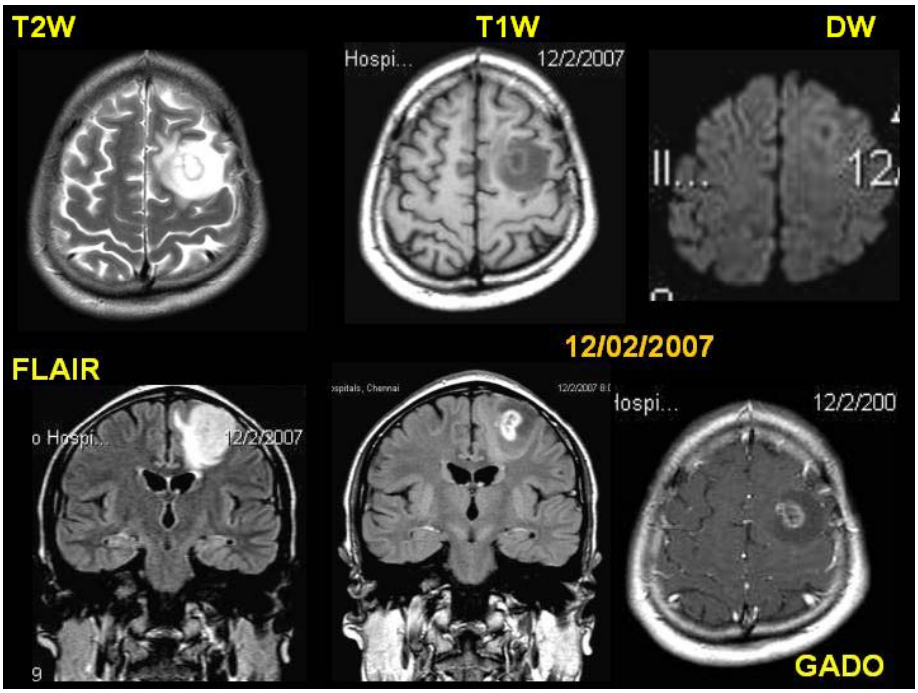

Fig. 3a: MRI shows, a small, nodular, peripheral enhancing lesion in the left frontal cortex mimicking a granuloma

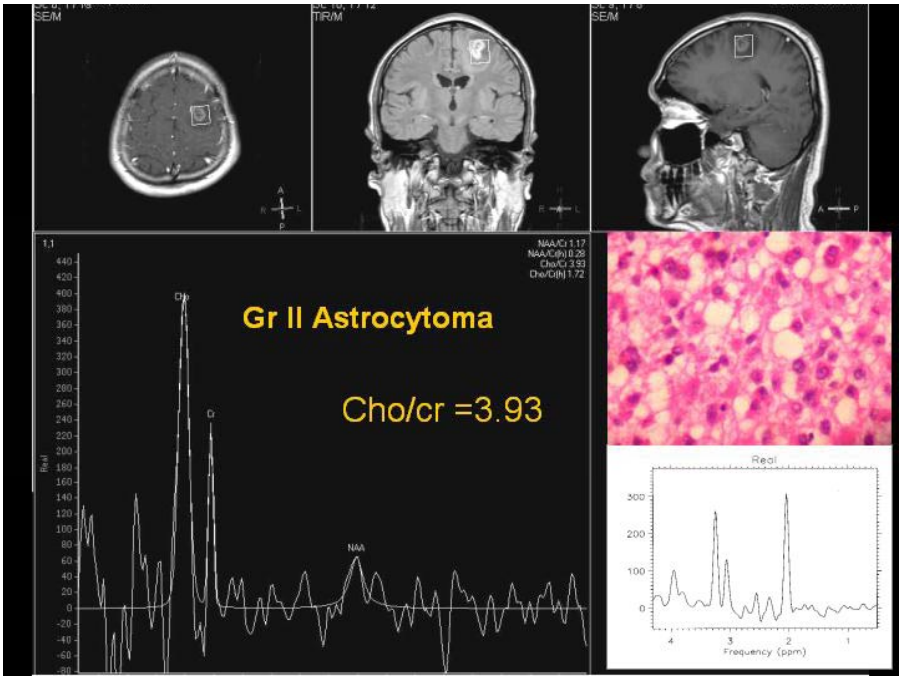

Fig. 3b: MRS reveals increased Cho/Cr ratio (3.93)with marked reduction of NAA peak suggesting a neoplasm ; Stereotactic biopsy : Grade II Astrocytoma

MRS changed the MRI diagnosis

Case No. 2 (contd.) : Post radiation follow up

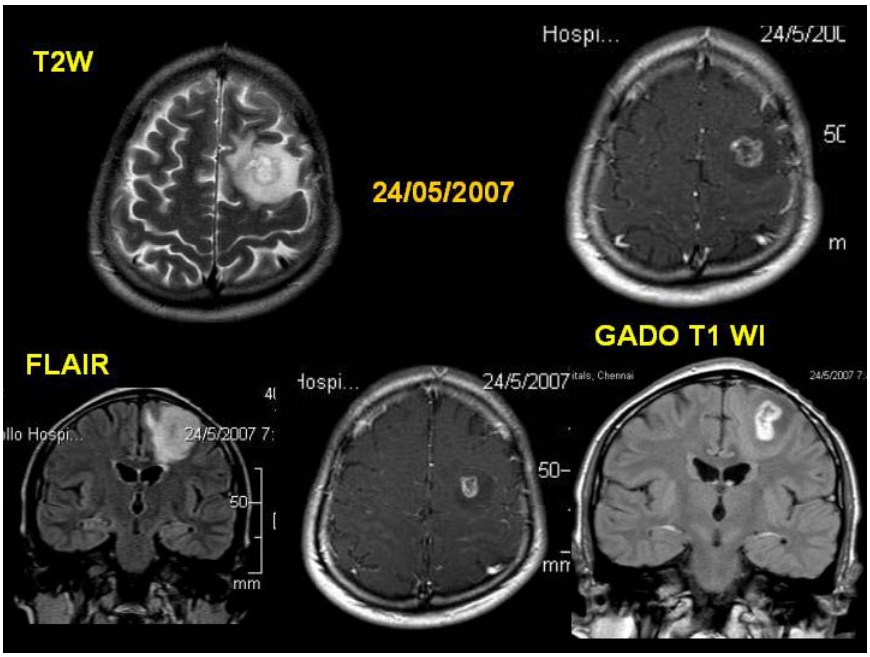

Fig. 3c: MRI after 3 months shows, a small, nodular, peripheral enhancing lesion with perilesional edema in the left frontal cortex as seen in pre-operative study- Recurrence

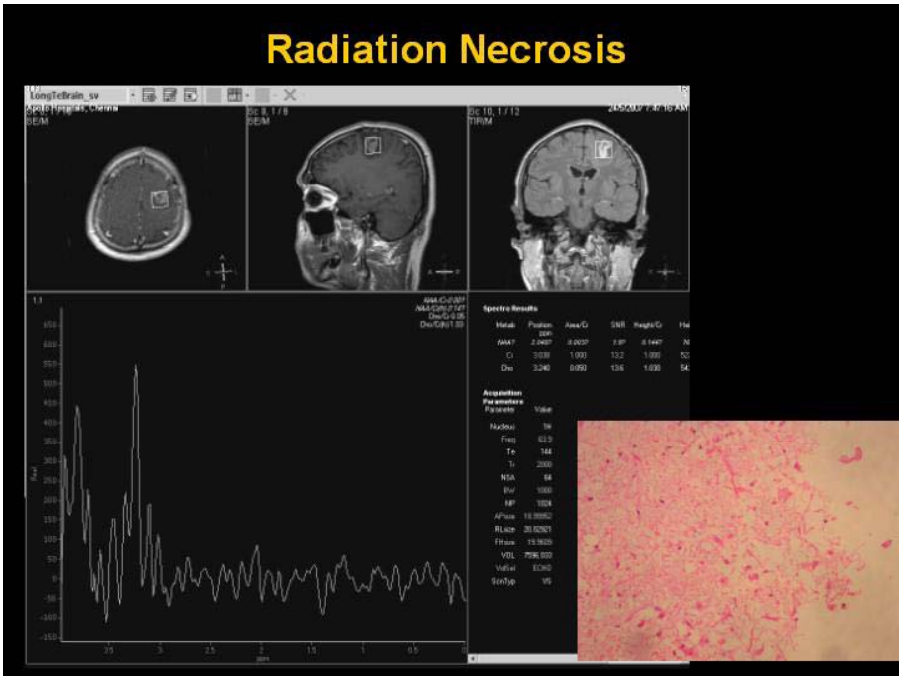

Fig. 3d: MRS reveals mild elevation of Cho peak with non-visualized NAA peak representing reactive changes
Stereotactic biopsy : Radiation changes

Case No. 3 : Twenty seven years, male presented with left side weakness for one week

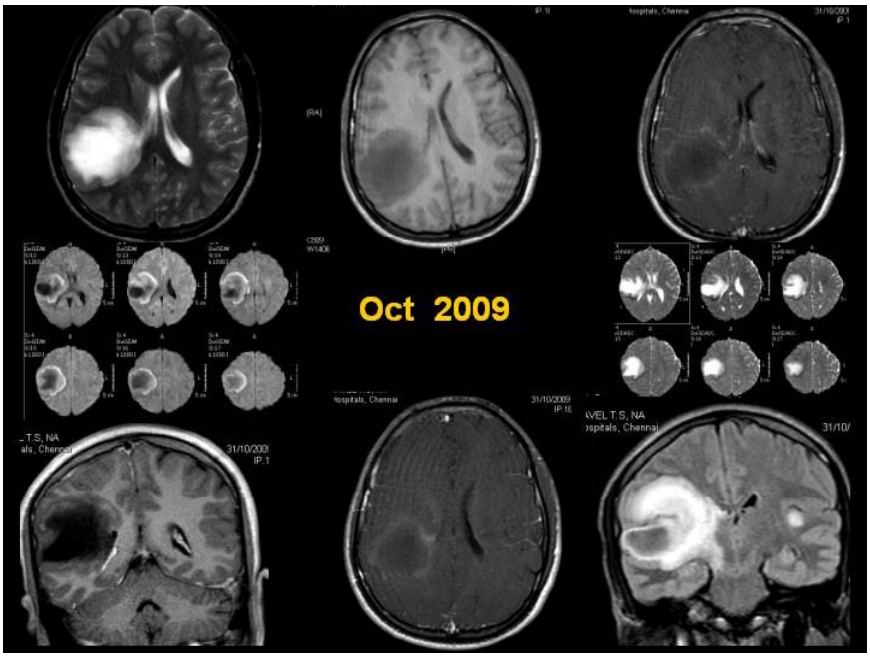

Fig. 4a: MRI shows a large, peripherally faint,indistinct enhancing lesion with perilesional edema and mass effect in the right temporal lobe; lesion reveals a peripheral rim of restricted diffusion on DW images suggesting a neoplasm

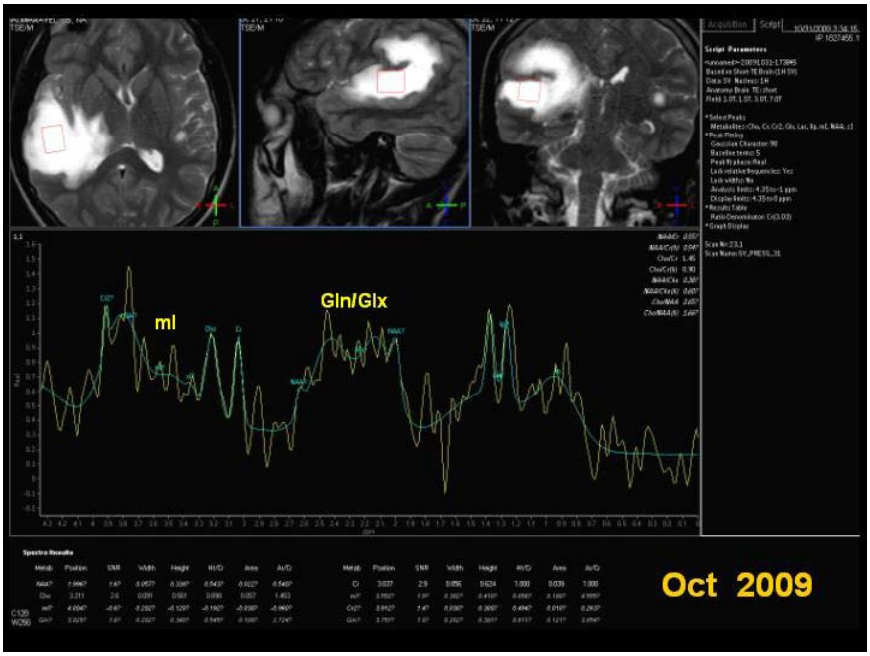

Fig. 4b: MRS reveals a broad peak between 2.1 and 2.5 ppm representing Gly/Gln and a myo-inositol peak; marked reduction in Cho and NAA suggesting non-neoplastic lesion; possibility of demyelinating disease is considered

Case No. 3 (contd.): Post medical treatment Follow up

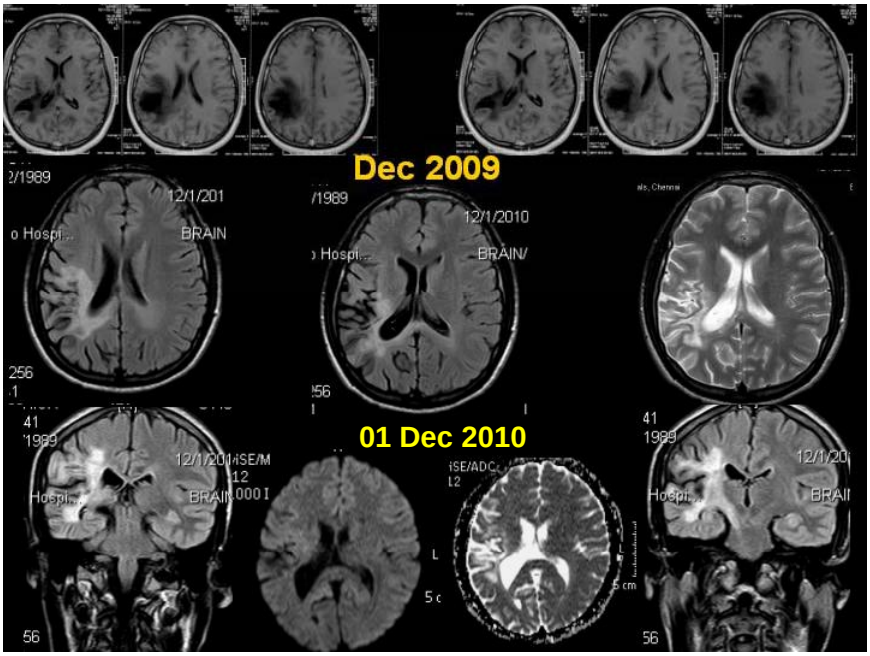

Fig. 4c: MRIs (after 2 months and 14 months)show significant reduction in the size of the lesion on Dec 2009; gliosis in subcortical and deep white matter with wallerian degeneration along the tract on Dec 2010 studies

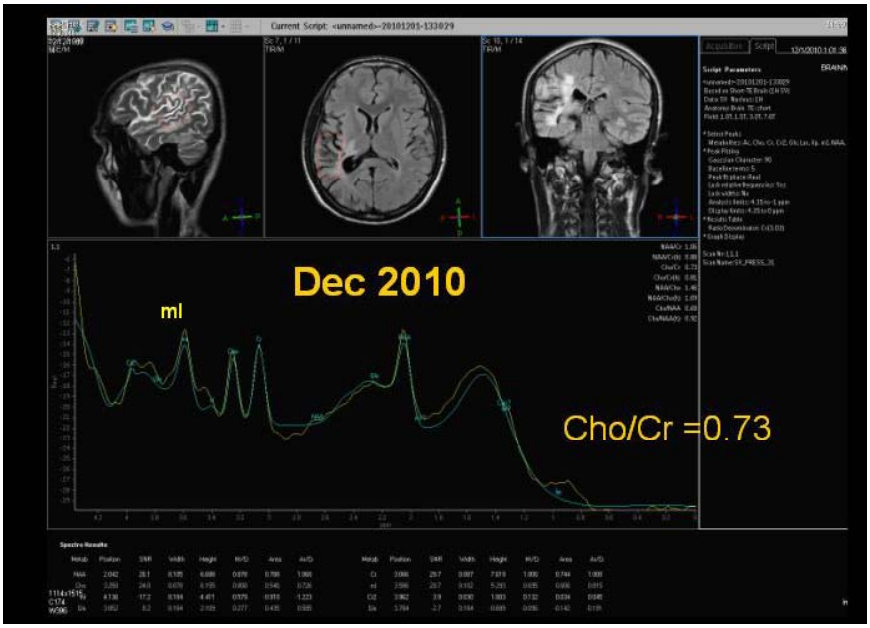

Fig. 4d: MRS reveals a myo-inositol peak; marked reduction in Cho and NAA and broad lipid peak representing chronic demyelinating disease

MRI aided MRS obviated need for biopsy or surgery in this patient

Case No. 4 : Twenty one years, Male presented with seizure disorder

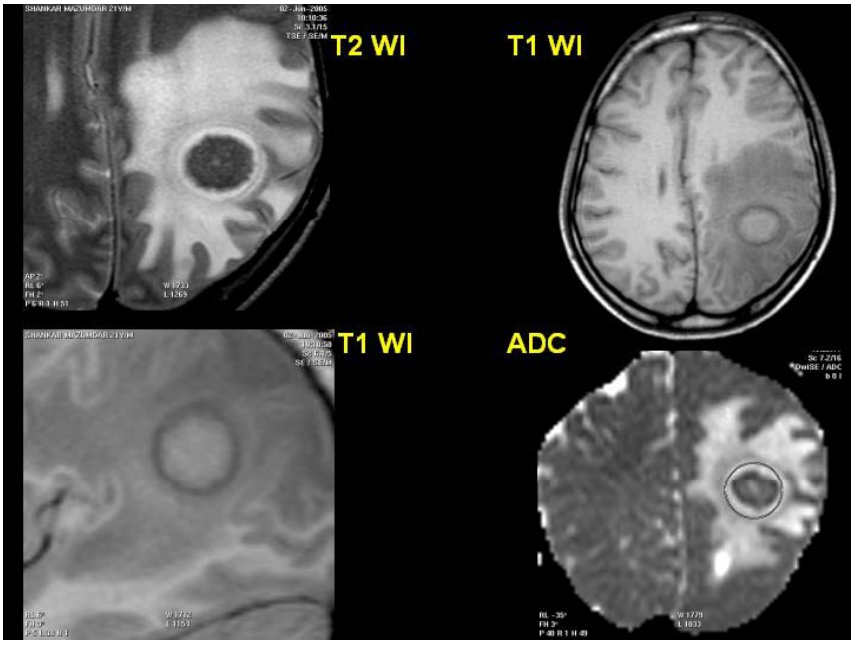

Fig. 5a: MRI shows, a circumscribed nodular, peripheral enhancing lesion with central hypointense area and hyperintense rim on T2 WI in the left parietal lobe ; ? Granuloma. ? Neoplasm

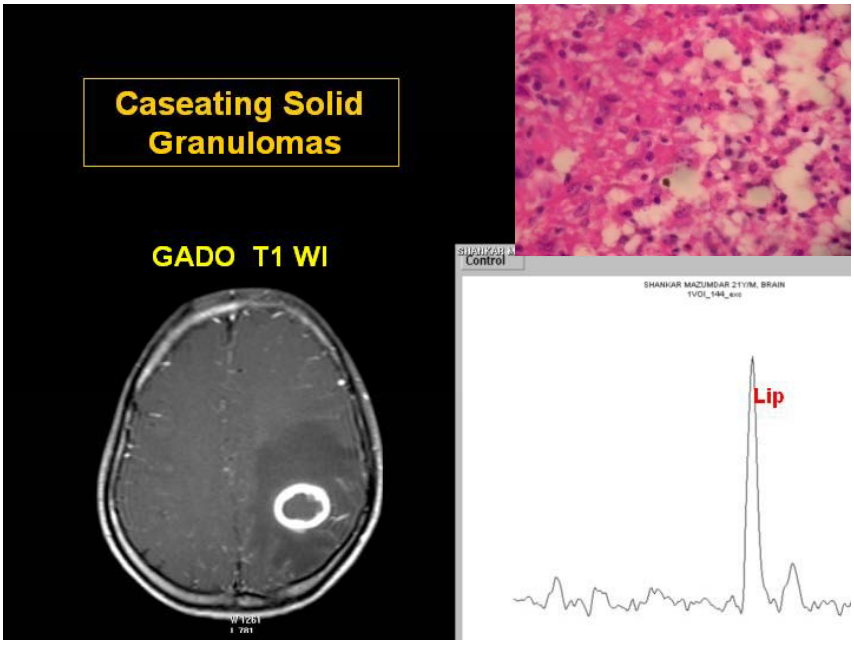

Fig. 5b: MRS reveals a sharp lipid peak at 1.3ppm and absence of Cho, NAA and other metabolites representing Tuberculoma

Case No. 5 : Forty six years, Male presented with seizure disorder

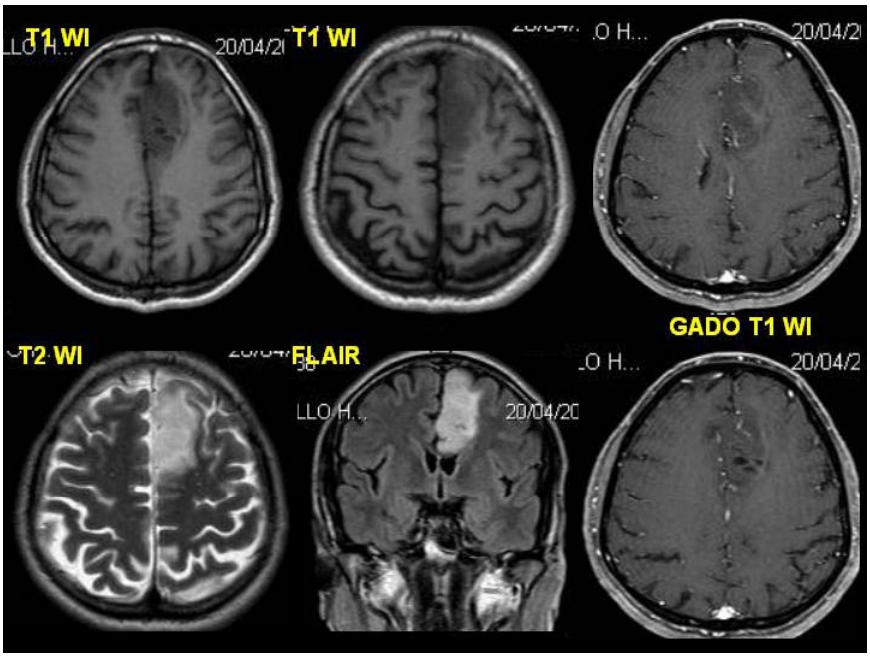

Fig. 6a: MRI shows, signal alteration on T2 WI in the left medial frontal cortex and non-enhancing on Post gadolinium contrast study – A nonspecific finding in the left frontal cortex – Focal cerebritis or neoplasm

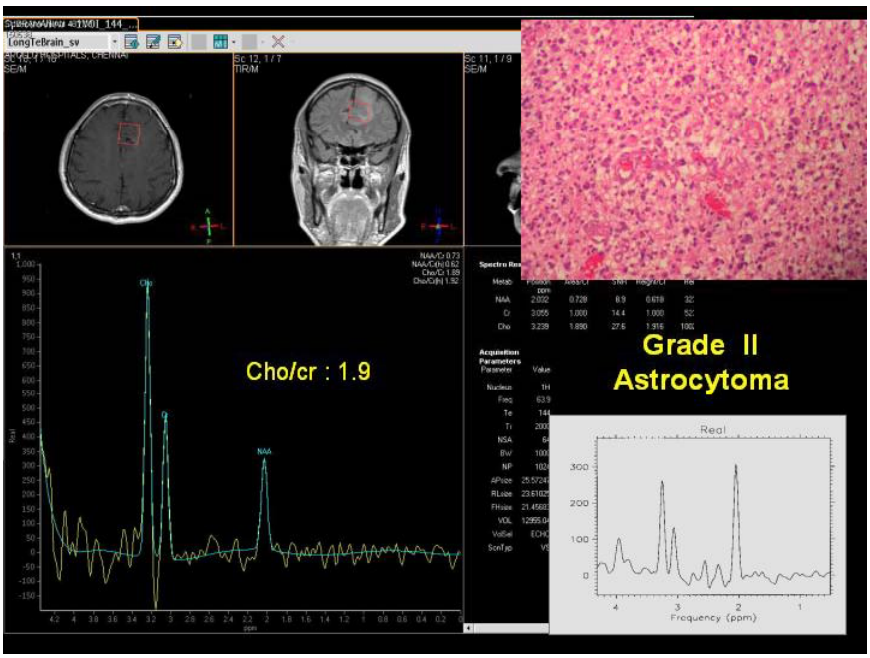

Fig. 6b: MRS reveals increased Cho/Cr ratio (1.9)with mild reduction of NAA peak suggesting a neoplasm ;
Stereotactic biopsy : Grade II Astrocytoma

Case No. 6 : Fifty seven years, Male presented headache and seizure -3 months

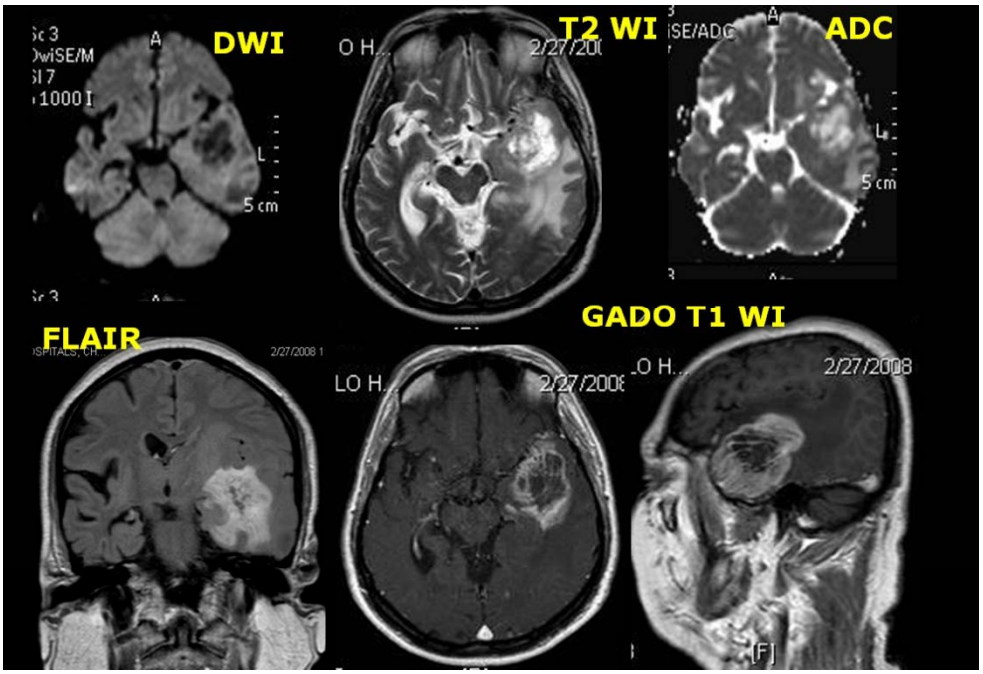

Fig No: 7 A. MRI shows, a large, thick nodular, peripheral enhancing necrotic lesion with edema and mass effect in the left temporal lobe representing high grade neoplasm

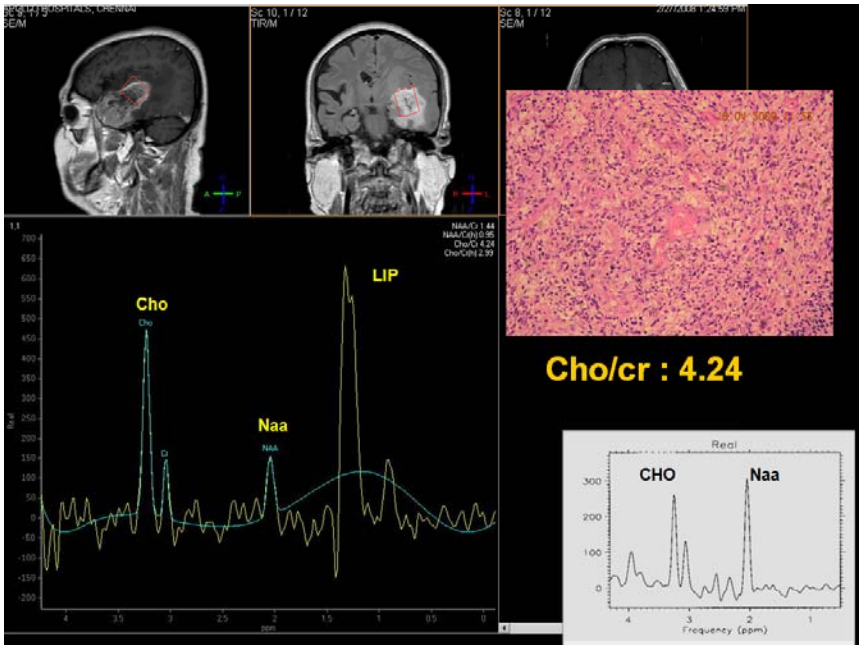

Fig No: 7 B. MRS reveals increased Cho/Cr ratio (4.24)with marked reduction of NAA peak and sharp increased in height of lipid peak - a high grade neoplasm
Biopsy : GBM

Case No. 7 : Twenty six years , Male presented with headache and vomiting

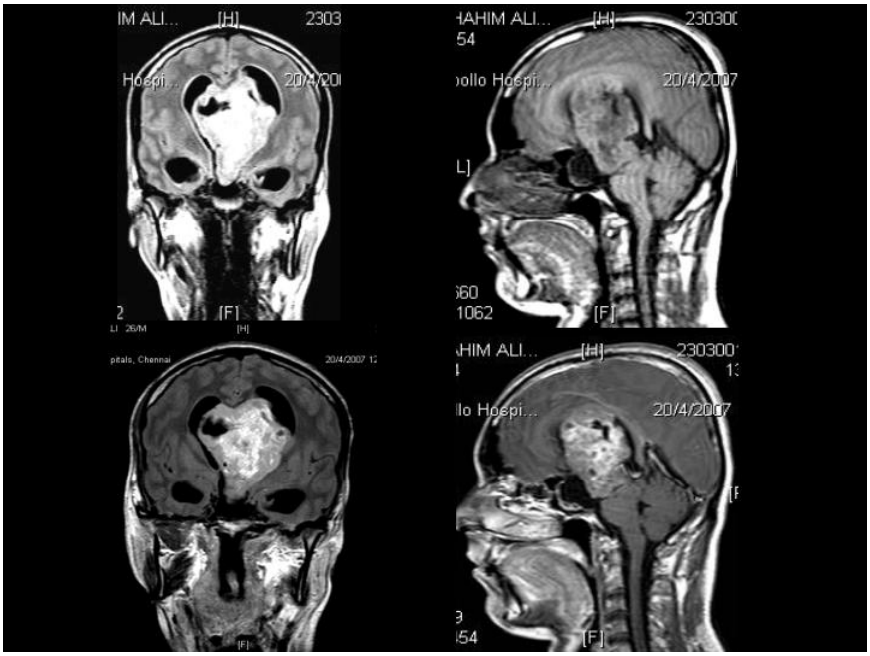

Fig. 8a: MRI shows, a large, midline, solid with cystic areas, intensely enhancing septal mass causing obstructive hydrocephalus-high grade neoplasm

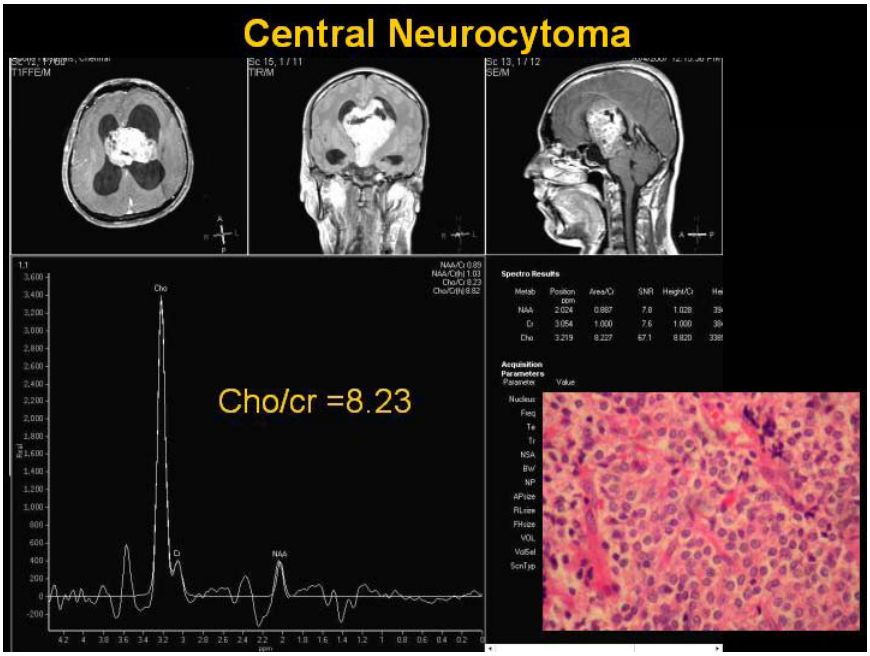

Fig. 8b: MRS reveals sharp increased choline height with Cho/Cr ratio (8.24) with marked reduction of NAA peak;
No lipid or lac peak seen. Biopsy : Central neurocytoma

Case No. 8 : 64Yrs male, presented with late onset seizure

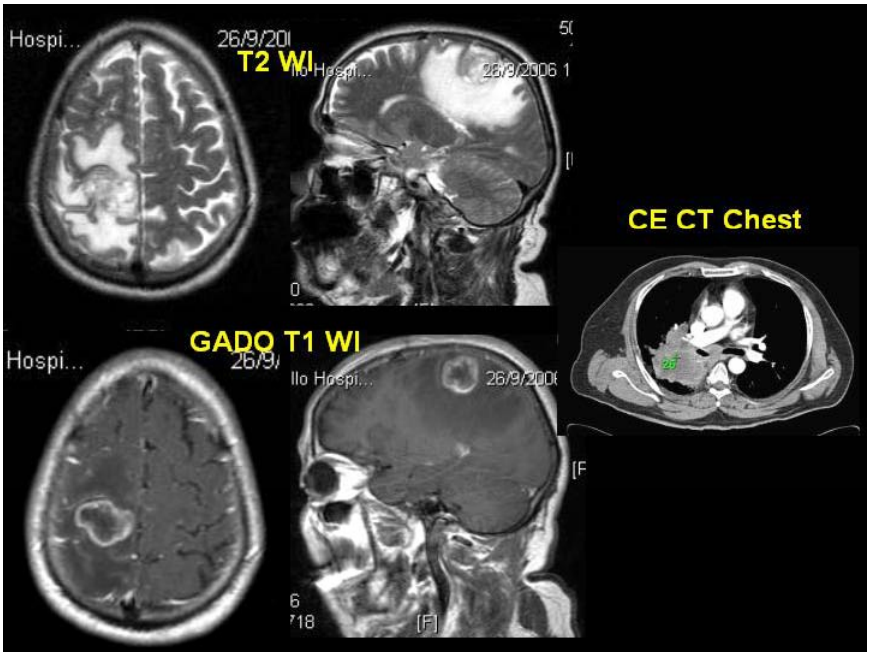

Fig. 9a: MRI shows a thick walled peripheral enhancing nodular lesion with area of necrosis and marked peri-enhancing edema in the right parietal lobe; CT chest reveals central bronchogenic carcinoma

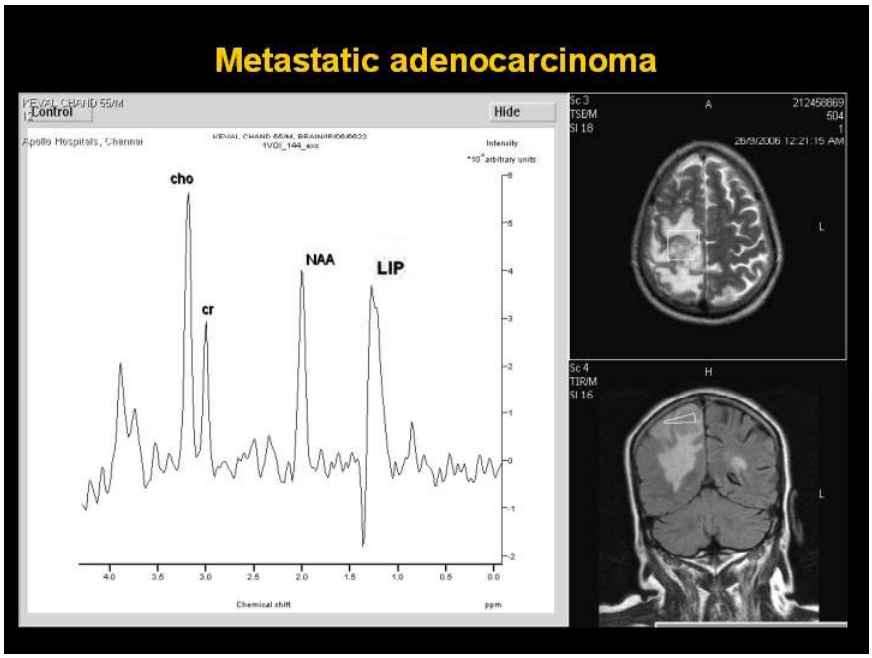

Fig. 9b: MRS reveals increased Cho/Cr ratio (3.1)with mild reduction of NAA peak and lipid elevation suggesting a necrotic neoplasm. Stereotactic biopsy : metastatic adenocarcinoma

Case No. 9 : Thirty one years , male presented with headache and seizure

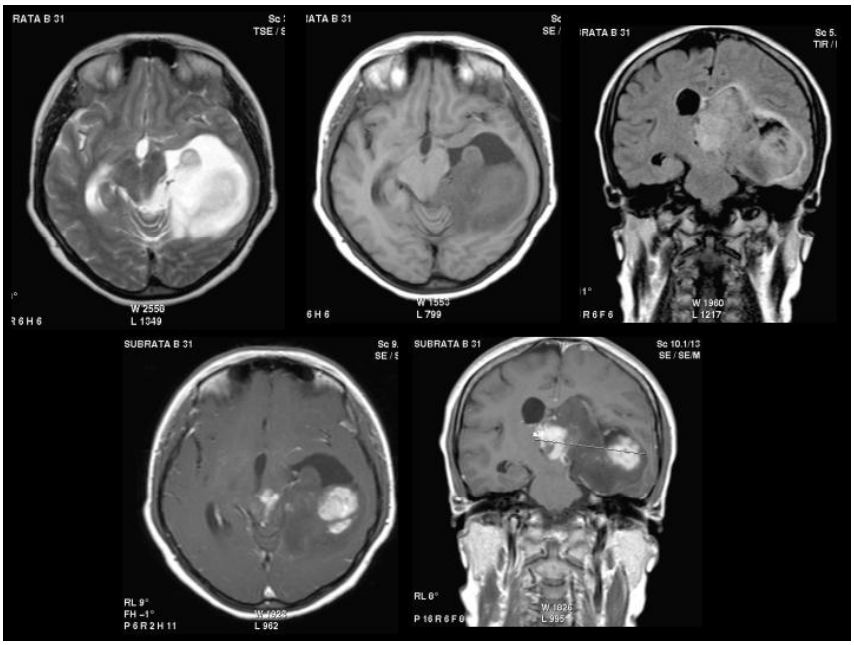

Fig. 10a: MRI shows large bulky, enhancing intra-ventricular mass in left temporal horn infiltrating into temporal lobe suggesting high grade neoplasm

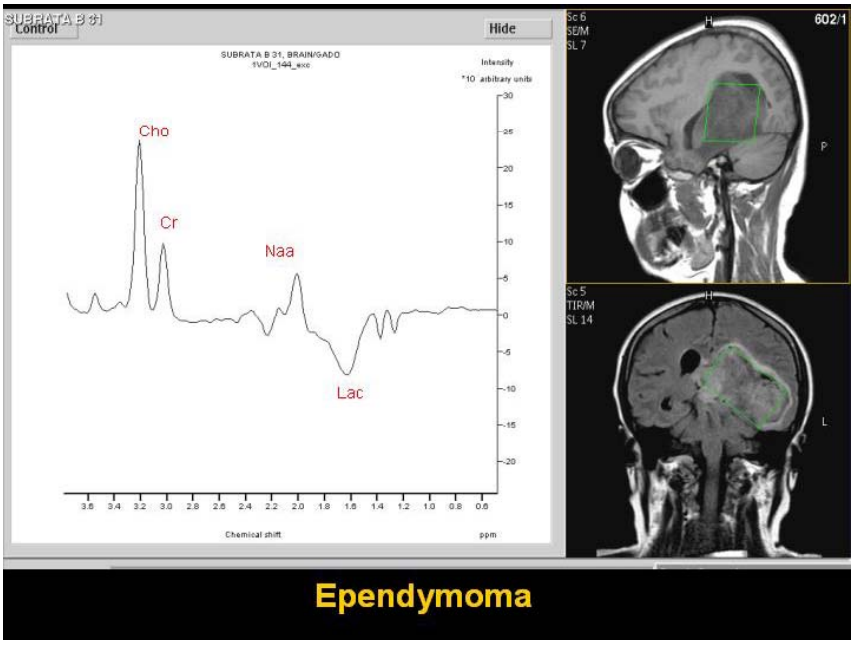

Fig. 10b: MRS reveals increased Cho/Cr ratio with gross reduction of NAA peak and inversion of lactate peak (TE of 144) indicating high grade neoplasm. Biopsy : Ependymoma

Case No. 10 : Seven years, child presented with cerebellar ataxia

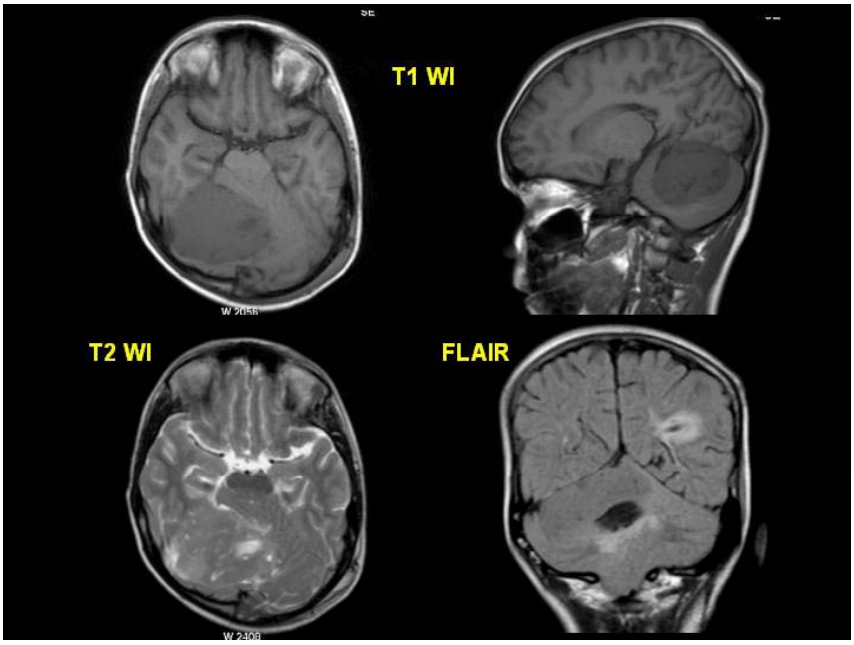

Fig. 11a: MRI shows a large, well-defined extra-axial neoplasm arising from the tentorium on right side causing mass effect on the cerebellum with tonsillar herniation -meningioma

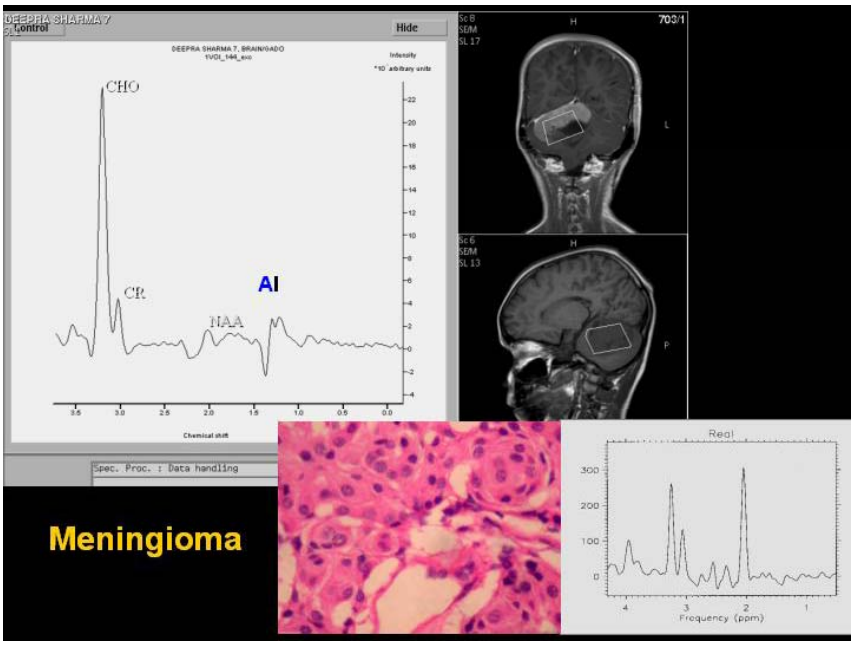

Fig. 11b: MRS(TE144) reveals sharp increased Choline height with Cho/Cr ratio (6.2)with marked reduction of NAA peak;
A small inverted peak at 1.4ppm representing alanine.
Biopsy : Meningioma

Case No. 11 : Fifty seven years, Male, a treated case of carcinoma Nasopharynx with RT, presented with headache for 3 months

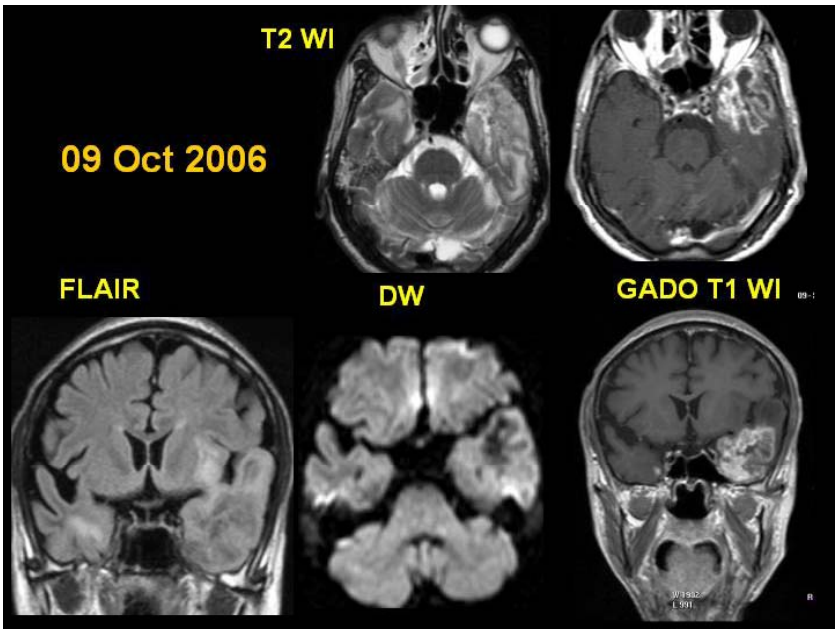

Fig. 12a: MRI shows large, lobulated, thick walled, peripheral enhancing lesion without significant mass effect in the left temporal lobe; another small lesion in the right lobe simulating metastases in view of clinical history.

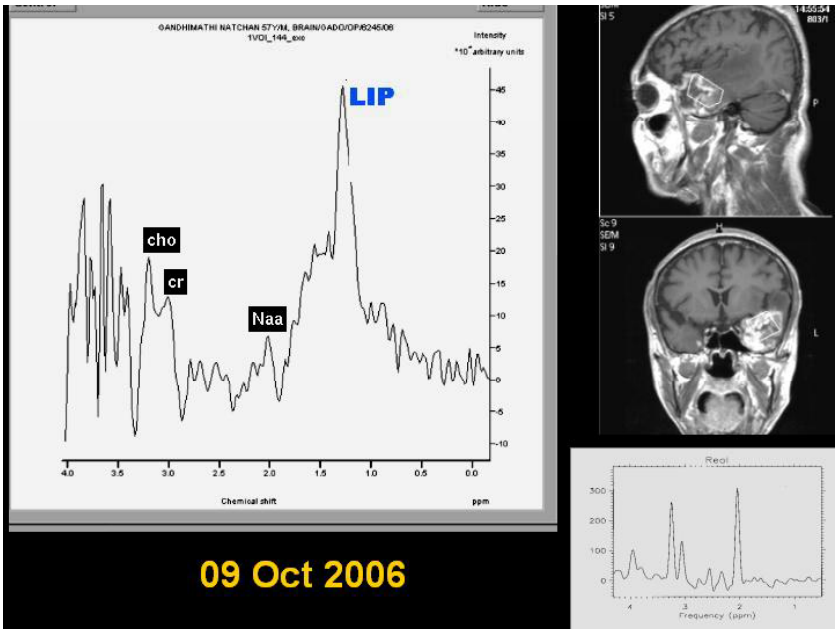

Fig. 12b: MRS reveals a broad based lipid peak between 0.6 and 1.9ppm ; marked reduction in Cho and NAA representing radiation necrosis

Case No. 11 : Follow up

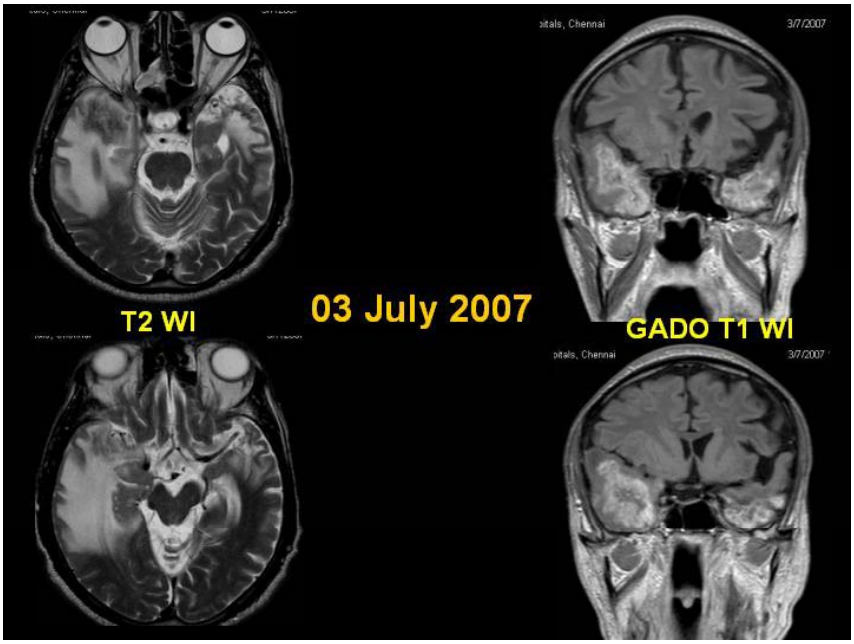

Fig. 12c: MRI after 9 months shows resolution of lesion in the left temporal lobe; lesion in the right temporal lobe appears more pronounced ; distribution of lesions consistent with radiation field

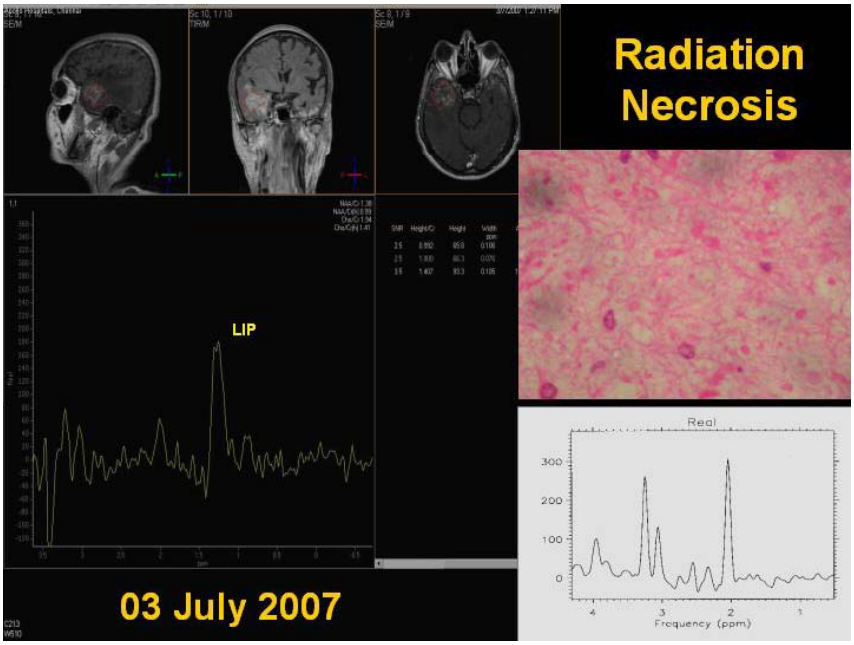

Fig. 12d: MRS reveals a sharp lipid peak at 1.3ppm; marked reduction in Cho and NAA representing radiation necrosis
Stereotactic biopsy of right temporal lesion: Radiation necrosis

Case No. 12 : Thirty three years, male diagnosed to have CNS Neuroblastoma

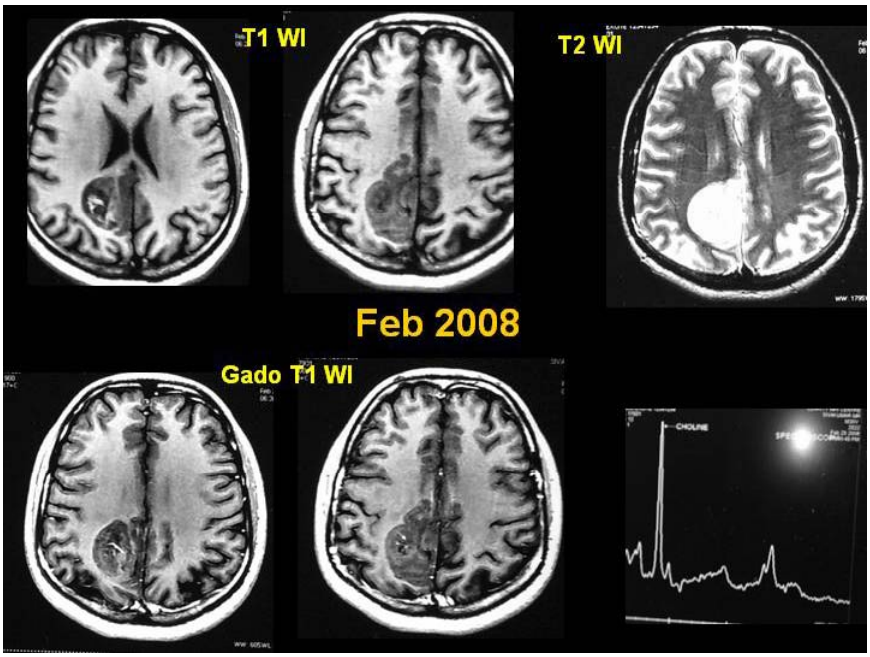

Fig. 13a: Preoperative MRI shows patchy enhancing lesion in right parietal cortex- surgery done ; biopsy :neuroblastoma (grade III)

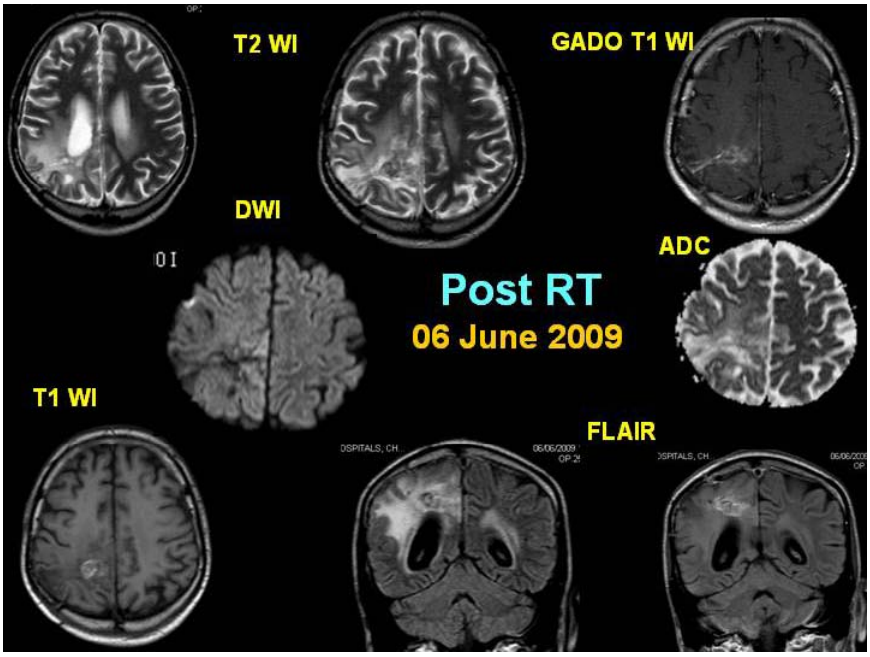

Fig. 13b: Post operative and post radiotherapy follow up of CNS Neuroblastoma- MRI after 15 months shows patchy enhancing areas in the right parietal lobe associated with area of gliosis suggesting doubtful recurrence

Case No. 12 : Post operative & Post RT follow up of CNS Neuroblastoma

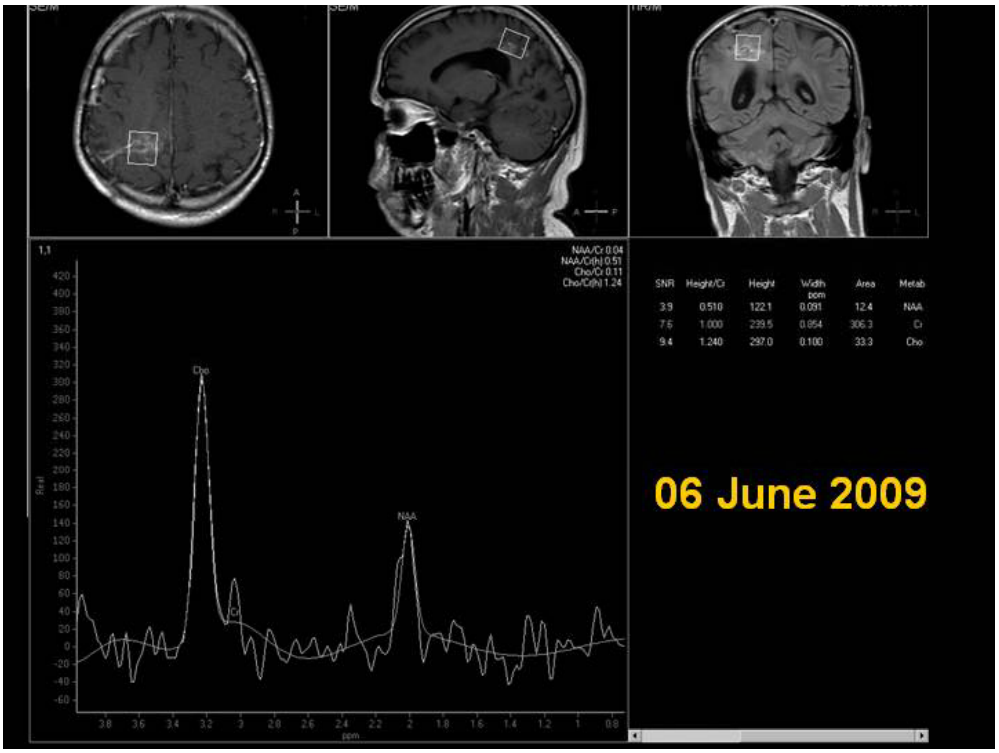

Fig. 13c: MRS reveals marked reduction in NAA and increased Cho/cr ratio suggesting reactive changes ; suggested follow up MRI with MRS

Case No. 12 : Follow up

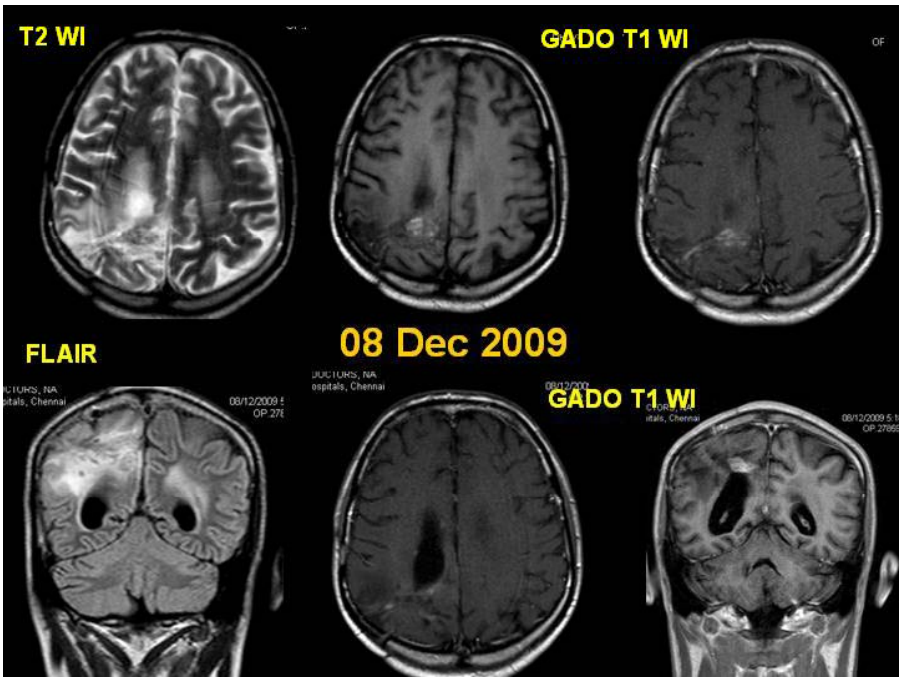

Fig. 13d: MRI after 21 months shows resolution of enhancing areas seen in the right parietal lobe

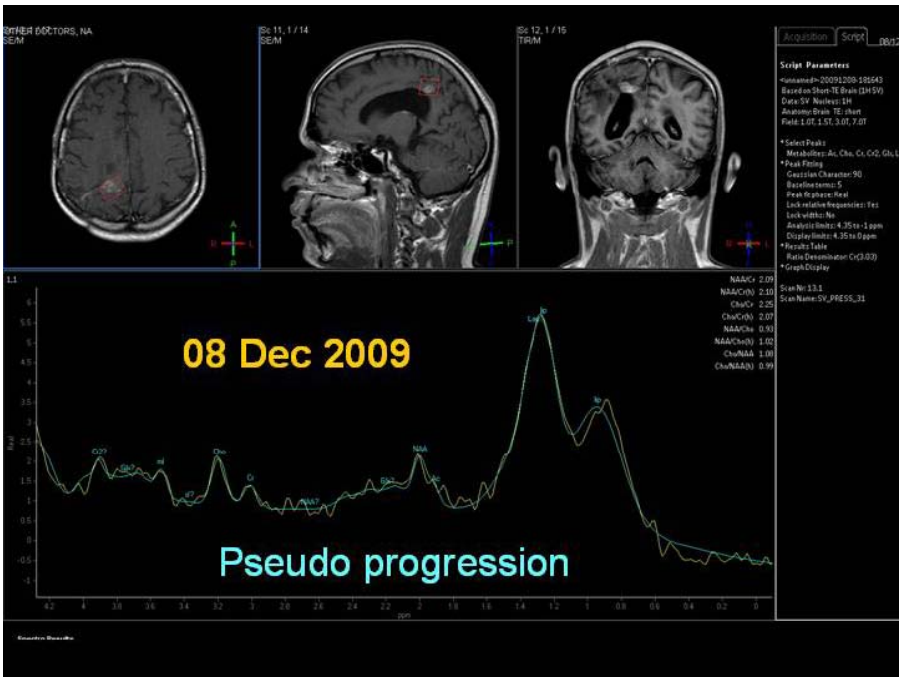

Fig. 13e: MRS (TE 31) reveals broad based lipid /lac peak between 0.6 and 1.6ppm; marked reduction in Cho and NAA representing treatment related changes.

Case No. 13 : Thirty five years, male presented with seizure

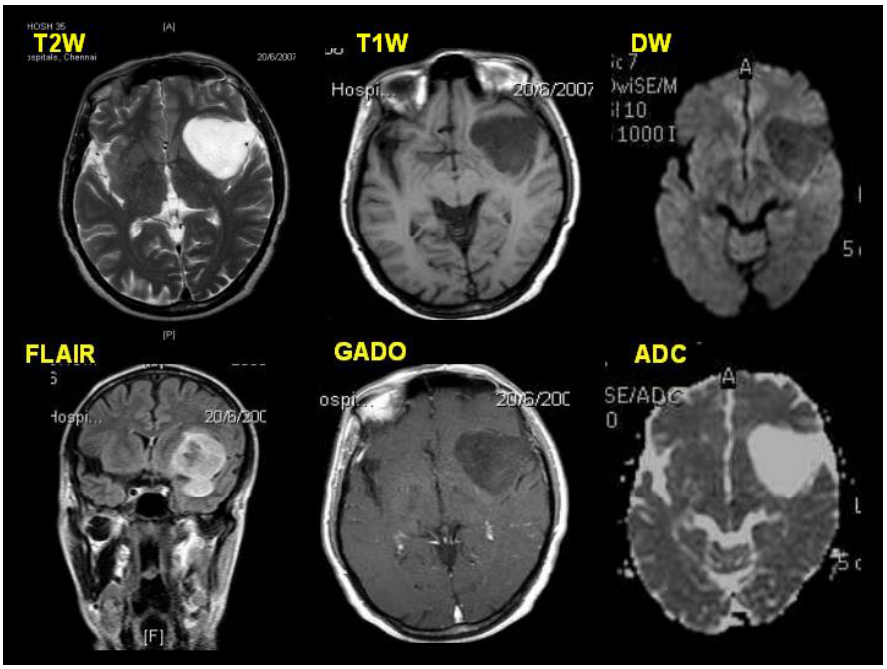

Fig. 14a: MRI shows a well-defined, non-enhancing lesion in the left fronto-temporal lobe; it displays hypointense on T1 WI, hyperintense on T2 WI and non –restricted on DWI. Non specific.

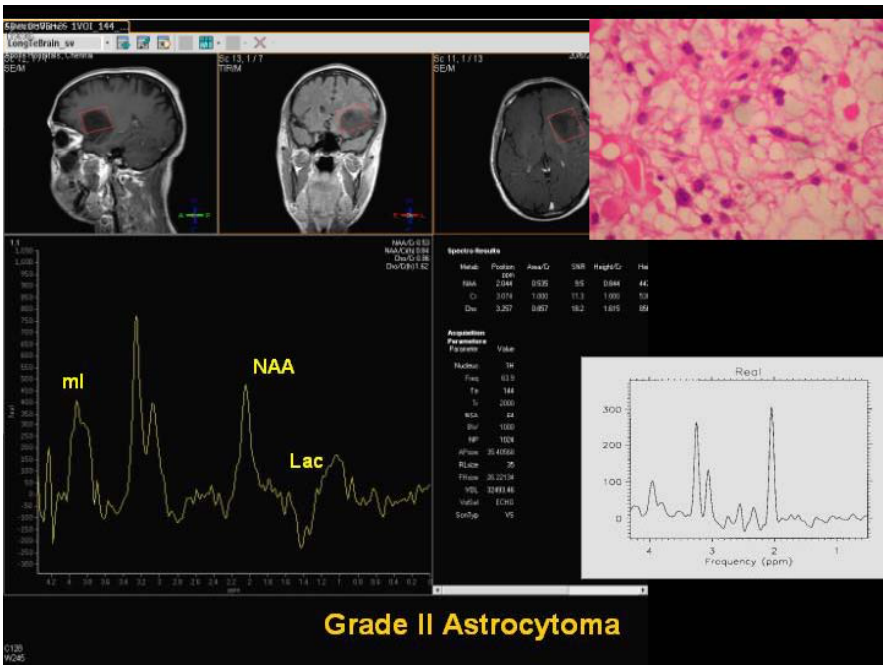

Fig. 14 b: MRS reveals mild increased Cho/Cr ratio with mild reduction of NAA peak, inversion of lactate peak (TE of 144) and detection of myoinositol peak suggesting neoplasm;
Biopsy : Grade II Astrocytoma

Case No. 14 : Fifty six years, male presented with headache and vomiting

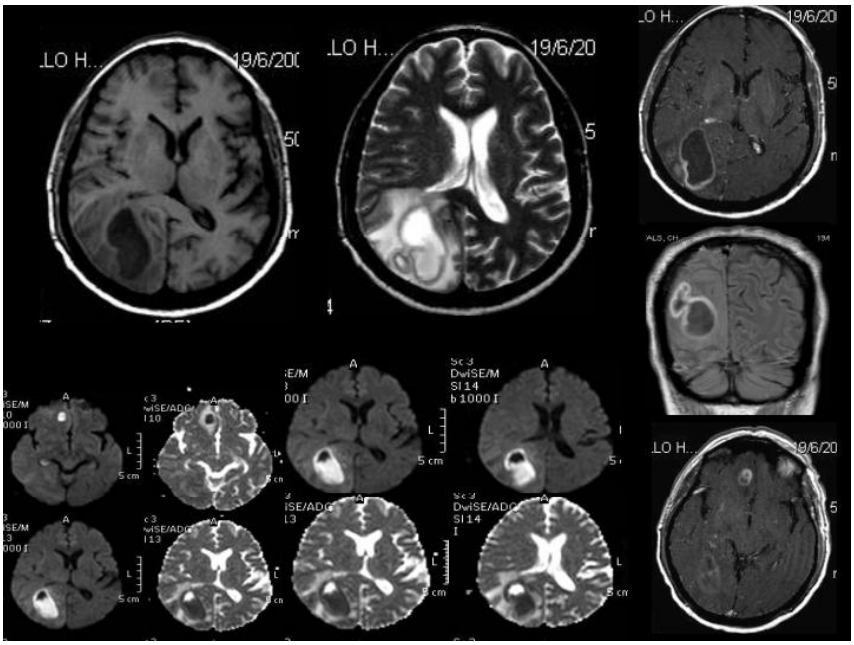

Fig. 15a: MRI shows two (one occipital and one at frontal lobes) peripheral enhancing cystic lesions with central hyperintense area and hypointense rim on T2 WI and restricted area on DWI suggestive of abscess

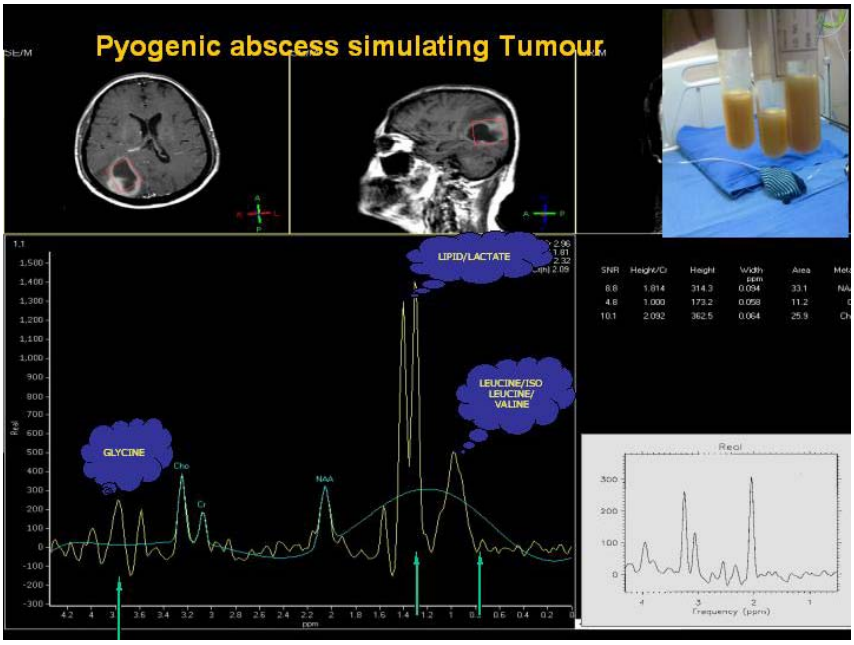

Fig. 15b: MRS reveals a sharp lipid peak at 1.3ppm,broad peak centered at 0.9ppm representing amino acid, and mild elevation of Cho/cr ratio and reduction of NAA representing pyogenic abscess

Case No. 15 : Nineteen years, male with headache for 2 months

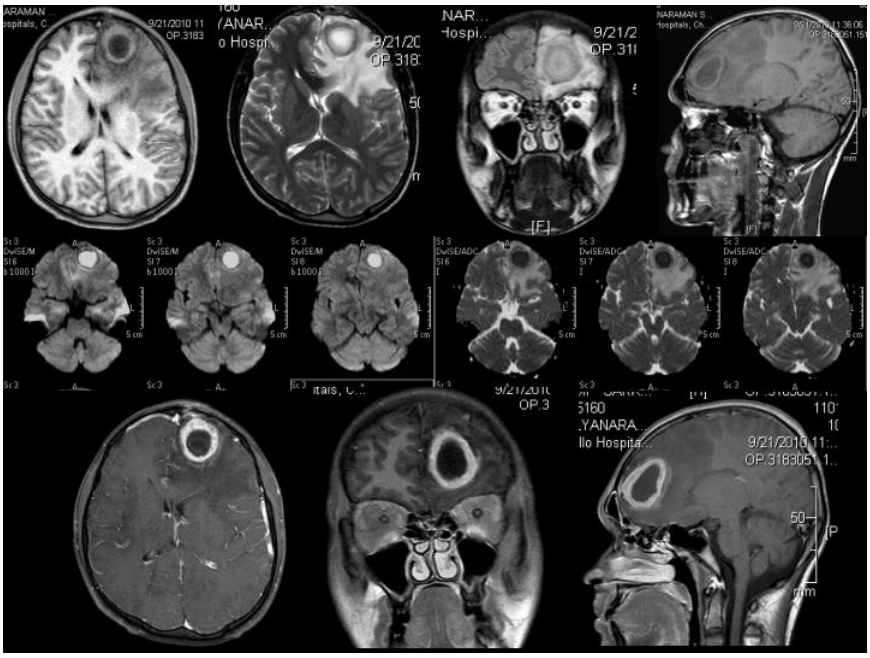

Fig. 16a: MRI shows a circumscribed cystic lesion with thick peripheral enhancing wall in the left frontal lobe; lesion displays central hyperintense area and hypointense rim on T2 WI and restricted area on DWI suggestive of abscess

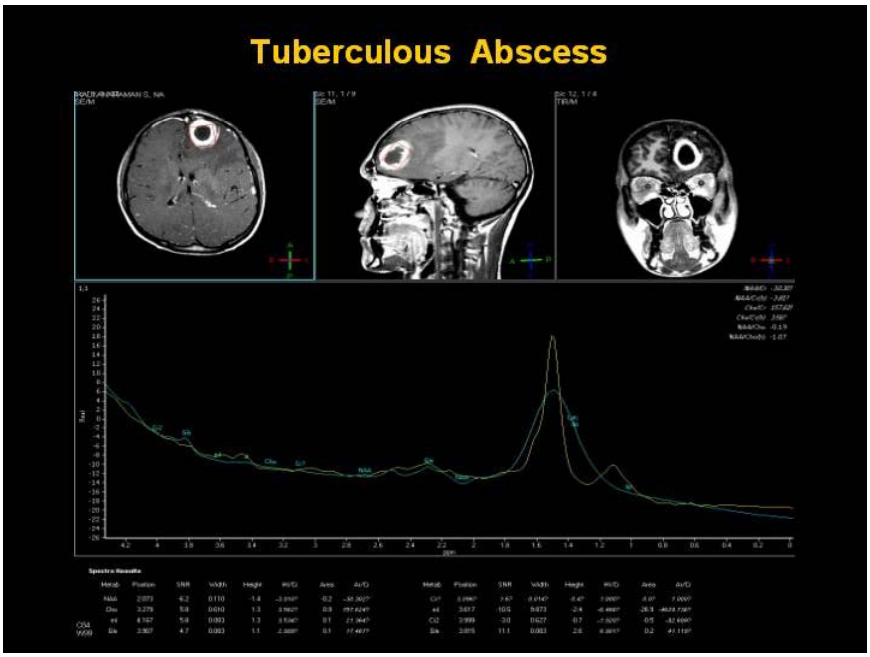

Fig. 16b: MRS reveals a broad lipid peak centered at 1.3ppm and absence of Cho, NAA and other metabolites representing Tuberculous abscess

Case No. 16 : Fifty five years, male presented with h/o headache for 8 months; he has cysts in liver.

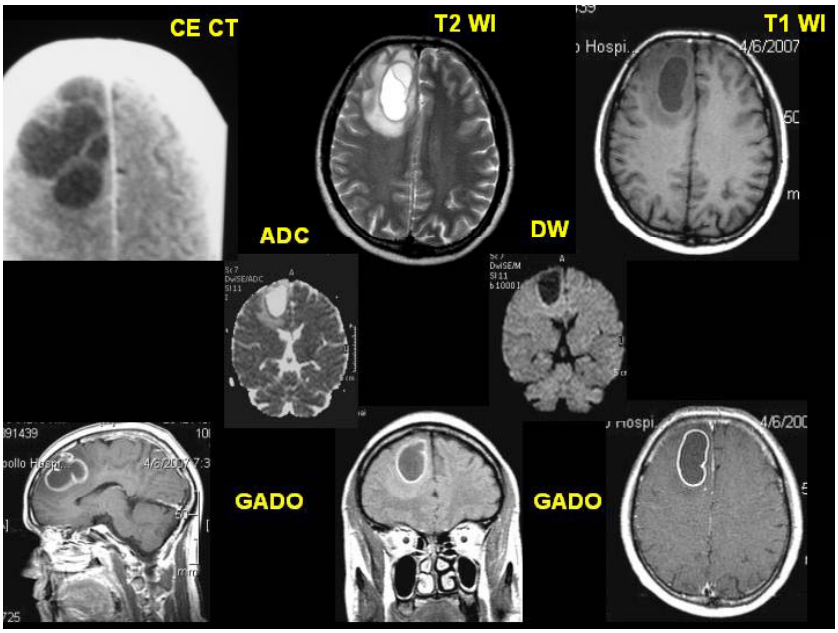

Fig. 17a: MRI shows multi-loculated, enhancing thinwalled, cystic lesion in the right frontal lobe; lesion displays non-restricted area on DWI suggestive of infected cyst.

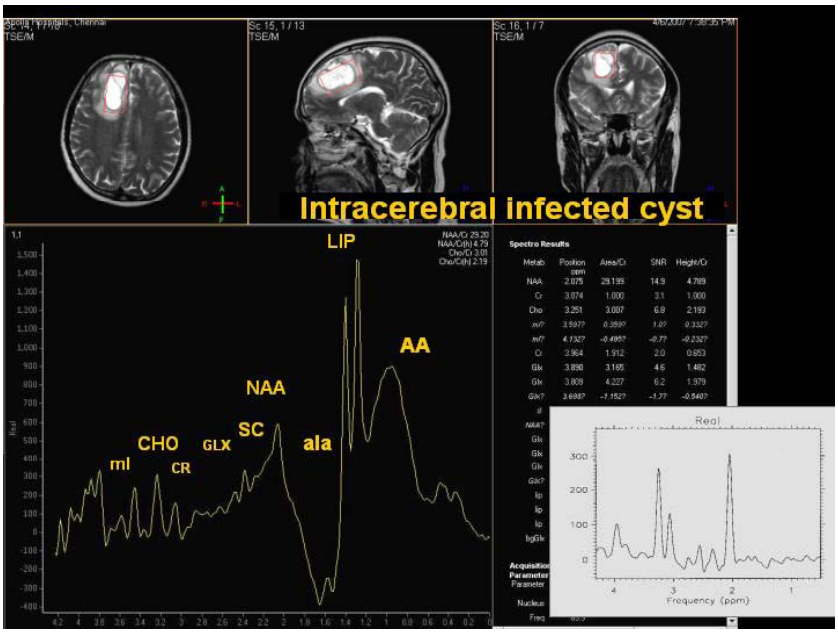

Fig. 17b: MRS reveals a sharp lipid peak at 1.3ppm,broad peak centered at 0.9ppm representing amino acid- acetate, alanine, and lactate mild elevation of Cho/cr ratio and reduction of NAA representing Infected cyst.
In view of multiple hydatid cysts in the liver, intracerebral Hydatid cyst is considered.

Case No. 17 : Twenty two years old male, immunocompromised, presented with headache & vomiting

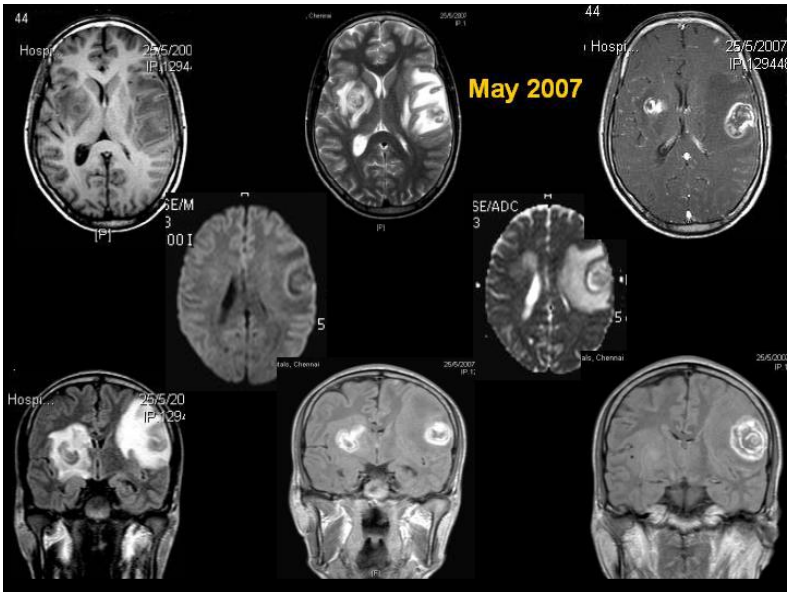

Fig. 18a: MRI shows multiple, nodular lesions with perilesional edema in both temporal lobes; lesions display multiple concentric layers of enhancement on post contrast study.

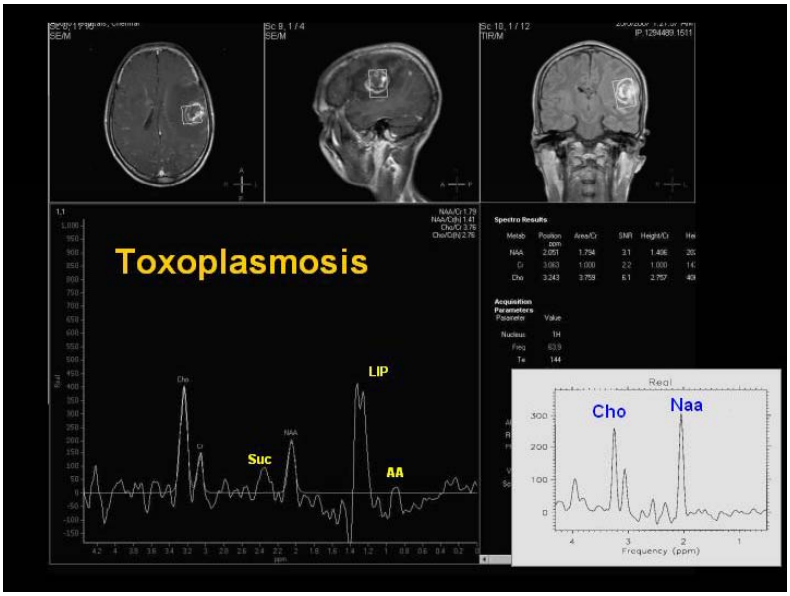

Fig. 18b: MRS reveals broad based lipid peak at 1.3ppm, small peak centered at 0.9ppm representing amino acid, small succinate peak at 2.4ppm, mild elevation of Cho/cr ratio and reduction of NAA representing Infected lesion.
Based on clinical and laboratory evidences , toxoplasmosis is considered.

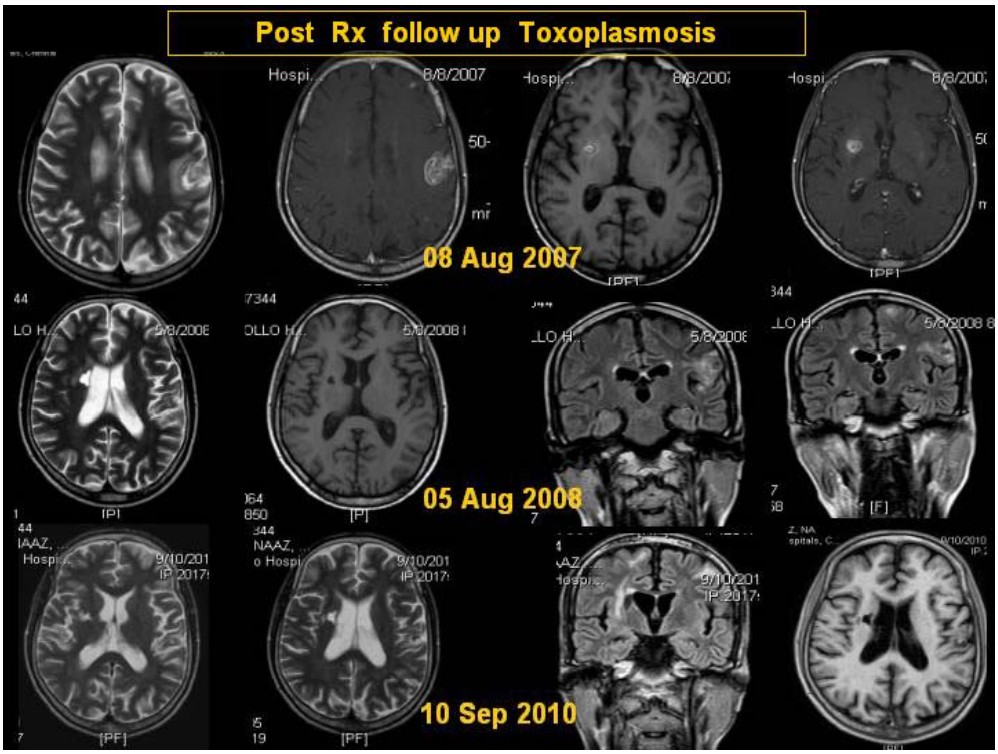

Fig. 18c: Post medical treatment Follow up MRIs (after 3months, 15 and 25 months) show partial to complete resolution of the lesions and gliosis.

Case No. 18 : Thirty four years, female presented with altered sensorium

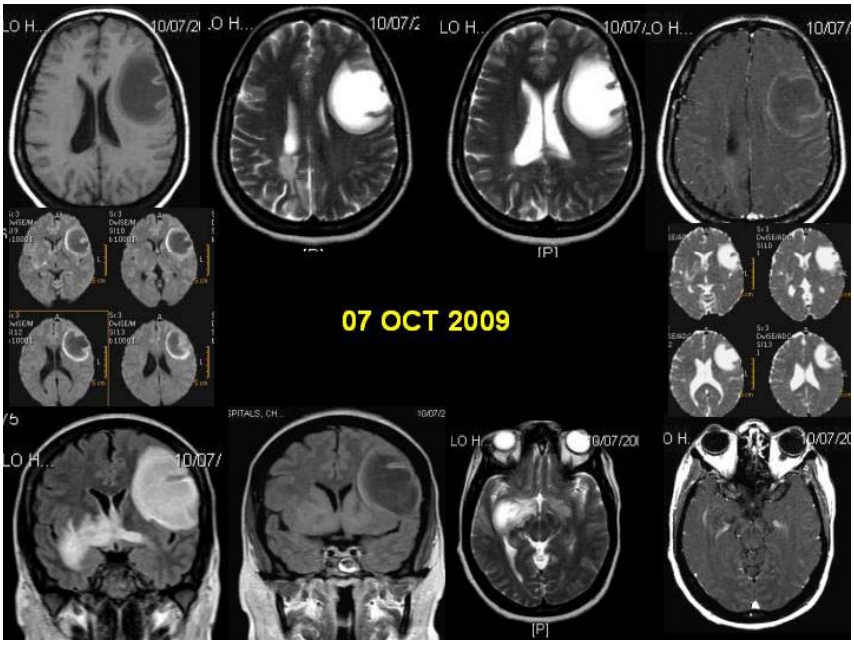

Fig. 19a: MRI shows two peripheral faint enhancing lesions with perilesional edema and mass effect in the left frontal and right temporal lobes; lesion reveals a peripheral rim of restricted diffusion on DW images suggesting neoplasm.

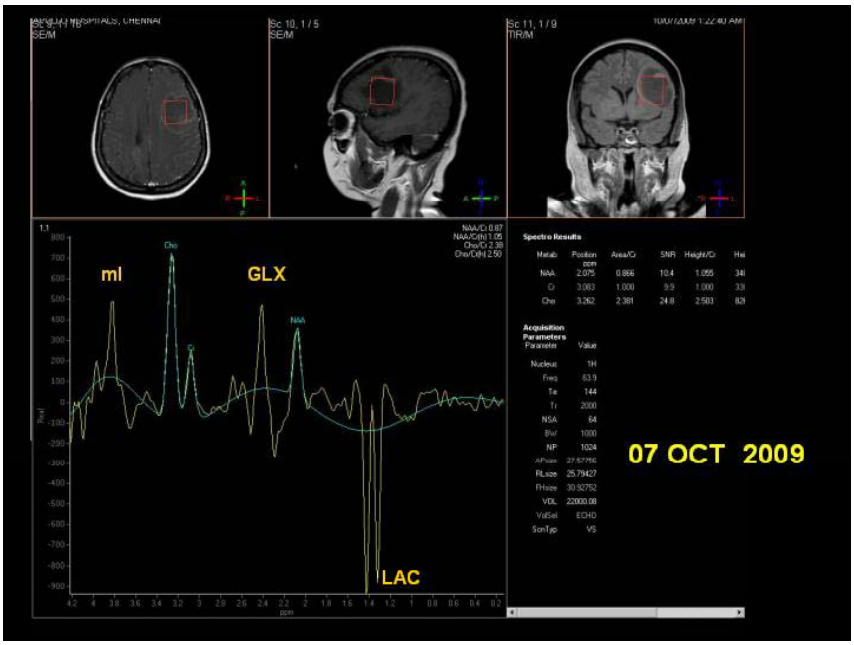

Fig. 19b: MRS reveals marked reduction in NAA/Cr and increased Cho/Cr ratios; peak at 2.4ppm representing Gly/Gln and a myo-inositol peak suggesting non-neoplastic lesion; possibility of demyelinating disease is considered.

MRS changed the MRI diagnosis

Case No. 18 : Post medical treatment follow up

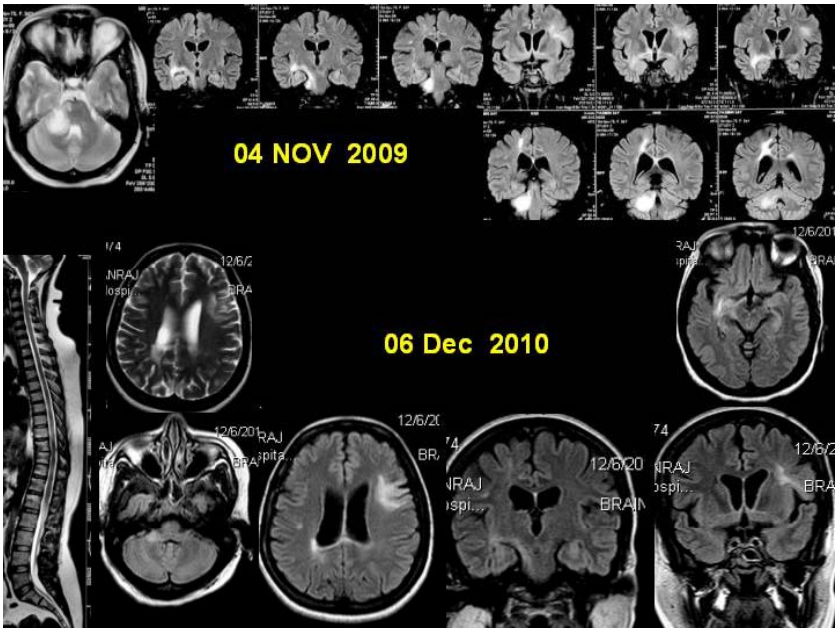

Fig. 19c: MRIs (after 1month and 13 months)show significant reduction in the size of the lesions in the left frontal and right temporal lobes on oct 2009;new lesion in right cerebellar peduncle; gliosis in subcortical and deep white matter with wallerian degeneration along the tract on Dec 2010 studies.

Fig. 19d: MRS reveals a myo-inositol peak; marked reduction in Cho and NAA and broad lipid peak representing chronic demyelinating disease.

MRI aided MRS obviated need for biopsy or surgery in this patient

Case No. 19 : Forty eight years, female presented with headache and left hemiparesis for 3 months

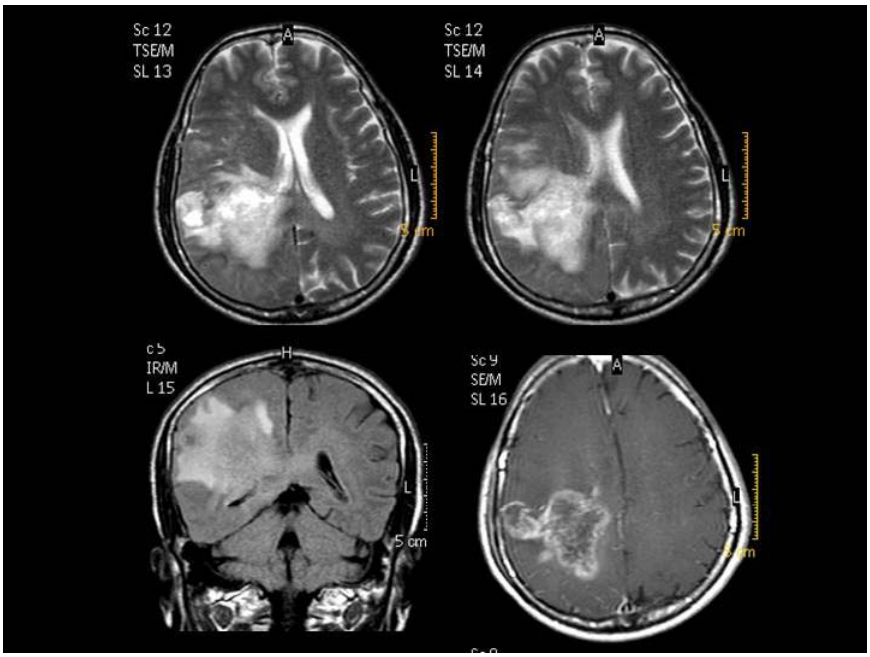

Fig. 20a: A.MRI shows a large, irregular, infiltrative, peripheral enhancing necrotic lesion with edema and mass effect in the right tempero parietal lobe representing high grade neoplasm

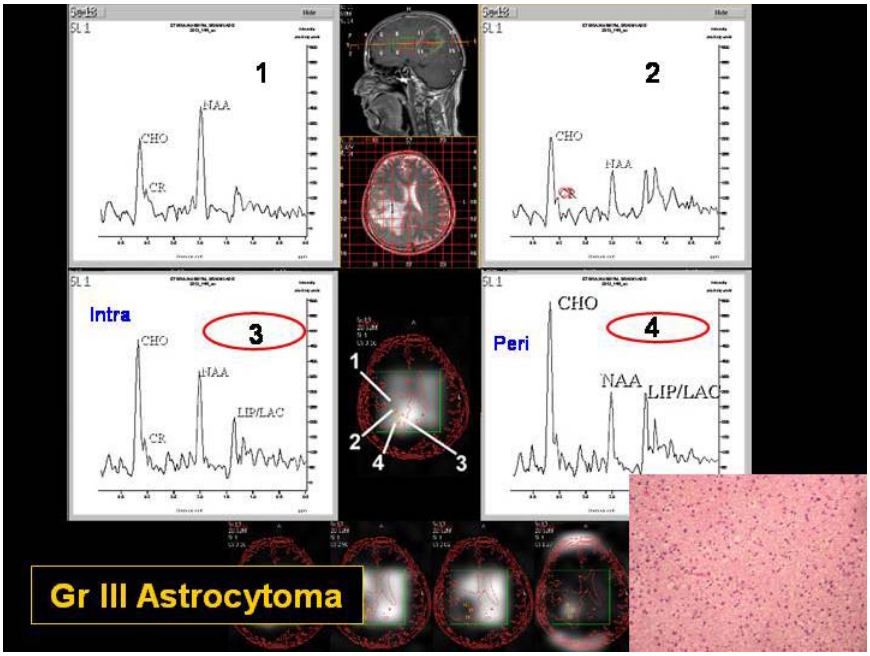

Fig. 20b: MV MRS reveals increased Cho/Cr and decreased NAA/Cho ratios, increased in height of lipid peak in the intra-tumoral and peri-enhancing areas representing high grade neoplasm. Biopsy : Grade III astrocytoma

Case No. 20 : Fifty seven years, Male presented with headache and slurring of speech for 2 weeks

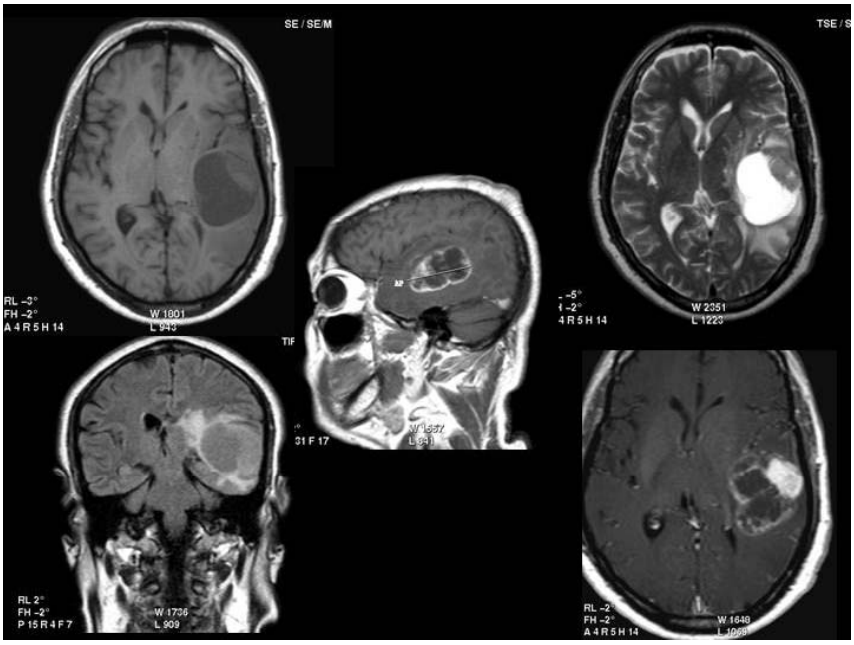

Fig. 21a: MRI shows a large, peripheral enhancing, ovoid lesion with edema and mass effect in the left temporal lobe representing high grade neoplasm

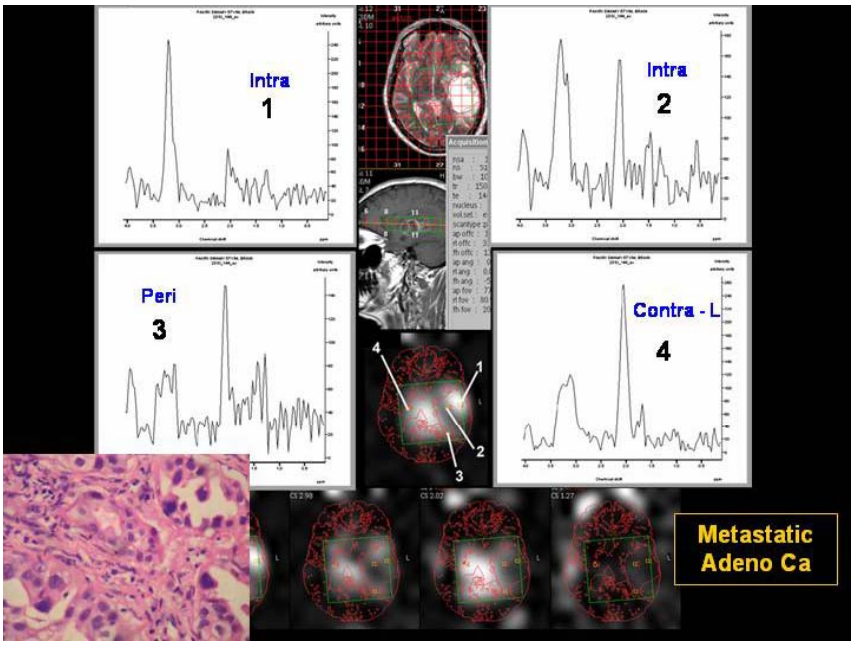

Fig. 21b: MV MRS reveals increased Cho/Cr and decreased NAA/Cho ratio in the intra-tumoral and normal spectra in the peri-enhancing areas representing non-infiltrative tumour. Biopsy : Metastatic adenocarcinoma

Case No. 21 :54 yrs male presented with seizure

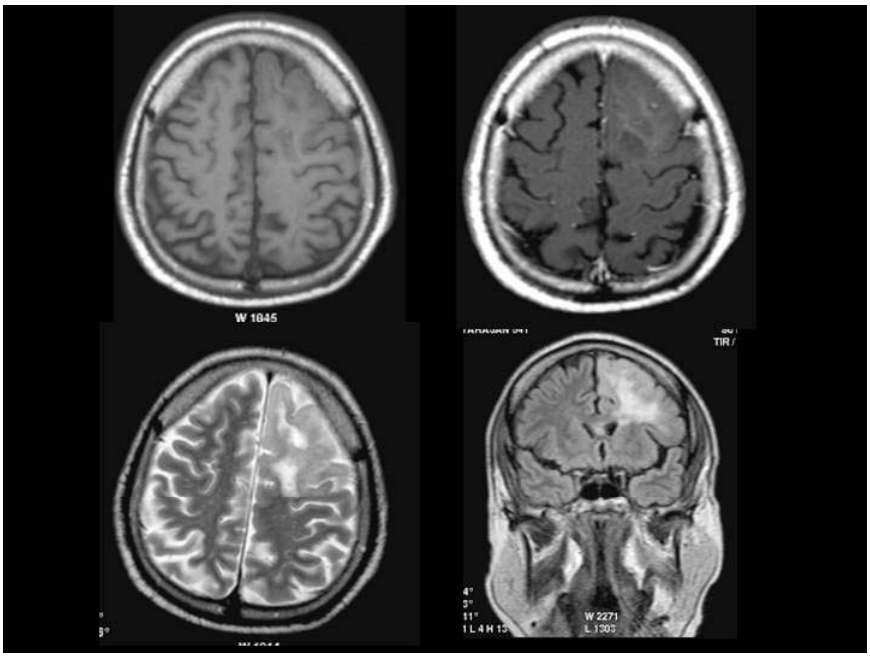

Fig. 22a: MRI shows thickening of gyri with signal alteration on T2 WI in the left medial frontal cortex and no enhancement on contrast study- low grade neoplasm

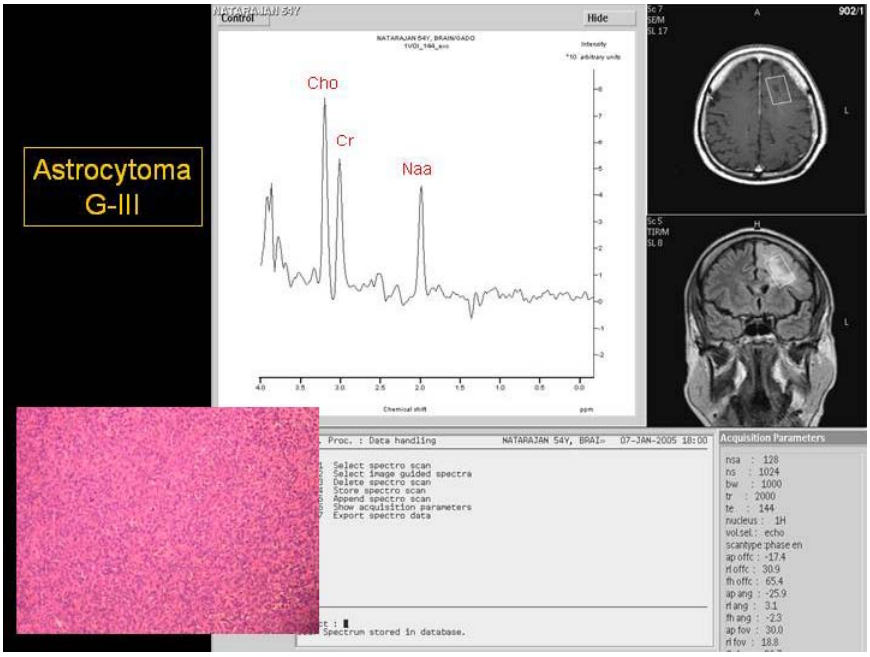

Fig. 22b: MRS reveals increased Cho/Cr ratio with mild reduction of NAA peak consistent with a neoplasm.
Stereotactic biopsy : Grade III Astrocytoma

Case No. 21 : Postoperative and post RT follow up

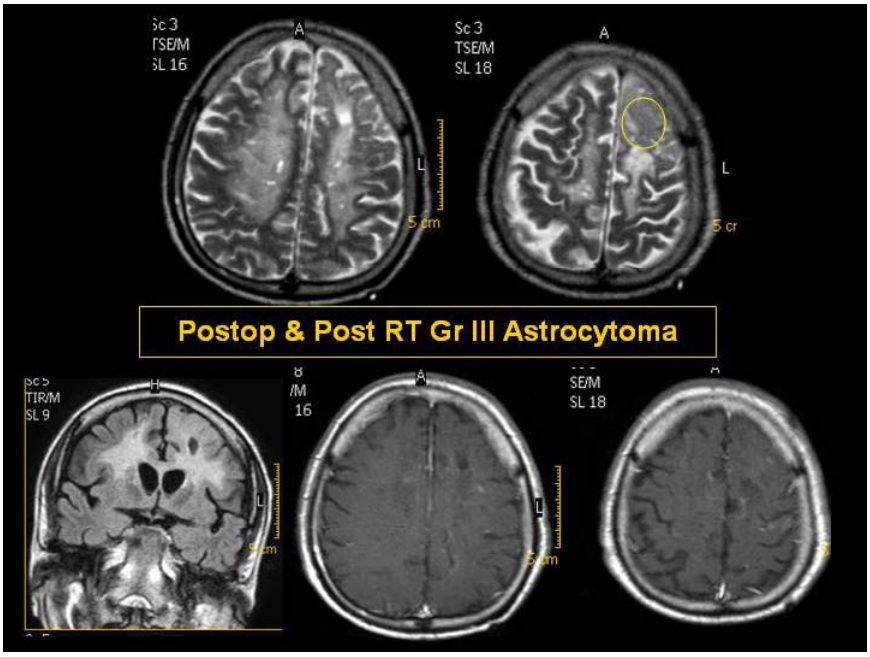

Fig. 22c: MRI shows signal alteration on T2 WI in deep white matter bilaterally representing post radiation leuko-encephalopthy

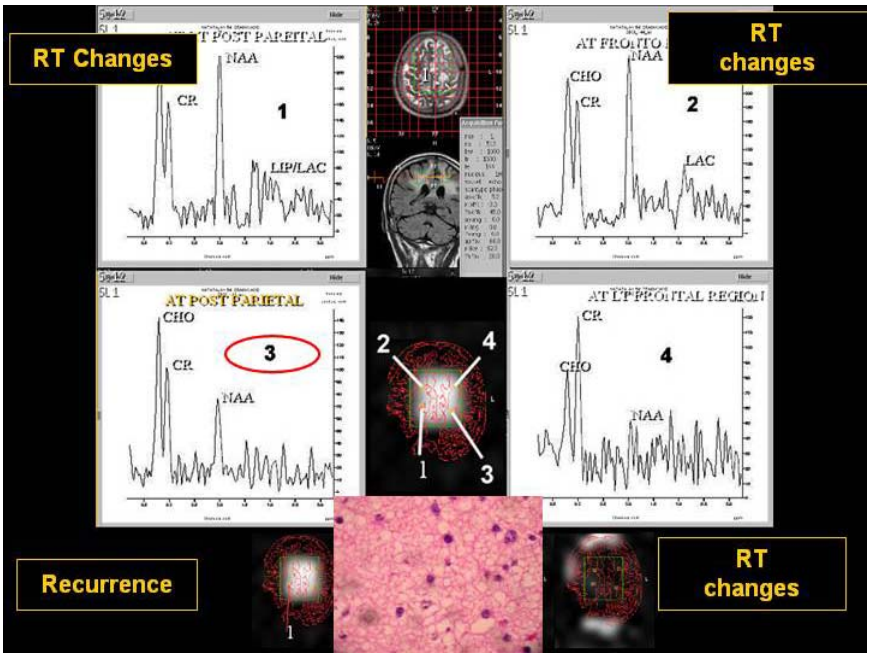

Fig. 22d: MV MRS reveals normal spectra with lipid/lac in both frontal and right parietal lobes representing treatment related changes; increased Cho/Cr and decreased NAA/Cho ratio in the left parietal lobe representing recurrence of tumour.
Biopsy : Tumour recurrence